January 2013

Synthesis And Catalytic Studies Of Zinc Complexes Of Amido-Oxazolinate Ligands

Srinivas Abbina

SYNTHESIS AND CATALYTIC STUDIES OF ZINC COMPLEXES OF AMIDO-
OXAZOLINATE LIGANDS

by

Srinivas Abbina
Masters of Science, Indian Institute of Technology, Guwahati, 2006

A Dissertation

Submitted to the Graduate Faculty

of the

University of North Dakota

in partial fulfillment of the requirements

for the degree of

Doctor of Philosophy

Grand Forks, North Dakota
December
2013

This dissertation, submitted by Srinivas Abbina in partial fulfillment of the requirements for the Degree of Doctor of Philosophy from the University of North Dakota, has been read by the Faculty Advisory Committee under whom the work has been done and is hereby approved.

_____
Dr. Guodong Du (Chairperson)

_____
Dr. Harmon Abrahamson

_____
Dr. Lothar Stahl

_____
Dr. Julia Xiaojun Zhao

_____
Dr. Santhosh K. Seelan

This dissertation meets the standards for the appearance, conforms to the style and format requirements of the Graduate School of the University of North Dakota, and is hereby approved.

_____
Dr. Wayne Swisher (Dean of the Graduate School)

_____
December 11, 2013

ii

PERMISSION

Title   SYNTHESIS AND CATALYTIC STUDIES OF ZINC COMPLEXES OF AMIDO-OXAZOLINATE LIGANDS

Department   Chemistry

Degree   Doctor of Philosophy

In presenting this dissertation in partial fulfillment of the requirements for a graduate degree from the University of North Dakota, I agree that the library of this University shall make it freely available for inspection. I further agree that permission for extensive copying for scholarly purposes may be granted by the professor who supervised my dissertation work or, in his absence, by the chairperson of the department or the dean of the Graduate School. It is understood that any copying or publication or other use of this dissertation or part thereof for financial gain shall not be allowed without my written permission. It is also understood that due recognition shall be given to me and to the University of North Dakota in any scholarly use which may be made of any material in my dissertation.

Signature   _____
                Srinivas Abbina

Date   12.09.2013

TABLE OF CONTENTS

List of Figures

x

ACKNOWLEDGEMENTS

Over the past five years, I have received constant support and encouragement from a great number of individuals. I owe my sincere gratitude to all those people who made this dissertation possible. First of all, I would like to express my deepest gratitude to my advisor Dr. Guodnong Du. His guidance has made this a thoughtful and rewarding journey. I have been fortunate enough to have an advisor who gave me the freedom to explore on my own and the guidance when my steps are faltered. His patience and support helped me to overcome many crisis situations and complete this dissertation.

It is great a pleasure to have a wonderful graduate committee members. I offer my sincere appreciation to all my committee members for the learning opportunities, insightful comments, and constructive criticisms that provided my committee members. I am also indebted to Chemistry Department (University of North Dakota), all faculty, and staff. Especially, I am thankful to Dr. Kubatova and Dr. Novikov for their assistance with ESI-MS and homonuclear decoupling NMR respectively. I am also grateful to Dr. Kolodka for assisting us in derving the gelpermeation chromatography data. I want to express my sincere thanks to North Dakota INBRE facility for helping us in providing MALDI-TOF data for our polymer samples. I would like to acknowledge Dr. Angel Ugrinov (North Dakota State University), Dr. Victor G. Young, Jr. (University of Minnesota, Twin Cities), Dr. Victor N. Nemykin (University of Minnesota, Duluth), Dr. Stahl, and Dr. Chu (UND)

for their time to resolve the crystal structures of zinc and nickel complexes. I have to give my special thanks to my previous group members (Dr. Binda and Dr. Lu) and current group members for providing very joyful working ambience. Many friends have helped me at different stages through out this graduation period. Their support and encouragement is uncotuntable. Most importantly, it would not have been possible without the support of my family. I would like to extend my heart-felt gratitude to all my family members for their encouragement throughout this endeavor.

ABSTRACT

This current work primarily focuses on the fundamental study of zinc complexes of amido-oxazolinate ligands that have shown a great deal of promise in their ability to catalyze various polymerization reactions. A family of new C_1-symmetric, monoanionic, amido-oxazolinate ligands containing oxazoline moiety has been synthesized in moderate to high yields (typically 30–95%) *via* a Pd-catalyzed amination reaction of chiral oxazolines with primary amines and amides. The obtained ligands were treated with $Zn[N(SiMe_3)_2]_2$ to generate the corresponding C_1-symmetric, monometallic zinc complexes. Single-crystal X-ray crystallographic studies confirm that most of the complexes are three-coordinate and mononuclear in nature. These complexes are viable initiators for alternating copolymerization of carbon dioxide (CO_2) and cyclohexene oxide (CHO), yielding moderate isotactic poly(cyclohexene carbonate) (PCHC) with good to high carbonate linkage and moderate molecular weights and PDI values, depending on the substituents. The asymmetric induction is generally low, with up to 71% SS unit in the main chain of the produced PCHCs.

A family of new chiral C_2-symmetric dinucleating amido-oxazolinate ligands that are bridged by three different linkers (*m*-phenylenediamine, 4-(4'-aminobenzyl)benzenamine, and 1,8-diaminoanthracene) has been synthesized in excellent yields (85-90%). Two-fold deprotonation of ligands with $Zn[N(SiMe_3)_2]_2$ in dry toluene generated a series of homoleptic bimetallic zinc complexes while the reaction of ligands

with one equiv. of Zn[N(SiMe$_3$)$_2$]$_2$ leads to formation of bischelating zinc amido-oxazolinate complexes in decent yield. All complexes were characterized by NMR spectroscopy (^{1}H, ^{13}C, COSY, and HETCOR). Dinucleating zinc complexes were also found to be efficient catalysts for asymmetric alternating copolymerization of CO$_2$ and CHO, generated highly pure isotactic poly(cyclohexene carbonate), irrespective of transformation of dinuclear complexes into mononuclear bis(amido-oxazolinate) complexes. The cooperative mechanism between the metal centers was evident by the enhanced catalytic activity of the dinucleating zinc complexes.

These results intrigued us to investigate the efficiency and stereo selectivity of our catalytic systems for ROP of *rac*-lactides. We have also explored the efficiency of zinc complexes of amido-oxazolinate ligands for the ring opening polymerization of *rac*-lactides at mild reaction conditions. These catalysts deliver a viable synthetic route to produce highly selective steroblock PLA ($P_m = 0.90$), an unprecedented selectivity in the case of zinc based catalysts. The same series of zinc complexes have also shown excellent activity for ring opening copolymerization of styrene oxide and cyclic anhydrides, including succinic anhydride, maleic anhydride, and phthalic anhydride. These catalysts exhibited unprecedented TOFs 8000 h^{-1} for coupling of styrene oxide and maleic anhydride. The ligand geometrical parameters strongly influence the stereochemistry of the obtained poly(styrene oxide-*co*-anhydride)s.

In addition to this, hydrosilylation of a variety of unsaturated organic substrates, including aldehydes, ketones, and imines are effectively reduced to alcohols and amines, respectively, using a high-valent nitridoruthenium(VI) compound as a catalyst and phenylsilane as a reductant. Mechanistic studies indicate that the catalysis proceeds via

silane activation rather than carbonyl activation, and the silane is likely activated via multiple pathways, including a radical-based pathway. The mechanistic investigation was carried out using a variety of spectroscopic and analytical techniques, including NMR spectroscopy, FT-IR spectrophotometry, gas chromatography (GC/FID and GC/MS), and high-resolution mass spectroscopy.

CHAPTER 1

GENERAL INTRODUCTION

1.1. Need of Sustainable Feedstocks

The domestic economies of the most nations still largely depend on their crude oil resources. The utilization of these crude oil resources ranges from energy production to synthesis of various polymeric materials/chemicals that are indispensable in variety of applications, including structural and packing materials, appliance, electronics, biomedical tools, and much more.[1,2,3,4] The rapid increase in global population has lead to a marked increase in the consumption and production of petroleum originated products. Synthetic plastics alone contribute for ~7-8% worldwide consumption of fossil fuel resources. According a recent survey in 2010, a single person in the U.S in average consumed approximately 140 kgs of plastics per year.[5,6] If the consumption of petroleum based feedstock is continued at the current pace, they will be depleted within next few centuries. In addition to the issues with synthesis of conventional polymers, disposal of synthetic polymers is also a huge environmental challenge.[7] Thus, it emphasizes the development of novel synthetic strategies for making biodegradable polymers using biorenewable resources instead of using petroleum based feedstock. While developing novel processing approaches, modifications of existing renewable polymers have been also attracting ever-increasing attention over the past two decades.[8,9,10] The target in this arena is the development of well-designed strategies for the future generation of polymeric materials

that will involve in controlled polymerizations of new monomers, extracted from the abundant carbon-based biorenewable resources. In an effort for the generation of widely-acceptable biodegradable polymers using renewable resources, a wealth of research has been focused on the synthesis and structural modifications of variety of polymers, including poly(lactide), poly(carbonates), and polyesters.

1.2. Polycarbonates

Carbon dioxide (CO_2) stands out as one of the most promising renewable resources because it is abundant, inexpensive, non-toxic, and non-flammable.[11,12,13a] Moreover, it has
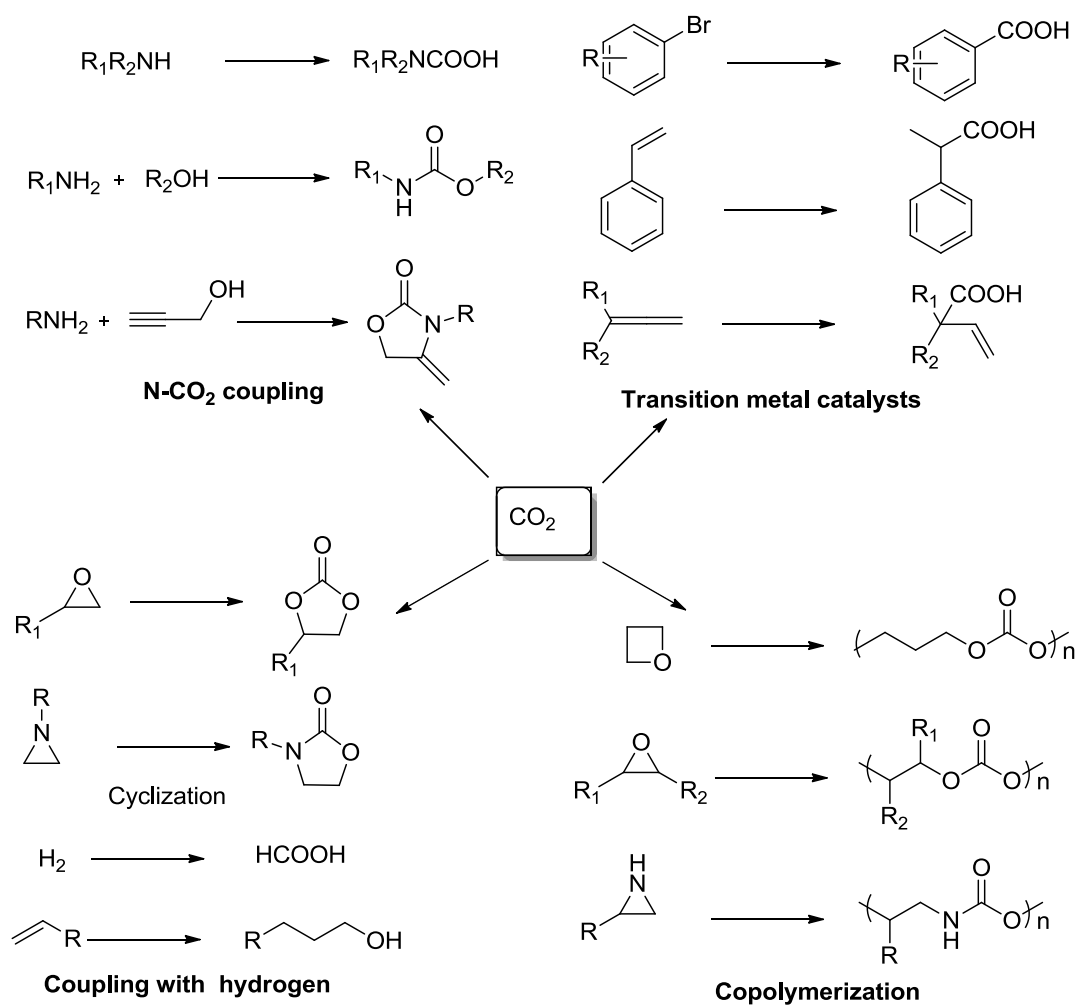
Figure 1. Potential applications of CO_2 as a chemical feedstock

2

been recently reported that the concentration of CO_2 in the atmosphere has increased to ~400 ppm and escalation of atmospheric CO_2 levels are further continued in the future.[13b] The primary sources accounting for the hike of CO_2 concentration are burning of fossil fuels, transportation, deforestation, and other human activities. Especially, the concentration of CO_2 in the atmosphere by human activities (5.5 Gt carbon per year) has kept steadily increasing during the last two hundred years.[14,15,16,17,18] Although the role of industrially-utilized CO_2 in reducing CO_2 levels in the atmosphere is under debate, it encourages the scientific community to utilize the CO_2 as an alternative feedstock to petroleum based resources as it meets the requirements of sustainable feedstock in the polymer industry. Moreover, the obtained CO_2 based polymers are generally biodegradable.[19]

However, the high thermodynamic stability of CO_2 makes it an ideal medium for various chemical processes.[20,21,22] To overcome this limitation, the coupling of CO_2 with highly reactive reagents has been well explored using variety of catalysts.[23,24,25] Figure **1** illustrates the potential usage of CO_2 as a chemical feedstock including large-scale production of urea, salicyclic acid and several carbonate-based materials.[26] In particular, over the past 40 years, significant efforts have been directed toward the catalytic coupling of heterocyclic compounds with carbon dioxide, especially the copolymerization of CO_2 and epoxides (propylene oxide (PO), cyclohexene oxide (CHO), and styrene oxide), due to a wide array of applications of the resulting polymeric materials.[27]

1.2.1. Origin of Polycarbonates (PC)s to Green Polycarbonates

Since the discovery of poly(bisphenol-A carbonate) (BPA-PC), a polycarbonate of bis(phenol-A), by D. W. Fox and H. Schnell independently, both aliphatic and aromatic

polycarbonates have been widely used in our daily life.[28] Due to the outstanding thermal, mechanical, optical, and electrical properties of polycarbonates, they have been used for various applications, including structural parts, household appliance parts, components of electrical/electronic devices, plasticizers, automotive applications, compact discs, impact resistant materials, reusable bottles, food and drink containers, and many other products.[27k, 29,30] The vital mechanical and thermal properties of polycarbonates are strongly dependent on their glass transition temperature (T_g) and few secondary transitions such as β- and γ - transitions below their glass transition temperature. The high T_g and melting point (T_m) of BPA-PC imparted thermal properties while higher β–transition values provided improves mechanical properties.[31] Until today, BPA-PC based polymers are widely manufactured by different companies with different trade names around the globe (Table 1).[32]

Table 1. Major manufacturers of polycarbonate plastics and corresponding trade names

Company	Trade Name
Sabic	LEXAN®
Bayer	MAKROLON®
Teijin Chemical Limited	PANLITE®
IDEMITSU	TARFLON®
Omay	Polyopt®
Nalge Nunc International	Nalgene®
Mobay Chemical Company	MERLON®

Industrial production of BPA-PC was carried out in the following two major routes: an interfacial reaction between monomer bisphenol-A and phosgene in the presence of dichloromethane and aq. NaOH and a melt polymerization process of bisphenol-A and diphenyl carbonate (Figure 2).[33,34] In both methods, the major concerns are usage of phosgene gas and monomer bisphenol-A (BPA). Phosgene gas is well-known for its highly toxic and corrosive nature. Even though diphenyl carbonate is an alternative to phosgene

gas, most often diphenyl carbonate is synthesized from phosgene gas and phenol. Moreover, the high temperatures are required in order to remove phenol and the degradation process of BPA-PC again generates the carcinogenic BPA.[35,36]
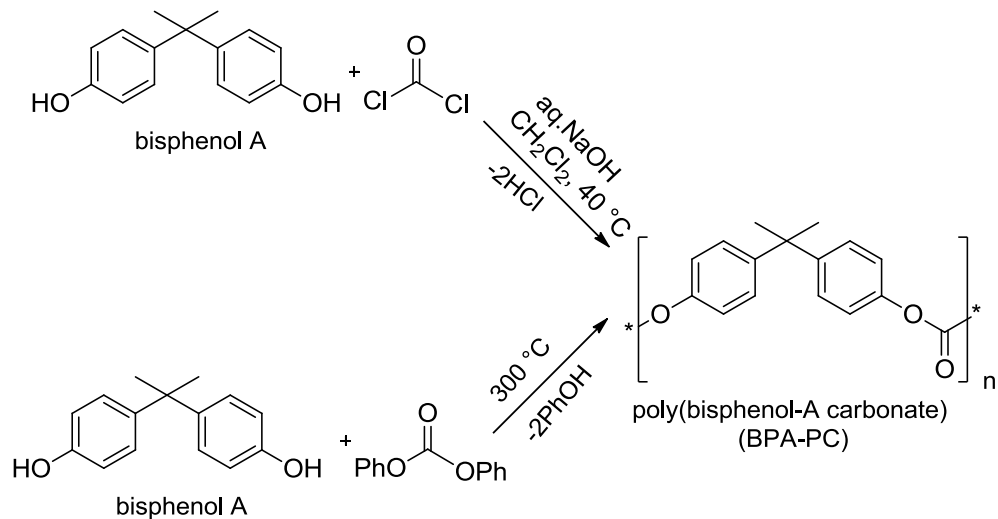
Figure 2. Primary industrial synthetic routes for the generation of BPA-PC

More recently, the usage of BPA products has become progressively more controversial due to its potential health hazards. A study by Centers for Disease Control and Prevention (CDC) in USA showed that low levels of BPA were found in samples of urine, human breast milk, and body fat of women. This study confirmed that the major source of BPA contamination is diet, e.g. BPA from canned foods and also BPA is leaching from polycarbonate beverage containers when they are subjected to heating.[37,38] The potential governmental regulations and health concerns of BPA would turn the attention of polymer scientific community toward green polycarbonates.

A more significant strategy for the synthesis of green PCs is the copolymerization of CO_2 with epoxides, most commonly used are CHO and PO, which is an alternative to the route that involves in the usage of phosgene and BPA. The widespread availability of naturally occurring epoxides and CO_2 will be another feature of this route; from this it

could be possible to generate a wide range of polycarbonates to address the current demands in the polymer industry. Moreover, this route is environmentally benign and the obtained polymers are biodegradable and biocompatible.[39] Few co-polymers that are derived from the copolymerization process are already commercialized, however, they are limited. The classical BPA-PCs and green PCs are belonging to the same category of PCs, however, they behave differently. The classical BPA-PC has a T_g of 150 °C whereas poly(cyclohexene carbonate) (PCHC) has T_g of 115 °C (Figure 3).
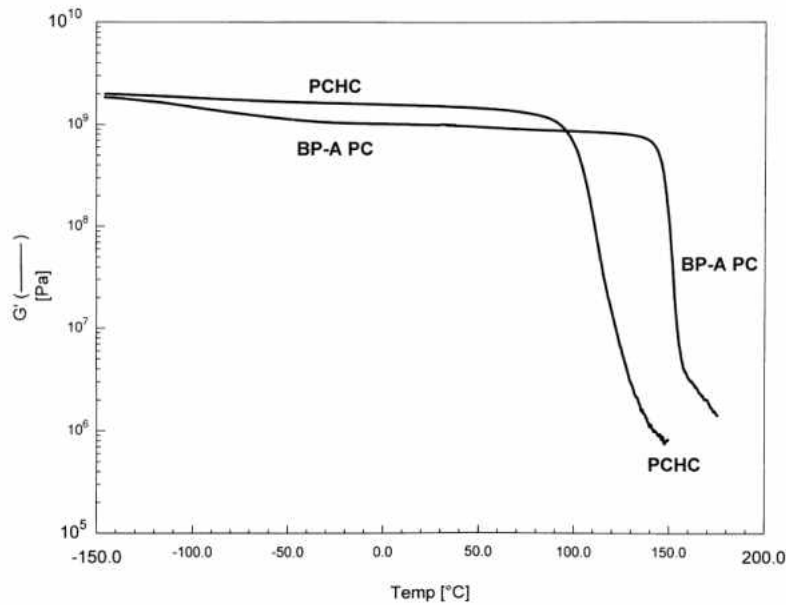
Figure 3. Comparison of glass transition temperatures (T_g/°C) of PCHC and BPA- PC[39]

The low T_g of PCHCs make them loss their stiffness at earlier temperature than BPA-PC and also their use for high temperature applications are limited.[40,41] The tensile properties, which quantify how polymers behave under stress, such as the yield stress, elongation at break, and stress at break of PCHC and BPA-PC are shown in Table 2. Yield stress and stress at break values of PCHC are significantly lower than the corresponding values of classical BPA-PC. It confirms the highly brittle nature of the PCHC compared

to the ductile BPA-PC. In contrast to this, the tensile modulus of PCHC is significantly higher than that of BPA-PC (Table 2). It implies the high stiffness of the PCHC.[39] The development of more economical synthetic methodologies and the synthesis of different new polycarbonates with improved material properties would definitely enhance their usage as bulk polymeric materials. As a result, an extensive amount of research has been devoted towards developing new and highly active catalysts for the generation of green polycarbonates.

Table 2. Comparison of thermal and mechanical properties of polycarbonates[39,42]

	$T_g/°C$	σ yield (MPa)	σ break (MPa)	strain at break (%)	tensile modulus (MPa)
BPA-PC	151	56-62	43-51	15-75	200-2800
PCHC	118	43-47	40-44	1.1-2.3	3500-3700
PPC	42	43 ± 2 (45)	7-30	600-1200	700-1400

PCHC: poly(cyclohexene carbonate), PPC: poly(propylene carbonate), BPA-PC: poly(bisphenol-A carbonate)

1.3. Alternating Copolymerization of Epoxides and Carbon Dioxide

1.3.1. Initial Studies in Copolymerization of CO_2 and Epoxides

In 1969, Inoue and coworkers first reported a heterogeneous zinc catalytic system, a 1:1 mixture of $ZnEt_2$ and water, for the alternating copolymerization of CO_2 and propylene oxide (PO) to produce low molecular weight poly(propylene carbonate) (PPC) with low turnover frequencies (TOF)s of 0.12 h^{-1} in very low yields at 80 °C and 20-30 atm of CO_2 pressure.[43] Following this initial discovery, several heterogeneous zinc based catalytic systems consisting of a combination of $ZnEt_2$ with dihydroxy alcohols (resorcinol),[44] carboxylic acids (benzoic acid, phthalic acid, acetic acid, succinic acid),[45] and primary amines[46], were employed for the copolymerization of CO_2 and PO. Shortly after these primary reports, Kuran and co-workers studied the effect of tri hydroxyl alcohols, such as pyrogallol and 4-bromopyrogallol on copolymerization of CO_2 with CHO

and PO. This catalytic system generated poly(propylene carbonate) (PPC) with TOFs up to 0.3 h⁻¹. [47,48] In order to develop the highly efficient catalyst, Hattori and co-workers synthesized a well-defined heterogeneous catalytic system using $Zn(OH)_2$ and glutaric acid for copolymerization of CO_2 and PO. This combination produced PPC with TOFs of 1.1 h⁻¹ at 60 °C and 30 atm pressure of CO_2.[49] At this point of time, they believed that catalytic activity of zinc glutarate might have originated from the unique morphology (including crystallinity and crystal size) of the catalyst rather than its surface area. Later on another efficient ZnO-based catalyst (half-ester/half-acid from maleic anhydride and 3,3,4,4,5,5,6,6,7,7,8,8,8-tridecafluorooctanol and then reacting it with ZnO),[50] was reported for the copolymerization of CO_2 and CHO. From these results, it was hypothesized that two labile hydrogens that are available from either alcohol or acid in catalytic system are very crucial so that the metal source ($ZnEt_2$ or $Zn(OH)_2$) and co-catalyst can form an active species containing zinc-oxygen bonds. However, these first-generation catalysts suffered from multiple active sites, solubility issues, low polymerization activites, undesired side products, and products with broad polydispersities. Moreover, the real active systems were not known as structures were poorly determined. To overcome these limitations with heterogeneous systems, single-site homogenous catalysts have been developed. It also gave an access to understanding the detailed mechanistic aspects of copolymerization process of CO_2 and epoxide at molecular levels. The first homogeneous well-defined, single-site catalyst for perfect alternating copolymerization of cyclohexene oxide and CO_2 was developed by Inoue *et al* in 1986, comprising an aluminum porphyrin ((TPP)AlX, TPP = 5,10,15,20-tetraphenylporphinato) complex with a co-catalyst quaternary ammonium or phosphonium salt, producing poly(cyclohexene carbonate) with

controlled molecular weights (3500-6000 g/mol) and narrow molecular weight distribution (Figure 4, **1**).[51] However, this reaction is very slow; it took about 13 days to reach completion of the reaction. This was the first achievement in living and alternating copolymerization of CO_2 and epoxides. Darensbourg *et al* developed effective homogenous catalysts, complexes of zinc phenoxides afforded from a reaction of substituted phenols with a solution of $Zn[N(SiMe_3)_2]_2$ in THF or diethyl ether, for both copolymerization of cyclohexene oxide and CO_2 and homopolymerization of cyclohexene oxide in neat conditions, to afford high molecular weight poly(cyclohexene carbonate)(PCHC) and poly(cyclohexene oxide) respectively (Figure 4).[52] Complex **3**, $(Ph_2PhO)_2Zn(Et_2O)_2$, generated a high molecular weight PCHC (Mn = 38000 g/mol, PDI = 4.5) with 91 % carbonate linkages and TOF of 2.4 h^{-1} under 55 atm of CO_2 pressure and 80 °C (Figure 4, **3**). However, these catalytic systems exhibited poor control over molecular weight of polymers. The high polydispersity indices (PDI) of the produced polymers are probably due to aggregations of the active species. Following this, complex **4** obtained by the addition of 2, 6-dihalophenols to $Zn[N(SiMe_3)_2]_2$, it is a binuclear four- coordinated zinc phenoxides with coordinated THF and displays with moderate TOFs of 7.6 h^{-1} (Figure

R= Me (2), R = Ph (3)
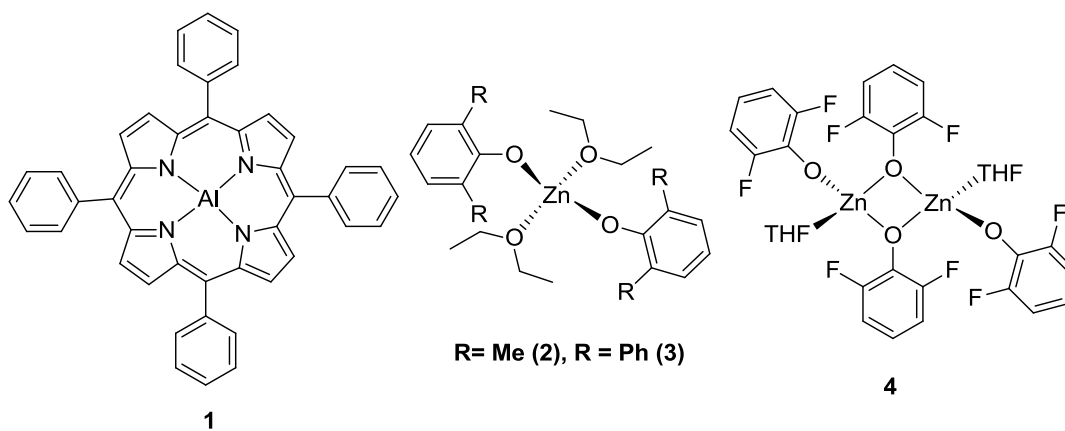
Figure 4. Homogeneous single-site catalysts for copolymerization of epoxide/CO_2 (**1**: porphyrin system, **2, 3,** and **4**: phenoxide systems)

4, **4**). Mechanistic studies confirmed that small groups (eg. Me) on phenyl groups easily facilitate the insertion of CO_2 into the Zn-OPh bond to yield methyl aryl carbonate intermediate without need of any additional coordination sites. Contrary to this, homopolymerization of epoxide required a binding site on the catalyst for the coordination of epoxide.[52]

Since this report, several examples of homogeneous catalysts have been reported for coupling of epoxides and CO_2; however, few metal-based catalysts were associated with great success. It is therefore, in the next sections a few interesting developments, catalysts centered with Cr, Co, and Zn metals, have been discussed.

1.3.2. Cobalt Catalysts for Epoxide–CO_2 Copolymerization

In 1979, Ikeda and co-workers used $Co(OAc)_2$ as a catalyst for copolymerization of PO and CO_2, yielding PPC with extremely low TOFs.[53] After this report, several cobalt
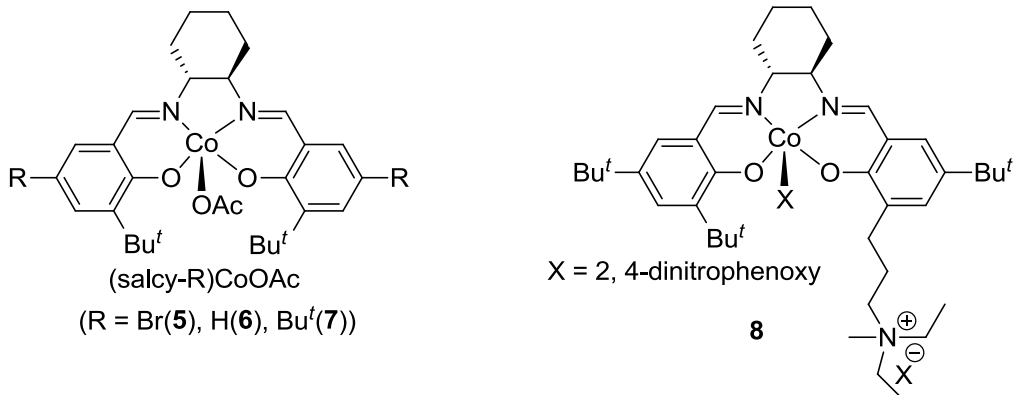
Figure 5. Cobalt salen complexes for epoxide and CO_2 copolymerization

complexes were explored. Recently, Coates and co-workers reported (salcy)CoOAc complexes without the combination of any co-catalysts for copolymerization of PO and CO_2 (Figure 5).[54] It was found that Co-salen based catalysts exhibited unprecedented selectivities for the generation of PPC without the formation of cyclic by-product propylene carbonate in measurable quantities. The resultant PPCs are highly alternated

with 95 % carbonate linkages at 25 °C and 55 atm of CO_2. Moreover, molecular weight distributions of the obtained polycarbonates are narrow and the polymerization process is immortal. In this case, pressure of the CO_2 was very crucial; at lower pressures, the catalyst was almost inactive. When enantiomerically pure (salcy-^{t}Bu)CoOAc (Figure 5, **7**) was employed for the copolymerization of (S)-PO and CO_2, it yielded isotactic (S)-PPC with highest reported selectivity of head-to-tail linkages (93%). The same complex gave a moderate selectivity (k $_{real}$ = 2.8) in the kinetic resolution of PO. Later on, Lu *et al* developed a binary Co-salen complex, chiral [(salcy)Co(III)X, X = -CH$_3$CO$_2$, -CCl$_3$CO$_2$, -OPh(NO$_2$)$_{x = 1,2,3}$] in conjunction with a co-catalyst quaternary ammonium salt. This complex was found to be an efficient catalyst for stereo and regio selective alternating copolymerization of CO_2 with epoxides under extremely mild reaction conditions.[55] Following this, Lu *et al* reported a Co(III)- salen complex where the salen ligand containing one quaternary ammonium salt on the third-position of one of the aromatic rings for alternating copolymerization of CHO and CO_2 to afford the corresponding highly alternating PCHC (Figure 5, **8**). Interestingly, this catalyst exhibited excellent activity and selectivity for PPC formation even at 120 °C and under very low pressure of 0.1 MPa.[56]

1.3.3. Chromium Catalysts for Epoxide–CO$_2$ Copolymerization

The first chromium complex employed for a copolymerization reaction came from the Holmes research group, who developed a fluorinated chromium porphyrin complex (Figure 6, **9**).[57] The catalyst with 4-dimethylaminopyridine (DMAP) as a co-catalyst showed high TOFs up to 173 h^{-1} for alternating copolymerization of CO_2 with CHO under harsh conditions (110 °C, supercritical (Sc) CO_2 at 222 atm). The fluorinated substituents on the porphyrin moiety gave better solubility for catalyst in supercritical CO_2.[57] Later on,

Darensbourg and Yarbrough reported a Cr-salen complex ((salcy-^{t}Bu)CrCl), which exhibited moderate activity (TOF = 32.2 h^{-1}) with the aid of a nucleophilic co-catalyst, N-methylimidazole (N-MeIm), for copolymerization of CHO and CO_2 without generating cyclic by-product (Figure 6, **10**). In the absence of co-catalyst, activity of the catalyst is predominately reduced to TOF = 10.4 h^{-1}.[58] The same catalyst was more selective toward propylene carbonate (PC) formation instead of PPC when it was used for copolymerization of PO and CHO at 80 °C. The activity of catalyst turned to PPC if the reaction temperature is reduced to 40 °C.[59]
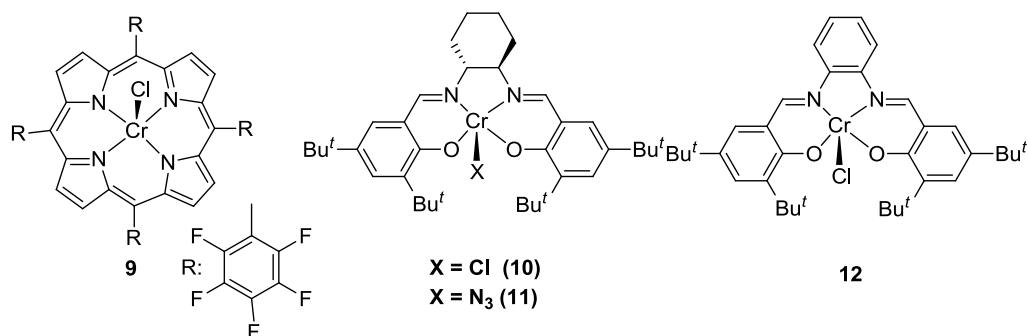
Figure 6. Chromium complexes for epoxide and CO_2 copolymerization

Subsequent studies on copolymerization of CO_2 with epoxides using (salcy-^{t}Bu)CrCl revealed that the formation of cyclic by-products such as CHC and PC required an energy barrier higher than the corresponding PCHC and PPC did.[60] Rieger *et al* studied copolymerization of PO and CO_2 using a slightly modified Cr- salen complex, (salph-^{t}Bu)CrCl and DMAP as co-catalyst, affording PPC with TOFs = 226 h^{-1} at 75 °C and 13 atm CO_2 (Figure 6, **12**).[61]The ratio of catalyst/co-catalyst can dramatically influence the formation of PPC and PC. For example, formation of PC is increased significantly if the concentration of co-catalyst is increased. After these results, a variety of co-catalysts have

been investigated with different combinations of ligand substitutions and initiating groups (Figure 7).[62,63,64,65,66] For instance, complex **18b** with PPN gave unprecedented TOFs of 1153 h^{-1} at 80 °C and 35 atm (Figure 6, **11**).[67]
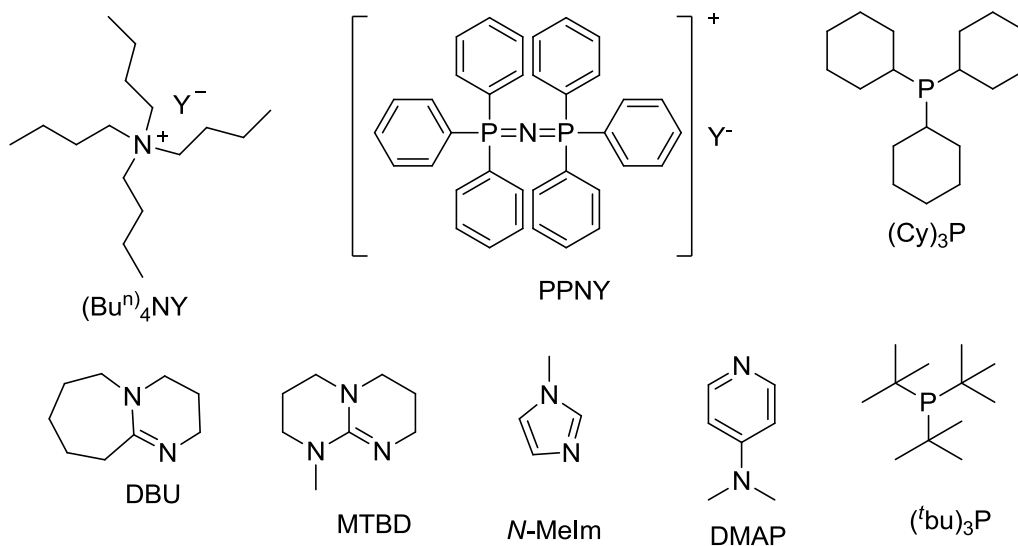
Y = I, Cl, Br, N$_3$, ClO$_4$, OBzF$_5$, OAc

Figure 7. Different co-catalysts for copolymerization of CO_2 and epoxides

1.3.4. Zinc Catalysts for Epoxide–CO_2 Copolymerization

A variety of zinc based catalysts have been studied for copolymerization of CO_2 and epoxides in the last 40 years. More attention shifted from heterogeneous catalysis to discrete, single-site, homogeneous catalysts as they gave unprecedented activities and selectivities for copolymerization of CO_2 and epoxide. Therefore, several zinc-based complexes have become work-horses for the catalysis of CO_2-epoxide coupling reactions. After the initial success with zinc phenoxides as viable initiators for copolymerization of epoxides with CO_2,[52] Darensbourg *et al* developed several zinc catalysts for the coupling of CO_2 and epoxides. Complex **13** was synthesized by the reaction of with 2, 6-disubstituted benzoic acids with Zn[N(SiMe$_3$)$_2$]$_2$ and the obtained complex was treated with

pyridine (Figure 8, **13**). Complex **13** was found to be an efficient initiator for copolymerization of CO_2 with CHO, yielding completely alternating PCHC (~100 % polycarbonate linkages) under mild reaction conditions.[68] Kim and co-workers reported zinc acetates ligated with pyridine alkoxides that (Figure 8, **14**) catalyze the copolymerization of CHO and CO_2, producing PCHC with only 63% of carbonate linkages (Mn of 9500 g/mol^{-1}, PDI of 2.4) and TOFs of 153 h^{-1}.[69]
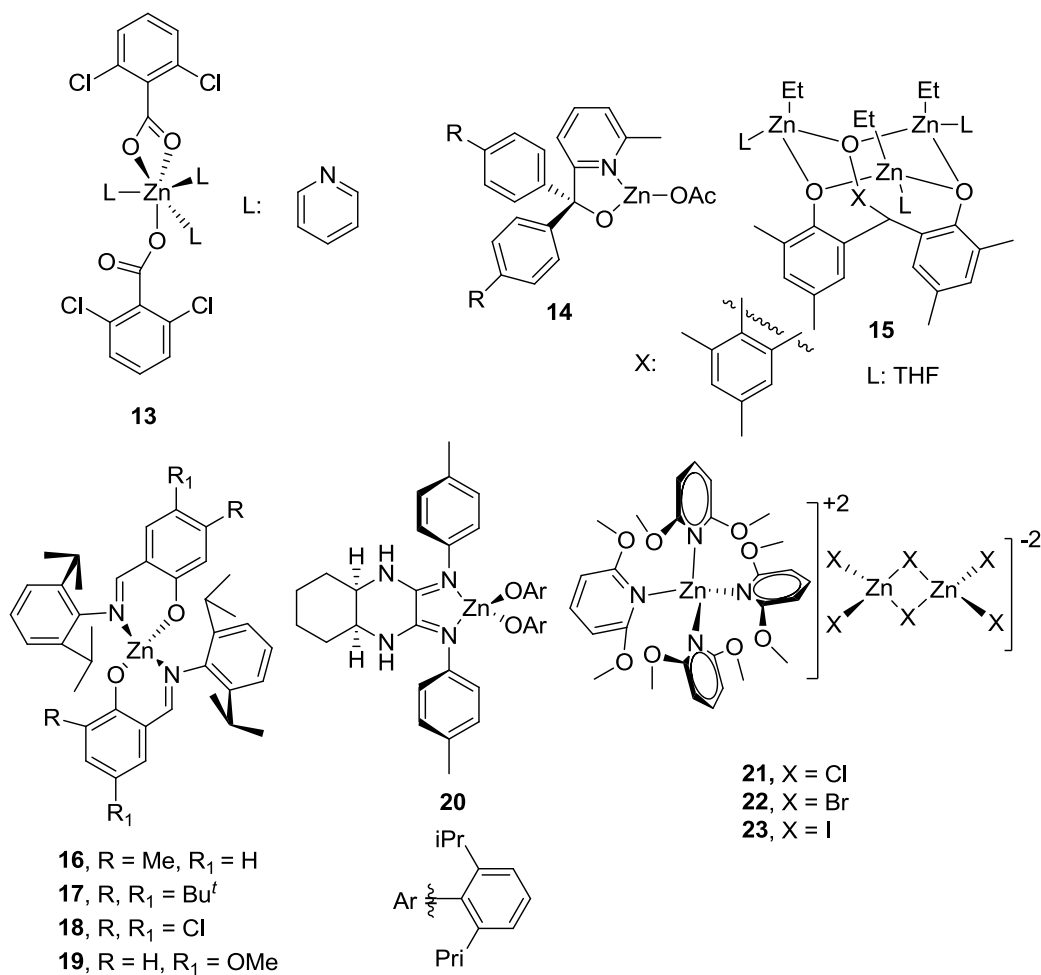
Figure 8. Various zinc complexes for copolymerization CO_2 and CHO

In a corresponding study, Dinger *et al* described a variety of phenoxide cluster compounds, synthesized from tris(3,5-dialkyl-2-hydroxyphenyl)methanes and $ZnEt_2$ that exhibited very low activity for the alternating copolymerization of CHO and CO_2 (Figure 8, **15**).[70]

In continuation of the above work, Darensbourg *et al* reported a series of bis(salicylaldiminato) zinc complexes, synthesized by treatment of salicylaldimine ligands with two equivalents of $Zn[N(SiMe_3)_2]_2$ in ethanol.[71] The polymerization activity of these zinc bis(salicyaldiminato) catalytic precursors was similar to the activities of the earlier reported zinc benzoxides. Subtle modifications in the R_1 and R_2 positions of the salicyaldimine ligand altered the polymerization behavior of the catalytic precursors (Figure 8, **16-19**). Later, Hampel *et al* synthesized number of quinoxaline-based zinc complexes that showed low activities (TOFs 4.9 h^{-1}) for coupling of CHO and CO_2, yielding PCHCs with broad polydispersities (PDI = 4.5) (Figure 8, **20**). It is believed that catalyst aggregations might lead to broad polydispersities of the resulting polycarbonates.[72] Later, Darensbourg *et al* illustrated that zinc adducts (Figure 8, **21-23**) were active for the hetero coupling of CHO of CO_2 and that the polymerization behavior of the catalysts is affected by the nature of halide ion. The fractional order (1.5) of the formation of PCHC reaction with respect to catalyst concentration suggested that both dimeric and monomeric complexes are involved in the copolymerization process.[73]

The major breakthrough was reported by Coates *et al* in 1998 for alternating copolymerization of CO_2 and epoxides. They investigated synthesis and applications of zinc based catalysts tailored with β-diketiminate ligands (BDI), where the steric and electronic factors can be easily tuned by varying the substitutents around the ligand frameworks to alter the catalytic activity.[74] This versatility in the ligand design is a useful tool in understanding mechanistic aspects of copolymerization process of CO_2/epoxides. The zinc(II) complex **24** has been synthesized by deprotanation of β-diketiminate ligand with n-butyllithium followed by a subsequent metathesis reaction with $Zn(OAc)_2$ (Figure

9, **24**). Complex **25** was obtained by treatment of BDI-H ligand with ZnEt$_2$ followed by MeOH (Figure 9, **25**)[74]. Complexes **24** and **25** exhibit very high and nearly identical activities (TOFs up to 494 h^{-1}) under mild reaction conditions (50°C, 100 psi of CO$_2$ pressure). The obtained polycarbonates are with high molecular weight and very narrow polydispersities (PDI= 1.07-1.17), moreover, the polymerization process is living.

Following this report, they investigated the required optimal complex geometry by varying the substitutions on the ligand framework and initiating groups ((BDI)ZnX, X= Cl, Br, Et, OMe, OAc, O^{i}Pr, N(SiMe$_3$)$_2$). It was found that the substitutions on ortho positions
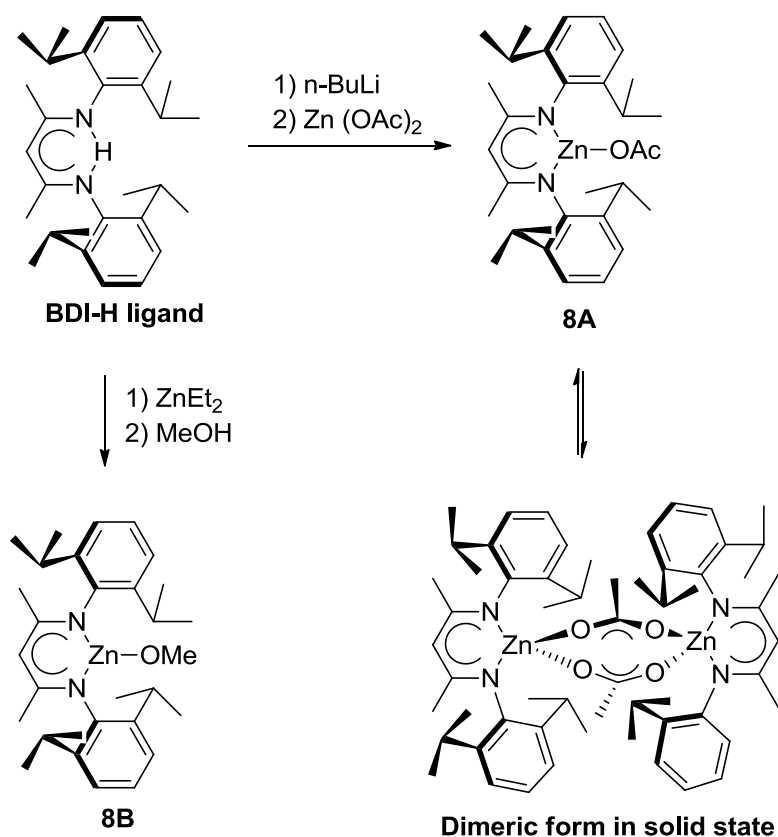
Figure 9. Zinc complexes for copolymerization of CO$_2$ and CHO

of the aniline group are very crucial. Comlplexes that incorporate isopropyl and ethyl groups (Figure 10, **27**, **28**) are very active, whereas substitution of methyl (Figure 10, **29**)

and n-propyl groups (Figure 10, **30**)   dramatically diminishes the polymerization activity of the zinc complexes.

From preliminary kinetic studies of the polymerization process, it is revealed that this catalytic polymerization reaction follows second order kinetics in terms of initiator concentration, which suggests that a bimetallic enchainment of the monomer is a major pathway. Therefore, it is believed that the complexes with methyl groups (which have a dimeric form in the solid state) are highly stable, do not possess enough steric hindrance that helps in equilibration of dimeric complexes into monomeric complexes, while complexes with n-propyl groups need a very high activation energy for bimetallic enchainment process. Replacement of methyl group with hydrogen on backbone of the complex prominently influenced the catalytic activity; activity of the complex is

X = OAc, OMe, ^{i}OPr, Cl, Br

catalyst	R$_1$	R$_2$	R$_3$	R$_4$	X
27	^{i}Pr	^{i}Pr	Me	H	OAc, OMe.O^{i}Pr
28	Et	Et	Me	H	OAc, OMe.O^{i}Pr
29	^{n}Pr	^{n}Pr	Me	H	OAc
30	Me	Me	Me	H	OAc
31	^{i}Pr	^{i}Pr	H	H	OMe
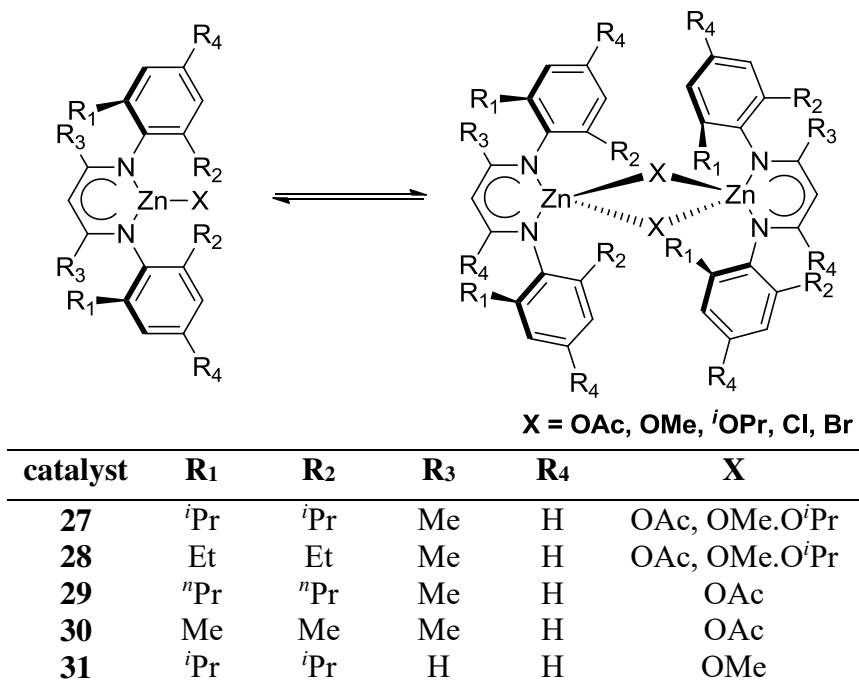
Figure 10. Synthesis of zinc complex of β-diketiminate ligands (BDI)

diminished significantly from 247 h^{-1} to 42 h^{-1} (Figure 10, **30**). Complexes with different initiating groups ((BDI-1)ZnX, where X = OAc, OMe, ^{i}OPr and N(SiMe$_3$)$_2$) have surprisingly similar polymerization behavior (Figure 11, **31–34**). All polymers have almost 95 % carbonate linkages in the polymeric backbone and controlled molecular weights distributions. It implies that all the complexes have same type of propagating species after

X: OAc (31), OMe (32), O^{i}Pr (33),
(N(SiMe$_3$)$_2$) (34), Et (35), Cl (36),
Br (37)

38
R$_1$ = Et, R$_2$ = ^{i}Pr
R$_3$ = H, R$_4$ = CF$_3$

39, X = OMe
R$_1$ = CN, R$_2$ = Me, R$_3$ = ^{i}Pr
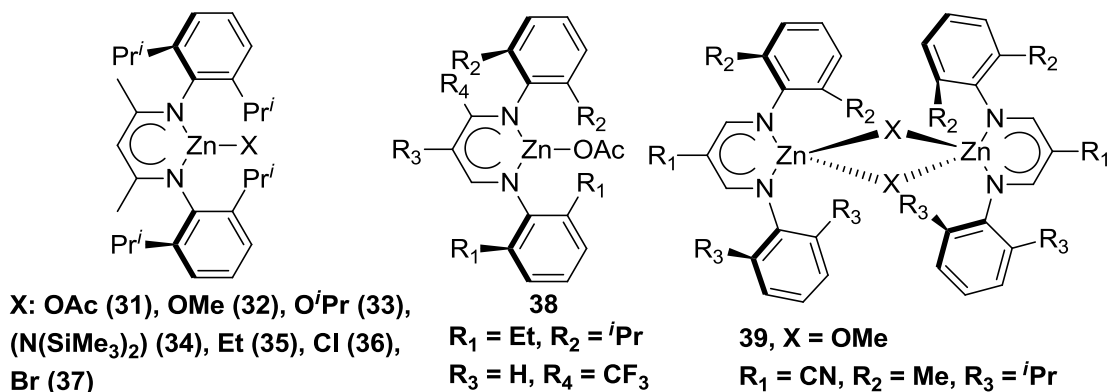
Figure 11. Versatile zinc complexes of BDI ligands

chain initiation step. The obtained polycarbonates are all atactic in nature, consisting of *trans*-cyclohexane linkages in the polymer main chain. It suggested that the back side attack of the epoxide in epoxide enchainment processes via a concerted fashion. Interestingly, complexes with initiating groups, Et, Cl, and Br, did not show polymerization activity (Figure 11, **35-37**). Polymerization activity can be dramatically influenced by subtle changes in electronic perturbation of (BDI)Zn complexes. Complex **38** is also highly active for PO and CO$_2$ copolymeriztion process, yielding PPC with 99 % carbonate linkages, with TOFs of 235 h^{-1} (Figure 11).[75] Catalyst **39**, with an electron-withdrawing cyano group exhibited remarkably high catalytic activity (TOFs: 2290 h^{-1}), however, the incorporated polycarbonate linkages (93%) are little low (Figure 11).[76] This high activity

might attribute to the more electron-deficient nature of the metal center, so that it would enhance the epoxide coordination.

1.3.5. Mechanism of Alternating Copolymerization of CO_2 and CHO

Coates and co-workers reported a comprehensive mechanistic study on copolymerization of CO_2 and epoxides.[77] The rate studies of copolymerization reactions indicate that the order of the reaction is 0, 1, and 1.0-1.8 in terms $[CO_2]$, [CHO], and [catalyst] respectively. It is believed that steric and electronic perturbations around the catalyst and temperature play a crucial role in determining the order of the reaction. From their investigation, authors concluded that bimetallic mechanism is more prominently operated, however, monometallic mechanism could be also accounted as a minor pathway (Figure 12, P : polymer chain).[77] The ratio of monomeric to dimeric active species will be increased with the rise of sterics and/or temperature; this leads to increase in the order of the reaction in initiator concentration.
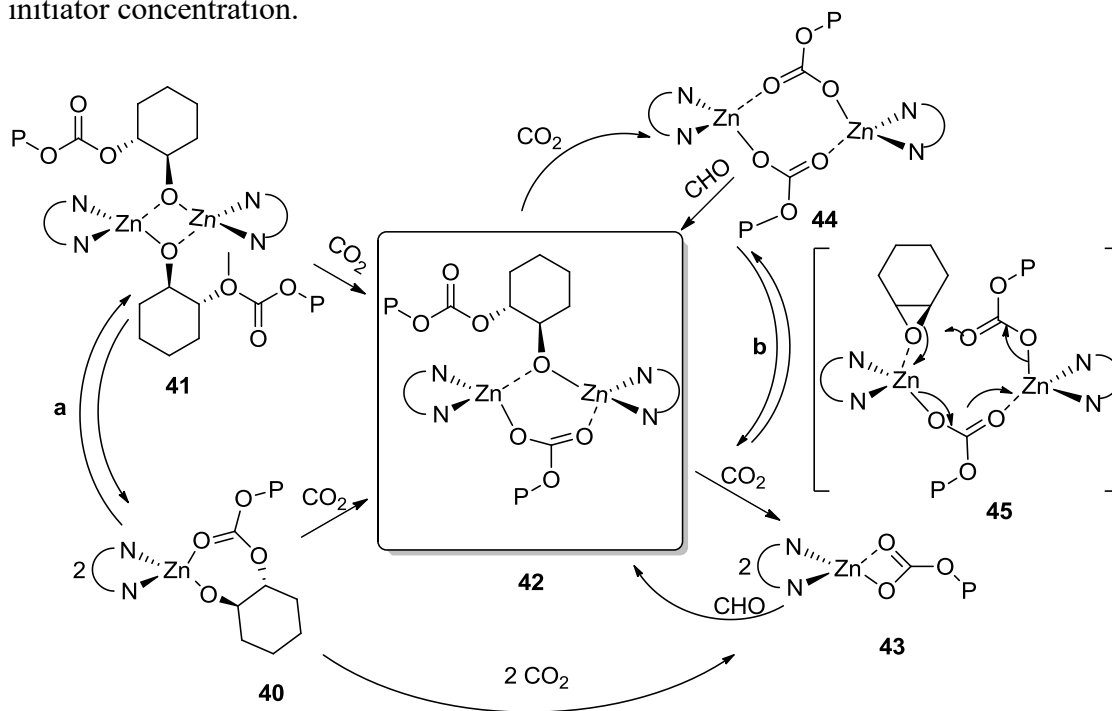
Figure 12. Mechanism of alternating copolymerization of CHO and CO_2[77]

The zinc alkoxide monomer (**40**) that is formed by insertion of CO_2 into Zn-OAc bond followed by CHO and its dimer (**41**) inserts CO_2 to yield either carbonate active species (**43**, **44**) or a dimeric species (**42**). This was the first step in the catalytic cycle. The formation of these active species depends on the steric and electronic factors of the BDI framework, propagating species, and temperature of the reaction. The dimeric active species (**44**), which have adequate steric hinderance to participate in a monomer/dimer equilibrium (Figure 12, route B), reacts with CHO to yield dimer **42**. From the analysis of the rate data, it is proposed that both **43** and **44** are acting as ground state species. The highly sterically hindered zinc complexes participate in the copolymerization process via a bimetallic transition state through both dimeric and monomeric ground states, where as less steric hindered zinc complexes proceed through only a dimeric ground state.[77] It is believed that, in the bimetallic transition state, one metal center coordinates the epoxide and the second metal center helps in attacking of the propagating carbonate species at the back side of the epoxide ring. Subsequently, the compound **42** reacts with CO_2 to complete one full catalytic cycle. This cycle is repeated to propagate the polymer chain.

1.4. Asymmetric Alternating Copolymerization of CO_2 and Epoxides

The thermal and mechanical properties of polymers, such as crystallization temperature, glass transition temperature, melting point, tensile strength, toughness, opacity, density, and strain at break are significantly reliant on microstructures of the polymers. There are several strategies to alter the physical properties of the polymers; coupling of CO_2 with various commercially and naturally available epoxides, stereo selective copolymerization, preparation of block polymers, and cross-linking polymerization methods. Especially, there has been a considerable interest in stero-regio

selective copolymerization of epoxides with CO_2 as this route can potentially change microstructures of the PCHCs and be a viable route to prepare the chiral enriched building blocks. In asymmetric copolymerization of CO_2 and epoxides, the most commonly used monomers are cyclohexene oxide and propylene oxide. The asymmetric copolymerization of CO_2 with CHO produces optically active polycarbonates, consisting with either (*R, R*) or (*S, S*)-trans 1,2-cyclohexaylene units, via inversion of the one of chiral centers of cyclohexane ring.[78]

In 1999, Nozaki *et al* first reported asymmetric alternating copolymerization of CO_2 and CHO using a chiral catalyst, 1:1 mixture of $ZnEt_2$ and (*S*)-α,α-diphenylpyrrolidine-2-ylmethanol (DPM)H, at 40 °C and 30 atm of CO_2 (Figure 13, **46**).[78] The polymer was obtained with 100 % carbonate linkages, molecular weight (*M*n) of 8400 g/mol, PDI of 2.2, and a T_g of 117 °C and the resultant PCHC is isotactic in nature. The obtained optical active polycarbonates were hydrolyzed by aq. NaOH, producing *trans*-cyclohexane-1,2-diol with 73% enantiomeric excess. The formation of chiral polycarbonate chain having trans-cyclohexane-1,2-diol confirmed that the CHO ring opening process proceeds via a S_N2–type mechanism (inversion configuration).
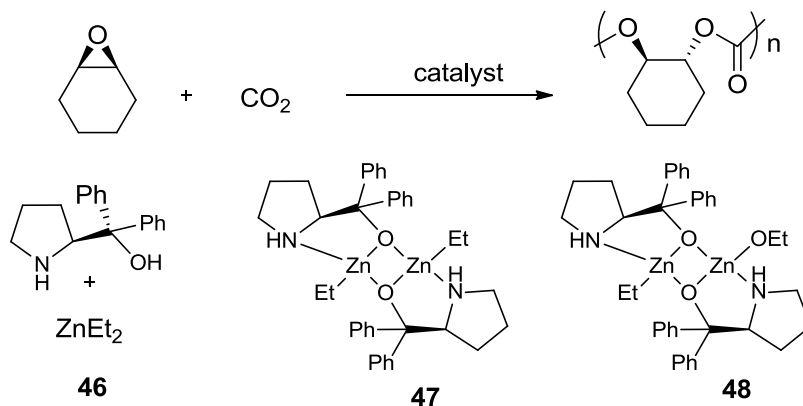
Figure 13. Chiral catalysts for asymmetric copolymerization of CO_2 and CHO

In their seminal work on asymmetric copolymerization of CO_2 and CHO, Nozaki *et al* developed a bimetallic zinc catalyst, synthesized by a reaction between $ZnEt_2$ and (DPM)H, for asymmetric coupling of CO_2 and CHO (Figure 13, **47**).[79] The structure of the dimeric zinc complex was identified by X-ray diffraction studies.

Each zinc center in the dimeric complex **47**, is coordinated by two bridging oxygen atoms, one ethyl group, and a pyrrolidine ring, arranged in a distorted tetrahedral geometry.
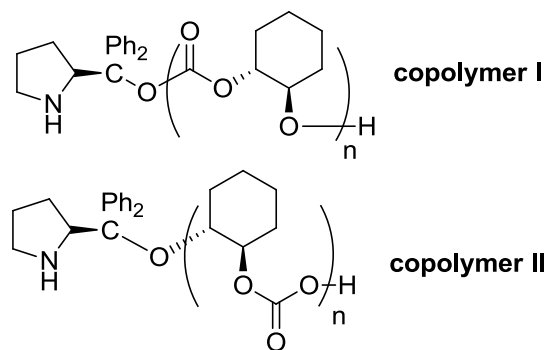
Figure 14. Two different copolymers with same end groups
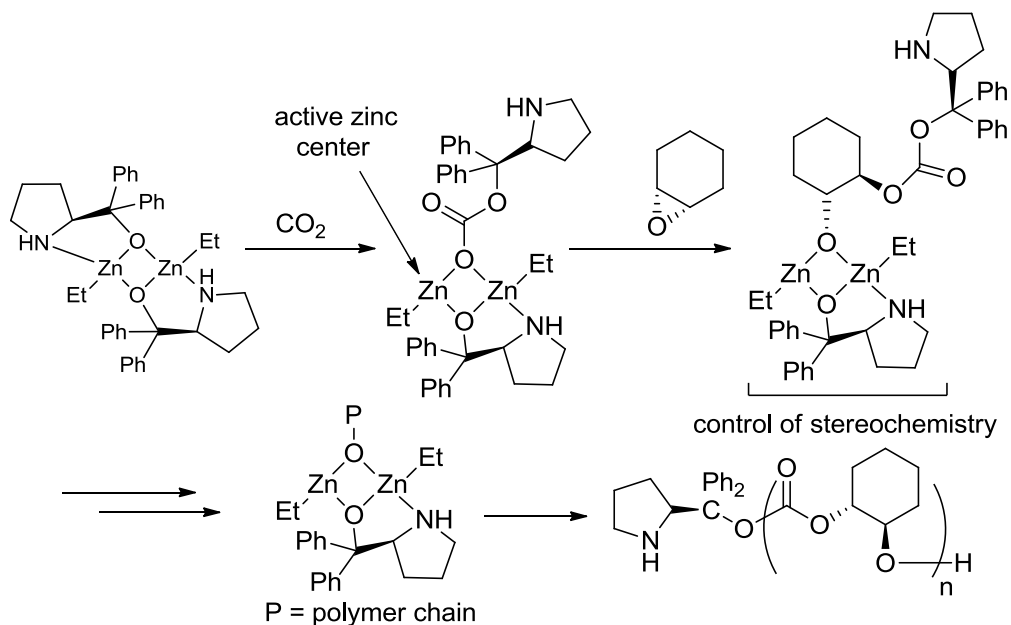
Figure 15. Plausible mechanism for asymmetric copolymerization of CO_2-CHO

The asymmetric coupling of CO_2 and CHO with complex **47** gave isotactic PCHC with lower enantiomeric excess (ee) of 49% while coupling with complex **48** stereoselectivity was improved up to 88 % ee (Figure 13, **48**). End-group determination by MALDI-TOF mass spectrometry gave useful clues about the copolymerization mechanism. The mass spectrum of PCHC appeared with two different series of polymers with same end group (Figure 14).[79] Based on end-group analysis and dilution studies, they proposed the above plausible mechanism (Figure 15).

In 2000, Coates and colleagues reported a series of well-defined, C_1-symmetric, chiral imine-oxazoline (IOX) ligated zinc bis(trimethylsilyl)amido complexes for the stereoselective, alternating copolymerization of CHO and CO_2.[80] By altering the substituents around the ligand framework, the optimized catalyst exhibited highest activity and stereoselectivity (Figure 16, **49**). X-ray diffraction studies revealed that complex **49** is a mononuclear, three-coordinate, and distorted trigonal in geometry. The aryl group is perpendicular to the IOX-zinc chelate ring and tert-butyl group is in a staggered conformation. It is believed that the high steric hindrance around the complex **49** precludes dimerization and solvent coordination with metal center. The catalyst **49** produced a chiral PCHC with 100% carbonate linkages, contained 88% *RR*-units in the main chain, with molecular weight of 14700 g mol^{-1}, PDI of 1.35, and T_g and T_m of respectively 120°C and 220°C. Similar to zinc complexes of β-diketiminate ligands for non-asymmetric copolymerization, the less bulky substitutents at the *ortho* position of the aryl group dramatically diminished the both activity and selectivity. The electron withdrawing group (CF_3) on the ligand backbone significantly increased its activity, but the selectivity is slightly compromised. Comparison of both experimental and theoretical intensities

(Bernoulli statistics) predicted that enantiomorphic-site control mechanism is operating in the copolymerization process.

49
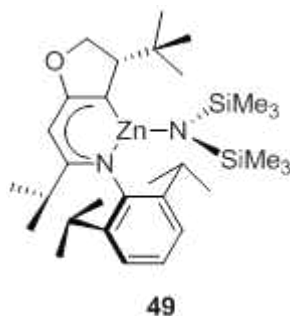
Figure 16. IOX ligand framework for asymmetric copolymerization

Recently, Coates and co-workers developed a series of new complexes (salen)CoX (salen = *N,N*-bis(salicylidene)-1,2-diaminoalkane; X = Cl, Br, I, OAc, OBzF$_5$) complexes as active catalysts for the copolymerization of cyclohexene oxide and CO_2 (Figure 17).[81] The majority of the complexes were synthesized by a metallation of salen-type ligands that were obtained by a condensation reaction of an aldehyde and a Schiff-base, with cobalt(II) acetate tetrahydrate and followed by oxidation reactions. They investigated the influence of axial ligand, backbone of the ligand, phenolate substituents, and CO_2 pressure on the copolymerization process. Although variation of the axial ligand had a small influence on the tacticity of the polymers, syndiotacticity of the obtained PCHC increased exceptionally when iodide was used as an initiating group (Figure 17, **50**). The highly sterically hindered complex **50,** (*rac*-(salen)CoBr), generated PCHC with unprecedented syndiotacticity of 81 % while enantiopure complex **52,** ((*R, R*)-(salen)CoBr) gave PCHC with 61 % syndiotacticity. The substitutents on the phenyl ring are also vital in achieving the desired stereoselectivity of the polymer main chain. Two tert-butyl groups on the phenyl group are

optimal to ensure the high selectivities. The structure of the catalyst dramatically influences the stereochemistry of the resultant PCHC (Figure 17).

According to previous assignments, all *m*-centered tetrads ([*mmm*], [*mmr*] and [*rmr*]) are correlated to a single resonance at 153.7 ppm and the *r*-centered tetrads ([*rrr*],

(salen)CoX
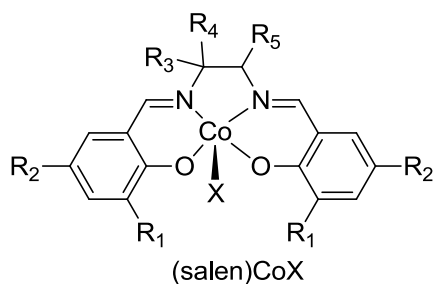
X = Cl, Br, I, OAc, OBzF$_5$

catalyst	R$_1$	R$_2$	R$_3$	R$_4$	R$_5$	X
50	Bu^t	Bu^t	H	Me	H	I
51	Bu^t	Bu^t	Me	Me	H	Br
52	Bu^t	Bu^t	Ph	H	trans-Ph	Br
53	Bu^t	Bu^t	H	Me	H	OBzF$_5$
54	Bu^t	Bu^t	H	trans-(CH$_2$)$_4$		OBzF$_5$
55	Me	H	H	Me	H	OBzF$_5$
56	cumyl	cumyl	H	trans-(CH$_2$)$_4$		Br
57	Bu^t	Bu^t	H	trans-(CH$_2$)$_4$		OAc
58	Bu^t	Bu^t	H	trans-(CH$_2$)$_4$		2,4,6-trinitro phenoxy
59	Bu^t	Bu^t	H	trans-(CH$_2$)$_4$		Br

Figure 17. A series of (salen)CoX complexes

[*rrm*], [*mrm*]) are correlated to a series of small peaks in the range of 153.3–153.1 ppm of the ^{13}C NMR spectrum of the poly(cyclohexne carbonate). In the case of isotactic PCHC, *m*-centered tetrads ([*mmm*], [*mmr*], and [*rmr*]) appeared more prominently whilst *r*-centered tetrads have a minor contribution. This is vice-versa in the case of syndiotactic PCHC. The common stereo-errors in poly(cyclohexene carbonate) main chain are caused by two different types of controlling mechanisms (Figure 18 and Figure 19). The first one is chain end control mechanism, where the stereochemistry of incoming monomer is controlled by the chirality of the chain-end. The second mechanism is enantiomorphic site

control; stereo regulation is controlled by the chirality of the catalyst. The obtained PCHC with catalyst **53**, (*rac*-(salen)CoOBzF$_5$) has ^{13}C NMR spectrum with four distinct resonances at 152.94, 153.06, 153.12 and 153.70 ppm. The up-field resonances at 152.94, 153.06, and 153.12 ppm correspond to *r*-centered resonances and the peak at 153.70 ppm
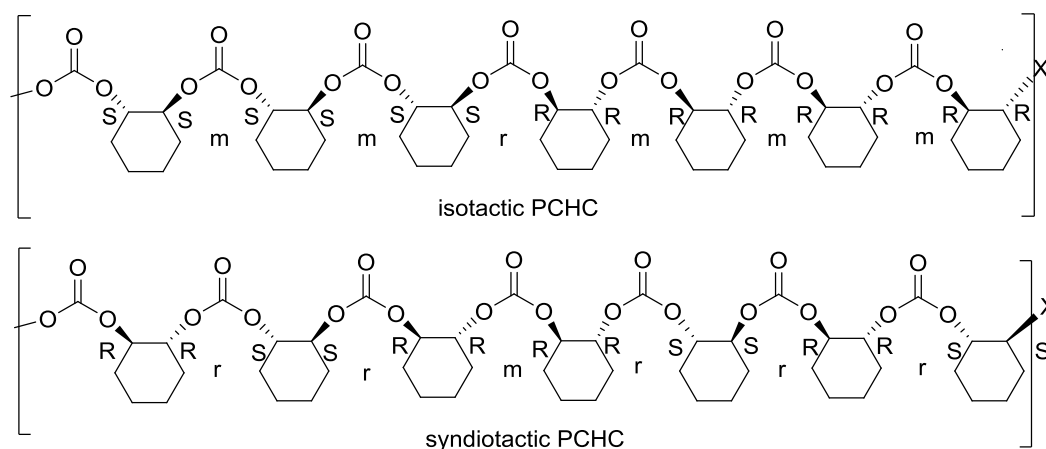
Figure 18. Common stereoerrors are caused by chain end control mechanism
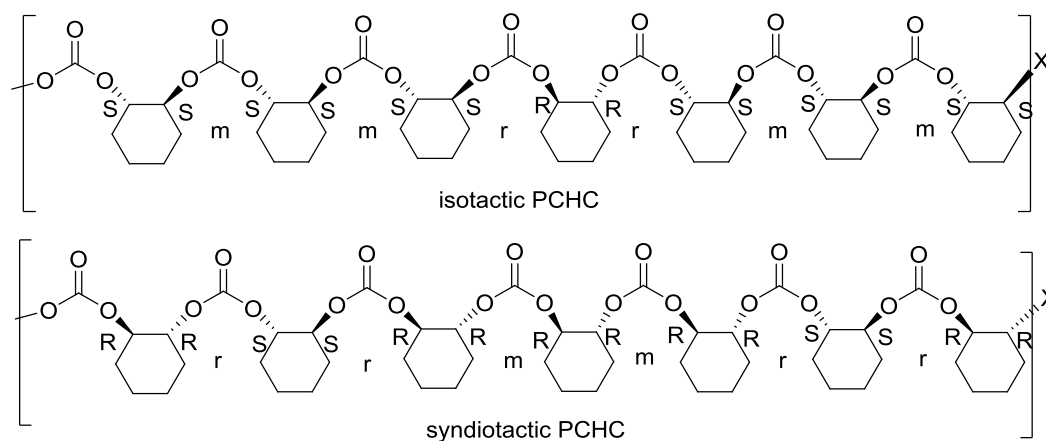
Figure 19. Stereoerrors are caused by enantiomorphic site control mechanism

correlated to *m*-centered resonances (Figure 20, **a**). Catalyst **54** ((*R,R*)-(salen)CoOBzF$_5$) and catalyst **55** (*rac*-(salen)CoOBzF$_5$) generated less syndiotactic PCHC (Figure 20, **b** and **c**) while catalyst **51** ((*R,R*)-(salen)CoBr) produced highly isotactic PCHC (Figure 20, **d**).
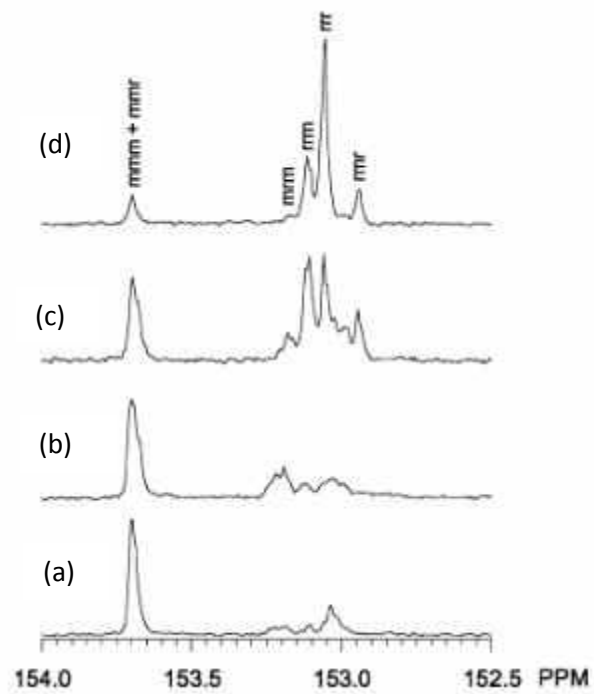
Figure 20. Carbonyl region of the poly(cyclohexene carbonate) in ^{13}C NMR spectrum
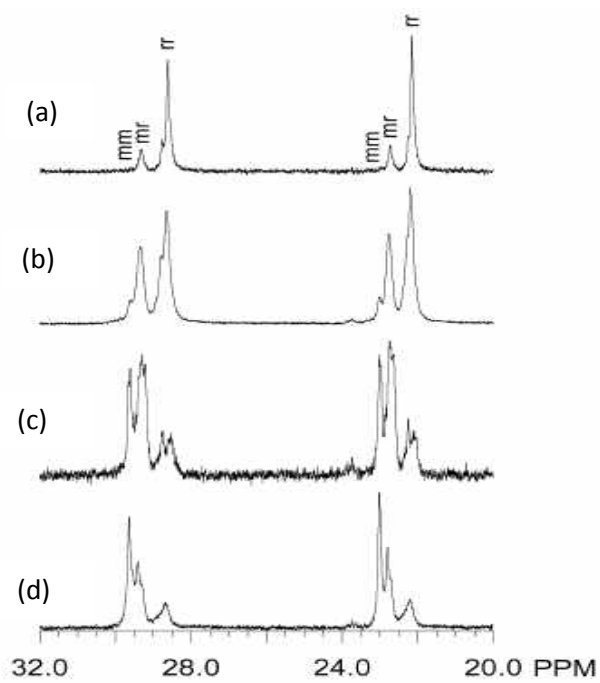
Figure 21. Methylene region of the poly(cyclohexene carbonate) in ^{13}C NMR spectrum

Along with the distinctive resonances of carbonyl groups of the polymer, the stereochemical information of the methylene carbons of the PCHC can be also studied by ^{13}C NMR spectroscopy. For syndiotactic PCHC, two series of two adjacent resonances ([*rr*] and [*mr*]) are found, assigned to the nonequivalent methylene carbons of the syndiotactic PCHC backbone (Figure 21, **a**). It was found that the intensity of [*rr*] triads is varied relatively to the intensity of syndiotacticity. In the case of less syndiotactic PCHC, the intensity of [*rr*] triads is low rather than the intensity of the [*mr*] triad resonances and additional two downfield [*mm*] triads are observed (Figure 21, **b** and **c**). For highly isotactic PCHC, the intensity of [*mm*] triad resonance is higher than the intensity of residual triads (Figure 21, **d**). More recently, Lu and co-workers reported the synthesis of highly isotactic PCHCs from desymetrization of *meso*-cyclohexene oxide using chiral salen Co(III) complexes in combination with bis(triphenylphosphine)-iminium chloride (PPNCl) as a co-catalyst (Figure 22, **60**).[82]

60
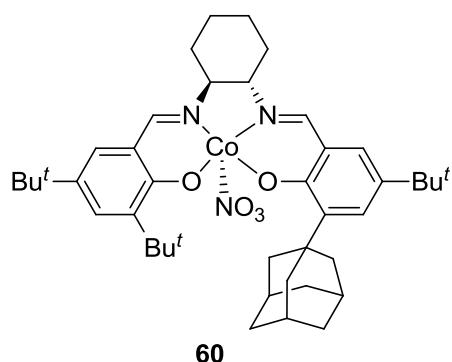
Figure 22. (Salen)Co(NO_3) complex for asymmetric copolymerization of CO_2 and CHO

The combination of enantiopure complex (*S,S*)-salenCo(III)(NO_3) and co-catalyst (PPNCl) significantly improved the enantioselectivity of PCHC up to 98:2 of *RR*:*SS,* in the presence of a chiral induction agent, (*S*)-2-methyltetrahydrofuran.

Significant efforts have also been carried out for the stereo-and regio selective copolymerization of CO_2 with propylene oxide (PO). The typical microstructures of the poly(propylene carbonate) are shown below (Figure **23**). Coates and coworkers reported that zinc (BDI) complex **38** for controlled stereo-and regioselective copolymerization of PO and CO_2, yielding PPC with poor selectivity (HH, TT, and HT in the ratio 23:23:54).[75] Later on, Qin *et al* used chiral salen cobalt complex **57** ([(*R,R*)-(salen)CoOAc]), for alternating copolymerization CO_2 and *rac*-PO to generate PPC with 80% head to tail (HT) linkages (Figure 17).[83] The same catalyst **57** showed highest activity for copolymerization of (*S*)-PO and CO_2, which produced highly isotactic PPC with 93 % of head-to-tail (HT) content. Addition of co-catalysts such as quaternary ammonium salts to the [(*R,R*)-(salen)CoX] complexes further enhances head to tail linkages of PPC under mild conditions.[84] Further, Lu *et al* showed that coupling of CO_2 and *rac*-PO catalyzed by combination of ([(*R,R*)-(salen)CoX]) **58** and cocatalyst [PPN]Cl, produced PPC with 94%
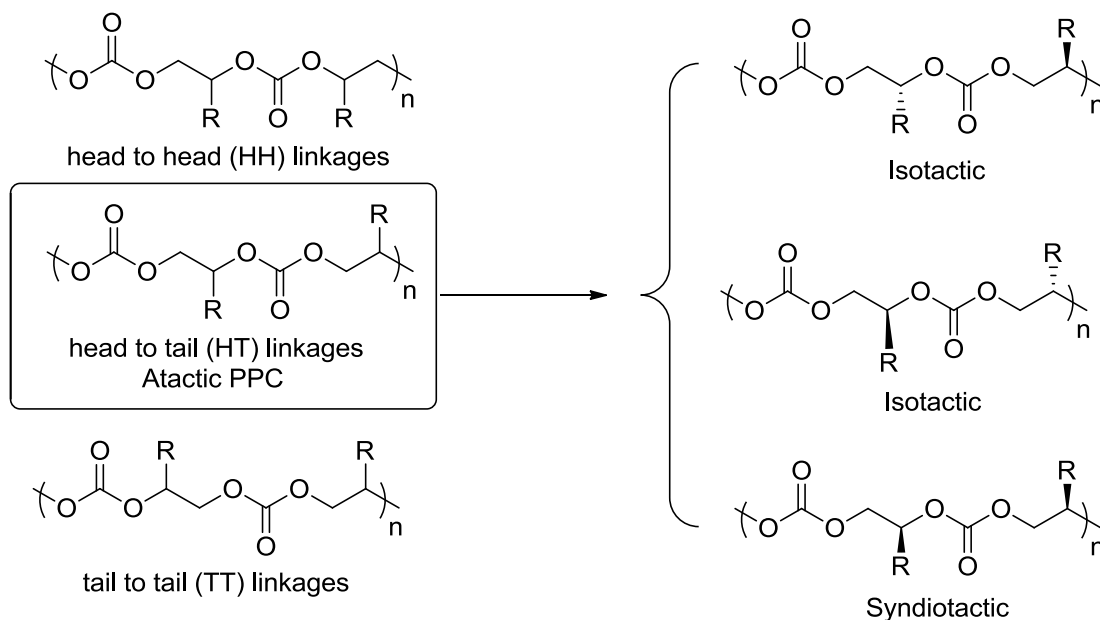
Figure 23. Microstructures of the PPC

head to tail linkages (Figure 17).[84] Stereochemistry of the catalyst, initiating group, and co-catalyst have remarkable influence on the microstructures of the PPC. Catalyst **54** with co-catalyst [PPN]Cl generated highly ordered isotactic PPC with an unprecedented activity of 620 h^{-1}. Interestingly, combination of catalyst **59** and [PPN]Cl generated highly ordered PPC for copolymerization of (*S*)-PO/CO_2 while the same catalyst combination gave a random polymer in the case of (*R*)-PO/CO_2 (Figure 17).[85]

1.5. Poly(lactide)$_s$

Biodegradable and biocompatible polymers, generated from renewable feedstock, have received much scientific attention due to depletion in crude oil based resources, global warming, and environmental awareness.[86] The production of polymers from non-petroleum resources, such as corn, sugar beets, and other biomass feedstock would thus help to reduce our dependence on consumption of nonrenewable resources, of which approximately 150 million tons are consumed annually as raw material for the production of synthetic plastics alone.[87] Poly(lactide) (PLA), a polymer of a cyclic diester of lactic acid, has become an attractive alternative to conventional polymers, with many potential applications ranging from bulk commodity materials to bio-medicinal products such as fibers, staples, sutures, drug delivery agents, and artificial tissue matrices.[88,89,90,91] In addition to the unique physical properties of PLA-based polymeric materials, they are also biocompatible, readily biodegradable, bioresorbable, and easily recycled. PLA is becoming increasingly inexpensive polymeric material due to rapid technological advancements and at the same time rise in the price of the corresponding petrochemical feedstocks. Recently, a joint venture, opened by Natureworks LLC, Cargill, and Teijen Limited, produced ~300 million lb of PLA anuually with a trade name Ingeo^{TM}, marketing the first commodity PLA polymer that is derived from corn instead of fossil fuels.[92]

The synthesis of PLA can be achieved *via* either polycondensation of lactic acid or chain growth polymerization, i.e. ring opening polymerization (ROP) of lactide. In

comparison to polycondensation reactions, ROP of lactides offers a great control over molecular weight, narrow polydispersities, and high levels of end-group fidelity of the resulting polymers.[93] Depending on the initiator, three different major mechanisms have been proposed for the ROP of lactides, including cationic, anionic, and coordination-insertion mechanisms.[94,95,96] The main driving force of ring-opening polymerization reactions is relief of the ring strain of cyclic ester monomers.

1.5.1. Cationic Ring-Opening Polymerization

Cationic polymerization mechanism involves the formation of cationic active initiating species; they later attack the lactide monomer. The resulting species, subsequently, are attacked by another monomer. The ring opening process proceeds *via* S_N2-type pathway (Figure 24). The cationic ring –opening polymerization is difficult to control and often yield only low molecular weight poly(lactides).[94]
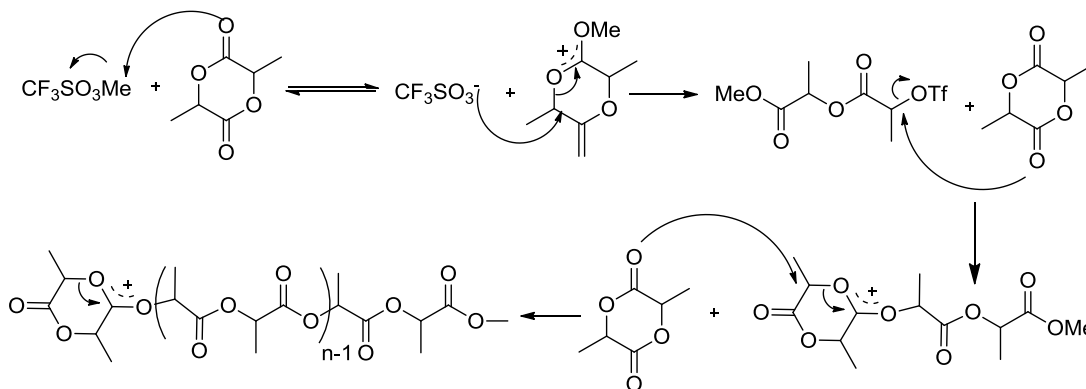
Figure 24. Mechanism of cationic ring-opening polymerization of ROP of lactides

1.5.2. Anionic Ring-Opening Polymerization

In anionic ring-opening polymerization, a nucleophile attacks either carbonyl carbon or carbon atom adjacent to the acyl-oxygen generating ring opened polymer. The major drawback in this mechanism is back-biting reactions that lead to formation of oligomers.

Although low-molecular weight polymers are commonly found products in this route, high molecular weight of the polymer can also be obtained using polar solvents (Figure 25).[95]
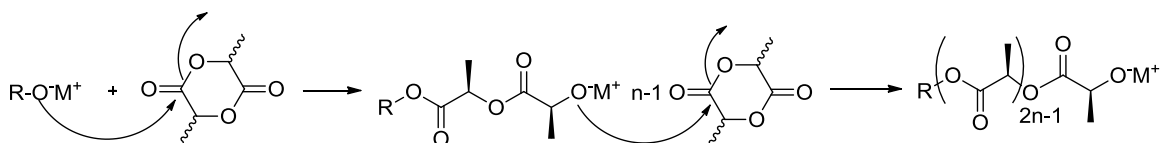
Figure 25. Mechanism of anionic ring-opening polymerization of ROP of lactides

1.5.3. Coordination-Insertion Ring-Opening Polymerization

The ROP of lactides, catalyzed by organo-metallic catalysts, is usually achieved through a coordination-insertion mechanism. Coordination-insertion ROP involves an insertion of the monomer into the metal-oxygen bond of the initiator or coordination of the lactide monomer to the metal center through its carbonyl oxygen. This step is crucial in controlling the stereoselectivity of the system (Figure 26).[96]
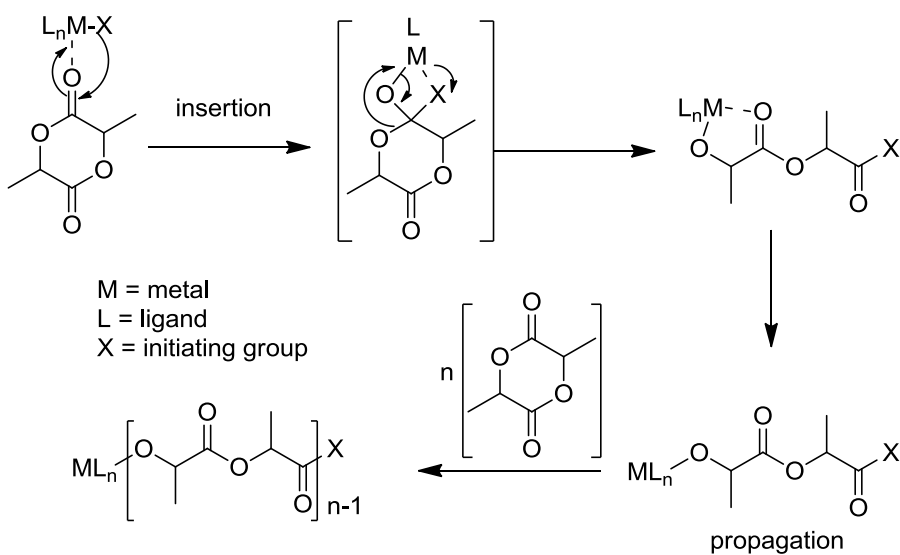
Figure 26. Co-ordination and insertion mechanism of ROP of lactides

Further, attack of acyl oxygen on the metal center and subsequent ring-opening of lactide monomer result in the formation of a new ring opened metal alkoxide species. These species are stabilized by coordination of carbonyl group that is in close proximity to the metal center as a lactate.
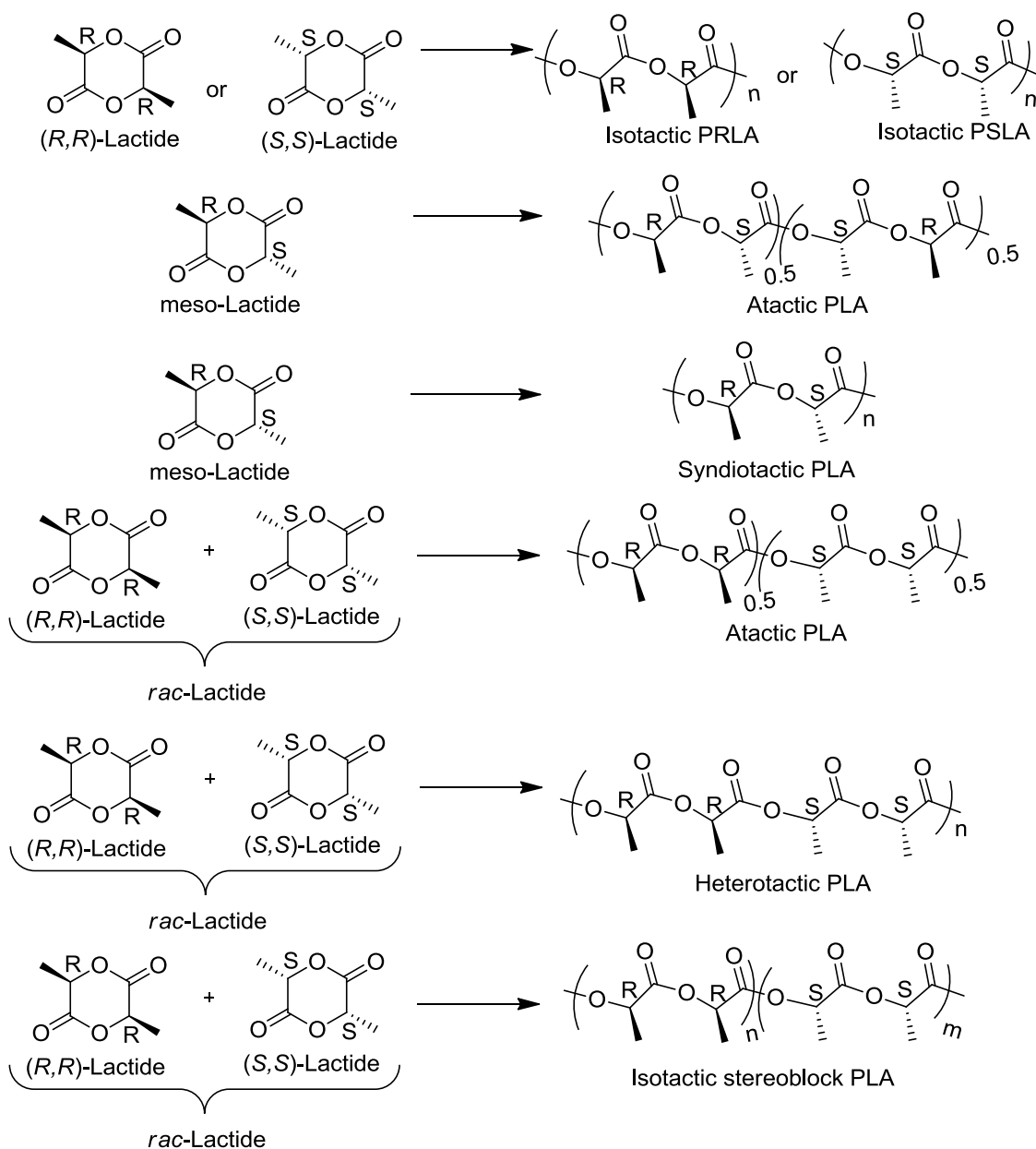
Figure 27. PLA microstructures derived from the stereocontrolled ROP of lactide

Tacticity or microstructures of the PLA can greatly influence the physical properties of the polymers. For instance, heterotactic PLA is crystalline, whereas atactic PLA is amorphous in nature. Therefore, there is a considerable interest in studying the stereochemistry of PLA. The stereochemical outcome of the polymer chain will be governed by two types of mechanisms, i.e. chain end growth and enantiomorphic site controls. In enantiomorphic site control mechanism, chirality of the propagating polymer chain depends on catalyst that determines the chirality of the next incoming monomer. In chain end control mechanism, chain end of the polymer chain governs the chirality of the next inserting monomer.[93]

The two chiral centers on a lactide monomer generate three different types of lactides; D-lactide (RR-configurations), L-lactide (SS-configurations), and *meso*-lactide (RS-configurations). Ring opening polymerization (ROP) of an enantiopure lactide either D- or L-lactide, which requires no polymerization stereocontrol, results in a pure isotactic polymer. In isotactic PLA, all stereocenters are aligned along the same side of the polymer backbone (Figure 27). On the other hand, in stereoselective ROP of either *meso*-lactide or *rac*-lactide, a plethora of ordered polymeric microstructures are generated. The stereoselective ROP of *meso*-lactide can lead to either syndiotactic PLA in which S and R stereocentres are perfectly alternated (SRSRSR) or heterotactic PLA in which the two stereocentres are doubly alternated (SSRRSSRR).[97] In the case of ROP of *rac*-lactides, three different types of stereoisomers are formed; heterotactic PLA that involved successive insertion of D- and L-lactide enantiomer units, isotactic stereo diblock isomer that is formed by the combination of two enantiopure poly(D-lactide) and poly(L-lactide) chains, and atactic polymer, produced by a random displacement of D- and L-lactide

enantiomer units. The degree of stereoselectivity, insertion errors, and chain exchange steps will impact the polymeric microstructures.[98]
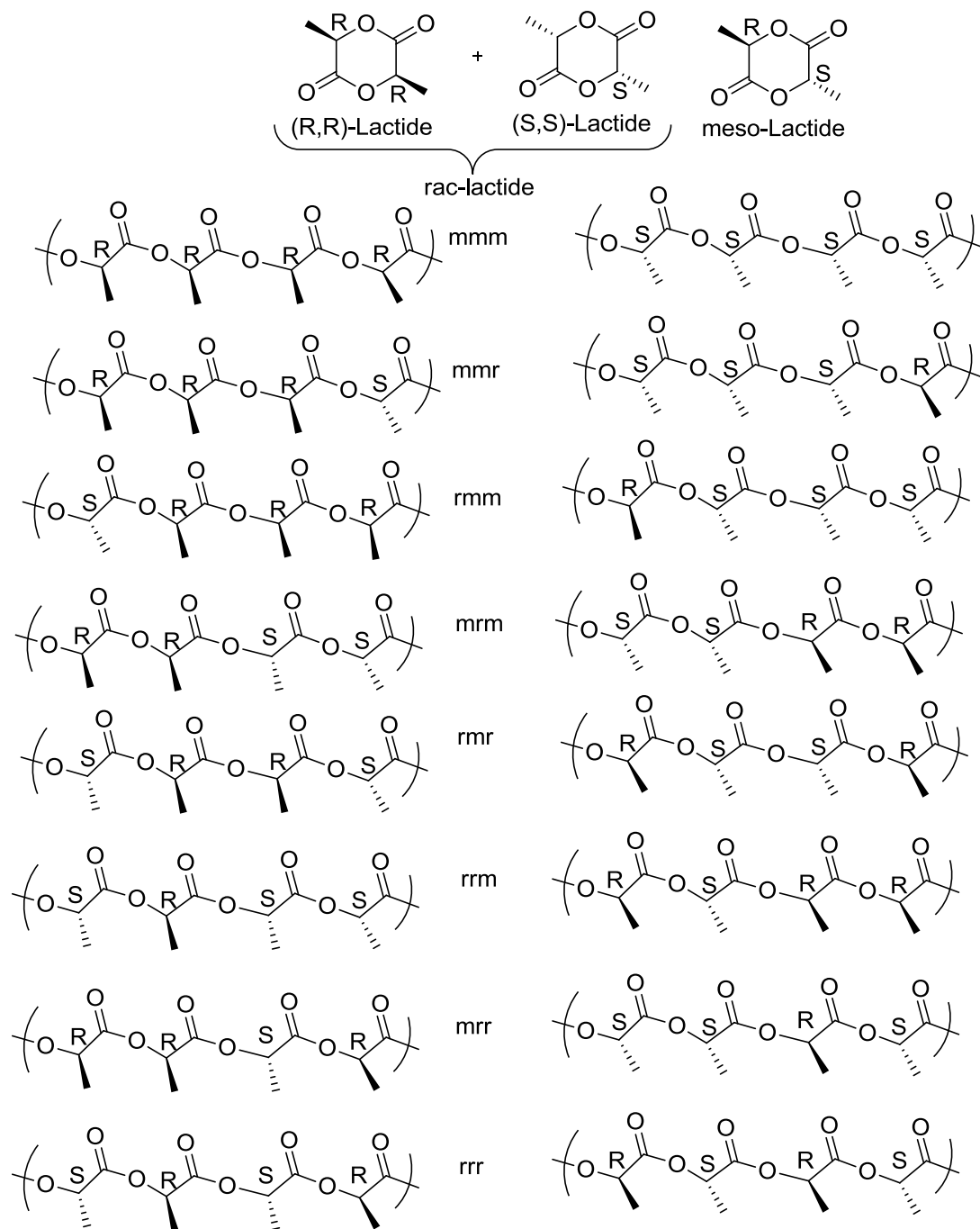
Figure 28. Observable tetrads of PLA by homonuclear decoupled ^{1}H NMR

According to Bovey formulations, 'm' or 'i' describes meso (adjacent stereocenters have the same chirality) and 'r'or's' describes racemic (adjacent stereocenters have differing in chirality) relationship between two stereocenters in a lactide monomer unit. At triad level, ROP of either racemic or meso-lactide generates two tetrads; *rm* and *mr*. Even though triads, pentads, and hexads are identified, they are often suffer with insufficient resolution, overlap of formed stereosequences or chemical shifts. In ROP of lactides, tetrad level stereosequences are the most commonly found and well resolved sequences.[98,99,100,101,102] The possible tetrad stereosequences are illustrated in Figure 28.[103]

As per previous assignments and Bernoulli enantiomorphic site control statistics, five tetrad sequences are the most commonly observed stereoerrors in PLA main chain.[104,105] The relative proportion of formation of tetrad sequences (degree of stereoselectivity) depends on the efficiency of the catalyst and the degree of control of insertion of racemic (*r*-diad) and meso (*m*-diad) sequences in the polymer backbone. The degree of stereoselectivity can be expressed as the probability of forming of either racemic diad (syndiotactic diad, P_r) or meso diad (isotactic, P_m) respectively. $P_r = 1.00$ indicates heterotactic in the case of ROP of *rac*-lactide and syndiotactic in the case of ROP of *meso*-lactide. $P_m = 1.00$ describes the isotactic polymers in the case of ROP of *rac*-lactide and heterotactic PLA in the case of ROP of *meso*-lactide. If $P_r = P_m = 0.5$, this means atactic polymer in ROP of both *rac* and *meso* lactides (Figure 26).[104] Many metal complexes have been extensively investigated for stereoselective ring opening polymerization of *rac*-lactides.

1.6. Poly(ester)s

To overcome the issues with conventional polymers, spectacular improvements have been made in synthesis of biodegradable and environmentally adaptable polymers using renewable resources during the last three decades. [106] Among the different types of polymers explored, polyesters constitute an important class of polymers as they are biodegradable and biocompatible.[107,108] Especially, aliphatic polyesters among the most commonly used biodegradable polymers in various medical applications,[109] such as drug delivery systems,[107] artificial tissues,[108] and commodity materials.[110] In general, polyesters are synthesized by polycondensation of diols and diacids or by ring-opening polymerization (ROP) of cyclic esters (Figure 29). The former route needs drastic conditions to remove water and it is highly energy intensive. In addition, highly accurate stoichiometries of monomers are essential in order to get high and controlled molecular weight polymers. In later route, the availability of cyclic ester monomers is limited to get the widespread polymer architectures.[111]
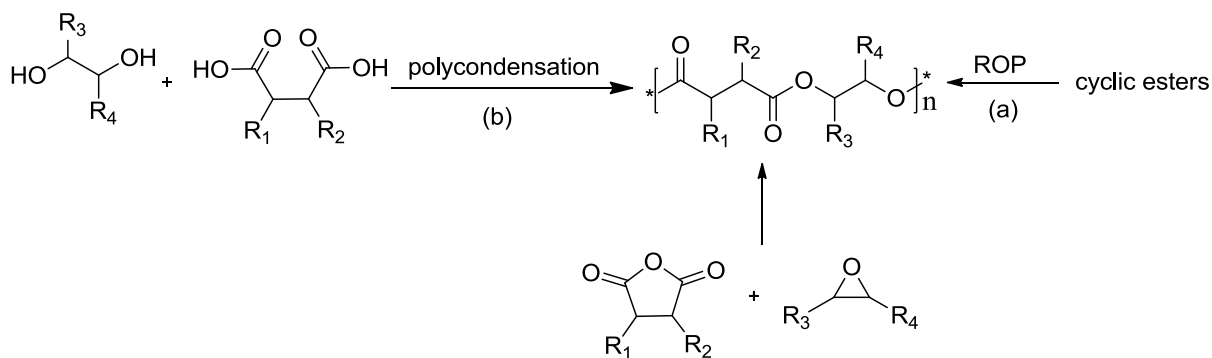
Figure 29. Common synthetic approaches to aliphatic polyesters

In contrast to these traditional routes, a wide variety of polyesters can be synthesized by the way of ring opening co- polymerization of cyclic anhydrides and epoxides due to nearly endless choices of monomer units.[112] Even though, the first catalytic coupling of oxiranes with anhydrides was reported in 1960s,[113] the undesirable by-products that are generated from homopolymerization of epoxides and the low molecular weight polymers hamper its popularity and improvements for quite some time. Recently, Inoue and co-workers reported a breakthrough using (tetraphenylporphyrinato)aluminum(III) ethoxide complexes (Figure 30, 1).[114] However, low molecular weight and long reaction times are still huge hurdles with this system. Followed by this report, Maeda and coworkers showed magnesium ethoxides as efficient initiators for ring-opening copolymerization of succinic anhydride (SA) with ethylene oxide (EO).[115] The recent reports on copolymerization of cylic oxiranes and anhydrides using diketiminate zinc complexes and chromium salophen and porphyrinato catalysts renewed the attention to this research area. More recently, Coates and co-workers reported cyno-diketiminate zinc complexes for copolymerization of aliphatic anhydrides and variety of epoxides, yielding copolymers with high molecular weight and narrow molecular weight distributions (Figure 30, 2).[116]
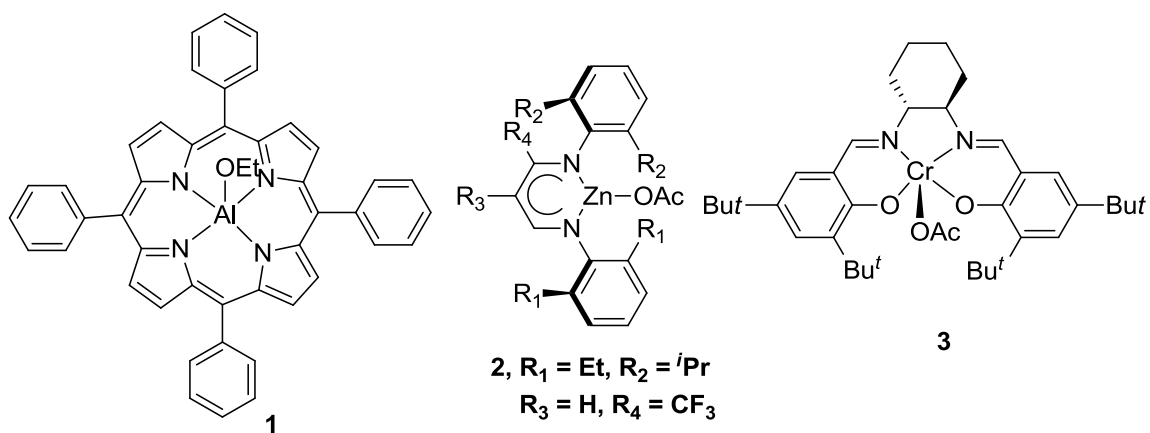
Figure 30. Popular catalysts for copolymerization of epoxides and anhydrides

Darensbourg *et al* reported alternating copolymerizaton of epoxides and anhydrides using salen-chromium(III) complexes (Figure 30, **3**) with the aid of co-catalysts, such as (bis(triphenyl phosphine)iminium) salts and tertrabutylammonium chlorides. The reaction rate studies confirmed that the rate-determining step was ring-opening of the oxirane by the enchained anhydride. [117] More investigations were carried out by Duchateau and co-workers on alternating ring-opening polymerization of epoxides and anhydrides using different metal salen chloride complexes ((salen)MCl, M = Al, Cr, Co; salen =N,N'-bis(3,5-di-tert-butylsalicylidene)diimine) and (tetraphenylprophyrinato)chromium complexes with conjunction of several co-catalysts.[118] It is confirmed that in most cases, the combination of chromium salophen chloride and bis-(triphenylphosphoranylidene)iminium chloride yielded best results. In common, catalysts showed lowest activity with N-heterocyclic co-catalysts. More recently, Coates and co-workers reported copolymerization of maleic anhydride with several terminal epoxides, catalyzed by a chromium(III) salen chloride complex, yielding highly alternating poly(esters) with narrow PDI values.[119]

1.7. References

1. Ross, M. L. The Oil Curse: How Petroleum Wealth Shapes the Development of Nations; Princeton University Press: Princeton, New Jersey, USA, **2012**.

2. Danner, H.; Braun, R. *Chem. Soc. Rev*. **1999**, *28*, 395–405.

3. Okada, M. *Prog. Polym. Sci*. **2002**, *27*, 87–133.

4. Gross, R. A.; Kalra, B *Science* **2002**, *297*, 803-807.

5. Yao, K.; Tang, C. *Macromolecules* **2013**, *46*, 1689−1712.

6. Stevens, E.S. Green Plastics; Princeton University Press, Princeton, New Jersey, **2002.**

7. Thompson, R. C.; Moore, C. J.; Saal, F. S.; Swan, S. H. *Phil. Trans. R. Soc. B* **2009,** *364***,** 2153–2166.

8. Gandini, A. *Green Chem*. **2011**, *13*, 1061−1083.

9. Mathers, R. T. *J. Polym. Sci., Part A: Polym. Chem.* **2012**, *50*, 1–15.

10. Gandini, A. *Macromolecules* **2008**, *41*, 9491−9504.

11. Kember, M. R.; Knight, P. D.; Reung, P. T. R.; Williams, C. K. *Angew. Chem., Int. Ed.* **2009**, *48*, 931–933.

12. Decortes, A.; Belmonte, M. M.; Benet-Buchholz, J.; Kleij, A. W. *Chem. Commun.* **2010**, *46*, 4580–4582.

13 (a) Zhang, Z.; Hu, S.; Song, J.; Li, W.; Yang, G.; Han, B. *ChemSusChem* **2009**, *2*, 234–238. (b) http://CO_2 now.org/. Accessed on 11.21.2013

14. Aresta, M.; Dibenedetto, A. *Dalton Trans*. **2007**, 2975–2992.

15. Prentice, I. C.; Farquhar, G. D.; Fasham, M. J. R.; Goulden, M. L.; Heimann, M.; Jaramillo, V. J.; Kheshgi, H. S.; Le Quere, C.; Scholes, R. J.; Wallace, D. W. R**.** The Carbon Cycle and Atmospheric Carbon Dioxide: **Intergovernmental Panel on Climate Change Third Assessment Report, 2001**.

16. Solomona, S.; Plattnerb, G-K.; Knuttic, R.; Friedlingstein, P. *PNAS*, **2006**, *106*, 1704–1709.

17. Department of Energy (US), International Energy Agency Report, 0484, **2009**.

18. Beer, C.; Reichstein, M.; Tomelleri, E.; Ciais, P.; Jung, M.; Carvalhais, N.; Rodenbeck, C.; Arain, M. A.; Baldocchi, D.; Bonan, G. B.; Bondeau, A.; Cescatti, A.; Lasslop, G.; Lindroth, A.; Lomas, M.; Luyssaert, S.; Margolis, H.; Oleson, K. W.; Roupsard, O.; Elmar Veenendaal, E.; Viovy, N.; Christopher Williams, C.; Woodward, F. I.; Papale, D. *Science* **2010**, *329*, 834–839.

19. Qin, Y.; Wang, X. *Biotechnol. J.* **2010**, *5*, 1164–1180.

20. (a) Kuran, W. *Prog. Polym. Sci.* **1998**, *23*, 919−992. (b) Ihata, O.; Kayaki, Y.; Ikariya, T. *Macromolecules* **2005**, *38*, 6429−6434.

21. Jessop, P. G.; Ikariya, T.; Noyori, R. *Chem. Rev.* **1999**, *99*, 475 –493.

22. Kendall, J. L.; Canelas, D. A.; Young, J. L.; De Simone, J. M. *Chem. Rev.* **1999**, *99*, 543 – 563.

23. Schafer, D.-C. A.; Saak, D.-C. W.; Haase, D.; Muller, T. *Angew. Chem., Int. Ed.* **2012**, *51*, 2981–2984.

24. Beckman, E. J. *Science* **1999**, *283*, 946 – 947.

25. Darensbourg, D. J.; Holtcamp, M. W. *Coord. Chem. Rev.* **1996**, *153*, 155–174.

26. Sakakura, T.; Choi, J-C.; Yasuda, H. *Chem. Rev.* **2007**, *107*, 2365–2387.

27. (a) Nakano, K.; Kobayashi, K.; Ohkawara, T.; Imoto, H.; Nozaki, K. *J. Am. Chem. Soc.* **2013**, *135*, 8456–8459. (b) Geschwind, J.; Frey, H. *Macromolecules* **2013**, *46*, 3280–3287. (c) Luinstra, G. A.; Borchardt, E. *Adv. Polym. Sci.* **2012**, *245*, 29–48. (d) Lu, X.-B.; Darensbourg, D. J. *Chem. Soc. Rev.* **2012**, *41*, 1462–1484. (e) Kember, M. R.; Buchard, A.; Williams, C. K. *Chem. Commun.* **2011**, *47*, 141−163. (f) Klaus, S.; Lehenmeier, M. W.; Anderson, C. E.; Rieger, B. *Coord. Chem. Rev.* **2011**, *255*, 1460−1479. (g) Lehenmeier, M. W; Bruckmeier, C.; Klaus, S.; Dengler, J. E.; Deglmann, P.; Ott, A.-K.; Rieger, B. *Chem. Eur. J.* **2011**, *17*, 8858–8869. (h) Darensbourg, D. J. *Inorg. Chem.* **2010**, *49*, 10765−10780. (i) Qin, Y.; Wang, X. *Biotechnol. J.* **2010**, *5*, 1164–1180. (j) Darensbourg, D. J. *Chem. Rev.* **2007**, *107*, 2388−2410. (k) Coates, W. G.; Moore, R. D. *Angew. Chem., Int. Ed.* **2004**, *43*, 6618–6639. (l) Darensbourg, D. J.; Mackiewicz, R. M.; Phelps, A. L.; Billodeaux, D. R. *Acc. Chem. Res.* **2004**, *37*, 836−844. (m) Nakano, K.; Kosaka, N.; Hiyama, T.; Nozaki, K. *Dalton Trans.* **2003**, 4039−4050.

28. *Handbook of Polycarbonate Science and Technology*; Legrand, D. G.; Bendler, J.T., Eds.; Marcel Dekker, Inc.: New York, **2000**.

29. Wang, S. J.; Du, L. C.; Zhao, X. S.; Meng, Y. Z.; Tjong, S. C. *J. Appl. Polym. Sci.* **2002**, *85*, 2327–2334.

30. Thorat, S. D.; Phillips, P. J.; Semenov, V.; Gakh, A. *J. Appl. Polym. Sci.* **2003**, *89*, 1163– 1176.

31. Nelson, A. M.; Long, T. M. *Polym. Int.* **2012**, *61*, 1485–1491.

32. http://www.matweb.com. Accessed on 08.18.2013.

33. Kim, W. B.; Joshi, U. A.; Lee, J. S. *Ind. Eng. Chem. Res.* **2004**, *43*, 1897–1914.

34. Gross, S. M.; Flowers, D.; Roberts, G.; Kiserow, D. J.; DeSimone, J. M. *Macromol.* **1999**, *32*, 3167–3169.

35. Grause, G.; Tsukada, N.; Hall, W. J.; Kameda, T.; Williams, P. T.; Yoshioka, T. *Polym. J.* **2010**, *42*, 438–442.

36. Tsintzou, G. P.; Antonakou, E. V.; Achilias, D. S. *J. Hazard. Mater.* **2012,** *241*, 137–

145.

37. Saal, F. S. V.; Hughes, C. *Environ. Health Persp.* **2005**, *113*, 926–933.

38. Jiang, X.; Ding, W.; Luan, C. *Can. J. Chem.* **2013**, *91*, 656–661.

39. Koninga, C.; Wildesonb, J.; Partona, R.; Pluma, B.; Steemana, P.; Darensbourg, D. J. *Polymer* **2001**, *42*, 3995–4004.

40. Li, G.; Qin, Y.; Wang, X.; Zhao, X.; Wang, F. *J. Polym. Res.* **2011**, *18*, 1177–1183.

41. Thorat, S. D.; Phillips, P. J.; Semenov, V.; Gakh, A. *J. Appl. Polym. Sci.* **2003**, *89*, 1163 – 1176.

42. Luinstra, G. A. *Polym. Rev.* **2008**, *48*, 192–219.

43. Inoue, S.; Tsuruta, K. H. *J. Polym Sci., Part B* **1969**, *7*, 287–292.

44. Kobayashi, M.; Tang, Y.-L., Tsuruta, T.; Inoue, S. *Makromol. Chem*. **1973**, *69*, 169–171.

45. Kobayashi, M.; Inoue, S.; Tsuruta, T. *J. Polym. Sci. Polym. Chem. Ed*. **1973**, *11*, 2383–2385.

46. Inoue, S.; Kobayashi, M.; Koinuma, H.; Tsuruta, T. *Makromol. Chem*. **1972**, *155*, 61–73.

47. Kuran, W.; Pasynkiewicz, S.; Skupinska, *J. Macromol. Chem. Phys*. **1976**, *177*, 1283–1292.

48. Kuran, W.; Pasynkiewicz, S.; Skupinska, *J. Makromol. Chem.* **1977**, *178*, 2149–2158.

49. Soga, K.; Imai, E.; Hattori, I. *Polym. J.* **1981**, *13*, 407–410.

50. Super, M. S.; Berluche, E.; Costello, C.; Beckman, E. J. *Macromolecules* **1997**, *30*, 368–372.

51. Aida, T.; Ishikawa, M.; Inoue, S. *Macromolecules* **1986**, *19*, 8–13.

52. Darensbourg, D. J.; Holtcamp, M. W.; Struck, G. E.; Zimmer, M. S.; Niezgoda, S. A.; Rainey, P.; Robertson, J. B.; Draper, J. D.; Reibenspies, J. H. *J. Am. Chem. Soc.* **1999**, *121*, 107–116.

53. Soga, K.; Uenishi, K.; Ikeda, S. *J. Polym. Sci. Polym, Chem. Ed.* **1979**, *17*, 415–423.
54. Qin, Z.; Thomas, C. M.; Lee, S.; Coates, G. W. *Angew. Chem., Int. Ed.* **2003**, *42*, 5484–5487.

55. Lu, X.-B.; Wang, Y. *Angew. Chem., Int. Ed.* **2004**, *43*, 3574–3577.

56. Ren , W-M.; Zhang, X.; Liu, Y.; Li, J.-F.; Wang, H.; Lu, X.-B. *Macromolecules*, **2010**, *43*, 1396–1402.

57. Mang, S.; Cooper, A. I.; Colclough, M. E.; Chauhan, N.; Holmes, A. B. *Macromolecules* **2000**, *33*, 303–308.

58. Darensbourg, D. J.; Yarbrough, J. C. *J. Am. Chem. Soc.* **2002**, *124*, 6335–6342.

59. Darensbourg, D. J.; Rodgers, J. L.; Fang, C. C. *Inorg. Chem.* **2003**, *42*, 4498–4500.

60. Darensbourg, D. J.; Yarbrough, J. C.; Ortiz, C.; Fang, C. C. *J. Am. Chem. Soc.* **2003**, *125*, 7586–7591.

61. Eberhardt, R.; Allmendinger, M.; Rieger, B. *Macromol. Rapid Comm.* **2003**, *24*, 194–196.

62. Darensbourg, D. J. and R. M. Mackiewicz, R. M. *J. Am. Chem. Soc.* **2005**, *127*, 14026–14038.

63. Darensbourg, D. J.; Mackiewicz, R. M.; Rodgers, J. L.; C. C. Fang, C. C.; Billodeaux, D. R.; Reibenspies, J. H. *Inorg. Chem.* **2004**, *43*, 6024–6034.

64. Darensbourg, D. J.; R. M. Mackiewicz, R. M.; J. L. Rodgers, J. L.; Phelps, A. L. *Inorg. Chem.* **2004**, *43*, 1831–1833.

65. Darensbourg, D. J.; Rodgers, J. L.; Fang, C. C. *Inorg. Chem.* **2003**, *42*, 4498–4500

66. Guo, L.; Wang, C.; Zhao, W.; Li, H.; Sun, W.; Shen, Z. *Dalton Trans.* **2009**, 5406–5410.

67. Darensbourg, D. J.; Mackiewicz, R. M.; Rodgers, J. L.; Phelps, A. L. *Inorg. Chem.* **2004**, *43*, 1831–183.

68. Darensbourg, D. J.; Wildeson, J. R.; Yarbrough. J. C. *Inorg. Chem.* **2002**, *41*, 973–980.

69. Kim, I.; Kim, S. M.; Ha, C. S.; Park, D. W. *Macromol. Rapid Commun.* **2004**, *25*, 888–893.

70. Dinger, M. B.; Scott, M. J. *Inorg. Chem.* **2001**, *40*, 1029–1036.

71. Darensbourg, D. J.; Rainey, P.; Yarbrough, J. *Inorg. Chem.* **2001**, *40,* 986–993.

72. Hampel, O.; Rode, C.; Walther, D.; Beckert, R.; Gorls, H. Z. *Naturforsch. B* **2002**, *57*, 946– 956.

73. (a) Darensbourg, D. J.; Lewis, S. J.; Rodgers, J. L.; Yarbrough, J. C. *Inorg. Chem.* **2003**, *42*, 581–589. (b) Super, M. S.; Berluche, E.; Costello, C.; Beckman, E. J. *Macromolecules* 1997, *30*, 368–372.

74. Cheng, M.; Lobkovsky, E. B.; Coates, G. W. *J. Am. Chem. Soc.* **1998,** *120,* 11018–11019.

75. Allen, S. D.; Moore, D. R.; Lobkovsky, E. B.; Coates. G. W. *J. Am. Chem. Soc.* **2002**, *124*, 14284–14285.

76. Moore, D. R.; Cheng, M.; Lobkovsky, E. B.; Coates, G. W. *Angew. Chem., Int. Ed.* **2002**, *41*, 2599–2602.

77. Moore, D. R.; Cheng, M.; Lobkovsky, E. B.; Coates, G. W. *J. Am. Chem. Soc*. **2003**, *125*, 11911–11924.

78. Nozaki, K.; Nakano, K.; Hiyama. T. *J. Am. Chem. Soc.* **1999**, *121*, 11008–11009.

79. Nakano, K.; Nozaki, K.; Hiyama, T. *J. Am. Chem. Soc.* **2003**, *125*, 5501–5510.

80. Cheng, M.; Darling, N. A.; Lobkovsky, E. B.; Coates, G. W. *Chem. Commun*. **2000**, 2007–2008.

81. Cohen, C. T.; Thomas, C. M.; Peretti, K. L.; Lobkovsky, E. B.; Coates. G. W. *Dalton Trans.* **2006**, 237–249.

82. Wu, G.-P.; Ren, W.-M.; Luo, Y.; Li, B.; Zhang, W.-Z.; Lu, X.-B. *J. Am. Chem. Soc.* **2012**, *134*, 5682−5688.

83. Qin, Z.; Thomas, C. M.; Lee, S.; Coates, G. W. *Angew. Chem., Int. Ed.* **2003**, *42*, 5484–5487.

84. Lu, X. -B.; Wang, Y. *Angew. Chem., Int. Ed.* **2004**, *43*, 3574–3577.

85. Cohen, C. T.; Chu, T.; Coates, G. W. *J. Am. Chem. Soc.* **2005**, *127*, 10869–10879.

86. (a) Wheaton, C. A.; Hayes, P. G.; Ireland, B. J. *Dalton Trans.* **2009**, 4832–4846. (b) Coates, G. W.; Hillmyer, M. A. *Macromolecules* **2009**, *42*, 7987−7989. (b) Gandini, A. Macromolecules **2008**, *41*, 9491−9504. (c) Williams, C. K.; Hillmyer, M. A. *Polym. Rev.* **2008**, *48*, 1−10. (d) Mecking, S. *Angew. Chem., Int. Ed.* **2004**, *43*, 1078−1085.

87. Biron, M, Thermosets and Composites. *Technical Information for Plastics Users;* 1st Ed. Elsevier Ltd: New York, **2003**; ch. 2, pp 32–33.

88. Chiellini, E.; Solaro, R. *Adv. Mater.* **1996**, *8*, 305-313.

89. Swift, G. *Acc. Chem. Res.* **1993**, *26*, 105-110.

90. Ikada, Y.; Tsuji, H. *Macromol. Rapid Commun.* **2000**, *21*, 117-132.
91. Chisholm, M. H.; Iyer, S. S.; Matison, M. E.; McCollum, D. G.; Pagel, M. *Chem. Commun.* **1997**, 1999–2002.

92.http://www.biocom.iastate.edu/workshop/2012workshop/presentations/bopp.pdf. Accessed on 09.08.2013.

93. Stanford, M. J.; Dove, A. P. *Chem. Soc. Rev.* **2010**, *39*, 486–494.

94. Lofgren, A.; Albertsson, A.-C., Dubois, P.; Jerome, R. *J. Macromol. Sci. Part C: Poly. Rev.* **1995**, *35*, 379–418.

95. Mecerreyes, D.; Jerome R.; Dubois, P. *Adv. Polym. Sci.* **1999**, *147*, 1063–1071.

96. Kricheldorf, H.; Kreiser-Saunders, I.; Jurgens, C.; Wolter, D. *Macromol. Symp.* **1996**, 103, 85–102.
97. Thomas, C. T. *Chem. Soc. Rev.* 2010, **39**, 165–173.

98. Doscotch, M. A.; Siepmann, J. I.; Munson, E. J. *Macromolecules* **1997**, *30*, 2422–2428.

99. Thakur, K. A. M.; Kean, R. T.; Hall, E. S.; Kolstad, J. J.; Munson, E. J. *Macromolecules* **1998**, *31*, 1487–1494.

100 . Chisholm, M. H.; Iyer, S. S.; McCollum, D. G.; Pagel, M.; Werner-Zwanziger, U. *Macromolecules* **1999**, *32*, 963–973.

101. Thakur, K. A. M.; Kean, R. T.; Zell, M. T.; Padden, B. E.; Munson, E. J. *Macromolecules* **1998**, *31*, 1487–1494.

102. Kasperczyk, J. E. *Macromolecules* **1995**, *28*, 3937–3939.

103. Chisholm, M. H.; Gallucci, J. C.; Quisenberry, K. T.; Zhou, Z. *Inorg. Chem.* **2008**, *47*, 2613–2624.

104. Ovitt, T. M.; Coates, G. W. *J. Am. Chem. Soc.* **2004**, *122*, 1316–1327.

105. Drouin, F.; Oguadinma, P. O.; Whitehorne, T. J. J.; Prudhomme, R. E.; Schaper, F. *Organometallics* **2010**, *29*, 2139–2147.

106. Dechy-Cabaret, O.; Martin-Vaca, B.; Bourissou, D. *Chem. Rev.* **2004**, *104*, 6147−6176.

107. (a) Okada, M. *Prog. Polym. Sci.* **2002**, *27*, 87–133. (b) Dechy-Cabaret, O.; Martin-Vaca, B.; Bourissou, D. *Chem. Rev.* **2004**, *104*, 6147–6176.

108. Coulembier, O.; Degee, P.; Hedrick, J. L.; Dubois, P. *Prog. Polym. Sci.* **2006**, *31*, 723–747.
109. Ikada, Y.; Tsuj, H. **2000**, *21,* 117–132.

110. Vink, E. T. H.; Ra´bago, K. R.; Glassner, D. A.; Springs, B.; O'Connor, R. P.; Kolstad, J.; Gruber, P. R. *Macromol. Biosci.* **2004**, *4*, 551-564.

111. (a) Thomas, C. M. *Chem. Soc. Rev.* **2010**, *39*, 165–173. (b) Robert, C.; Montigny, F.; Thomas, C. T. *Nature Commun.* **2011**, *2*, 586−592. (c) Kricheldorf, H. R. *Chem. Rev.* **2009**, *109*, 5579−5594.

112. (a) Hua, Z.; Qi, G.; Chen, S. *J. Appl. Polym. Sci.* **2004**, *93*, 1788–1792. (b) Takasu, A.; Ito, M.; Inai, Y.; Hirabayashi, T.; Nishimura, Y. *Polym. J.* **1999**, *31*, 961–969.

113. Fischer, R. F. *J. Polym. Sci.* **1960**, *44*, 155−172.

114. (a) Aida, T.; Inoue, S. *J. Am. Chem. Soc.* **1985**, *107*, 1358–1364. (b) Aida, T.; Sanuki, K.; Inoue, S. *Macromolecules* **1985**, *18*, 1049–1055.

115. Maeda, Y. *Polymer* **1997**, *38*, 4719-4725.

116. Jeske, R. C.; DiCiccio, A. M.; Coates, G. W. *J. Am. Chem. Soc.* **2007**, *129*, 11330−11331.

117. Darensbourg, D. J.; Poland, R. P.; Escobedo, C. *Macromolecules* **2012**, *45*, 2242−2248

118. (a) Nejad, E. H.; Melis, C. G. W.; Vermeer, T. J.; Koning, C. E.; Duchateau, R. *Macromolecules* **2012**, *45*, 1770−1776. (b) Nejad, E. H.; Paoniasari, A..; Melis, C. G. W.; Koning, C. E.; Duchateau, R. *Macromolecules* **2013***, 46,* 631−637. (c) Huijser, S.; Nejad, E. H.; Sablong, R.; Jong, C. D.; Koning, C. E.; Duchateau, R. *Macromolecules* **2011**, *44*, 1132–1139.

119. DiCiccio, A. M.; Coates, G. W. *J. Am. Chem. Soc.* **2011**, *133*, 10724–10727.

CHAPTER 2

MODULAR SYNTHESIS OF CHIRAL β- DIKETIMINATO-TYPE LIGANDS
CONTAINING 2-OXAZOLINE MOEITY VIA PALLADIUM-CATALYZED
AMINATION

2.1. Introduction

Because the reactivity and selectivity of metal catalysts are largely determined by

the auxiliary ligands, ligand design has been a central theme in catalysis, particularly in

asymmetric synthesis, which continues to be of great academic and industrial importance.[1]

One of the challenges is to derive efficient chiral catalysts for asymmetric induction in

different substrates with subtle variations. Since it is not expected that a single catalyst will

work for a wide range of substrates, an efficient strategy towards new catalysts would be

the design of a search pathway that provides access to a large number of structurally

similar ligands with tunable yet diverse substituents.[2] Indeed, many researchers have

sought to develop asymmetric catalysts by screening a large pool of chiral ligands.[3] To this

end, a modular approach for the ligand library construction is highly desirable.[4]

β-Diketiminato ligands (Figure 31A) have received great attention in coordination

chemistry due to the ease of fine tuning of the steric and electronic properties.[5] These

ligands are monoanionic upon deprotonation and form strong bonds with metals, usually

in a bidentate fashion. Various β-diketiminato metal complexes have been employed in a

number of catalytic reactions.[6,7] In a broader sense, the monoanionic, anilinido-imino

ligands (Figure 31B) can be included as a variation of the regular β-diketiminato

framework.[8] One example is the *ortho*-oxazoline substituted anilines, in which aniline nitrogens are typically not further functionalized.[9] Due to the presence of an aromatic ring, the resonance in the backbone is attenuated in comparison with the regular ligands and this may offer opportunity for electronic differentiation and stereocontrol upon coordination.[10] Given their extensive applications, it is somewhat surprising that the chiral variants of β-diketiminato ligands are relatively less developed in the literature,[11,12] although these moieties are often incorporated as subcomponents of multidentate or macrocyclic ligands in chiral environments.[13] In principle, stereo-directing groups can be introduced into all the R^1– R^5 substituents. Of particular interest are ligands with chiral substituents at the periphery (R^1 and R^5) that are in close proximity with the open coordination site where catalysis is taking place. Among these, monoanionic, chiral semicorrin[14] and bisoxazoline ligands[15] are some of the successful examples, where chiral substituents are intro- duced at the periphery (R^1 and $R^{5)}$ positions. Another approach is to incorporate axial chirality at the backbone, as demonstrated in ligands derived from isoquinoline and 2- aminonaphthalene[16] and in binaphthyl surrogates based on inner N–H–N hydrogen bonding.[17] Variation of backbone with stereogenic heteroatoms can also lead to axial chirality.[18]
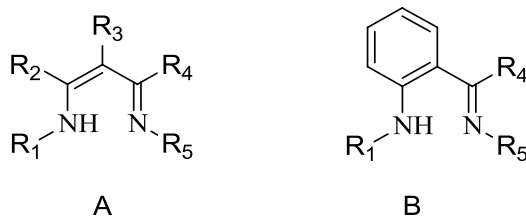
Figure 31. (A) β-Diketiminato ligands where R_1-R_5 substituents can be stereogenic. (B) Anilinido-imino variations

In our effort of constructing a chiral ligand framework, we have envisioned a modular approach for the synthesis of a library of chiral β-diketiminato type ligands based

on the direct coupling of two independent building blocks. The synthetic target (see Scheme 1) is a type of anilinido-imino ligands, with imine nitrogen from a chiral oxazoline moiety and amine nitrogen from an aniline/amide moiety. For the modular assembly, a choice of readily available chiral building blocks is critical. The 2-oxazoline was chosen as the imine nitrogen subunit because chiral oxazolines have widespread use as ligands and are readily accessible from the chiral pool of amino alcohols.[19] The ability of varying both chiral and stereo-directing centers independently allows the opportunity to explore the syn synergy between them. Herein we report the synthesis and characterization of a library of new chiral β-diketiminato type ligands via the Pd-catalyzed Buchwald–Hartwig amination reaction (Scheme 1).

2.2. Results and Discussion

We started out to synthesize a series of β-diketiminato type ligands containing one or two chiral substituents at the periphery, which are in close proximity with the open coordination site where catalysis would take place. By independently varying two points of diversity, the oxazoline fragment R and the amine component (R′), a library of chiral β-diketiminato type ligands **L1–L24** has been generated in a modular fashion (Scheme 1).
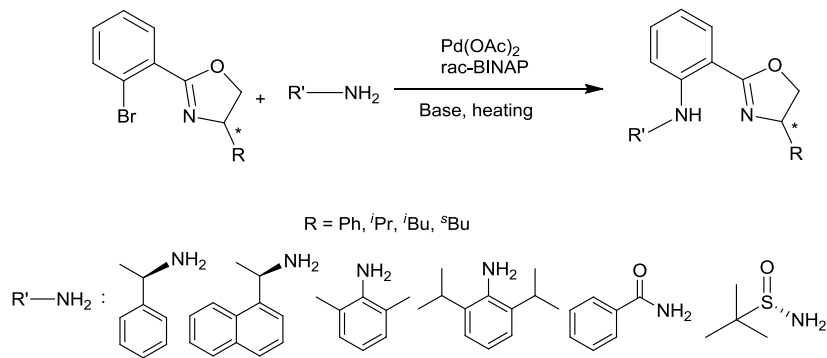
Scheme 1. Synthesis of chiral β-diketiminato type ligands

51

Chiral 2-(2′-bromophenyl)oxazolines **1a–d** were prepared from readily available chiral amino alcohols in a single step via two methods (Scheme 2).[20] In our hands, the second method seems to give better yields in shorter reaction time and offers another possibility to modify the aryl backbone. The resulting compounds **1a–d** were utilized as the coupling partners for the preparation of chiral bdiketiminato type ligand variants (see below).
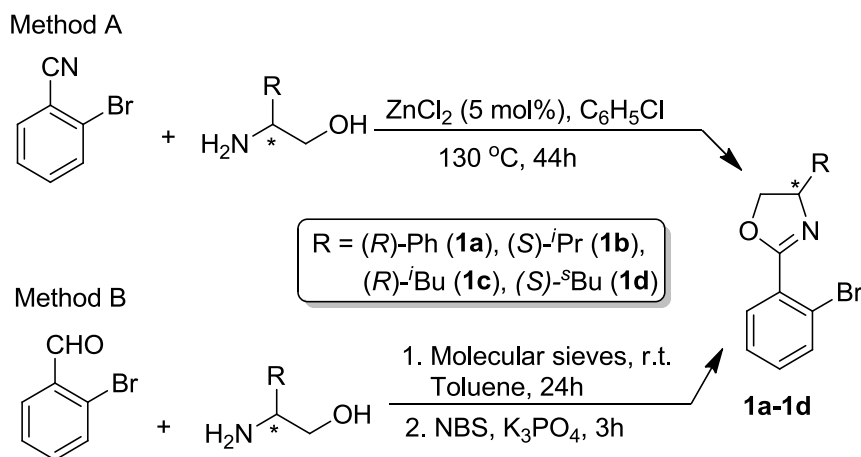
Scheme 2. Synthesis of chiral 2-oxazolines
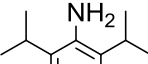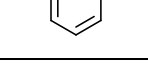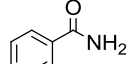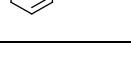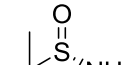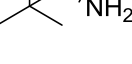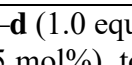
The desired chiral β-diketiminato-type compounds **L1–L24** (Figure 31) were synthesized via a cross coupling strategy, joining the chiral oxazoline and amine/amide moieties in a modular fashion (Scheme 1). The Pd-catalyzed Buchwald–Hartwig amination reaction was chosen because it has been extensively studied and modified with significant improvements for the cross coupling reaction of aryl or alkyl halides with amines or amides.[22,23] It has been previously employed in the library synthesis, including examples involving chiral oxazolines.[24,25] In principle, other cross coupling protocols such as Cu-catalyzed amination could be applied as well. Thus, heating a mixture of chiral oxazolines **1a–d** and (R)- α-methylbenzylamine in the presence of a catalytic amount of Pd(OAc)$_2$-BINAP under refluxing toluene afforded compounds **L1–L4** in moderate yields after purification by

52

column chromatography (see Table 3, entries 1–4). Compounds **L1** and **L3** were obtained as yellow solids while **L2** and **L4** are oily.

In order to vary the amine terminal, the phenyl substituent R′ in **L1**–**L4** was replaced with naphthalene, a sterically bulkier substituent. Thus, ligands **L5**–**L8** were similarly synthesized from Pd-catalyzed amination of chiral oxazo- lines **1a**–**d** with (*R*)-1-(1-naphthyl)ethylamine in moderate yields as oily compounds (Table 3, entries 5–8). It is noted that the synthesis of **L1**, **L7**, and **L8** required longer reaction times and the isolated yields were generally rather low. Attempts were made to improve the coupling reactions without much success; yields of 30–73% were typically obtained for the series of alkylamines, in part, due to formation of several unidentified by-products and subsequent difficulty in isolation. Use of state of the art phosphine ligands instead of BINAP, or other coupling protocols such as Cu-catalyzed amination may improve the yields, and efforts along these lines are ongoing.

We were interested in the effect of one stereogenic center in conjunction with a bulky substituent on catalytic selec- tivity. In this context, *ortho*-substituted anilines were used as the coupling partners. 2,6-Dimethylaniline and 2,6-diisopropylaniline were separately treated with chiral ox- azolines **1a**–**d** under similar conditions as above to afford ligands **L9**–**L16**. Yields of this series were generally higher (63–84%; see Table 3), presumably due to the enhanced nucleophilicity upon deprotonation of arylamines compared to alkylamines utilized in ligands **L1**–**L8**.

Table 3. Pd-Catalyzed Amination Reactions of Chiral Oxazolines **1a–d** with Primary Alky- or Arylamines and Amides[a]

Entry	R	R'NH$_2$	Ligand	Time (h)	Yield (%)[b]
1	Ph		**L1**	68	35[c]
2	*i*-Pr		**L2**	37	47
3	*i*-Bu		**L3**	40	56
4	*s*-Bu		**L4**	37	44
5	Ph		**L5**	24	50[c]
6	*i*-Pr		**L6**	24	73
7	*i*-Bu		**L7**	67	30
8	*s*-Bu		**L8**	67	36
9	Ph		**L9**	48	84
10	*i*-Pr		**L10**	48	77
11	*i*-Bu		**L11**	48	74
12	*s*-Bu		**L12**	48	83
13	Ph		**L13**	48	80
14	*i*-Pr		**L14**	48	84
15	*i*-Bu		**L15**	48	75
16	*s*-Bu		**L16**	48	63
17	Ph		**L17**[d]	20	98
18	*i*-Pr		**L18**[d]	20	95
19	*i*-Bu		**L19**[d]	32	98
20	*s*-Bu		**L20**[d]	20	99
21	Ph		**L21**[d]	5 d	84
22	*i*-Pr		**L22**[d]	5 d	60
23	*i*-Bu		**L23**[d]	2 d	70
24	*s*-Bu		**L24**[d]	2 d	<10

[a]Reaction conditions: oxazoline **1a–d** (1.0 equiv), amine (1.2 equiv),*t*-BuONa (1.4 equiv), Pd(OAc)$_2$ (5 mol%), *rac*-BINAP (5 mol%), toluene, 120 °C. [b]Isolated yields. [c]Exists as a ~9:1 mixture of two stereoisomers. [d]Reaction conditions: oxazoline **1a–d** (1.0 equiv), benzamide or sulfonamide (4.0 equiv), Cs$_2$CO$_3$ (2 equiv), Pd(OAc)$_2$ (10 mol%), *rac*-BINAP (20 mol%), toluene, heating
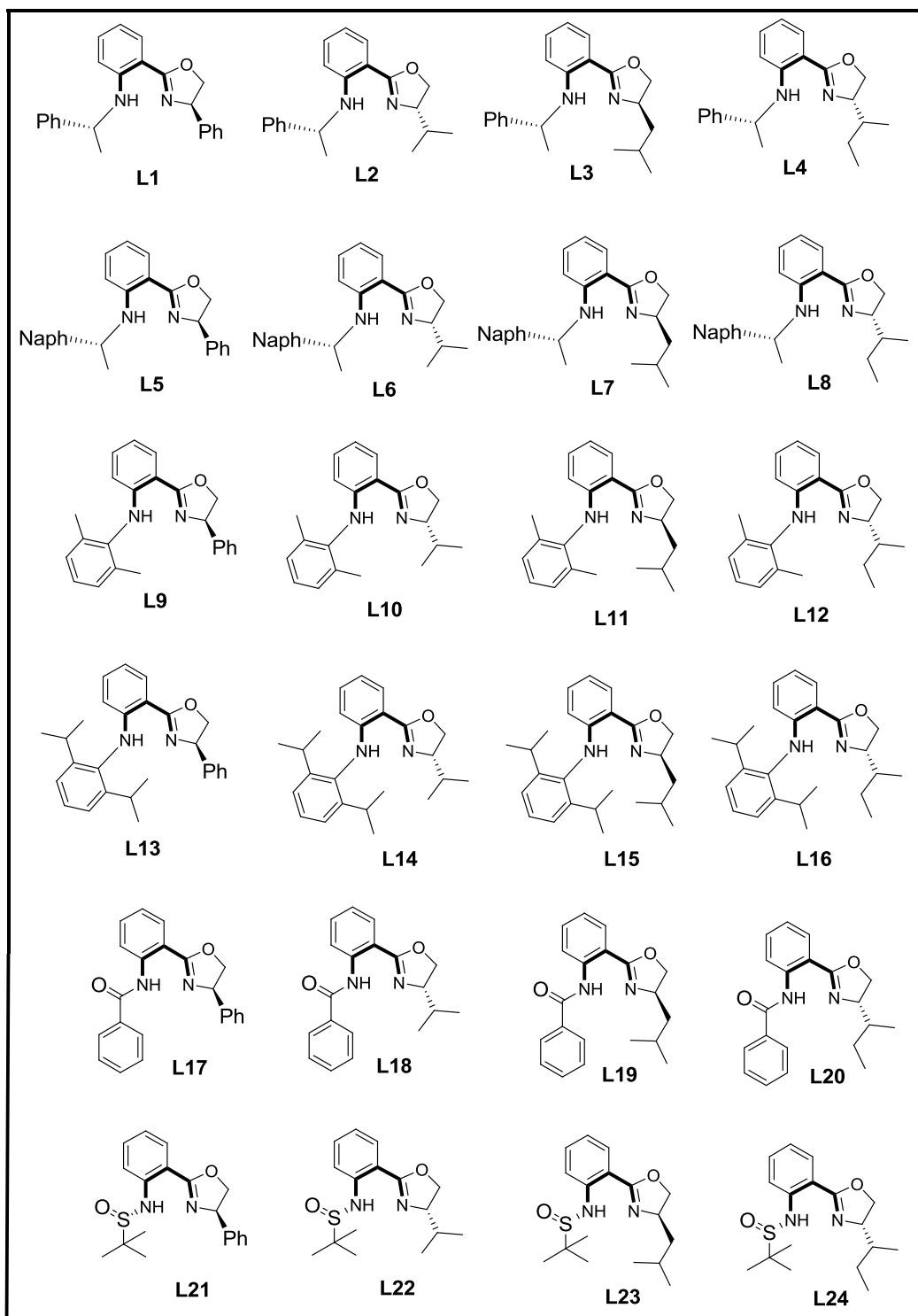
Figure 32. Structure of ligands **L1–L24**

A primary amide as a coupling partner was also employed to synthesize ligands **L17–L20**. Initial attempts under same conditions afforded minimal amount of the desired products, possibly because of the side reactions at high temperatures.[8d] In subsequent experiments, the reaction temperature was reduced to 100°C, the Pd and BINAP loadings were increased to 10 mol% and 20 mol%, respectively, and 4 equivalents of the amide (see Table 3) were employed. Under these conditions, compounds **L17–L20** were obtained in very high yields (>95%) and in shorter reaction times (see Table 3). This approach can be used to expand the library of chiral β-diketiminato type ligands to incorporate chiral amide substituents when they are potentially beneficial, and a pool of chiral amides is available as well.

Under similar conditions, a chiral sulfinamide, (*S*)-*tert*-butylsulfinamide,[26] can be coupled to the oxazoline moiety, resulting in compounds **L21–L24**. The reactions require longer reaction times, and the yields are generally good (60–84%), except the one with *sec*-butyl substituent (**L24**), despite the structural similarity and multiple attempts. To the best of our knowledge, sulfinamides have not previously been studied as coupling partners in the Buchwald–Hartwig amination reaction.

The structures of the synthesized compounds **L1–L24** are shown in Figure 32, and they have been characterized by ^{1}H and ^{13}C NMR spectroscopy. Characteristic peak is the NH signal in the downfield region of 9–10 ppm for **L1–L16**, 13.2–13.4 ppm for **L17–L20**, and 11–12 ppm for **L21– L24**. The observation is consistent with the presence of an intramolecular hydrogen bonding interaction between the NH group and the imino nitrogen, which is typical for this type of compounds. Also noteworthy is that the ^{1}H NMR (CDCl_3) spectra of **L1** and **L5** showed two distinct N-H peaks at $\delta = 9.08$ and 8.82 (minor) for **L1**; and at $\delta = 9.21$ and 8.88 (minor) for **L5**, respectively. Guiry and co-workers have

also observed the presence of two distinct NH peaks in a similar ligand framework.[27] At an elevated temperature (30 °C), these peaks coalesced to a single resonance, which is attributed to the presence of rotamers resulting from hindered rotation. When ligand **L1** was subjected to the VT-NMR experiment in the range of 0–55 °C, however, no obvious shift or coalescence was observed, suggesting the presence of a mixture of diastere- omers resulting from minor racemization. Preliminary investigations suggested that the racemization occurred at the oxazoline side, not the amine side; this process is rather specific to oxazolines with aryl substituents at the 4-position.[21] It should be noted that, in the isolated samples, only one set of signals was detected for the remaining ligands. Furthermore, the formulation of these compounds was confirmed with mass spectrometry (GC- MS and HRMS) and optical rotations, which are in agreement with the intended structures.

2.3. Conclusions

In conclusion, a library of twenty four new chiral β- diketiminato type ligands containing an oxazoline moiety has been synthesized via the Pd-catalyzed Buchwald–Hartwig amination reaction of chiral oxazolines and primary amines and amides. By independently varying two components (R and R'), this modular synthetic approach opens a pathway to obtain different combinations of chirality (e.g., *RR*, *RS*, *SS*, and *SR*), allowing exploration of the synergistic interactions between two chiral or stereo-directing centers in catalysis. It also offers the oppor- tunity to introduce additional coordinating groups to stabilize the ligation. The ligand framework presented here should be widely applicable in a range of metal- based catalytic reactions. These compounds themselves are also potential chiral proton sources,[17] with the NH proton located in a chiral microenvironment.

Considering the availability of large numbers of various chiral amines and amides, this methodology will allow the synthesis of a large family of new chiral β-diketiminato-type ligands for high throughput screening in asymmetric catalysis as well as in other applications. Our ongoing efforts involve optimizing and expanding the chiral β-diketiminato type ligands and searching for applications in other asymmetric catalyses.

2.3. Experimental Section

All air- or moisture-sensitive reactions were carried out under a dry N_2 atmosphere, employing standard Schlenk line and dry box techniques. Solvents were dried over Na/benzophenone and distilled under N_2. Deuterated solvents were purchased from Cambridge Isotope Laboratory and used as received. 2-(2'-Bromophenyl)oxazolines **1a–d** were prepared and purified according to a modified literature procedure. 2-Bromobenzonitrile, 2-bromobenzaldehyde, (*S*)-*tert*-butylsulfinamide, (*R*)-2-phenylglycinol, (*R*)-a-methylben- zylamine, (*R*)-(+)-1-(1-naphthyl)ethylamine, (*R*)-leucinol, *N*-bro- mosuccinimide, Cs_2CO_3, and K_3PO_4 tribasic were purchased from Aldrich while *L*-valinol and *L*-isoleucinol were purchased from Fluka and used as received.

All ^1H and ^{13}C NMR spectra were recorded on a Bruker Avance-500NMR spectrometer and referenced to the residual peaks in $CDCl_3$ or C_6D_6 at 298 K. Melting points were obtained on a Mel-Temp apparatus and were uncorrected. Optical rotations were recorded on a Rudolph Autopol III polarimeter with sodium D line (589 nm) at room temperature. GC/MS analyses were performed on an HP 5890 GC/HP 5971/B MSD system with electron impact ionization (70 eV). High-resolution mass spectrometry (HRMS) was

performed using high-resolution time of flight G1969A instrumentation (Agilent, Santa Clara, CA, USA).

General procedure for amination of chiral oxazolines with primary amines

An oven dried Schlenk flask was charged with 5 mol% Pd(OAc)$_2$, 5 mol% *rac*-BINAP, 1.0 equiv of chiral aryl bromide (**1a–1d**), 1.2 equiv of the appropriate primary amine, 1.4 equiv of sodium *tert*-butoxide and dry degassed toluene (15 mL), and the mixture was refluxed under nitrogen flow at 120 °C until an appropriate amount of the ligand was formed as judged by TLC and ^{1}H NMR spectroscopy. The crude product was then purified by column chromatography on silica gel eluted with a mixture of hexanes and ethyl acetate.

(4*R*)-4,5-Dihydro-2-(2′-(*R*-α-methyl-benzylamine)phenyl)-4-phenyloxazole   (L1).
Yield: 35%. mp: 56–59 °C. [α]$_D$ = –367.5 (c = 1.00, CHCl$_3$). ^{1}H NMR (500.1 MHz; CDCl$_3$; 298 K): δ$_H$ 1.54 (3H, d, *J* = 5.0 Hz, ArCH(*Me*)N), 4.13 (1H, t, *J* = 5.0 Hz, NCH(R)C*H*$_2$O), 4.59 (1H, q, *J* 5.0 Hz, ArC*H*(Me)N), 4.72 (1H, t, *J* = 5.0 Hz, NCH(R)C*H*$_2$O), 5.54 (1H, t, *J* = 5.0 Hz, NC*H*(R)CH$_2$O), 6.45 (1H, d, *J* = 10.0 Hz, Ar*H*), 6.57 (1H, t, *J* = 10.0 Hz, Ar*H*), 7.13 (1H, t, *J* = 10.0 Hz, Ar*H*), 7.18 (1H, d, *J* = 10.0 Hz, Ar*H*), 7.29 (1H, t, *J* = 10.0 Hz, Ar*H*), 7.35 (2H, m, Ar*H*), 7.78 (2H, d, *J* = 5.0 Hz, Ar*H*), 9.08 (1H, s, ArN*H*). ^{13}C NMR (125.8 MHz; CDCl$_3$; 298 K): δ$_{C\{H\}}$ 24.1 (ArCH(*Me*)N), 59.4 (Ar*C*H(Me)N), 69.0 (NCH(R)*C*H$_2$O), 71.8 (N*C*H(R)CH$_2$O), 107.3 (arom-*C*H), 110.9 (arom-*C*H), 113.5 (arom-*C*H), 124.8 (arom-*C*H), 125.4 (arom-*C*H), 125.7 (arom-*C*H), 126.4 (arom-*C*H), 127.5 (arom-*C*H), 127.6 (arom-*C*H), 128.9 (arom-*C*H), 131.5 (arom-*C*H), 141.9 (arom-*C*H), 144.4 (arom-*C*H), 147.4 (arom-*C*H), 164.7 (arom-*C*H). HRMS (ESI) calcd for C$_{23}$H$_{23}$N$_2$O [M+H]$^+$ 343.18048; found *m/z* 343.18155. GC/MS *m/z* 342 [M]$^+$, 327, 207, 194, 129.

(4*S*)-4,5-Dihydro-2-(2′-(*R*-α-methyl-benzylamine)phenyl)-4-*iso*-propyloxazole **(L2).**

Yield: 47%. [α]$_D$ = –250.0 (c = 1.00, CHCl$_3$). ^{1}H NMR (500.1 MHz; CDCl$_3$; 298 K): δ$_H$ 0.91 (3H, d, *J* = 5.0 Hz, *i*-Pr), 0.98 (3H, d, *J* = 5.0 Hz, *i*-Pr), 1.51 (3H, d, *J* = 5.0 Hz, ArCH(*Me*)N), 1.71 (1H, m, *i*-Pr), 3.92 (1H, t, *J* = 5.0 Hz, NC*H*(R)CH$_2$O), 4.05 (1H, t, *J* = 5.0 Hz, NCH(R)C*H$_2$*O), 4.26 (1H, t, *J* = 5.0 Hz, NCH(R)C*H$_2$*O), 4.56 (1H, q, *J* = 5.0 Hz, ArC*H*(Me)N), 6.38 (1H, d, *J* = 10.0 Hz, Ar*H*), 6.46 (1H, t, *J* = 10.0 Hz, Ar*H*), 7.02 (1H, t, *J* = 10.0 Hz, Ar*H*), 7.13 (1H, d, *J* = 10.0 Hz, Ar*H*), 7.22 (1H, m, Ar*H*), 7.28 (3H, m, Ar*H*), 7.63 (1H, d, *J* = 5.0 Hz, Ar*H*), 9.09 (1H, s, ArN*H*). ^{13}C NMR (125.8 MHz; CDCl$_3$; 298 K): δ$_{C\{H\}}$ 19.0 (*Me*CH(Me)), 19.3 (MeCH(*Me*)), 25.2 (ArCH(*Me*)N), 33.7 (Me*C*H(Me)), 52.9 (Ar*C*H(Me)N), 69.1 (N*C*H(R)CH$_2$O), 73.1 (NCH(R)*C*H$_2$O), 108.8 (arom-*C*H), 111.9 (arom-*C*H), 114.5 (arom-*C*H), 126.0 (arom-*C*H), 126.9 (arom-*C*H), 128.8 (arom-*C*H), 129.9 (arom-*C*H), 132.3 (arom-*C*H), 145.7 (arom-*C*H), 148.4 (arom-*C*H), 164.1 (arom-*C*H). HRMS (ESI) calcd for C$_{20}$H$_{25}$N$_2$O [M+H]$^+$ 309.19614; found *m/z* 309.19786. GC/MS *m/z* 308 [M]$^+$, 293. 222, 207, 194, 152, 129. Anal. Calcd for C$_{20}$H$_{24}$N$_2$O: C, 77.89; H, 7.84; N, 9.08. Found: C, 77.69; H, 7.99; N, 9.07.

(4*R*)-4,5-Dihydro-2-(2′-(*R*-α-methyl-benzylamine)phenyl)-4-*iso*-butyloxazole **(L3).**

Yield: 56%. mp: 65–68 °C. [α]$_D$ = –262.0 (c = 1.00, CHCl$_3$). ^{1}H NMR (500.1 MHz; CDCl$_3$; 298 K): δ$_H$ 0.89 (6H, d, *J* = 5.0 Hz, *i*-Pr), 1.35 (1H, m, *i*-PrC*H$_2$*), 1.49 (3H, d, *J* = 5.0 Hz, ArCH(*Me*)N), 1.56 (1H, m, *i*-PrC*H$_2$*), 1.84 (1H, m, *i*-Pr), 3.77 (1H, t, *J* = 5.0 Hz, NC*H*(R)CH$_2$O), 4.33 (2H, m, NCH(R)C*H$_2$*O), 4.50 (1H, q, *J* = 5.0 Hz, ArC*H*(Me)N), 6.33 (1H, d, *J* = 10.0 Hz, Ar*H*), 6.46 (1H, t, *J* = 10.0 Hz, Ar*H*), 7.02 (1H, t, *J* = 10.0 Hz, Ar*H*), 7.13 (1H, m, Ar*H*), 7.21 (1H, m, Ar*H*), 7.23 (3H, m, Ar*H*), 7.64 (1H, d, *J* = 5.0 Hz, Ar*H*), 9.02 (1H, s, ArN*H*). ^{13}C NMR (125.8 MHz; CDCl$_3$; 298 K): δ$_{C\{H\}}$ 22.6 (*Me*CH(Me)CH$_2$),

23.4 (MeCH(*Me*)CH₂), 25.3 (Me*C*H(Me)CH₂), 26.1 (ArCH(*Me*)N), 46.0 (MeCH(Me)*C*H₂), 53.2 (Ar*C*H(Me)N), 65.4 (NCH(R)*C*H₂O), 71.5 (N*C*H(R)CH₂O), 108.9 (arom-*C*H), 111.9 (arom-*C*H), 114.6 (arom-*C*H), 125.8 (arom-*C*H), 126.0 (arom-*C*H), 126.9 (arom-*C*H), 128.8 (arom-*C*H), 129.1 (arom-*C*H), 129.8 (arom-*C*H), 132.3 (arom-*C*H), 145.7 (arom-*C*H), 148.4 (arom-*C*H), 164.0 (arom-*C*H). HRMS (ESI) calcd for C₂₁H₂₇N₂O [M+H]⁺ 323.21179; found *m/z* 323.21277. GC/MS *m/z* 322 [M]⁺, 307, 207, 194, 129.

(4*S*)-4,5-Dihydro-2-(2′-(*R*-α-methyl-benzylamine)phenyl)-4-*sec*-butyloxazole (L4).
Yield: 44%. [α]$_D$ = −223.7 (c = 1.00, CHCl₃). ¹H NMR (500.1 MHz; CDCl₃; 298 K): δ$_H$ 0.79 (1H, m, MeCH₂C*H*(Me), 0.86 (3H, d, *J* = 5.0 Hz, MeCH₂CH(*Me*), 0.90 (3H, t, *J* = 5.0 Hz, *Me*CH₂CH(Me), 1.25 (1H, m, MeC*H*₂CH(Me), 1.51 (3H, d, *J* = 5.0 Hz, ArCH(*Me*)N), 1.60 (1H, m, MeC*H*₂CH(Me), 3.91 (1H, t, *J* = 5.0 Hz, NC*H*(R)CH₂O), 4.16 (1H, m, NCH(R)C*H*₂O), 4.26 (1H, m, NCH(R)C*H*₂O), 4.55 (1H, q, *J* = 5.0 Hz, ArC*H*(Me)N), 6.40 (1H, d, *J* = 10.0 Hz, Ar*H*), 6.47 (1H, t, *J* = 10.0 Hz, Ar*H*), 7.04 (1H, t, *J* = 10.0 Hz, Ar*H*), 7.14 (1H, t, *J* = 10.0 Hz, Ar*H*), 7.19 (1H, m, Ar*H*), 7.25 (3H, m, Ar*H*), 7.63 (1H, d, *J* = 5.0 Hz, Ar*H*), 9.07 (1H, s, ArN*H*). ¹³C NMR (125.8 MHz; CDCl₃; 298 K): δ$_{C\{H\}}$ 11.4 (MeCH(CH₂*Me*)), 15.4 (*Me*CH(CH₂Me)), 25.1 (Me*C*H(CH₂Me)), 26.2 (ArCH(*Me*)N), 40.1 (MeCH(*C*H₂Me)), 52.9 (Ar*C*H(Me)N), 65.9 (NCH(R)*C*H₂O), 71.8 (N*C*H(R)CH₂O), 108.8 (arom-*C*H), 111.8 (arom-*C*H), 114.5 (arom-*C*H), 126.0 (arom-*C*H), 126.9 (arom-*C*H), 128.8 (arom-*C*H), 129.9 (arom-*C*H), 132.3 (arom-*C*H), 145.7 (arom-*C*H), 148.4 (arom-*C*H), 164.0 (arom-*C*H). HRMS (ESI) calcd for C₂₁H₂₇N₂O [M+H]⁺ 323.21179; found *m/z* 323.21346. GC/MS *m/z* 322 [M]⁺, 307, 265, 207, 194, 129.

(4*R*)-4,5-Dihydro-2-(2′-(*R*-1-(1-naphthyl)ethylamine)phenyl)-4-phenyloxazole (L5).

Yield: 50%. [α]$_D$ = –303.7 (c = 1.00, CHCl$_3$). ^{1}H NMR (500.1 MHz; CDCl$_3$; 298 K): δ$_H$ 1.57 (3H, d, J = 5.0 Hz, ArCH(*Me*)N), 4.05 (1H, t, J = 5.0 Hz, NCH(R)C*H*$_2$O), 4.62 (1H,t,*J*=5.0 Hz, NCH(R)C*H*$_2$O), 5.28 (1H, q, J = 5.0 Hz, ArC*H*(Me)N), 5.48 (1H, t, J = 5.0 Hz, NC*H*(R)CH$_2$O), 6.19 (1H, d, J = 5.0 Hz, Ar*H*), 6.48 (1H, t, J = 5.0 Hz, Ar*H*), 6.94 (1H, t, J = 5.0 Hz, Ar*H*), 7.22 (1H, d, J = 5.0 Hz, Ar*H*), 7.25 (1H, m, Ar*H*), 7.30 (2H, m, Ar*H*), 7.38–7.48 (5H, m, Ar*H*), 7.64 (1H, d, J = 5.0 Hz, Ar*H*), 7.71 (1H, d, J = 5.0 Hz, Ar*H*), 7.81 (1H, d, J = 5.0 Hz, Ar*H*), 8.10 (1H, d, J = 5.0 Hz, Ar*H*), 9.16 (1H, s, ArN*H*). ^{13}C NMR (125.8 MHz; CDCl$_3$; 298 K): δ$_{C\{H\}}$ 24.3 (ArCH(*Me*)N), 49.8 (ArCH(Me)N), 70.5 (NCH(R)*C*H$_2$O), 73.3 (N*C*H(R)CH$_2$O), 108.8 (arom-*C*H), 112.4 (arom-*C*H), 115.0 (arom-*C*H), 122.9 (arom-*C*H), 125.8 (arom-*C*H), 126.1 (arom-*C*H), 126.4 (arom-*C*H), 126.8 (arom-*C*H), 127.7 (arom-*C*H), 128.0 (arom-*C*H), 129.2 (arom-*C*H), 129.6 (arom-*C*H), 130.3 (arom-*C*H), 131.0 (arom-*C*H), 133.0 (arom-*C*H), 134.5 (arom-*C*H), 140.7 (arom-*C*H), 143.4 (arom-*C*H), 148.7 (arom-*C*H), 165.9 (arom-*C*H). HRMS (ESI) calcd for C$_{27}$H$_{25}$N$_2$O [M+H]$^+$ 393.19614; found *m/z* 393.19700. GC/MS *m/z* 391, 281, 207, 193, 167, 149.

(4*S*)-4,5-Dihydro-2-(2′-(*R*-1-(1-naphthyl)-ethylamine)phenyl)-4-*iso*-propyloxazole (L6). Yield: 73%. [α]$_D$ = –359.4 (c = 1.00, CHCl$_3$). ^{1}H NMR (500.1 MHz; CDCl$_3$; 298 K): δ$_H$ 1.06 (3H, d, J = 5.0 Hz, *i*-Pr), 1.12 (3H, d, J = 5.0 Hz, *i*-Pr), 1.82 (3H, d, J = 5.0 Hz, ArCH(*Me*)N), 1.87 (1H, m, *i*-Pr), 4.10 (1H, t, J = 5.0 Hz, NC*H*(R)CH$_2$O), 4.25 (1H, q, J = 5.0 Hz, ArC*H*(Me)N), 4.43 (1H, t, J = 5.0 Hz, NCH(R)C*H*$_2$O), 5.51 (1H, t, J = 5.0 Hz, NCH(R)C*H*$_2$O), 6.40 (1H, d, J = 10.0 Hz, Ar*H*), 6.60 (1H, t, J = 10.0 Hz, Ar*H*), 7.08 (1H, t, J = 10.0 Hz, Ar*H*), 7.44 (1H, t, J = 10.0 Hz, Ar*H*), 7.65–7.56 (3H, m, Ar*H*), 7.82–7.78 (2H, m, Ar*H*), 7.98 (1H, d, J = 10.0 Hz, Ar*H*), 8.29 (1H, d, J = 10.0 Hz, Ar*H*), 9.44 (1H, b,

ArNH). ^{13}C NMR (125.8 MHz; CDCl$_3$; 298 K): δ$_{C\{H\}}$ 19.2 (*Me*CH(Me)), 19.6 (MeCH(*Me*)), 24.2 (ArCH(*Me*)N), 34.0 (Me*C*H(Me)), 49.4 (Ar*C*H(Me)N), 69.4 (N*C*H(R)CH$_2$O), 73.4 (NCH(R)*C*H$_2$O), 109.1 (arom-*C*H), 112.2 (arom-*C*H), 114.9 (arom-*C*H), 122.8 (arom-*C*H), 123.0 (arom-*C*H), 125.9 (arom-*C*H), 126.4 (arom-*C*H), 127.8 (arom-*C*H), 129.6 (arom-*C*H), 130.1 (arom-*C*H), 131.2 (arom-*C*H), 132.6 (arom-*C*H), 134.5 (arom-*C*H), 140.9 (arom-*C*H), 148.4 (arom-*C*H), 164.4 (arom-*C*H).HRMS (ESI) calcd for C$_{24}$H$_{27}$N$_2$O [M+H]$^+$ 359.21179; found *m/z* 359.21334. GC/MS *m/z* 358 [M]$^+$, 355, 281, 221, 147.

(4*R*)-4,5-Dihydro-2-(2′-(*R*-1-(1-naphthyl)-ethylamine)phenyl)-4-*iso*-butyloxazole (L7). Yield: 30%. [α]$_D$ = –318.3 (c = 1.00, CHCl$_3$). ^{1}H NMR (500.1 MHz; CDCl$_3$; 298 K): δ$_H$ 1.07 (6H, m, *i*-Pr), 1.52 (1H, m, *i*-PrC*H$_2$*), 1.71 (1H, m, *i*-PrC*H$_2$*), 1.78 (3H, d, *J* = 5.0 Hz, ArCH(*Me*)N), 2.01 (1H, m, *i*-Pr), 3.95 (1H, t, *J* = 5.0 Hz, NC*H*(R)CH$_2$O), 4.52 (2H, m, NCH(R)C*H$_2$*O), 5.43 (1H, q, *J* = 5.0 Hz, ArC*H*(Me)N), 6.31 (1H, d, *J* = 5.0 Hz, Ar*H*), 6.58 (1H, t, *J* = 5.0 Hz, Ar*H*), 7.04 (1H, t, *J* = 5.0 Hz, Ar*H*), 7.43 (1H, t, *J* = 5.0 Hz, Ar*H*), 7.66–7.55 (3H, m, Ar*H*), 7.80–7.77 (2H, m, Ar*H*), 7.97 (1H, d, *J* = 10.0 Hz, Ar*H*), 8.27 (1H, d, *J* = 10.0 Hz, Ar*H*), 9.32 (1H, s, ArN*H*). ^{13}C NMR (125.8 MHz; CDCl$_3$; 298 K): δ$_{C\{H\}}$ 22.9 (*Me*CH(Me)CH$_2$), 23.7 (MeCH(*Me*)CH$_2$), 24.2 (Me*C*H(Me)CH$_2$), 26.4 (ArCH(*Me*)N), 46.3 (MeCH(Me)*C*H$_2$), 49.6 (Ar*C*H(Me)N), 65.6 (N*C*H(R)CH$_2$O), 71.8 (NCH(R)*C*H$_2$O), 109.2 (arom-*C*H), 112.3 (arom-*C*H), 114.9 (arom-*C*H), 122.8 (arom-*C*H), 122.9 (arom-*C*H), 125.8 (arom-*C*H), 126.4 (arom-*C*H), 127.7 (arom-*C*H), 129.6 (arom-*C*H), 130.1 (arom-*C*H), 131.0 (arom-*C*H), 132.6 (arom-*C*H), 134.5 (arom-*C*H), 140.8 (arom-*C*H), 148.4 (arom-*C*H), 164.3 (arom-*C*H). HRMS (ESI) calcd for C$_{25}$H$_{29}$N$_2$O [M+H]$^+$ 373.22744; found *m/z* 373.22927. GC/MS *m/z* 362, 341, 238, 217, 147.

(4S)-4,5-Dihydro-2-(2′-(R-1-(1-naphthyl)-ethylamine)phenyl)-4-*sec*-butyloxazole

(L8). Yield: 36%. [α]$_D$ = −303.1 (c = 1.00, CHCl$_3$). ^{1}H NMR (500.1 MHz; CDCl$_3$; 298 K):

δ$_H$ 0.97 (6H, m, *Me*CH$_2$CH(*Me*)), 1.03 (1H, m, MeCH$_2$C*H*(Me)), 1.59 (2H, m,

MeC*H$_2$*CH(Me)), 1.80 (3H, d, *J* = 5.0 Hz, ArCH(*Me*)N), 4.09 (1H, t, *J* =5.0 Hz,

NC*H*(R)CH$_2$O), 4.32 (1H, t, *J* = 5.0 Hz, NCH(R)C*H$_2$*O), 4.43 (1H, t, *J* = 5.0 Hz,

NCH(R)C*H$_2$*O), 5.47 (1H, q, *J* = 5.0 Hz, ArC*H*(Me)N), 6.39 (1H, d, *J* = 5.0 Hz, Ar*H*), 6.58

(1H, t, *J* = 5.0 Hz, Ar*H*), 7.07 (1H, t, *J* = 5.0 Hz, Ar*H*), 7.44 (1H, t, *J* = 5.0 Hz, Ar*H*), 7.63–

7.55 (3H, m, Ar*H*), 7.79 (2H, d, *J* = 10.0 Hz, Ar*H*), 7.96 (1H, d, *J* = 10.0 Hz, Ar*H*), 8.27

(1H, d, *J* = 10.0 Hz, Ar*H*), 9.39 (1H, s, ArN*H*). ^{13}C NMR (125.8 MHz; CDCl$_3$; 298 K):

δ$_{C\{H\}}$ 11.7 (MeCH(CH$_2$*Me*)), 14.6 (*Me*CH(CH$_2$Me)), 25.7 (Me*C*H(CH$_2$Me)), 35.1

(ArCH(*Me*)N), 40.3 (MeCH(*C*H$_2$Me)), 49.4 (Ar*C*H(Me)N), 69.2 (NCH(R)*C*H$_2$O), 72.0

(N*C*H(R)CH$_2$O), 109.1 (arom-*C*H), 112.1 (arom-*C*H), 114.8 (arom-*C*H), 122.8 (arom-

*C*H), 123.0 (arom-*C*H), 125.8 (arom-*C*H), 126.4 (arom-*C*H), 127.7 (arom-*C*H), 129.6

(arom-*C*H), 130.1 (arom-*C*H), 131.2 (arom-*C*H), 132.6 (arom-*C*H), 134.5 (arom-*C*H),

140.9 (arom-*C*H), 148.2 (arom-*C*H), 164.3 (arom-*C*H). HRMS (ESI) calcd for C$_{25}$H$_{29}$N$_2$O

[M+H]$^+$ 373.22744; found *m/z* 373.22947. GC/MS *m/z* 372 [M]$^+$, 357, 272, 257, 243, 155.

(4R)-4,5-Dihydro-2-(2′-(2,6-dimethylaniline)phenyl)-4-phenyloxazole (L9). Yield:

84%. mp: 110–115 ºC. [α]$_D$ = −7.1 (c = 0.98, CHCl$_3$). ^{1}H NMR (500.1 MHz; CDCl$_3$; 298

K): δ$_H$ 2.12 (3H, s, Ar*Me*), 2.16 (3H, s, Ar*Me*), 4.12 (1H, t, *J* = 5.0 Hz, NCH(R)C*H$_2$*O),

4.70 (1H, t, *J* 5.0 Hz, NCH(R)C*H$_2$*O), 5.41 (1H, t, *J* = 5.0 Hz, NC*H*(R)CH$_2$O), 6.25 (1H,

d, *J* = 10.0 Hz, Ar*H*), 6.60 (1H, t, *J* = 10.0 Hz, Ar*H*), 7.03 (3H, m, Ar*H*), 7.13 (1H, t, *J* =

10.0 Hz, Ar*H*), 7.25 (5H, m, Ar*H*), 7.81 (1H, d, *J* = 10.0 Hz, Ar*H*), 9.91 (1H, s, ArN*H*).

^{13}C NMR (125.8 MHz; CDCl$_3$; 298 K): δ$_{C\{H\}}$ 20.1 (Ar*Me*), 32.1 (Ar*Me*), 70.1

(NCH(R)*C*H₂O), 73.0 (N*C*H(R)CH₂O), 108.1 (arom-*C*H), 112.3 (arom-*C*H), 116.5 (arom-*C*H), 126.2 (arom-*C*H), 126.6 (arom-*C*H), 127.5 (arom-*C*H), 127.7 (arom-*C*H), 128.2 (arom-*C*H), 128.4 (arom-*C*H), 130.0 (arom-*C*H), 133.8 (arom-*C*H), 136.4 (arom-*C*H),137.1 (arom-*C*H), 138.1 (arom-*C*H), 140.4 (arom-*C*H), 143.0 (arom-*C*H), 147.6 (arom-*C*H), 148.0 (arom-*C*H), 165.2 (arom-*C*H). HRMS (ESI) calcd for $C_{23}H_{23}N_2O$ [M+H]⁺ 343.18048; found *m/z* 343.18171. GC/MS *m/z* 342 [M]⁺, 222, 194, 120. Anal. Calcd for $C_{23}H_{22}N_2O$: C, 80.67; H, 6.48; N, 8.18. Found: C, 80.09; H, 6.60; N, 8.10.

(4*S*)-4,5-Dihydro-2-(2′-(2,6-dimethylaniline)phenyl)-4-*iso*-propyloxazole (L10). Yield: 77%. [α]_D = −7.8 (c = 2.30, CHCl₃). ¹H NMR (500.1 MHz; CDCl₃; 298 K): δ_H 0.92 (3H, d, *J* = 5.0 Hz, MeCH*Me*), 0.98 (3H, d, *J* = 5.0 Hz, *Me*CHMe), 1.81 (1H, m, MeC*H*Me), 2.19 (6H, s, Ar*Me*), 4.03 (1H, *J* = 5.0 Hz, NCH(R)C*H₂*O), 4.19 (1H, *J* = 5.0 Hz, NCH(R)C*H₂*O), 4.34 (1H, t, *J* = 5.0 Hz, NC*H*(R)CH₂O), 6.21 (1H, d, *J* = 10.0 Hz, Ar*H*), 6.61 (1H, t, *J* = 10.0 Hz, Ar*H*), 7.12 (3H, m, Ar*H*), 7.27 (1H, m, Ar*H*) 7.78 (1H, d, *J* = 10.0 Hz, Ar*H*), 9.96 (1H, s, ArN*H*). ¹³C NMR (125.8 MHz; CDCl₃; 298 K): δ_{C{H}} 18.8 (*Me*CH*Me*), 19.0 (*Me*CH*Me*), 19.1 (Me*C*HMe), 21.4 (Ar*Me*), 34.2 (Ar*Me*), 70.1 (NCH(R)*C*H₂O), 73.2 (N*C*H(R)CH₂O), 109.0 (arom-*C*H), 112.1 (arom-*C*H), 115.7 (arom-*C*H), 126.6 (arom-*C*H), 128.8 (arom-*C*H), 128.9 (arom-*C*H), 130.2 (arom-*C*H), 132.5 (arom-*C*H), 136.9 (arom-*C*H) 137.3 (arom-*C*H), 138.6 (arom-*C*H), 148.1 (arom-*C*H), 164.3 (arom-*C*H). HRMS (ESI) calcd for $C_{20}H_{26}N_2O$ [M+H]⁺ 309.19614; found *m/z* 309.19726. GC/MS *m/z* 308 [M]⁺, 265, 222, 194.

(4*R*)-4,5-Dihydro-2-(2′-(2,6-dimethylaniline)phenyl)-4-*iso*-butyloxazole (L11). Yield: 74%. [α]_D = +12.2 (c = 1.50, CHCl₃). ¹H NMR (500.1 MHz; CDCl₃; 298 K): δ_H 0.91 (6H, d, *J* = 5.0 Hz, *i*-Pr), 1.18 (1H, m, *i*-Pr), 1.46 (1H, m, *i*-PrC*H₂*), 1.78 (1H, m, *i*-PrC*H₂*),

65

2.13 (6H, s, Ar*Me*) 3.84 (1H, t, *J* = 5.0 Hz, NC*H*(R)CH$_2$O), 4.35 (2H, m, NCH(R)C*H*$_2$O), 6.10 (1H, d, *J* = 10.0 Hz, Ar*H*), 6.56 (1H, t, *J* = 10.0 Hz, Ar*H*), 7.04 (4H, m, Ar*H*), 7.71 (1H, d, *J* = 10.0 Hz, Ar*H*), 9.86 (1H, s; ArN*H*). ^{13}C NMR (125.8 MHz; CDCl$_3$; 298 K): δ$_{C\{H\}}$ 14.6 (*Me*CH(CH$_2$)*Me*), 18.8 (*Me*CH(CH$_2$)*Me*), 23.0 (Me*C*H(CH$_2$)Me), 24.1 (*Me*CH(*C*H$_2$)Me), 26.1 (Ar*Me*), 46.3 (Ar*Me*), 65.6 (N*C*H$_2$(R)CH$_2$O) 71.8 (N*C*H$_2$(R)CH$_2$O) 108.9 (arom-*C*H), 112.2 (arom-*C*H), 115.3 (arom-*C*H), 126.2 (arom-*C*H), 128.4 (arom-*C*H), 129.3 (arom-*C*H), 130.1 (arom-*C*H), 133.1 (arom-*C*H), 136.7 (arom-*C*H), 137.4 (arom-*C*H), 138.6 (arom-*C*H), 148.1 (arom-*C*H), 164.2 (arom-*C*H). HRMS (ESI) calcd for C$_{21}$H$_{26}$N$_2$O [M+H]$^+$ 323.21179; found *m/z* 323.21451. GC/MS *m/z* 322 [M]$^+$, 194, 222, 180. Anal. Calcd for C$_{21}$H$_{26}$N$_2$O: C, 78.22; H, 8.13; N, 8.69. Found: C, 77.83; H, 8.81; N, 8.65.

(4*S*)-4,5-Dihydro-2-(2′-(2,6-dimethylaniline)phenyl)-4-*sec*-butyloxazole (L12). Yield: 83%. [α]$_D$ = +20.0 (c = 1.00, CHCl$_3$). ^{1}H NMR (500.1 MHz; CDCl$_3$; 298 K): δ$_H$ 0.94 (6H, m, *Me*CH$_2$CH*Me*), 1.38 (1H, m, MeC*H*$_2$CHMe), 1.60 (1H, m, MeC*H*$_2$CHMe), 1.84 (1H, m, MeCH$_2$C*H*Me), 2.18 (6H, s, Ar*Me*), 3.88 (1H, t, *J* = 5.0 Hz, NC*H*(R)CH$_2$O), 4.42 (2H, t, *J* = 5.0 Hz, NCH(R)C*H*$_2$O), 6.22 (1H, d, *J* = 10.0 Hz, Ar*H*), 6.62 (1H, t, *J* = 10.0 Hz, Ar*H*), 7.09 (3H, m, Ar*H*), 7.25 (1H, m, Ar*H*), 7.73 (1H, d, *J* = 10.0 Hz, Ar*H*), 9.91 (1H, s, ArN*H*). ^{13}C NMR (125.8 MHz; CDCl$_3$; 298 K): δ$_{C\{H\}}$ 11.7 (*Me*CHCH$_2$*Me*), 14.7 (*Me*CHCH$_2$*Me*), 15.1 (Me*C*HCH$_2$Me), 18.8 (MeCH*C*H$_2$Me), 26.2 (Ar*Me*), 39.9 (Ar*Me*), 68.6 (N*C*H(R)CH$_2$O), 71.6 (N*C*H(R)CH$_2$O), 108.9 (arom-*C*H), 112.1 (arom-*C*H), 115.7 (arom-*C*H), 126.5 (arom-*C*H), 128.7 (arom-*C*H), 130.1 (arom-*C*H), 131.9 (arom-*C*H), 137.0 (arom-*C*H), 137.1 (arom-*C*H), 138.5 (arom-*C*H), 148.0 (arom-*C*H), 164.6 (arom-

CH). HRMS (ESI) calcd for $C_{21}H_{28}N_2O$ [M+H]$^+$ 323.21179; found *m/z* 323.21403. GC/MS *m/z* 322 [M]$^+$, 222, 194, 208.

(4*R*)-4,5-Dihydro-2-(2′-(2,6-diisopropylaniline)phenyl)-4-phenyloxazole (L13). Yield: 80%. mp: 80–85 ºC. [α]$_D$ = +53.3 (c = 1.00, CHCl$_3$). ^{1}H NMR (500.1 MHz; CDCl$_3$; 298 K): δ$_H$ 0.98 (3H, d, *J* = 5.0 Hz*, MeCHMe*), 1.01 (3H, d, *J* = 5.0 Hz*, MeCHMe*), 1.09 (6H, d, *J* = 5.0 Hz*, MeCHMe*), 3.00 (2H, m, Me*CH*Me), 4.13 (1H, t, *J* = 5.0 Hz, NCH(R)C*H₂*O), 4.67 (1H, t, *J* 5.0, NCH(R)C*H₂*O), 5.44 (1H, t, *J* 5.0*,* NC*H*(R)CH₂O), 6.22 (1H, d, *J* 10, Ar*H*), 6.60 (1H, t, *J* = 10.0 Hz, Ar*H*), 6.77 (1H, t, *J* = 10.0 Hz, Ar*H*), 7.03 (3H, d, *J* = 10.0 Hz, Ar*H*), 7.43–7.28 (5H, m, Ar*H*), 8.06 (1H, d, *J* = 10.0 Hz*,* Ar*H*), 9.89 (1H, s*,* ArN*H*). ^{13}C NMR (125.8 MHz; CDCl$_3$; 298 K): δ$_{C\{H\}}$ 22.4 (MeCH*Me*), 23.0 (*Me*CHMe), 24.4 (MeCH*Me*), 24.9 **(***Me*CHMe), 28.1 (Me*C*HMe), 28.6 (Me*C*HMe), 70.1 (N*C*H(R)CH₂O), 73.2 (NCH(R)*C*H₂O), 107.7 (arom-*C*H), 112.2 (arom-*C*H), 115.1 (arom-*C*H), 118.7 (arom-*C*H), 122.9 (arom-*C*H), 124.0 (arom-*C*H), 126.6 (arom-*C*H), 127.7 (arom-*C*H), 128.9 (arom-*C*H), 130.0 (arom-*C*H), 133.7 (arom-*C*H), 136.1 (arom-*C*H), 140.5 (arom-*C*H), 143.0 (arom-*C*H), 148.9 (arom-*C*H), 149.7 (arom-*C*H), 165.5 (arom-*C*H). HRMS (ESI) calcd for $C_{27}H_{32}N_2O$ [M+H]$^+$ 399.24309; found *m/z* 399.24452. GC/MS *m/z* 398 [M]$^+$, 236, 220, 193.

(4*S*)-4,5-Dihydro-2-(2,6-diisopropylaniline)phenyl)-4-*iso*-propyloxazole (L14). Yield: 84%. [α]$_D$ = +6.9 (c = 1.00, CHCl$_3$). ^{1}H NMR (500.1 MHz; CDCl$_3$; 298 K): δ$_H$ 0.88 (3H, d, *J* = 5.0 Hz*, MeCHMe*), 0.94 (3H, d, *J* = 5.0 Hz, MeCH*Me*), 1.03 (3H, d, *J* = 5.0 Hz, *Me*CHMe), 1.16 (6H, m, MeCH*Me*), 1.24 (3H, d, *J* = 5.0 Hz, MeCH*Me*), 1.76 (1H, m, Me*CH*Me), 3.01 (2H, m, 2 x Me*CH*Me), 4.01 (1H, t, *J* = 5.0 Hz, NCH(R)C*H₂*O), 4.14 (1H, t, *J* = 5.0 Hz, NCH(R)C*H₂*O), 4.31 (1H, t, *J* = 5.0 Hz, NC*H*(R)CH₂O), 6.14 (1H, d, *J* =

10.0 Hz, Ar*H*), 6.51 (1H, t, *J* = 10.0 Hz*, *Ar*H*), 7.04 (1H, t, *J* = 10.0 Hz*, *Ar*H*), 7.21 (2H, m, Ar*H*), 7.26 (1H, t, *J* = 10.0 Hz, Ar*H*) 7.71 (1H, d, *J* = 10.0 Hz*, *Ar*H*), 9.81 (1H, s, ArN*H*). ^{13}C NMR (125.8 MHz; CDCl$_3$; 298 K): $\delta_{C\{H\}}$ 18.4 (MeCH*Me*), 18.5 (MeCH*Me*), 23.0 (Me*CH**Me*), 24.7 (*Me*CHMe), 24.8 (*Me*CHMe), 28.3 (*Me*CHMe), 28.4 (MeCHMe), 30.7 (Me*C*HMe), 33.2 (Me*C*HMe), 68.8 (NCH(R)*C*H$_2$O), 72.7 (N*C*H(R)CH$_2$O), 108.6 (arom-*C*H), 112.4 (arom-*C*H), 115.2 (arom-*C*H), 119.0 (arom-*C*H), 122.9 (arom-*C*H), 124.1 (arom-*C*H), 127.5 (arom-*C*H), 129.8 (arom-*C*H), 132.6 (arom-*C*H), 135.7 (arom-*C*H), 140.8 (arom-*C*H), 148.2 (arom-*C*H), 150.0 (arom-*C*H), 164.3 (arom-*C*H). HRMS (ESI) calcd for C$_{24}$H$_{34}$N$_2$O [M+H]$^+$ 365.25874; found *m/z* 365.26028. GC/MS *m/z* 364 [M]$^+$, 236, 162, 114.

(4*R*)-4,5-Dihydro-2-(2′-(2,6-diisopropylaniline)phenyl)-4-*iso*-butyloxazole   **(L15).** Yield: 75%. mp: 65–68 ºC. [α]$_D$ = +2.8 (c = 1.00, CHCl$_3$). ^{1}H NMR (500.1 MHz; CDCl$_3$; 298 K): δ_H 0.90 (6H, d, *J* = 5.0 Hz*, *i-Pr), 1.11–1.05 (12H, m, *Me*CH*Me*), 1.34 (1H, m, *i*-PrC*H$_2$*), 1.57 (1H, m, *i*-PrC*H$_2$*), 1.82 (1H, m, *i*-Pr), 3.10 (2H, m, 2 x MeC*H*Me), 3.84 (1H, t, *J* = 5.0 Hz, NC*H*(R)CH$_2$O), 4.35 (2H, m, NCH(R)C*H$_2$*O), 6.16 (1H, d, *J* = 10.0 Hz, Ar*H*), 6.55 (1H, t, *J* = 10.0 Hz*, *Ar*H*), 7.04 (1H, t, *J* = 10.0 Hz*, *Ar*H*), 7.20 (3H, m, Ar*H*), 7.74 (1H, d, *J* = 10.0 Hz*, *Ar*H*), 9.88 (1H, s*, *ArN*H*). ^{13}C NMR (125.8 MHz; CDCl$_3$; 298 K): $\delta_{C\{H\}}$ 22.4 (*Me*CH(CH$_2$)Me), 22.6 (MeCH(CH$_2$)*Me*), 23.0 (MeCH(*CH$_2$*)Me), 23.2 (*Me*CHMe), 24.9 (*Me*CHMe), 25.0 (*Me*CHMe), 25.7 (*Me*CHMe), 28.5 (*Me*CH(CH$_2$)Me), 28.9 (*Me*CHMe), 46.3(Me*C*HMe), 65.2 NCH(R)*C*H$_2$O), 71.8 (N*C*H(R)CH$_2$O), 108.1 (arom-*C*H), 112.1 (arom-*C*H), 114.8 (arom-*C*H), 118.7 (arom-*C*H), 122.8 (arom-*C*H), 124.1 (arom-*C*H), 127.6 (arom-*C*H), 129.8 (arom-*C*H), 132.2 (arom-*C*H), 135.4 (arom-

CH), 147.8 (arom-*C*H), 149.2 (arom-*C*H), 164.1 (arom-*C*H). HRMS (ESI) calcd for C₂₅H₃₆N₂O [M+H]⁺ 379.27439; found *m/z* 379.27593. GC/MS *m/z* 378 [M]⁺ 236, 128, 162.

(4*S*)-4,5-Dihydro-2-(2′-(2,6-diisopropyl-aniline)phenyl)-4-*sec*-butyloxazole   (L16).

Yield: 63%. mp: 58–62 ℃. [α]$_D$ = +18.7 (c = 1.00, CHCl₃). ¹H NMR (500.1 MHz; CDCl₃; 298 K): δ$_H$ 0.82 (3H, d, *J* = 5.0 Hz, MeCH₂CH*Me*), 0.89 (3H, t, *J* = 5.0 Hz, *Me*CH₂CHMe), 1.11–1.04 (12H, m, *Me*CH*Me*), 1.22 (2H, m, MeC*H₂*CHMe), 1.57 (1H, m, MeCH₂C*H*Me), 3.08 (2H, m, 2 x MeC*H*Me), 3.95 (1H, t, *J* = 5.0 Hz, NC*H*(R)CH₂O), 4.22 (1H, t, *J* 5.0 Hz, NCH(R)C*H₂*O), 4.35 (1H, t, *J* 5.0 Hz, NCH(R)C*H₂*O), 6.12 (1H, d, *J* = 10.0 Hz, Ar*H*), 6.56 (1H, t, *J* = 10.0 Hz*,* Ar*H*), 7.04 (1H, t, *J* = 10.0 Hz*,* Ar*H*), 7.21 (2H, m, Ar*H*), 7.25 (1H, t, *J* = 10.0 Hz, Ar*H*) 7.69 (H, d, *J* = 10.0 Hz*,* Ar*H*), 9.93 (1H, s*,* ArN*H*). ¹³C NMR (125.8 MHz; CDCl₃; 298 K): δ$_{C\{H\}}$ 11.7 (*Me*CHCH₂*Me*), 14.7 (MeCHCH₂Me), 14.8 (*Me*CHCH₂*Me*), 22.5 (*Me*CH*Me*), 23.3 (*Me*CH*Me*), 25.2 (*Me*CH*Me*), 26.3 (*Me*CH*Me*), 28.5 (Me*C*HCH2Me), 28.5 (Me*C*HMe), 39.7 (Me*C*HMe), 68.6 (N*C*H(R)CH₂O), 71.8 (NCH(R)*C*H₂O), 108.2 (arom-*C*H), 112.0 (arom-*C*H), 115.2 (arom-*C*H), 118.8 (arom-*C*H), 123.0 (arom-*C*H), 123.9 (arom-*C*H), 127.5 (arom-*C*H), 129.7 (arom-*C*H), 132.4 (arom-*C*H), 135.5 (arom-*C*H), 147.8 (arom-*C*H), 149.7 (arom-*C*H), 164.1 (arom-*C*H). HRMS (ESI) calcd for C₂₅H₃₆N₂O [M+H]⁺ 379.27439; found *m/z* 379.27582. GC/MS *m/z* 378 [M]⁺, 236, 128, 162.

General procedure for amination of chiral oxazolines with amides

An oven dried Schlenk flask was charged with 10 mol% Pd(OAc)₂, 20 mol% *rac*-BINAP, 1.0 equiv of chiral aryl bromide (**1a–1d**), 4.0 equiv of benzamide or sulfinamide, 2.0 equiv of cesium carbonate and dry degassed toluene (15 mL), and the mixture was heated under

nitrogen flow until an appropriate amount of the ligand was formed as judged by TLC and

^{1}H NMR spectroscopy. The crude product was then purified by column chromatography.

(4*R*)-4,5-Dihydro-2-(2′-(benzamide)phenyl)-4-phenyloxazole (L17). Yield: 98%. mp: 118–122 °C. $[\alpha]_D = -132.2$ (c = 1.00, CHCl$_3$). ^{1}H NMR (500.1 MHz; C$_6$D$_6$; 298 K): δ_H 3.81 (1H, t, *J* = 10.0 Hz, NCH(R)C*H*$_2$O), 4.20 (1H, t, *J* = 10.0 Hz, NCH(R)C*H*$_2$O), 5.08 (1H, t, *J* = 10.0 Hz, NC*H*(R)CH$_2$O), 6.96 (1H, t, *J* = 10.0 Hz, Ar*H*), 7.07 (2H, t, *J* = 10.0 Hz, Ar*H*), 7.11-7.28 (6H, m, Ar*H*), 7.38 (1H, t, *J* = 10.0 Hz, Ar*H*), 8.06 (1H, d, *J* = 5.0 Hz, Ar*H*), 8.24 (2H, d, *J* = 5.0 Hz, Ar*H*), 9.65 (1H, d, *J* = 5.0 Hz, Ar*H*), 13.37 (1H, s, ArN*H*). ^{13}C NMR (125.8 MHz; C$_6$D$_6$; 298 K): $\delta_{C\{H\}}$ 70.3 (NCH(R)*C*H$_2$O), 73.3 (N*C*H(R)CH$_2$O), 113.7 (arom-*C*H), 120.5 (arom-*C*H), 122.6 (arom-*C*H), 127.2 (arom-*C*H), 128.0 (arom-*C*H), 128.2 (arom-*C*H), 128.4 (arom-*C*H), 128.7 (arom-*C*H), 129.2 (arom-*C*H), 129.8 (arom-*C*H), 131.7 (arom-*C*H), 133.5 (arom-*C*H), 136.0 (arom-*C*H), 141.7 (arom-*C*H), 142.0 (arom-*C*H), 165.3 (arom-*C*H), 166.0 (arom-*C*H). HRMS (ESI) calcd for C$_{22}$H$_{19}$N$_2$O$_2$ [M+H]$^+$ 343.1441; found *m/z* 343.14494. GC/MS *m/z* 342 [M]$^+$, 341, 325251, 207, 147.

(4*S*)-4,5-Dihydro-2-(2′-(benzamide)phenyl)-4-*iso*-propyloxazole (L18). Yield: 95%. $[\alpha]_D = +83.0$ (c = 1.00, CHCl$_3$). ^{1}H NMR (500.1 MHz; C$_6$D$_6$; 298 K): δ_H 0.78 (3H, d, *J* = 5.0 Hz, *i*-Pr), 0.88 (3H, d, *J* = 5.0 Hz, *i*-Pr), 1.52 (1H, m, *i*-Pr), 3.68 (1H, t, *J* 10.0 Hz, NC*H*(R)CH$_2$O), 3.81 (1H, t, *J* = 10.0 Hz, NCH(R)C*H*$_2$O), 4.02 (1H, t, *J* = 10.0 Hz, NCH(R)C*H*$_2$O), 6.94 (1H, d, *J* = 10.0 Hz, Ar*H*), 7.31 (3H, m, Ar*H*), 7.39 (1H, t, *J* = 10.0 Hz, Ar*H*), 7.97 (1H, d, *J* = 10.0 Hz, Ar*H*), 8.34 (2H, m, Ar*H*), 9.53 (1H, d, *J* = 10.0 Hz, Ar*H*), 13.29 (1H, s, ArN*H*). ^{13}C NMR (125.8 MHz; C$_6$D$_6$; 298 K): $\delta_{C\{H\}}$ 19.0 (*Me*CH(Me)), 19.2 (MeCH(*Me*)), 33.4 (Me*C*H(Me)), 69.6 (NCH(R)*C*H$_2$O), 73.2 (N*C*H(R)CH$_2$O), 113.9 (arom-*C*H), 120.3 (arom-*C*H), 122.5 (arom-*C*H), 127.6 (arom-*C*H), 128.0 (arom-*C*H),

128.2 (arom-*C*H), 128.8 (arom-*C*H), 129.8 (arom-*C*H), 131.9 (arom-*C*H), 133.0 (arom-*C*H), 136.2 (arom-*C*H), 141.4 (arom-*C*H), 164.2 (arom-*C*H), 165.9 (arom-*C*H). HRMS (ESI) calcd for $C_{19}H_{21}N_2O_2$ [M+H]$^+$ 309.15975; found *m/z* 309.16149. GC/MS *m/z* 308 [M]$^+$, 250, 207, 178, 146.

(4*R*)-4,5-Dihydro-2-(2′-(benzamide)phenyl)-4-*iso*-butyloxazole (L19). Yield: 98%. mp: 86–89 ºC. [α]$_D$ = −16.6 (c = 1.00, CHCl$_3$). ^{1}H NMR (500.1 MHz; C$_6$D$_6$; 298 K): δ$_H$ 0.85 (3H, d, *J* = 5.0 Hz, *i*-Pr), 0.94 (3H, d, *J* = 5.0 Hz, *i*-Pr), 1.03 (2H, m, *i*-PrC*H*$_2$), 1.40 (1H, m, *i*-Pr), 3.50 (1H, t, *J* = 5.0 Hz, NC*H*(R)CH$_2$O), 4.03 (2H, m, NCH(R)C*H*$_2$O), 6.95 (1H, t, *J* = 10.0 Hz, Ar*H*), 7.32 (3H, m, Ar*H*), 7.38 (1H, t, *J* = 10.0 Hz, Ar*H*), 7.99 (1H, d, *J* = 10.0 Hz, Ar*H*), 8.32 (2H, m, Ar*H*), 9.55 (1H, d, *J* = 10.0 Hz, Ar*H*), 13.21 (1H, s, ArN*H*). ^{13}C NMR (125.8 MHz; C$_6$D$_6$; 298 K): δ$_{C\{H\}}$ 20.8 (*Me*CH(Me)CH$_2$), 22.1 (MeCH(*Me*)CH$_2$), 25.4 (Me*C*H(Me)CH$_2$), 45.8 (MeCH(Me)*C*H$_2$), 65.0 (N*C*H(R)CH$_2$O), 71.9 (NCH(R)*C*H$_2$O), 114.1 (arom-*C*H), 120.4 (arom-*C*H), 122.0 (arom-*C*H), 122.5 (arom-*C*H), 124.2 (arom-*C*H), 127.7 (arom-*C*H), 128.8 (arom-*C*H), 129.7 (arom-*C*H), 132.3 (arom-*C*H), 133.9 (arom-*C*H), 141.3 (arom-*C*H), 164.0 (arom-*C*H), 165.9 (arom-*C*H). HRMS (ESI) calcd for $C_{20}H_{23}N_2O_2$ [M+H]$^+$ 323.17540; found *m/z* 323.17817. GC/MS *m/z* 322 [M]$^+$, 265, 245, 224, 146.

(4*S*)-4,5-Dihydro-2-(2′-(benzamide)phenyl)-4-*sec*-butyloxazole (L20). Yield: 99%. [α]$_D$ = +99.0 (c = 1.00, CHCl$_3$). ^{1}H NMR (500.1 MHz; C$_6$D$_6$; 298 K): δ$_H$ 0.73 (3H, d, *J* = 5.0 Hz, MeCH$_2$CH(*Me*), 0.83 (3H, t, *J* = 5.0 Hz, *Me*CH$_2$CH(Me), 1.11 (1H, m, MeC*H*$_2$CH(Me), 1.38 (1H, m, MeC*H*$_2$CH(Me), 1.50 (1H, m, MeC*H*$_2$CH(Me), 3.70 (1H, t, *J* = 5.0 Hz, NC*H*(R)CH$_2$O), 3.93 (1H, m, NCH(R)C*H*$_2$O), 4.02 (1H, m, NCH(R)C*H*$_2$O), 6.95 (1H, t, *J* = 10.0 Hz, Ar*H*), 7.33 (3H, m, Ar*H*), 7.40 (1H, t, *J* = 10.0 Hz, Ar*H*), 7.98

(1H, d, J = 5.0 Hz, ArH), 8.29 (2H, m, ArH), 9.49 (1H, d, J = 10.0 Hz, ArH), 13.19 (1H, s, ArNH). ^{13}C NMR (125.8 MHz; C$_6$D$_6$; 298 K): $\delta_{C\{H\}}$ 11.9 (MeCH(CH$_2$$Me$)), 15.3 ($Me$CH(CH$_2$Me)), 26.0 (Me$C$H(CH$_2$Me)), 39.8 (MeCH($CH_2$Me)), 63.4 (NCH(R)$CH_2$O), 71.9 (N$C$H(R)CH$_2$O), 114.0 (arom-$C$H), 120.3 (arom-$C$H), 122.5 (arom-$C$H), 127.5 (arom-$C$H), 128.2 (arom-$C$H), 129.1 (arom-$C$H), 131.9 (arom-$C$H), 132.3 (arom-$C$H), 132.4 (arom-$C$H), 132.9 (arom-$C$H), 136.2 (arom-$C$H), 141.3 (arom-$C$H), 164.0 (arom-$C$H), 166.0 (arom-$C$H). HRMS (ESI) calcd for C$_{20}$H$_{23}$N$_2$O$_2$ [M+H]$^+$ 323.17540; found m/z 323.17860. GC/MS m/z 322 [M]$^+$, 265, 245, 146.

(4R)-4,5-Dihydro-2-(2′-((S)-*tert*-butylsulfinamide)phenyl)-4-phenyloxazole (L21).
Yield: 84 %. mp: 120–122 ºC. [α]$_D$ = -113.2 (c = 1.0, CHCl$_3$). ^{1}H NMR (500.1 MHz; C$_6$D$_6$; 298 K): δ_H 1.27 (9H, s, Bu^t), 3.81 (1H, t, J 10.0, ArCH(N)CH_2O), 4.21 (1H, t, J 10.0, ArCH(N)CH_2O), 5.13 (1H, t, J 10.0, ArCH(N)CH$_2$O), 6.86 (1H, t, J 10.0, ArH), 7.15–7.28 (6H, b, ArH), 7.68 (1H, d, J 10.0, ArH), 8.02 (1H, d, J 10.0, ArH), 11.43 (1H, s, ArNH). ^{13}C NMR (125.8 MHz; C$_6$D$_6$; 298 K): $\delta_{C\{H\}}$ 22.8 (Bu^t), 56.8 (Bu^t), 70.1 (ArCH(N)CH$_2$O), 73.4 (ArCH(N)CH$_2$O), 112.5 (arom-CH), 115.4 (arom-CH), 120.3 (arom-CH), 127.1 (arom-CH), 128.0 (arom-CH), 128.3 (arom-CH), 128.5 (arom-CH), 129.1 (arom-CH), 130.4 (arom-CH), 133.3 (arom-CH), 142.7 (arom-CH), 146.1 (arom-CH), 165.2 (arom-CH). HRMS (ESI) calcd for C$_{19}$H$_{22}$N$_2$O$_2$S [M+H]$^+$ 343.14747; found m/z 343.15012. GC/MS (EI): m/z 238, 207, 180, 131,118. GC/MS (CI): m/z 342 (M$^+$). Anal. Calcd for C$_{19}$H$_{22}$N$_2$O$_2$S: C, 66.64; H, 6.48; N, 8.18. Found: C, 66.67; H, 6.52; N, 8.09.

(4S)-4,5-Dihydro-2-(2′-((S)-*tert*-butylsulfinamide)phenyl)-4-isopropyloxazole (L22).
Yield: 60 %. [α]$_D$ = +66.5 (c = 0.75, CHCl$_3$). ^{1}H NMR (500.1 MHz; C$_6$D$_6$; 298 K): δ_H 0.82

(3H, d, *J* 10.0, *i*-Pr), 0.97 (3H, d, *J* 10.0, *i*-Pr), 1.37 (9H, s, *Bu*^{t}), 1.52 (1H, m, *J* 5.0, *i*-Pr), 3.68 (1H, t, *J* 10.0, ArC*H*(N)CH$_2$O), 3.82 (1H, t, *J* 10.0, ArCH(N)C*H*$_2$O), 4.02 (1H, t, *J* 10.0, ArCH(N)C*H*$_2$O), 6.83 (1H, t, *J* 10.0, Ar*H*), 7.19 (1H, t, *J* 10.0, Ar*H*), 7.59 (1H, d, *J* 10.0, Ar*H*), 8.02 (1H, d, *J* 10.0, Ar*H*), 11.29 (1H, s, ArN*H*). ^{13}C NMR (125.8 MHz; C$_6$D$_6$; 298 K): δ$_{C\{H\}}$ 18.8 (*Me*CH(Me)), 19.0 (MeCH(*Me*)), 22.9 (*Bu*^{t}), 33.4 (MeC*H*(Me)), 56.4 (*Bu*^{t}), 69.4 (ArCH(N)*C*H$_2$O), 73.2 (Ar*C*H(N)CH$_2$O), 113.1 (arom-*C*H), 116.0 (arom-*C*H), 120.3 (arom-*C*H), 130.2 (arom-*C*H), 132.9 (arom-*C*H), 146.2 (arom-*C*H), 164.2 (arom-*C*H). HRMS (ESI) calcd for C$_{16}$H$_{25}$N$_2$O$_2$S [M+H]$^+$ 309.16422; found *m/z* 309.16874. GC/MS: *m/z* 204, 161, 133, 119, 106.

(4*R*)-4,5-Dihydro-2-(2′-((*S*)-tert-butylsulfonamide)phenyl-4-isobutyloxazole (L23).
Yield: 70%. [α]$_D$ = +85.4 (c = 0.57, CHCl$_3$). ^{1}H NMR (500.1 MHz; CDCl$_3$; 298 K): δ$_H$ 0.94 (6H, m, (C*H*$_3$)$_2$CHCH$_2$), 1.25 (9H, s, ^{t}*Bu*), 1.63 (2H, m, (CH$_3$)$_2$CHC*H*$_2$), 1.83 (1H, m, (CH$_3$)$_2$C*H*CH$_2$), 3.87 (1H, t, *J* 6.32, ArC(N)C*H*CH$_2$O), 4.11 (1H, t, *J* 7.55, ArC(N)CHC*H*$_2$O), 4.40 (1H, t, *J* 6.95, ArC(N)CHC*H*$_2$O), 6.90 (1H, t, *J* 8.48, Ar*H*), 7.35 (1H, t, *J* 7.95, Ar*H*), 7.41 (1H, d, *J* 8.03, Ar*H*), 7.71 (1H, d, *J* 8.48, Ar*H*), 11.04 (1H, s, ArN*H*). ^{13}C NMR (125.8 MHz; CDCl$_3$; 298 K): δ$_{C\{H\}}$ 22.3 (*Me*(CH)CH$_2$*Me*), 22.8 (^{t}*Bu*), 23.1 (Me(*C*H)CH$_2$Me), 45.7 (Me(CH)*C*H$_2$Me), 56.7 (*C*Me$_3$), 64.8 (ArC(N)*C*HCH$_2$O), 71.7 (Ar*C*(N)CHCH$_2$O), 112.6 (arom-*C*H), 115.1 (arom-*C*H), 120.1 (arom-*C*H), 129.1 (arom-*C*H), 132.6 (arom-*C*H), 144.9 (arom-*C*H), 163.6 (arom-*C*H). HRMS (ESI) calcd for C$_{17}$H$_{27}$N$_2$O$_2$S [M+H]$^+$ 323.17987; found *m/z* 323.18379. GC/MS: *m/z* 264, 216, 161, 145,120.

(4*S*)-4,5-Dihydro-2-(2′-((*S*)-*tert*-butylsulfonamide)phenyl-4-*sec*-butyloxazole (L24).

Yield: <10%. $[\alpha]_D$ = +64.1 (c = 0.85, CHCl$_3$). ^{1}H NMR (500.1 MHz; CDCl$_3$; 298 K): δ_H 0.75 (3H, m, (C*H$_3$*)$_2$CHCH$_2$), 0.89 (1H, m, (CH$_3$)$_2$CHC*H$_2$*), 0.91 (3H, m, (C*H$_3$*)$_2$CHC*H$_2$*), 0.94 (1H, m, (CH$_3$)$_2$CHC*H$_2$*), 1.28 (1H, m, (CH$_3$)$_2$C*H*CH$_2$), 1.38 (9H, s, ^{t}*Bu*), 4.13 (1H, t, *J* 8.48, ArC(N)C*H*CH$_2$O), 4.26 (1H, t, *J* 8.08, ArC(N)CHC*H$_2$*O), 4.36 (1H, t, *J* 8.90, ArC(N)CHC*H$_2$*O), 6.93 (1H, t, *J* 7.64, Ar*H*), 7.37 (1H, t, *J* 8.33, Ar*H*), 7.46 (1H, d, *J* 8.52, Ar*H*), 7.77 (1H, d, *J* 7.22, Ar*H*), 11.06 (1H, s, ArN*H*). ^{13}C NMR (125.8 MHz; CDCl$_3$; 298 K): $\delta_{C\{H\}}$ 11.3 (Me(CH)CH$_2$*Me*), 15.0 (*Me*(CH)CH$_2$Me), 23.0 (^{t}*Bu*), 25.9 (Me(CH)*C*H$_2$Me), 39.5 (Me(*C*H)CH$_2$Me), 56.9 (*C*Me$_3$), 69.0 (ArC(N)CHCH$_2$O), 71.6 (Ar*C*(N)CHCH$_2$O), 112.6 (arom-*C*H), 115.2 (arom-*C*H), 123.8 (arom-*C*H), 132.3 (arom-*C*H), 132.8 (arom-*C*H), 145.0 (arom-*C*H), 163.7 (arom-*C*H). HRMS (ESI) calcd for C$_{17}$H$_{27}$N$_2$O$_2$S [M+H]$^+$ 323.17987; found *m/z* 323.18127. GC/MS: *m/z* 218, 178, 161, 133.

2.5. References

1. (a) Walsh, P. J. Kozlowski, M. C. *Fundamentals in Asymmetric Catalysis*; USB: Sausalito, CA, **2008**. (b) Jacobsen, E. N.; Pfaltz, A.; Yamamoto, H. *Comprehensive Asymmetric Catalysi*s; Springer: Heidelberg, Germany, **1999**. (c) Martin, R.; Buchwald, S. L. *Acc. Chem. Res*. **2008**, *41*, 1461–1473. (d) Heitbaum, M.; Glorius, F.; Escher, I. *Angew. Chem., Int. Ed.* **2006**, *45,* 4732–4762.

2. Hoveyda, A. H.; Hird, A. W.; Kacprzynski, M. A. *Chem. Commun*. **2004**, 1779–1785.

3. (a) Lu, Y.; Johnstone, T. C.; Arndtsen, B. A. *J. Am. Chem. Soc*. **2009**, *131*, 11284–11285 (b) Shi, B.-F.; Maugel, N.; Zhang, Y.-H.; Yu, J.-Q. *Angew. Chem., Int. Ed.* **2008**, *47,* 4882–4886. (c) Blaser, H.-U.; Pugin, B.; Spindler, F.; Thommen, M. *Acc. Chem. Res*. **2007**, *40*, 1240–1250. (d) Cesar, V.; Bellemin-Laponnaz, S.; Wadepohl, H.; Gade, L. H. *Chem. Eur. J.* **2005**, *11*, 2862–2873.

4. Pfaltz, A.; Drury, W. J., III *Proc. Natl. Acad. Sci. USA* **2004**, 101, 5723–5276.

5. (a) Bourget-Merle, L.; Lappert, M. F.; Severn, J. R. *Chem. Rev.* **2002**, *102*, 3031–3065. (b) Bourget-Merle, L.; Cheng, Y.; Doyle, D. J.; Hitchcock, P. B.; Khvostov, A. V.; Lappert, M. F.; Protchenko, V.; Wei, X. *ACS Symposium Series* **2006**, *917*, 192–207. (c) Holland, P. L. *Acc. Chem. Res*. **2008**, *41*, 905–914. (d) Mindiola, D. J. *Comments Inorg. Chem*. **2008**, *29*, 73–92. (e) Chomitz, W. A.; Arnold, J. *Chem. Eur. J.* **2009**, *15*, 2020–2030.

6. (a) Badiei, Y. M.; Dinescu, A.; Dai, X.; Palomino, R. M.; Heinemann, F. W.; Cundari, T. R.; Warren, T. H. *Angew. Chem., Int. Ed.* **2008**, *47,* 9961–9964. (b) Eckert, N. A.; Bones, E. M.; Lachicotte, R. J.; Holland, P. L. *Inorg. Chem*. **2003**, *42*, 1720–1725. (c) Cheng, M.; Moore, D. R.; Reczek, J. J.; Chamberlain, B. M.; Lobkovsky, E. B.; Coates, G. W. *J. Am. Chem. Soc*. **2001**, *123*, 8738–8749.

7. (a) Champouret, Y.; Baisch, U.; Poli, R.; Tang, L.; Conway, J. L.; Smith, K. M. *Angew. Chem. Int. Ed.* **2008**, *47,* 6069–6072. (b) Lazarov, B. B.; Hampel, F.; Hultzsch, K. C.; Doz, P. *Z. Anorg. Allg. Chem*. **2007**, *633*, 2367–2373. (c) Vollmerhaus, R.; Rahim, M.; Tomaszewski, R.; Xin, S.; Taylor, N. J.; Collins, S. *Organometallics* **2000**, *19*, 2161–2169.

8. (a) Li, J.; Tian, D.; Song, H.; Wang, C.; Zhu, X.; Cui, C.; Cheng, J.-P. *Organometallics* **2008**, *27*, 1605–1611. (b) Chen, C.-T.; Chan, C.-Y.; Huang, C.-A.; Chen, M.-T.; Peng, K.-F. *Dalton Trans*. **2007**, 4073–4078. (c) Badiei, Y. M.; Krishnaswamy, A.; Melzer, M. M.; Warren, T. H. *J. Am. Chem. Soc*. **2006**, *128*, 15056–15057. (d) Gao, H.; Guo, W.; Bao, F.; Gui, G.; Zhang, J.; Zhu, F.; Wu, Q. *Organometallics* **2004**, *23*, 6273–6280.

9. (a) Luo, F. –T.; Ravi, V. K.; Xue, C. *Tetrahedron* **2006**, *62*, 9365–9372. (b) Gomez, M.; Jansat, S.; Muller, G.; Aullon, G.; Maestro, M. A. *Eur. J. Inorg. Chem*. **2005**, 4341–4351. (c) Pfaltz, A.; *J. Heterocyclic Chem*. **1999**, *36,* 1437–1451.

10. Cortright, S. B.; Johnston, J. N. *Angew. Chem., Int. Ed*. **2002**, *41*, 345–348.

11. (a) Drouin, F.; Oguadinma, P. O.; Whitehouse, T. J. J.; Prud'homme, R. E.; Schaper, F. *Organometallics* **2010**, *29*, 2139–2147. (b) El-Zoghbi, I.; Latreche, S.; Schaper, F. *Organometallics* **2010**, *29*, 1551–1559. (c) Oguadinma, P. O.; Schaper, F. *Organometallics* **2009**, *28*, 4089–4097. (d) Cheng, M.; Darling, N. A.; Lobkovsky, E. B.; Coates, G. W. *Chem. Commun*. **2000**, 2007–2008. (e) Bertilsson, S. K.; Tedenborg, L.; Alonso, D. A.; Anderson, P. G. *Organometallics* **1999**, *18*, 1281–1286. (f) Wan, Z.-K.; Choi, H.-w.; Kang, F.-A.; Nakajima, K.; Demeke, D.; Kishi, Y. *Org. Lett*. **2002**, *4*, 4431–4434. (g) Brunner, H.; Rahman, A. F. M. *Z. Naturforsch,* **1983**, *38b*, 1332–1338. (h) Zhou, Y.-B.; Tang, F.-Y.; Xu, H.-D.; Wu, X.-Y.; Ma, J.-A.; Zhou, Q.-L. *Tetrahedron: Asymmetry* **2002**, *13*, 469–473. (i) Buch, F.; Harder, S. *Z. Naturforsch,, B: Chem. Sci*. **2008**, *63*, 169–173.

12. (a) Köhler, V.; Mazet, C.; Toussaint, A.; Kulicke, K.; Häussinger, D.; Neuburger, M.; Schaffner, S.; Kaiser, S.; Pfaltz, A. *Chem. Eur. J*. **2008**, 14, 8530–8539. (b) Mazet, C.; Köhler, V.; Roseblade, S.; Toussaint, A.; Pfaltz, A. *Chimia* **2006**, *60*, 195–198.

13. (a) End, N.; Macko, L.; Zehnder, M.; Pfaltz, A. *Chem. Eur. J*. **1998**, *4*, 818–824. (b) Chen, Y.; Ruppel, J. V.; Zhang, X. P. *J. Am. Chem. Soc*. **2007**, *129*, 12074–12075.

14. (a) Pfaltz, A. *Acc. Chem. Res*. **1993**, *26*, 339–345. (b) Leutenegger, U.; Madin, A.; Pfaltz, A. *Angew. Chem., Int. Ed*. **1989**, *28*, 60–61.

15. (a) Dagorne, S.; Bellemin-Laponnaz, S.; Maisse-Francois, A. *Eur. J. Inorg. Chem*. **2007**, 913–925. (b) Sibi, M. P.; Asano, Y. *J. Am. Chem. Soc*. **2001**, *123*, 9708–9709. (c) Mueller, D.; Umbricht, G.; Weber, B.; Pfaltz, A. *Helv. Chim. Acta* **1991**, *74*, 232–240. (d) Lowenthal, R. E.; Abiko, A.; Masamune, S. *Tetrahedron Lett*. **1990**, *31*, 6005–6008.

16. (a) Luesse, S. B.; Counceller, C. M.; Wilt, J. C.; Perkins, B. R.; Johnston, J. N. *Org. Lett*. **2008**, *10*, 2445–2447. (b) Cortright, S. B.; Huffman, J. C.; Yoder, R. A.; Coalter, J. N., III; Johnston, J. N. *Organometallics* **2004**, *23*, 2238–2250. (c) Cortright, S. B.; Yoder, R. A.; Johnston, J. N. *Heterocycles* **2004**, *62*, 223–227.

17. Kawabata, T.; Jiang, C.; Hayashi, K.; Tsubaki, K.; Yoshimura, T.; Majumdar, S.; Sasamori, T.; Tokitoh, N. *J. Am. Chem. Soc*. **2009**, *131*, 54–55.

18. Barrett, A. G. M.; Gray, A. A.; Hill, M. S.; Hitchcock, P. B.; Procopiou, P. A.; White, A. J. P. *Inorg. Chem*. **2006**, *45*, 3352–3358.

19. (a) Schneider, N.; Bellemin-Laponnaz, S.; Wadepohl, H.; Gade, L. H. *Eur. J. Inorg. Chem*. **2008**, 5587–5598. (b) Hargaden, G. C.; McManus, H. A.; Cozzi, P. G.; Guiry, P. J. *Org. Biomol. Chem*. **2007**, *5*, 763–766. (c) Lu, S. –F.; Du, D. –M.; Zhang, S. –W.; Xu, J. *Tetrahedron: Asymmetry* **2004**, *15*, 3433–3441. (d) Inoue, M.; Nakada, M. *Org. Lett*. **2004**, *6*, 2977–2980. (e) Inoue, M.; Suzuki, T.; Nakada, M. *J. Am. Chem. Soc*. **2003**, *125*, 1140–1141. (f) Miller, J. J.; Rajaram, S.; Pfaffenroth, C.; Sigman, M. S. *Tetrahedron* **2009**, *65*, 3110–3119. (g) McManus, H. A.; Cozzi, P. G.; Guiry, P. J. *Adv. Synth. Catal*. **2006**, *348*, 551–558. (h) McManus, H .; Guiry, P. J. *Chem. Rev*. **2004**, *104*, 4151–4202. (i) Hargaden, G.; Guiry, P. J. *Chem. Rev*. **2009**, *109*, 2505–2550.

20. (a) Zhou, Q-L.; Pfaltz, A. *Tetrahedron* **1994**, *50*, 4467–4478. (b) Schwekendiek, K.; Glorius, F. *Synthesis,* **2006**, *18*, 2996–3002.

21. See Supporting Information for more details.

22. (a) Surry, D. S.; S. L. Buchwald, S. L. *Angew.. Chem., Int. Ed*. **2008**, *47*, 6338–6361. (b) Surry, D. S.; Buchwald, S. L. *Chem. Sci*. **2010**, *1*, 13–31.

23. (a) Wolfe, J. P.; Wagaw, S.; Buchwald, S. L. *J. Am. Chem. Soc*. **1996**, *118*, 7215–7216. (b) Li, J. J.; Wang, Z.; Mitchell, L. H. *J. Org. Chem*. **2007**, *72*, 3606–3607. (c) Wolfe, J. P.; Buchwald, S. L. *J. Org. Chem*. **2000**, *65*, 1144–1157. (d) Chen, Y.; Fields, K. B.; Zhang, X. P. *J. Am. Chem. Soc*. **2004**, *126*, 14718–14719. (e) Bolm, C.; Hildebrand, J. P. *J. Org. Chem*. **2000**, *65*, 169–175. (f) Kamikawa, K.; Sugimoto, S.; Uemura, M. *J. Org. Chem*. **1998**, *63*, 8407–8410.

24. (a) McManus, H. A.; Guiry, P. J. *J. Org. Chem*. **2002**, *67*, 8566–8573. (b) Coeffard, V.; Muller-Bunz, H.; Guiry, P. J. *Org. Biomol. Chem*. **2009**, *7*, 1723–1734. (c) Doherty, S.; Knight, J. G.; Smyth, C. H.; Sore, N. T.; Rath, R. K.; McFarlane, W.; Harrington, R. W.; Clegg, W. *Organometallics,* **2006**, *25*, 4341–50. (d) McKeon, S.; Muller-Benz, H,; Guiry, P. J. *Eur. J. Org. Chem*. **2009**, 4833–4841.

25. (a) Xie, X.; Zhang, T. Y.; Zhang, Z. *J. Org. Chem*. **2006**, *71*, 6522–6529. (b) Gao, G. –Y.; Chen, Y.; Zhang, X. P. *Org. Lett*. **2004**, *6*, 1837–1840.

26. Tobak, M. T.; Herbage, M. A.; Ellman, J. A. *Chem. Rev*. **2010**, *110*, 3600–3740.

27. Hargaden, G. C.; Muller-Bunz, H.; Guiry, P. J. *Eur. J. Org. Chem*. **2007**, 4235–4243.

CHAPTER-3

CHIRAL AMIDO-OXAZOLINATE ZINC COMPLEXES FOR ALTERNATING
COPOLYMERIZATION OF CO_2 AND CYCLOHEXENE OXIDE

3.1. Introduction

Utilization of carbon dioxide (CO_2) as a renewable C1feedstock has attracted
increased interest due to its low cost, nontoxicity, and availability in nature and from many
industrial processes.[1] Given its thermodynamic and kinetic stability, one approach is to
couple CO_2 with high-energy, ring-strained heterocyclic molecules, leading to formation
of alternating copolymers.[2] The most widely studied one is the alternating
copolymerization of CO_2 with epoxides, in the presence of catalysts/cocatalysts.[3,4] The
resultant aliphatic polycarbonates possess attractive properties, such as biodegradability
and low oxygen permeability, and are regarded as promising new generation materials as
alternatives to conventional petrochemical-derived polymers. Consequently, much effort
has been devoted toward the development of efficient catalysts for alternating
copolymerization of CO_2 with epoxides. Beginning with Inoue's discovery of the
$ZnEt_2/H_2O$ catalyst in 1969,[5] a wide array of catalytic systems of metal complexes with
various ligands, such as phenoxides,[6] salen and its derivatives,[3a,7] porphyrins,[8] and others,[9]
have been explored to promote the transformation. In particular, zinc-β-diketiminate
complexes (Figure 33, A) developed by Coates[10] have been prominent for the
copolymerization of CO_2 with epoxides mainly due to their high catalytic activity and

precise control over molecular weight and polydispersity. Furthermore, the system is consistent with a living polymerization process.[10,11] A number of strategies have been exploited to improve the thermal and mechanical properties of polycarbonates and to expand their applications.[3] These include copolymerization with epoxide momomers other than the commonly applied cyclohexene oxide (CHO) and propylene oxide (PO),[12] terpolymerization with two different epoxides or other types of monomers,[13] and polymer chain cross-linking.[14] Inspired by the success of chiral catalysts in asymmetric organic synthesis, another
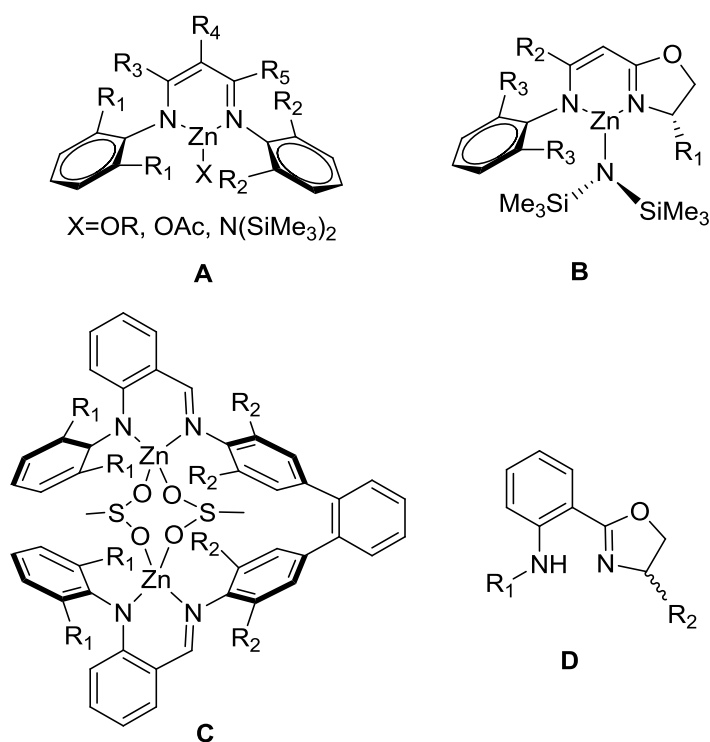
Figure 33. Structrual variants of β-diketiminate ligands

strategy is to use them to impart control over the absolute and relative stereochemistry of the resulting polycarbonates. The first examples of asymmetric copolymerization of CO_2 and CHO were reported by Nozaki, with a 1:1 mixture of (S)-diphenyl(pyrrolidin-2-

yl)methanol and $ZnEt_2$ as a chiral catalyst,[15] and by Coates, with a series of well-defined, Zn imine-oxazoline catalysts (Figure 33, B).[16] The main-chain chirality of the poly(cyclohexene carbonate) (PCHC) was determined to be 70% ee and up to 72% ee, respectively, after hydrolysis to 1,2-trans-cyclohexane diol. The former was improved to 80% ee by judicious adjustment of reaction conditions based on mechanistic understandings.[17] Despite its dinuclear nature, Trost's zinc complex was shown to induce rather low enantioselectivity (18% ee) in alternating copolymerization of CO_2 and CHO.[18] Along with the developments of zinc-based catalysts, cobalt and chromium salen complexes were also widely investigated for this asymmetric coupling as well as with racemic epoxides.[19] Remarkably, the highest enantioselectivity to date (96% ee) for PCHC was achieved with an unsymmetric enantiopure Co(III)-salen catalyst in combination with a cocatalyst, bis(triphenylphosphine)iminium chloride.[20] Additionally, this approach may serve as a useful method for enantioselective desymmetrization of meso-epoxides and kinetic resolution of racemic epoxides. Monoanionic and chelating β-diketiminate ligands have found widespread use in coordination chemistry and catalysis.[21] Modulation of substituents around the ligand skeleton can Figurestrongly influence the steric and electronic behavior of the ligands[22] and enables them to be used in numerous catalytic applications.[23] Likewise, isoelectronic and structurally related variants of β-diketiminate ligands, such as triazapentadienates, formazanates, anilido-aldimines, and imine-oxazolinates, have also been examined for different catalytic reactions.[24] Particularly, the anilido-aldimine moiety has been incorporated into dinucleating zinc complexes (Figure 33, C) that show high activity toward CO_2/CHO copolymerization.[25] However, the chiral version of these ligands is relatively less explored in catalysis;[26] the Coates's Zn imine-

oxazoline catalysts are an eminent example.[16] Recently, we have prepared a series of unsymmetrical β-diketimine-type ligands incorporating a chiral 2-oxazoline moiety (Figure 33, D).[27] On the basis of the studies mentioned above,[16,25] their zinc complexes are expected to be effective initiators for alternating copolymerization of CO_2 and CHO. Although being C_1 symmetric, they could be advantageous, as the dissymmetric environment is postulated to enhance the asymmetric induction in the CO_2/CHO copolymerization.[20] Herein, we present the synthesis and characterization of zinc complexes of several C_1-symmetric chiral amido-oxazolinate ligands and their catalytic applications in the alternating copolymerization of CO_2 and CHO.

3.2. Results and Discussion

3.2.1. Synthesis of Zinc Complexes

The chiral, unsymmetrical amido-oxazolinate ligands, a variation of β-diketimine type, have been obtained via a palladium-catalyzed Buchwald−Hartwig amination reaction (Scheme 3).[27] The modular approach allows independent variations of the two stereodirecting groups (R_1 and R_2) in the ligand framework, and various substituents are incorporated into the framework in order to explore the steric and electronic effects of substituents and their possible synergy in catalysis.

Following previous reports,[10b] the zinc amide complexes (**2a−m**) were prepared by treatment of the free ligands with 1 equiv. of $Zn[N(SiMe_3)_2]_2$ in dry toluene at room temperature (Scheme 2).[28] The desired products were readily isolated in high yields within a few hours. In comparison, similar reactions with conventional β-diketiminate ligands were carried out under higher temperature (80 °C) and with longer times (20 h to days).[10b]

In the ^{1}H NMR spectra, the disappearance of the free ligand NH signals around 10−11 ppm and the appearance of new broad singlets in the upfield region at 0.1 to −0.05 ppm are consistent with the incorporation of a single amidooxazolinate ligand in the products. The new broad signals, assigned to the trimethylsilyl groups, usually appear as one singlet at ambient temperature that integrates to 18 protons; however, two broad singlets were observed in some cases for N(SiMe$_3$)$_2$ protons. The splitting may indicate restricted rotation of the N(SiMe$_3$)$_2$ group, resulting from its steric interaction with the substituents on either side, e.g., ^{t}Bu (**2c**, **2m**) or D^{i}PP (**2g**, **2h**), or with another −N(SiMe$_3$)$_2$ group in a dimeric arrangement (**2k**, **2l**). In the ^{13}C NMR spectra, the peaks around 4.80−5.50 ppm were assigned to the carbon of the silyl group, consistent with the formation of the amidooxazolinate zinc complexes.

	R1	R2		R1	R2
a	2,6-DMP	(S)-^{i}Pr	g	2,6-D^{i}PP	(S)-^{i}Pr
b	2,6-DMP	(S)-^{s}Bu	h	2,6-D^{i}PP	(R)-^{i}Bu
c	2,6-DMP	(S)-^{t}Bu	i	(R)-CHMePh	(R)-^{i}Bu
d	2,6-DMP	(R)-^{i}Bu	j	(R)-CHMeNaph	(S)-^{i}Pr
e	2,6-DMP	(R)-Ph	k	COPh	(S)-^{i}Pr
f	3,5-BTP	(R)-Ph	l	COPh	(R)-^{i}Bu
			m	(S)-SO^{t}Bu	(R)-^{i}Bu
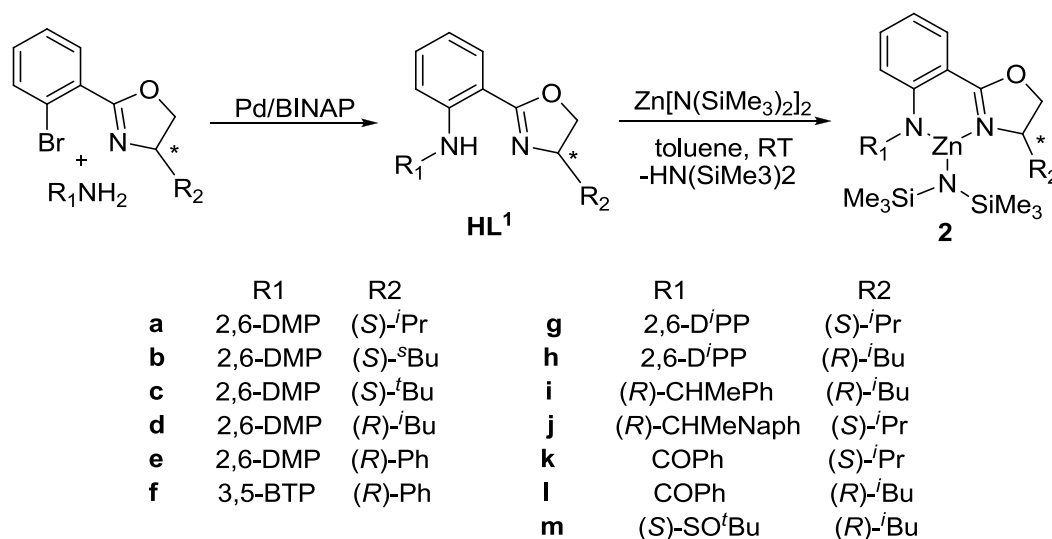
Scheme 3. Synthesis of ligands and zinc amide complexes

Formation of homoleptic bis-ligated zinc complexes was not observed, which may suggest that the steric bulk of the ligands is sufficient to stabilize the unsaturated, three-coordinate metal center and prevent the coordination of an additional ligand. In fact,

treatment of complex **2a** with excess THF or pyridine shows no sign of binding, as judged by ^{1}H NMR. However, when the steric bulk is reduced, e.g., in **2k** and **2l**, additional set of signals appears in the ^{1}H NMR spectra. For example, besides the septet at 1.60 ppm, assigned to the methine proton of $-CH(CH_3)_2$ in **2k**, a smaller septet at 1.86 ppm is also observed.[29] This is attributed to the monomer/dimer equilibrium in solution (Scheme 4), which is further supported by dilution studies of **2k** using ^{1}H NMR. The relative intensity of the aforementioned signals varies with dilution. As the dilution of the solution was increased, **2k** became a more monomeric species, from which $K_{eq} = 75.4$ M^{-1} (20 °C in CDCl$_3$) can be derived. The value is analogous to an acetate bridged β-diketiminate dimer ($K_{eq} = 207$ M^{-1} at 20 °C in C$_6$D$_6$).[10d] Addition of THF or pyridine has little effect on the equilibrium. This may suggest that the side-arm amide oxygen can coordinate intramolecularly or form a bridge between two metals. In the solid state, compound **2k** exists as an amide oxygen-bridged dimer, as confirmed by the X-ray structural analysis. However, compound **2m**, with a sulfinamido side arm, shows no evidence of dimer/monomer equilibrium, and a single set of signals is observed in the ^{1}H NMR spectrum. It is possible that **2m** exists as a monomeric species with sulfinamido oxygen weakly coordinated to the zinc center. Given the interest in bimetallic catalysis, the obse-
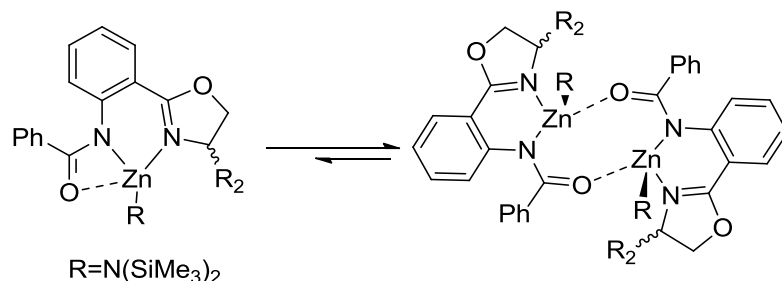
Scheme 4. Monomer/dimer equilibrium for **2k** and **2l**

-rvation here with **2k** and **2l** may suggest a different approach to constructing bimetallic systems. As zinc β-diketiminate complexes with various initiating groups are known for the copolymerization reaction of epoxides and CO_2, we attempted to synthesize zinc complexes with alkoxide and carboxylate groups, starting from different zinc precursors, such as $Zn(OAc)_2$ and $ZnCl_2$, after deprotonation of ligands with ^nBuLi.[10a–d] However, no desired complex was isolated from these reactions. In an alternative route, the zinc amide complex (**2a**) was allowed to react with a stoichiometric amount of 2-propanol, and formation of alkoxide was indicated by the new peaks at 3.42 and 1.60 ppm for (**L^{1a}**)Zn-O^{i}Pr. However, the reaction appeared to be complicated by side reactions, and attempted purification led to the decomposition of complex to free ligand. These observations are in contrast with the conventional zinc β-diketiminate complexes and may be a reflection of the inherent basicity of the amido nitrogen in the present system.[25]

3.2.2. X-ray Structures

Single crystals of compound **2a** were obtained from concentrated solutions in toluene at −20 °C. The solid-state structure was determined by single-crystal X-ray diffraction techniques; the X-ray crystal data and data collection and refinement parameters are summarized in Table S1 in the Supporting Information (Table S1). The structure of complex **2a** is depicted in Figure 34 with selected bond distances and bond angles. In agreement with the solution NMR data, **2a** is a monometallic, C_1-symmetric, three-coordinate zinc complex, and the geometry at zinc metal was best described as trigonal planar, as the sum of the bond angles around the zinc atom is 359.48°.
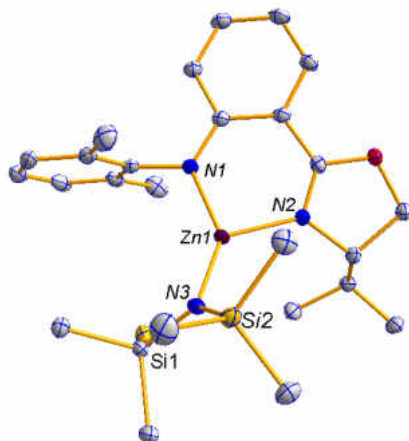
Figure 34. ORTEP drawing of complex **2a** with thermal ellipsoids drawn at the 50 % probability level. Selected bond distances (Å) and bond angles (°): Zn–N(1) 1.915(10), Zn–N(2) 1.968(9), Zn–N(3) 1.874(9), N(1)–Zn–N(2) 94.98(4), N(1)–Zn–N(3) 139.15(4), N(2)–Zn–N(3) 125.35(4). Hydrogen atoms are omitted for clarity.

The chelating amido-oxazolinate ligand forms a slightly puckered six-membered ring with the zinc metal through its two nitrogen atoms. The bond distance of $Zn-N_{imino}$ (1.968(9) Å) is considerably longer than that of $Zn-N_{amido}$ (1.915(10) Å), presumably due to the stronger interaction with the anionic amido nitrogen. The difference (~0.05 Å) is similar to those in other unsymmetrical NN bidentate ligation with less resonance character,[30] but longer than those in more symmetrical, β-diketiminate complexes (0.01−0.04 Å).[10b,31] The bond distance of Zn−N3 (1.874(9) Å) is on the shorter end of the Zn−Nsilylamide bonds reported.[31,32] The bond angle of N1−Zn−N3 (139.15(4)°) is larger than that of N2 −Zn−N3 (125.35(4)°), due to higher steric repulsion between the DMP group and the N(SiMe₃)₂ group. This leads to the N(SiMe₃)₂ group tilting toward the imine side. On the other hand, due to the chiral center at the 4- oxazoline position (S configuration), the plane defined by N3− Si1−Si2 is not perpendicular to the N1−N2−N3 coordination plane; instead, it is twisted 31.43(3)° from its regular perpendicular position, with one of the silyl groups staying away from the ^{i}Pr group on the same side. In turn, the DMP group is 17.66(4)° away from perpendicular to the plane defined by N(1)−N(2)−N(3) due to steric repulsions.

Moreover, the bite angle N1−Zn−N2 was sharper than the other bonds (N1−Zn−N3, N2−Zn−N3). To further probe the influence of the chiral center on the conformation of the
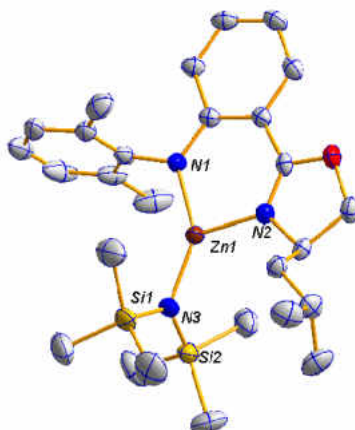
Figure 35. ORTEP drawing of complex **2d** with thermal ellipsoids drawn at the 50 % probability level. Selected bond distances (Å) and bond angles (deg): Zn–N(1) 1.912(15), Zn–N(2) 1.975(16), Zn–N(3) 1.877(15), N(1)–Zn–N(2) 95.84(6), N(1)–Zn–N(3) 142.72(7), N(2)–Zn– N(3) 121.43(7). Hydrogen atoms are omitted for clarity.

zinc complexes, we determined the X-ray crystal structure of **2d**, containing an *R* configuration at the 4-oxazoline position with a ^{i}Bu group. The modification of the chiral configuration on the oxazoline ring did not lead to considerable changes in the coordination geometry around the metal center. Complex **2d** was isomorphic with **2a**, featuring a distorted trigonal-planar geometry and similar geometric parameters (Figure 35). The smaller bond angle of N2−Zn− N3 = 121.43(7)° in **2d** compared to **2a** (125.35(4)°) can beattributed to the smaller steric bulk of ^{i}Bu (**2d**) compared to ^{i}Pr (**2a**), which imposes less repulsion with the trimethylsilyl group. In accord with this, the six-membered chelating ring is almost planar; the Zn atom is displaced only by 0.0877(2) Å from the plane through other five atoms. Because of the *R* configuration at the chiral center, the silylamido groups twisted in the opposite orientation (compared with that in **2a**), but to a lesser extent (8.54(7)° vs 31.43(3)° in **2a**), again due to ^{i}Bu being less demanding than ^{i}Pr. The DMP group is slightly tilted, by 12.81(6)°, from its perpendicular position.
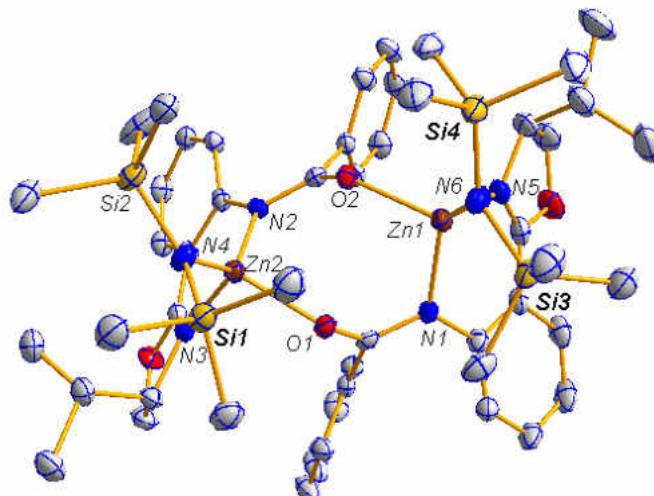
Figure 36. ORTEP drawing of complex **2k** with thermal ellipsoids drawn at the 50 % probability level. Selected bond distances (Å) and bond angles (deg): Zn(1)–N(1) 2.032(2), Zn(1)–N(5) 2.075(2), Zn(1)–N(6) 1.921(19), Zn(1)–O(2) 2.025(16), N(1)–C(1)1.321(3), O(1)–C(1)1.271(3), N(1) –Zn(1)–N(5) 88.42(8), N(1)–Zn(1)–N(6) 132.52(8), N(5)–Zn(1)–N(6) 115.02(8), N(1)–Zn(1)–O(2) 100.22(7), N(5)–Zn(1)–O(2) 99.32(7). Hydrogen atoms are omitted for clarity.

Suitable crystals of complex **2k** were obtained from recrystallization in dry toluene at room temperature, and single-crystal X-ray determinations confirm its dimeric form in the solid state (Figure 36). The two zinc centers are bridged by the amide oxygen of the other ligand to form a tub-like eightmembered ring (Zn1−N1−C1−O1−Zn2−N2−C2−O2). Each zinc metal is ligated with the two nitrogens of the ligand, one nitrogen of the silylamide, and one oxygen atom from benzamide in a distorted tetrahedral geometry. The bond distances of Zn−N are considerably longer than those in monomeric zinc complexes **2a** and **2d**, but are typical of tetrahedron geometry due to its more crowded environment than the trigonal-planar geometry.[33] The relative distances follow a similar pattern to that in monomeric zinc complexes, as Zn−Nimino (2.075(2) Å) is ~0.043 Å longer than Zn−Namido (2.032(2) Å) and Zn−Nsilylamide (1.921(19) Å) is the shortest. The two bis(trimethylsilyl)amido groups are oriented in a *syn* fashion. The isopropyl groups on the oxazoline ring and the amido phenyl groups are arranged in an *anti* manner with respect to the NN chelate.

3.2.3. Copolymerization Studies

Our interest in the present system has been twofold. First, we investigate the zinc complexes as potential catalysts for alternating copolymerization of CO_2 and CHO. Second, we want to address the effect of the ligand design on the asymmetric incorporation of CHO monomer into the polymer chain. Compound **2a** was used as a catalyst for initial optimization. Reaction conditions such as temperature, reaction time, pressure of the CO_2, and additive were varied. The selectivity, or the percentage of polycarbonate linkage, was determined by measuring the relative intensity of the methine proton signals of the carbonate linkage (δ = 4.6 ppm) and ether linkage (δ = 3.4 ppm). In no cases was the generation of cyclic carbonate observed (δ = 4.0 ppm). Selected results are listed in Table 4. It is observed that the temperature and CO_2 pressure have a strong influence on the outcome of the copolymerization. The catalyst was inactive at room temperature. As expected, the conversion and carbonate linkages improved with the increasing CO_2 pressure from 100 to 500 psi (entries **2−4**). However, further increase in pressure seemed to be detrimental (entry 5). When the initiating group was changed from $N(SiMe_3)_2$ to an alkoxide $-O^iPr$ by in situ addition of 1 equiv. of ^iPrOH, comparable results were observed (entry **6** vs **4**). Despite the reasonable conversion, only low yields of polycarbonates were isolated, in part due to some weight loss during the reaction (up to 30%). The cause is unclear, but running the reaction without stirring seemed to alleviate the loss, as isolated yields are significantly higher (entry **7**), at the expense of longer reaction time and slightly lower carbonate linkage. Raising the temperature to 75 °C increased the conversion and shortened the time to 20 h without sacrificing yield and selectivity (entry **8**).

Table 4. Screening of the conditions for copolymerization of CO_2 and CHO[a]

entry	temp. (°C)	pressure (PSI)	t/h	stirring (rpm)	conversion (%)[b]	yield (%)[c]	carbonate linkages (%)[d]
1	RT	100	24	1000	0	-	-
2	50	100	24	1000	42	12	75
3	50	250	24	1000	59	7	85
4	50	500	24	1000	60	15	93
5	50	750	24	1000	27	11	75
6[e]	50	500	24	1000	60	13	96
7[f]	50	500	48	n. s.	62	38	81
8[f]	75	500	20	n. s.	80	36	85

[a]Reaction conditions: Copolymerization reactions were run in neat cyclohexene oxide (CHO) using 1 mol % catalyst **2a**. [b]Determined by ^1H NMR spectroscopy on crude reaction mixture. [c]Isolated yield assuming 100% polycarbonates. [d]Calculated by the integration of methine resonances in ^1H NMR spectra of polymers. [e]With added ^iPrOH (1 equiv to **2a**). [f]Not stirred

To investigate the effect of ligand architecture on catalytic performance, complexes **2a-m** with systematic modifications in substituents were employed for CHO and CO2 copolymerization under optimized conditions (500 psi of CO_2 pressure, 75 °C, without stirring, 20 h). The results are summarized in Table 5. Although the reaction rate is slow, with a TOF generally around $3-4h^{-1}$, all the compounds showed appreciable activity, and a white powdery polymer was isolated after workup. It appeared that the conversions were capped at ~80%, as increased reaction time showed little improvement, probably due to the high viscosity at the end of the reaction.[34] Little or no cyclic carbonate was noted; up to 95% polycarbonate linkage (**2b**) was obtained in the polymers. This level of selectivity is lower than the optimized β-diketiminato zinc catalysts,[10] but is comparable with the more closely related anilido-aldimine zinc catalysts.[25] Electron-withdrawing groups are known to increase the Lewis acidity and catalytic activity of the metal.[10,16] However, introduction of CF_3 groups at the meta positions of the phenyl group significantly raised the catalytic activity of **2f** toward homopolymerization of CHO, as only a small amount of

polycarbonate linkage (6%) was incorporated, although the molecular weight is high (26.2 kg/mol). Introduction of a second alkyl chiral group at the amido side (**2i**, **2j)** led to lower conversion, presumably because the free rotation of the less bulky substituents on amido nitrogen may hinder CHO entrance to the active site.[4c,10b,35] Restricted rotation of the aniline has been observed to be important in facilitating catalytic activity in olefin polymerization.[36] Despite the less bulky substituent in **2k** and **2l**, both showed high conversion, which may be indicative of bimetallic action. However, compound **2m** with sulfinamide was very sluggish, and it afforded a polymer with high polyether linkage and narrow PDI value.

Table 5. Copolymerization of CHO and CO_2 using catalysts **2a-2m**[a]

entry	cat.	conv. (%)[b]	carbonate linkages (%)[c]	m-centered tetrad (%)[d]	yield (%)[e]	Mn (kg/mol)[f]	PDI[f]	SS/RR[g]
1	**2a**	80	85	69	36	6.5	1.3	42/58
2	**2b**	77	95	67	18	13.4	4.2[h]	i
3	**2c**	69	90	69	32	3.1	1.4	48/52
4	**2d**	62	72	66	18	9.1	2.0	56/44
5	**2e**	66	85	62	23	11.6	7.0[h]	52/48
6	**2f**	83	6	-	42	26.1	1.9	-
7	**2g**	82	56	70	32	6.1	1.7	41/59
8	**2h**	81	72	72	43	11.3	1.6	71/29
9	**2i**	58	90	65	20	14.1	7.0[h]	53/47
10	**2j**	59	60	43	13	2.9	1.2	i
11	**2k**	78	69	63	17	4.1	1.5	48/52
12	**2l**	81	83	70	16	2.6	1.2	52/48
13	**2m**	18	49	70	4	7.0	1.1	44/56

[a]Copolymerization reactions were carried out in neat CHO at 75 °C with [CHO]: [catalyst] = 100:1 at 500 PSI of CO_2. [b]Determined by ^{1}H NMR spectroscopy. [c]Calculated by the integration of methine resonances in ^{1}H NMR spectra of polymers. [d]Determined by ^{13}C NMR spectroscopy. [e]Isolated yields, assuming 100% polycarbonates. [f]Determined by gel permeation chromatography calibrated with polystyrene standards in tetrahydrofuran. [g]Determined by chiral GC on diols after hydrolysis. [h]Bimodel distribution of polymer. [i]racemic

The molecular weight of the polycarbonate was determined by GPC against a polystyrene standard. The polycarbonate produced by the zinc catalysts showed similar or lower molecular weight compared with calculated values based on conversion, indicative of the presence of a chain transfer process during the reaction, and the molecular weight distribution is somewhat broad (PDI 1.1−2.0). In a few cases (**2b**, **2e**, and **2i**), the PDI values were inflated by the presence of an additional peak at higher molecular weights.[29] The bimodal distributions of polycarbonates have been noted in several zinc-catalyzed copolymerizations and may arise from the presence of multiple active sites or monomer/dimer equilibrium of the catalytic species.[8a,37] The microstructure (tacticity) of the resulting polymers was characterized by ^{13}C NMR spectroscopy. Typically three distinct resonances were observed at 154.03, 153.52, and 153.37 ppm in the carbonyl regions of PCHCs (Figure **37a**).
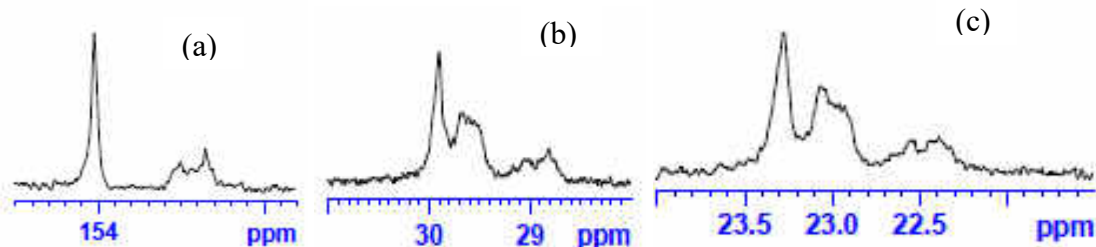
Figure 37. ^{13}C-NMR spectrum of the poly (cyclohexene carbonate) generated by catalyst **2c**. (a): carbonyl region; both (b) and (c): methylene region

Based on the previous assignments, [16,38] the largest peak at 154.03 ppm was correlated to *m*-centered tetrads ([*mmm*] and [*mmr*]), and the remaining tetrad upfield resonances (δ = 153.52 and 153.37 ppm) were assigned to the *r*-centered tetrads ([*mrm*] and [*mrr*]). The other common tetrads in isotactic polymers [*rmr*] and [*rrr*] were not observed. In accord with this, two series of methylene triad resonances were observed corresponding to two nonequivalent methylene carbons in the ^{13}C NMR spectra (Figure

37b and **c**). The two downfield resonances (δ = 29.90 (**b**), 23.28 (**c**)) correspond to [*mm*] triads, and the intensity is relatively higher than the other triads [*mr*] (δ = 29.66 (**b**), 23.06 (**c**)) and [*rr*] (δ = 29.05 (**b**), 22.54 (**c**)). The other peaks in this region correspond to polyether linkage.[15,38] On the basis of these assignments, most of the catalysts yield isoenriched PCHC with high *m*-centered tetrads. Increased steric bulk in the catalysts seems to favor higher microstructure regularity in the resultant polycarbonates, as the highest isotacticity (72% *m*-centered tetrads) was obtained with catalyst **2h**, which bears 2,6-D*i*PP and *i*Bu groups on its ligand backbone. Curiously, catalyst **2j** produces a slightly syndioenriched PCHC with 57% *r*-centered tetrads, which is a rather rare case.[38] The two different configurations of chiral centers might have influence on this reverse selectivity.

To further investigate the microstructure assignment and reaction mechanisms, statistical methods were applied to simulate the tetrad distributions observed in PCHC.[16,38] When two models based on chain-end control and enantiomorphic site control mechanisms are compared, the latter seems to give better agreement between calculated and observed tetrad intensities.[29,39] The enantioselectivity parameter α, the probability of an *R* monomer unit adding at the *R* site or an *S* monomer unit adding at the *S* site, has been calculated, with the highest value being 0.85 with **2h**.[29] The numbers are comparable with those obtained with zinc imine-oxazoline catalysts.[16] On this basis we hypothesize the present system follows an enantiomorphic site control mechanism.[11,16] However, this process may be competitive with a chain-end control mechanism.[38]

The hydrolysis of resulting copolymers, by an alkali treatment, followed by neutralization with 1 M HCl, gave 1,2-trans-cyclohexanediol in 70−80% isolated yields. Chiral GC analysis of the diol indicates that these chiral catalysts can induce asymmetry

during the copolymerization, although the enantiomeric excess was generally low (Table 5). Among them, catalyst **2h** exhibited the highest enantiomeric excess of 71:29 (SS:RR) (Table 5, entry **8**). It should be noted that catalyst **2h** also afforded the highest isotacticity in the series. When compared with related zinc imine-oxazoline catalysts (see Figure 33, B) with an *RR*:*SS* ratio up to 86:14,[16] the stereoselectivity exhibited by the present catalysts is low, especially considering the resemblance in their structural features and the similarity in the enantioselectivity parameter α. The exact reason is not understood at the moment, although it is suspected that the low selectivity of the present system might be due to some electronic effect resulting from attenuated resonance in the ligand backbone.[40] Nevertheless, they have the same sense of chiral induction, and the chirality of the diol is mostly influenced by the configuration of the oxazoline substituents, as an R configuration at the 4-oxazoline position results in enrichment of opposite configurations in the diol unit.[16] The combination of a bulky group at the amide side and a long, bulky group at the imine side seems to work best. The second chiral group at the amide side may also play a significant role; however, a synergistic interaction between the two is not observed.

3.3. Conclusions

A family of new chiral zinc complexes has been synthesized via the reaction of $Zn[N(SiMe_3)_2]_2$ and the corresponding C_1-symmetric, monoanionic amido-oxazolinate ligands (HL**1a−m**). While most of them exist as mononuclear complexes, as confirmed by single-crystal X-ray structural analysis of **2a** and **2d**, complexes **2k** and **2l**, with less bulky substituents, are dimeric in the solid state and are in equilibrium between monomer and dimer in solution. All of them are shown to be viable initiators for copolymerization of CO_2 and CHO, yielding polymers with up to 95% polycarbonate linkage and moderate

molecular weights and polydispersity values. Modifications around the ligand architecture have a significant influence on the polymerization process. The resultant polymers are isotactic with enriched m-centered tetrads, except for **2j**, which produces a syndioenriched PCHC. Induction of main chain chirality is feasible, with up to 42% ee obtained with **2h**, and can be correlated roughly with the chiral centers in ligands, although enantioselectivity is usually very low. In general, catalysts with one chiral center on the oxazoline moiety (R_2 position) and a sufficiently bulky group on the amido nitrogen (R_1 position) seem to provide better structural requirements for activity and selectivity. Current efforts are under way for a better understanding of the effect of ligand architecture in the copolymerization process and improving the activity and selectivity of the catalysts.

3.4. Experimental Conditions

General Procedures: All reactions that involved compounds sensitive to air and/or moisture were carried out under a dry nitrogen atmosphere using freshly dried solvents and standard Schlenk line and glovebox techniques. All chemicals were purchased from Aldrich except where noted. Toluene was distilled under nitrogen from Na/benzophenone. $CDCl_3$ and C_6D_6 were dried over CaH_2 and Na/benzophenone, respectively, and distilled and degassed prior to use. Carbon dioxide (Airgas, high purity, 99.995%) was used as received. Cyclohexene oxide was distilled from CaH_2 following three freeze−pump−thaw cycles and stored in a glovebox prior to use. Zinc bis(trimethylsilyl)amide was prepared according to the literature.[41]

NMR spectra were recorded on a Bruker AVANCE-500 NMR spectrometer (^{1}H and ^{13}C). Chiral GC analysis was carried out on an Agilent 7890 with FID detector using

a chiral column (cyclodex-B, 30 m × 0.250 mm × 0.25 μm). The temperature program was as follows: injector temperature 250 °C, detector 300 °C, oven initial temperature 120 °C, hold for 30 min, ramp at 30 °C/min to 200 °C, hold for 10 min. Inlet flow: 85 mL/min (split mode, 68:1). Gel permeation chromatography (GPC) analysis was performed on a Varian Prostar, using a PLgel 5 μm Mixed-D column, a Prostar 355 RI detector, and THF as eluent at a flow rate of 1 mL/min (20 °C). Polystyrene standards were used for calibration.

Synthesis of Zinc Complexes

Synthesis of (4S)-4,5-dihydro-2-[2'-(2,6-dimethylanilino)phenyl]-4-$tert$-butyloxazole (HL^{1c}). Synthesis of this new ligand was performed analogously following the literature. Yield (98 %). ^{1}H NMR (500.1 MHz; CDCl$_3$; 298 K): 0.95 (9H, s, C(CH_3)$_3$), 2.22 (6H, s, ArMe), 4.27 (2H, m, NCH(R)CH_2O), 4.30 (1H, m, NCH(R)CH$_2$O), 6.23 (1H, d, J = 8.80, m-PhHN), 6.65 (1H, t, J = 7.50, p-PhH(CH$_3$)$_2$), 7.10-7.15 (4H, br, ArH), 7.79 (1H, d, J = 7.90, o-PhHN), 10.01 (1H, br, NH). ^{13}C NMR (125.8 MHz; CDCl$_3$; 298 K): 18.62 (ArMe), 26.07 (C(CH$_3$)$_3$), 34.10 (C(CH$_3$)$_3$), 67.02 (NCH(R)CH$_2$O), 76.42 (NCH(R)CH$_2$O), 108.66, 112.72, 115.35, 126.22, 129.90, 132.29 (CH$_{arom}$).136.47, 137.03, 138.23, 147.84, 164.05 (C_{quart}). GC/MS: m/z = 322[M]$^+$, 307, 291, 222, 208, 194. HRMS (ESI): m/z calcd for C$_{21}$H$_{26}$N$_2$O [M]$^+$: 322.20451; found: 322.21233

Synthesis of (4R)-4,5-dihydro-2-[2'-(3,5-bis(trifluoromethyl)anilino)phenyl]-4-phenyloxazole(HL^{1f}). Synthesis of this new ligand was performed analogously following the literature. Yield (66 %). ^{1}H NMR (500.1 MHz; CDCl$_3$; 298 K): 3.84 (1H, t = 8.12, NCH(R)CH$_2$O), 4.39 (1H, t, J = 8.80, NCH(R)CH_2O), 5.51 (1H, m, t, J = 8.70, NCH(R)CH_2O), 6.46 (1H, d, J = 7.8 m-PhHN), 6.96 (3H, m, ArH), 7.02-7.04 (4H, m, ArH), 7.05-7.09 (3H, m, ArH), 7.60 (1H, dr, J = 8.2, o-PhHN), 10.51 (1H, br, NH). ^{13}C NMR

(125.8 MHz; CDCl$_3$; 298 K): 70.32 (NCH(R)CH_2O), 73.62 (NCH(R)CH_2O), 112.27 (Ar-CF_3), 114.35 (Ar-CF_3), 115.29, 119.67, 119.80, 120.01, 122.44, 124.60, 126.70, 128.02, 129.07, 130.78 (CH_{arom}) 132.20, 132.77, 133.27, 142.31, 143.60, 143.98, 163.40 (C_{quart}). GC/MS: m/z = 450[M]$^+$, 331, 331, 304. HRMS (ESI): m/z calcd for $C_{23}H_{17}F_6N_2O$ [M+H]$^+$: 451.12451; found: 451.12450.

Synthesis of [(L^{1a})ZnN(SiMe$_3$)$_2$] (2a). A solution of ligand **HL^{1a}** (414 mg, 1.342 mmol) in toluene (10 mL) was added into zinc bis(trimethylsilyl)amide (543 mg, 1.406 mmol) in toluene (5 mL) at room temperature. After being stirred for 8 hr, the pale yellow solution was dried *in vacuo*, giving the desired compound as yellow powder (98 %, 704 mg). Recrystallization from toluene at -20 °C gave yellow colored crystals (90 %, 643 mg) suitable for single crystal X-ray diffraction analysis. ^{1}H NMR (500.1 MHz; CDCl$_3$; 298 K): -0.15 (18H, s, N(SiMe$_3$)$_2$), 0.90 (3H, d, J = 7.14, (CH_3)$_2$CH), 1.02 (3H, d, J = 7.10, (CH_3)$_2$CH), 2.01 (3H, s, ArMe), 2.24 (3H, s, ArMe), 2.41 (1H, m, (CH$_3$)$_2$CH), 4.39 (1H, t, J = 7.10, NCH(R)CH$_2$O), 4.47 (1H, t, J = 8.0, NCH(R)CH_2O), 4.51(1H, m, NCH(R)CH_2O), 6.22 (1H, d, J =8.70, m-PhHN), 6.45 (1H, t, J = 8.10, p-PhH(CH$_3$)$_2$), 7.01 (1H, t, J = 7.94, m-PhHN), 7.08 (2H, br, m-PhH(CH$_3$)$_2$), 7.16 (1H, t, J = 7.84, p-PhHN), 7.82 (1H, d, J = 8.06 o-PhHN). ^{13}C NMR (125.8 MHz; CDCl$_3$; 298 K): 4.87 (SiMe_3), 15.10 ((CH)Me_2), 19.10 (ArMe), 19.16 (ArMe), 31.38 ((CH)Me$_2$), 66.94 (NCH(R)CH$_2$O), 69.24 (NCH(R)CH_2O), 103.86, 113.05, 116.24, 124.41, 129.99, 131.60 (CH_{arom}), 134.25, 134.51, 147.2, 157.18, 169.50 (C_{quart}). Anal. Calcd for $C_{26}H_{41}N_3OSi_2Zn$: C, 58.57; H, 7.75; N, 7.88. Found: C, 57.18; H 7.91; N, 7.58.

Synthesis of [(L^{1b})ZnN(SiMe$_3$)$_2$] (2b). A solution of ligand **HL^{1b}** (237 mg, 0.735 mmol) in toluene (5 mL) was added into zinc bis(trimethylsilyl)amide (283 mg, 0.735 mmol) in

toluene (5 mL) at room temperature. After being stirred for 8 hr, the pale yellow colored solution was dried *in vacuo*, giving the desired compound as yellow powder (89%, 357 mg). ^{1}H NMR (500.1 MHz; CDCl$_3$; 298 K): -0.24 (18H, s, C*H*$_3$), 0.84 (3H, m, C*H*$_3$CHCH$_2$CH$_3$), 1.02 (3H, m, CH$_3$CHCH$_2$C*H*$_3$), 1.27 (1H, m, CH$_3$CHC*H*$_2$ CH$_3$), 1.34 (1H, m, CH$_3$CHC*H*$_2$CH$_3$), 1.43 (1H, m, CH$_3$C*H*CH$_2$CH$_3$), 2.00 (3H, s, Ar*Me*), 2.18 (3H, s, Ar*Me*), 4.49 (1H, t, *J* = 8.54, NC*H*(R)CH$_2$O), 4.55 (1H, t, *J* = 9.67, NCH(R)C*H*$_2$O), 4.61 (1H, t, *J* = 8.55, NCH(R)C*H*$_2$O), 6.23 (1H, d, *J* = 9.30, *m*-Ph*H*N), 6.47 (1H, t, *J* = 7.90, *p*-Ph*H*(CH$_3$)$_2$), 7.01 (1H, t, *J* = 7.67, *p*-Ph*H*N), 7.07 (1H, br, *m-PhHN*), 7.23-7.48 (2H, br, *m*-Ph*H*(CH$_3$)$_2$), 7.81 (1H, d, *J* = 8.29, *o*-Ph*H*N). ^{13}C NMR (125.8 MHz; CDCl$_3$; 298 K): 4.80 (Si*Me*$_3$), 12.10 (CHCH$_2$(*CH*$_3$)$_2$), 12.21 (CHCH$_2$(*CH*$_3$)$_2$), 18.69 (Ar*Me*), 18.98 (Ar*Me*), 26.85 (CHC*H*$_2$(CH$_3$)$_2$), 37.98 (*C*HCH$_2$(CH$_3$)$_2$), 66.61 (N*C*H(R)CH$_2$O), 68.17 (NCH(R)*C*H$_2$O), 103.96, 113.03, 116.25, 124.36, 125.53, 128.47 (*C*H$_{arom}$), 131.02, 131.20, 134.41, 147.22, 157.11, 169.45 (*C*$_{quart}$). Anal. Calcd for C$_{27}$H$_{43}$N$_3$OSi$_2$Zn·0.2C$_7$H$_8$: C, 60.30; H, 7.95; N, 7.43. Found: C, 60.39; H 7.61; N, 6.67.

Synthesis of [(L^{1c})ZnN(SiMe$_3$)$_2$] (2c). To a solution of ligand **HL^{1c}** (113 mg, 0.350 mmol) in toluene (5 mL), zinc bis(trimethylsilyl)amide (135 mg, 0.351 mmol) was added at room temperature. After being stirred for 8 hr, ^{1}H NMR confirmed the incomplete conversion of the ligand into zinc complex. An additional amount of zinc bis(trimethylsilyl)amide (8 mg, 0.021 mmol) was added. After 4 hr of stirring, the yellow colored solution was dried *in vacuo*, giving the desired compound as yellow powder (92 %, 177 mg). ^{1}H NMR (500.1 MHz; CDCl$_3$; 298 K): -0.36 (9H, s, C*H*$_3$), 0.04 (9H, s, C*H*$_3$), 1.01 (9H, s, C(C*H*$_3$)$_3$), 2.23 (3H, s, Ar*Me*), 2.27 (3H, s, Ar*Me*), 4.21 (1H, m, NC*H*(R)CH$_2$O), 4.40 (1H, t, *J* = 9.70, NCH(R)C*H*$_2$O), 4.56 (1H, m, NCH(R)C*H*$_2$O), 6.20 (1H, d, *J* = 9.13, *m*-Ph*H*N), 6.42 (1H,

m, *p*-Ph*H*(CH$_3$)$_2$), 7.02-7.18 (3H, m, Ar*H*), 7.20 (1H, m, Ar*H*), 7.83 (1H, d, *J* = 8.28, *o*-Ph*H*N). ^{13}C NMR (125.8 MHz; CDCl$_3$; 298 K): 5.19 (Si*Me*$_3$), 5.28 (Si*Me*$_3$), 18.46 (Ar*Me*), 18.84 (Ar*Me*), 25.27 (C(*C*H$_3$)$_3$), 34.95 (*C*(CH$_3$)$_3$), 68.41 (N*C*H(R)CH$_2$O), 73.34 (NCH(R)*C*H$_2$O), 103.37, 112.85, 115.82, 124.50, 128.99, 129.28, 131.81 (*C*H$_{arom}$).134.20, 134.62, 134.78, 147.09, 157.37, 170.54 (*C*$_{quart}$).

Synthesis of [(L^{1d})ZnN(SiMe$_3$)$_2$] (2d). A solution of ligand **HL^{1d}** (316 mg, 0.980 mmol) in toluene (10 mL) was added into zinc bis(trimethylsilyl)amide (378 mg, 0.980 mmol) in toluene (5 mL) at room temperature. After being stirred for 8 hr, the pale yellow colored solution was dried *in vacuo*, giving the desired compound as yellow powder (552 mg). The light yellow colored solid was recrystallized from toluene at -20 °C to give yellow colored crystals (93%, 502 mg). ^{1}H NMR (500.1 MHz; CDCl$_3$; 298 K): -0.01 (18H, s, C*H*$_3$), 1.21 (6H, m, CH$_2$CH(C*H*$_3$)$_2$), 1.74 (1H, m, CH$_2$C*H*(CH$_3$)$_2$), 1.93 (1H, m, C*H*$_2$CH(CH$_3$)$_2$), 2.22 (3H, s, Ar*Me*), 2.39 (3H, s, Ar*Me*), 2.45 (1H, m, C*H*$_2$CH(CH$_3$)$_2$), 4.39 (1H, t, *J* = 8.23, NC*H*(R)CH$_2$O), 4.74 (1H, m, NCH(R)C*H*$_2$O), 4.84 (1H, t, *J* = 8.90, NCH(R)C*H*$_2$O), 6.42 (1H, d, *J* = 8.90, *m*-Ph*H*N), 6.63 (1H, m, *p*-Ph*H*(CH$_3$)$_2$, 7.19 (1H, br, *p*-Ph*H*N), 7.33 (2H, m, *m*-Ph*H*(CH$_3$)$_2$), 7.45 (1H, m, *m*-Ph*H*(CH$_3$)$_2$), 8.03 (1H, d, *J* = 8.50, *o*-Ph*H*N). ^{13}C NMR (125.8 MHz; CDCl$_3$; 298 K): 5.04 (Si*Me*$_3$), 18.71 (CHCH$_2$(*C*H$_3$)$_2$), 19.07 (CHCH$_2$(*C*H$_3$)$_2$), 22.23 (CH*C*H$_2$(CH$_3$)$_2$), 23.96 (Ar*Me*), 25.83 (Ar*Me*), 45.68 (*C*H$_2$CH(CH$_3$)$_2$), 63.60 (N*C*H(R)CH$_2$O), 71.80 (NCH(R)CH$_2$O), 104.03, 113.10, 116.26, 124.39, 125.47, 128.56, 129.03 (*C*H$_{arom}$), 134.04, 134.17, 134.47, 147.27, 157.05, 169.50 (*C*$_{quart}$). Anal. Calcd for C$_{27}$H$_{43}$N$_3$OSi$_2$Zn: C, 59.26; H, 7.92; N, 7.68. Found: C, 59.04; H 7.84; N, 7.44.

Synthesis of [(L^{1e})ZnN(SiMe$_3$)$_2$] (2e). To a solution of the ligand **HL^{1e}** (265 mg, 0.774 mmol) in toluene (10 mL), zinc bis(trimethylsilyl)amide (301 mg, 0.780 mmol) was added

at room temperature. After being stirred for 8 hr, the pale yellow colored solution was dried *in vacuo*, giving the desired compound as yellow powder (96%, 421 mg). ^{1}H NMR (500.1 MHz; CDCl$_3$; 298 K): -0.35 (18H, s, N(SiMe$_3$)$_2$), 1.98 (3H, s, ArMe), 2.23 (3H, s, ArMe), 4.53 (1H, m, NC*H*(R)CH$_2$O), 4.90 (1H, t, *J* = 8.90, NCH(R)C*H*$_2$O), 5.53 (1H, m, NCH(R)C*H*$_2$O), 6.27 (1H, d, *J* = 8.85, *m*-Ph*H*N), 6.50 (1H, t, *J* = 7.57, *p*-Ph*H*(CH$_3$)$_2$), 6.99 (1H, t, *J* = 7.81, *p*-Ph*H*N), 7.06 (1H, m, *m*-Ph*H*N), 7.12 (2H, m, *m*-Ph*H*(CH$_3$)$_2$), 7.35-7.40 (5H, m, C$_3$H$_3$NOPh*H*), 7.93 (1H, d, *J* = 8.37, *o*-Ph*H*N). ^{13}C NMR (125.8 MHz; CDCl$_3$; 298 K): 4.87 (Si*Me*$_3$), 18.67 (Ar*Me*), 18.98 (Ar*Me*), 68.11 (NCH(R)C*H*$_2$O), 74.0 (NCH(R)C*H*$_2$O), 103.86, 116.40, 118.24, 121.33, 124.39, 125.54, 127.09, 128.46, 128.92, 129.27, 129.50, 131.67 (*C*H$_{arom}$), 134.00, 134.09, 134.70, 141.34, 147.10, 157.46, 170.19 (*C*$_{quart}$). Anal. Calcd for C$_{29}$H$_{39}$N$_3$OSi$_2$Zn·0.5CH$_2$Cl$_2$: C, 58.11; H, 6.61; N, 6.89. Found: C, 58.25; H 6.79; N, 6.43.

Synthesis of [(L^{1f})ZnN(SiMe$_3$)$_2$] (2f). To a solution of ligand **HL^{1f}** (79 mg, 0.175 mmol) in toluene (4 mL), zinc bis(trimethylsilyl)amide (68 mg, 0.175 mmol) was added at room temperature. After being stirred for 8 hr, the pale yellow colored solution was dried in *vacuo*, giving the desired compound as yellow powder (68 %, 82 mg). ^{1}H NMR (500.1 MHz; CDCl$_3$; 298 K): -0.32 (18H, s, C*H*$_3$), 4.56 (1H, m, NC*H*(R)CH$_2$O), 4.93 (1H, t, *J* = 7.80, NCH(R)C*H*$_2$O), 5.51 (1H, m, NCH(R)C*H*$_2$O), 6.46 (2H, m, Ar*H*), 7.06 (1H, m, Ar*H*), 7.19 (2H, m, Ar*H*), 7.33-7.44 (3H, m, Ar*H*), 7.53 (2H, m, Ar*H*), 7.58 (1H, br, Ar*H*), 8.02 (1H, d, *J* = 9.35, *o*-Ph*H*N). ^{13}C NMR (125.8 MHz; CDCl$_3$): 5.52 (Si*Me*$_3$), 68.45 (NCH(R)C*H*$_2$O), 74.39 (NCH(R)C*H*$_2$O),115.30 (*C*F$_3$), 117.50 (*C*F$_3$), 122.50, 124.70, 125.55, 126.84, 127.33, 128.47, 128.62, 129.30, 129.74, 132.14 (*C*H$_{arom}$), 133.14, 135.22, 140.41, 152.67, 156.69, 157.38, 170.50 (*C*$_{quart}$).

Synthesis of [(L^{1g})ZnN(SiMe$_3$)$_2$] (2g). To a solution of ligand **HL^{1g}** (400 mg, 1.097 mmol) in toluene (15 mL), zinc bis(trimethylsilyl)amide (424 mg, 1.098 mmol) was added at room temperature. After being stirred for 8 hr, the yellow colored solution was dried *in vacuo*, giving the desired compound as yellow powder (89%, 575 mg). ^{1}H NMR (500.1 MHz; CDCl$_3$; 298 K): -0.30 (9H, s, C*H$_3$*), 0.03 (9H, s, C*H$_3$*), 0.92 (3H, d, *J* = 6.81, CH(C*H$_3$*)$_2$), 1.07 (6H, d, *J* = 7.03, ArCH(C*H$_3$*)$_2$), 1.17 (3H, d, *J* = 6.91, CH(C*H$_3$*)$_2$), 1.29 (6H, d, *J* = 6.75, ArCH(C*H$_3$*)$_2$), 1.57 (1H, m, C*H*(CH$_3$)$_2$), 3.02 (1H, m, ArC*H*(CH$_3$)$_2$), 3.28 (1H, m, ArC*H*(CH$_3$)$_2$), 4.40 (1H, t, *J* = 7.75, NC*H*(R)CH$_2$O), 4.47 (1H, t, *J* = 8.49, NCH(R)C*H$_2$*O), 4.54 (1H, m, NCH(R)C*H$_2$*O), 6.25 (1H, d, *J* = 9.25, *m*-Ph*H*N), 6.44 (1H, t, *J* = 8.49, *p*-Ph*H*(CH$_3$)$_2$), 7.19 (1H, t, *J* = 7.13, *m*-Ph*H*N), 7.20-7.24 (3H, m, Ar*H*), 7.81 (1H, d, *J* = 8.41, *o*-Ph*H*N). ^{13}C NMR (125.8 MHz; CDCl$_3$; 298 K): 5.10 (Si*Me$_3$*), 5.19 (Si*Me$_3$*), 21.20 (CH(*C*H$_3$)$_2$), 22.40 (CH(*C*H$_3$)$_2$), 24.25 (*C*H(CH$_3$)$_2$), 25.68 (ArCH(*C*H$_3$)$_2$), 26.54 (ArCH(*C*H$_3$)$_2$), 27.92 (ArCH(*C*H$_3$)$_2$), 28.92 (ArCH(*C*H$_3$)$_2$), 39.25 (Ar*C*H(CH$_3$)$_2$), 41.01 (Ar*C*H(CH$_3$)$_2$), 63.01 (N*C*H(R)CH$_2$O), 73.55 (NCH(R)*C*H$_2$O), 105.05, 112.12, 116.60, 122.26, 124.53, 127.46, 128.27 (*C*H$_{arom}$), 132.42, 136.49, 138.48, 144.89, 155.88, 168.54 (*C*$_{quart}$).

Synthesis of [(L^{1h})ZnN(SiMe$_3$)$_2$] (2h). To a solution of ligand **HL^{1h}** (137 mg, 0.362 mmol) in toluene (6 mL), zinc bis(trimethylsilyl)amide (140 mg, 0.362 mmol) was added at room temperature and stirred for 8 hr. The pale yellow colored solution was dried *in vacuo*, to give a yellow compound (89%, 195 mg). ^{1}H NMR (500.1 MHz; CDCl$_3$; 298 K): -0.22 (9H, s, C*H$_3$*), 0.03 (9H, s, C*H$_3$*), 0.92 (3H, d, *J* = 6.81, CH$_2$CH(C*H$_3$*)$_2$), 1.07 (6H, d, *J* = 7.03, ArCH(C*H$_3$*)$_2$), 1.17 (3H, d, *J* = 6.91, CH$_2$CH(C*H$_3$*)$_2$), 1.29 (6H, d, *J* = 6.75, ArCH(C*H$_3$*)$_2$), 1.57 (1H, m, CH$_2$C*H*(CH$_3$)$_2$), 1.76 (1H, m, C*H$_2$*CH(CH$_3$)$_2$), 2.22 (1H, m, C*H$_2$*CH(CH$_3$)$_2$),

3.07 (1H, m, ArC*H*(CH₃)₂), 3.28 (1H, m, ArC*H*(CH₃)₂), 4.26 (1H, t, *J* = 7.75, NC*H*(R)CH₂O), 4.60 (1H, m, NCH(R)C*H₂*O), 4.66 (1H, t, *J* = 8.49, NCH(R)C*H₂*O), 6.26 (1H, d, *J* = 9.25, *m*-Ph*H*N), 6.44 (1H, t, *J* = 8.49, *p*-Ph*H*(CH₃)₂), 7.05 (1H, t, *J* = 7.13, *m*-Ph*H*N), 7.20-7.28 (3H, m, Ar*H*), 7.83 (1H, d, *J* = 8.41, *o*-Ph*H*N). ^{13}C NMR (125.8 MHz; CDCl₃; 298 K): 5.21 (Si*Me₃*), 5.30 (Si*Me₃*), 22.30 (CHCH₂(*CH₃*)₂), 23.86 (CHCH₂(*CH₃*)₂), 24.25 (*C*HCH₂(CH₃)₂), 24.55 (CH*C*H₂(CH₃)₂), 25.33 (ArCH(*CH₃*)₂), 25.54 (ArCH(*CH₃*)₂), 25.92 (ArCH(*CH₃*)₂), 25.98 (ArCH(*CH₃*)₂), 28.25 (Ar*C*H(CH₃)₂), 45.01 (Ar*C*H(CH₃)₂), 63.61 (N*C*H(R)CH₂O), 71.55 (NCH(R)*C*H₂O), 104.05, 113.12, 118.60, 124.26, 125.53, 128.46, 131.25 (*C*H$_{arom}$), 133.61, 138.10, 144.61, 144.90, 158.59, 169.50 (*C*$_{quart}$).

Synthesis of [(L^{1i})ZnN(SiMe₃)₂] (2i). To a solution of ligand **HL^{1i}** (56 mg, 0.173 mmol) in toluene (10 mL), zinc bis(trimethylsilyl)amide (67 mg, 0.173 mmol) was added at room temperature and the mixture was stirred for 8 hr. The pale yellow colored solution was dried *in vacuo*, to afford the desired compound as yellow powder (68 %, 65 mg). ^{1}H NMR (500.1 MHz; CDCl₃; 298 K): 0.21 (18H, s, C*H₃*), 1.12 (6H, m, CH₂CH(C*H₃*)₂), 1.32 (1H, m, CH₂C*H*(CH₃)₂), 1.56 (1H, m, C*H₂*CH(CH₃)₂), 1.74 (1H, m, C*H₂*CH(CH₃)₂), 2.22 (3H, d, *J* = 8.35, ArCHC*H₃*), 4.18 (1H, m, ArC*H*CH₃), 4.58 (2H, m, NC*H*(R)C*H₂*O), 5.05 (1H, m, NCH(R)C*H₂*O), 6.50 (1H, t, *J* = 9.35, *m*-Ph*H*N), 6.83 (1H, d, *J* = 9.35, *m*-Ph*H*N), 7.12 (2H, t, *J* = 8.13, *o*-Ph*H*), 7.20-7.28 (4H, m, ArH), 7.97 (1H, d, *J* = 6.45, *o*-Ph*H*N). ^{13}C NMR (125.8 MHz; CDCl₃; 298 K): 5.52 (Si*Me₃*), 21.68 (CHCH₂(*CH₃*)₂), 24.14 (*C*HCH₂(CH₃)₂), 26.25 (ArCH*C*H₃), 44.68 (CH*C*H₂(CH₃)₂), 58.08 (Ar*C*HCH₃), 63.85 (N*C*H(R)CH₂O), 71.20 (NCH(R)*C*H₂O), 104.97, 112.56, 116.92, 126.34, 128.44, 128.62, 129.87, 131.85, 134.26 (*C*H$_{arom}$), 147.21, 158.03, 169.51 (*C*$_{quart}$). Anal. Calcd for C₂₇H₄₃N₃OSi₂Zn: C, 59.26; H, 7.92; N, 7.68. Found: C, 59.35; H 7.68; N, 7.73.

Synthesis of [(L^{1j})ZnN(SiMe$_3$)$_2$] (2j). To a solution of ligand **HL^{1j}** (283 mg, 0.790 mmol) in toluene (10 mL), zinc bis(trimethylsilyl)amide (305 mg, 0.790 mmol) was added at room temperature. After being stirred for 8 hr, the pale yellow colored solution was dried *in vacuo*, giving the desired compound as yellow powder (88 %, 405 mg). ^{1}H NMR (500.1 MHz; CDCl$_3$; 298 K): 0.04 (18H, s, CH_3), 0.89 (3H, d, J = 7.60, CH(CH_3)$_2$), 1.04 (3H, d, J = 8.01, CH(CH_3)$_2$), 1.98 (3H, d, J = 8.22, ArCHCH_3), 2.67 (1H, m, CH(CH$_3$)$_2$), 4.42 (2H, m, NCH(R)CH_2O), 4.61 (1H, m, NCH(R)CH_2O), 5.50 (1H, br, C$_{12}H_{11}$), 6.40 (1H, t, J = 7.80, *p*-PhHN), 6.45 (1H, d, J = 9.35, *m*-PhHN), 6.97 (1H, t, J = 7.80, *m*-PhHN), 7.20 (1H, d, J = 7.80, ArH), 7.33 (1H, t, J = 9.35, ArH), 7.55 (1H, m, ArH), 7.61 (1H, t, J = 9.35, ArH), 7.71 (1H, d, J = 9.35, *o*-PhHN), 7.85 (1H, d, J = 9.35, ArH), 7.92 (1H, d, J = 9.35, ArH), 8.25 (1H, d, J = 9.35, ArH). ^{13}C NMR (125.8 MHz; CDCl$_3$; 298 K): 5.50 (SiMe_3), 14.35 (CH(CH_3)$_2$), 19.37 (CH(CH_3)$_2$), 28.31(ArCHCH_3), 30.44 (CH(CH$_3$)$_2$), 55.50 (ArCH(CH$_3$)), 66.13 (NCH(R)CH_2O), 69.27 NCH(R)CH$_2$O), 105.20, 112.70, 117.22, 121.78, 123.06, 125.52, 126.13, 127.0, 128.40, 129.30, 131.04 (CH_{arom}), 134.43, 142.20, 147.95, 159.62, 160.73, 169.53 (C$_{quart}$). Anal. Calcd for C$_{30}$H$_{43}$N$_3$OSi$_2$Zn·0.2C$_7$H$_8$: C, 62.68; H, 7.47; N, 6.98. Found: C, 62.59; H, 7.25; N, 6.32.

Synthesis of [(L^{1k})ZnN(SiMe$_3$)$_2$] (2k). To a solution of ligand **HL^{1k}** (333 mg, 1.081 mmol) in toluene (6 mL), zinc bis(trimethylsilyl)amide (418 mg, 1.082 mmol) was added at room temperature. After being stirred for 8 hr, the pale yellow colored solution was dried *in vacuo*, and the residue was recrystallized from toluene at -30 °C to afford **2k** (84 %, 483 mg) as light pinkish crystals. ^{1}H NMR (500.1 MHz; CDCl$_3$; 298 K; peaks for the minor species are only partially identified due to overlap): Major: 0.06 (9H, s, CH_3), 0.09 (9H, s, CH_3), 0.64 (3H, d, J = 7.12,CH(CH_3)$_2$), 0.68 (3H, d, J = 7.12,CH(CH_3)$_2$), 1.60 (1H, m,

CH(CH$_3$)$_2$), 4.09 (1H, m, NCH(R)CH$_2$O), 4.28 (1H, t, J = 7.91, NCH(R)CH_2O), 4.35 (1H,

t, J = 7.09, NCH(R)CH_2O), 6.87 (1H, d, J = 9.210, m-PhHN), 7.10 (4H, m, ArH), 7.20-

7.25 (6H, m, ArH), 7.45 (2H, d, J = 9.41, COPh-H), 7.73 (1H, d, J = 9.41, o-PhHN). Minor:

0.59 (3H, d, J = 7.09, CH(CH_3)$_2$), 0.84 (3H, d, J = 7.06, CH(CH_3)$_2$), 1.86 (1H, m,

CH(CH$_3$)$_2$), 6.96 (1H, t, J = 9.49, m-PhHN), 7.62 (2H, d, J = 8.81, COPh-H), 7.69 (1H, d,

J = 9.50, o-PhHN). ^{13}C NMR (125.8 MHz; CDCl$_3$; 298 K): Major: 5.95 (SiMe_3), 14.86

((CH)Me_2), 18.93 ((CH)Me_2), 30.24 ((CH)Me$_2$), 67.56 (NCH(R)CH$_2$O), 69.61

(NCH(R)CH$_2$O), 121.32, 127.32, 128.28, 128.43, 129.22, 129.66, 130.66, 133.56, 138.05

(CH$_{arom}$), 140.77, 151.41, 168.82, 176.34 (C_{quart}). Minor: 5.69 (SiMe_3), 15.58 ((CH)Me_2),

19.26 ((CH)Me_2), 31.13 ((CH)Me$_2$), 68.03 (NCH(R)CH$_2$O), 69.98 (NCH(R)CH$_2$O),

120.31, 127.63, 127.90, 128.53, 128.79, 129.06, 130.06, 132.98, 137.45 (CH$_{arom}$), 139.58,

150.87, 168.40, 176.14 (C_{quart}). Anal. Calcd. for C$_{50}$H$_{74}$N$_6$O$_4$Si$_4$Zn$_2$·0.4C$_7$H$_8$: C, 57.49; H,

7.05; N, 7.62. Found: C, 57.88; H, 6.56; N, 7.65.

Synthesis of [(L^{1l})ZnN(SiMe$_3$)$_2$] (2l). To a solution of ligand **HL^{1l}** (68 mg, 0.211 mmol)

in toluene (6 mL), zinc bis(trimethylsilyl)amide (84 mg, 0.211 mmol) was added at room

temperature. After being stirred for 8 hr, the pale yellow colored solution was dried *in*

vacuo, giving the desired compound as yellow powder (98%, 113 mg). ^{1}H NMR (500.1

MHz; CDCl$_3$; 298 K; peaks for the minor species are only partially identified due to

overlap): Major: -0.04 (9H, s, CH_3), 0.08 (9H, s, CH_3), 0.62 (3H, d, J = 7.15,

CH$_2$CH(CH_3)$_2$), 0.97 (3H, d, J = 6.80, CH$_2$CH(CH_3)$_2$), 1.27 (1H, m, CH$_2$CH(CH$_3$)$_2$), 1.50

(1H, m, CH_2CH(CH$_3$)$_2$), 1.73 (1H, m, CH_2CH(CH$_3$)$_2$), 3.75 (1H, t, J = 9.10,

NCH(R)CH$_2$O), 4.50 (2H, t, J = 8.90, NCH(R)CH_2O), 6.84 (2H, m, ArH), 7.04 (2H, m,

ArH), 7.16 (1H, m, ArH), 7.52 (1H, m, ArH), 7.63 (2H, m, ArH), 7.91 (1H, d, J = 8.10, o-

Ph*H*N).　　Minor: 0.52 (3H, d, *J* = 6.50*,* CH$_2$CH(C*H$_3$*)$_2$), 1.04 (3H, d, *J* = 6.80, CH$_2$CH(C*H$_3$*)$_2$), 1.24 (1H, m, CH$_2$C*H*(CH$_3$)$_2$), 1.44 (1H, m, C*H$_2$*CH(CH$_3$)$_2$), 1.93 (1H, m, C*H$_2$*CH(CH$_3$)$_2$), 4.00 (1H, m, NC*H*(R)CH$_2$O), 4.14 (1H, m, NCH(R)C*H$_2$*O), 4.22 (1H, m, NCH(R)C*H$_2$*O), 6.94 (2H, m, Ar*H*), 7.36 (1H, m, Ar*H*), 8.11 (1H, d, *J* = 7.50, *o*-Ph*H*N).

^{13}C NMR (125.8 MHz; CDCl$_3$; 298 K): Major: 5.85 (Si*Me$_3$*), 21.12 (CHCH$_2$(*C*H$_3$)$_2$), 22.36 (CHCH$_2$(*C*H$_3$)$_2$), 24.01 (*C*HCH$_2$(CH$_3$)$_2$), 25.02 (CH*C*H$_2$(CH$_3$)$_2$), 67.61 (N*C*H(R)CH$_2$O), 74.55 (NCH(R)*C*H$_2$O), 104.05, 113.12, 119.60, 124.26, 125.53, 128.46, 133.61, 138.10, 145.49 (*C*H$_{arom}$), 158.19, 165.09, 169.50, 176.18 (*C$_{quart}$*). Minor: 5.01 (Si*Me$_3$*), 20.01 (CHCH$_2$(*C*H$_3$)$_2$), 23.01 (CHCH$_2$(*C*H$_3$)$_2$), 24.18 (*C*HCH$_2$(CH$_3$)$_2$), 26.12 (CH*C*H$_2$(CH$_3$)$_2$), 69.76 (N*C*H(R)CH$_2$O), 77.85 (NCH(R)*C*H$_2$O), 104.35, 113.32, 119.01, 124.89, 126.01, 129.06, 133.89, 139.08, 145.01(*C*H$_{arom}$), 158.59, 165.89, 170.04, 176.30 (*C$_{quart}$*).

Synthesis of [(L^{1m}) ZnN(SiMe$_3$)$_2$] (2m). To a solution of ligand **HL^{1m}** (364 mg, 1.129 mmol) in toluene (15 mL), zinc bis(trimethylsilyl)amide (436 mg, 1.129 mmol) was added at room temperature. After being stirred for 8 hr, the pale red colored solution was dried *in vacuo*, giving the desired compound as yellow powder (86%, 531 mg). ^{1}H NMR (500.1 MHz; CDCl$_3$; 298 K): -0.28 (9H, s, C*H$_3$*), 0.07 (9H, s, C*H$_3$*), 0.92 (6H, br, CH$_2$CH(C*H$_3$*)$_2$), 1.11 (2H, m, C*H$_2$*CH(CH$_3$)$_2$), 1.31 (1H, m, CH$_2$C*H*(CH$_3$)$_2$), 1.54 (9H, s, C(C*H$_3$*)$_3$), 2.81 (1H, t, *J* = 8.83, NC*H*(R)CH$_2$O), 3.69 (1H, t, *J* = 6.91, NCH(R)C*H$_2$*O), 4.06 (1H, t, *J* = 8.49, NCH(R)C*H$_2$*O), 6.86 (1H, t, *J* = 7.63, *p*-Ph*H*N), 7.04 (1H, d, *J* = 8.23, *m*-Ph*H*N), 7.32 (1H, t, *J* = 7.93, *m*-Ph*H*N), 7.69 (1H, d, *J* = 7.93, *o*-Ph*H*N). ^{13}C NMR (125.8 MHz; CDCl$_3$; 298 K): 5.20 (Si*Me$_3$*), 5.75 (Si*Me$_3$*), 21.28 (CHCH$_2$(*C*H$_3$)$_2$), 23.68 (CHCH$_2$(*C*H$_3$)$_2$), 25.08 (*C*HCH$_2$(CH$_3$)$_2$), 25.93 (C(*C*H$_3$)$_3$), 43.17 (CH*C*H$_2$(CH$_3$)$_2$), 59.56 (*C*(CH$_3$)$_3$), 65.30 (N*C*H(R)CH$_2$O),70.51 (NCH(R)*C*H$_2$O), 115.72, 119.02, 123.49, 131.09 (*C*H$_{arom}$), 145.95,

154.52, 165.72 (C_{quart}). Anal. Calcd. for $C_{23}H_{43}N_3O_2SSi_2Zn\cdot0.3C_7H_8$: C, 52.51; H, 7.99; N, 7.29. Found: C, 52.69; H 7.66; N, 7.32.

Copolymerization of Cyclohexene Oxide/CO2. In a glovebox, a 60 mL Teflon-lined Parr high-pressure reactor vessel that was previously dried in an oven was charged with a zinc catalyst (1 mol%) and CHO (1 equiv). The vessel was sealed, taken out of the glovebox, and brought to desired temperature and CO_2 pressure. After the mixture was stirred for the allotted time, it was cooled and a small aliquot of reaction mixture was taken for ^{1}H NMR spectroscopy to determine the conversion. When no further conversion was noted, the polymerization mixture was transferred into a round-bottom flask with CH_2Cl_2 (3-5 mL), and the polymer was precipitated from addition of methanol (18-30 mL). After separation, the polymer was dried in *vacuo* to constant weight to determine the yield. Molecular weight (M_n) and PDIs were determined by GPC using polystyrene standards.

Hydrolysis of Polymers and Chiral GC Analysis. In a typical procedure, a small round bottom flask was loaded with polycarbonate (20 mg, 0.141 mmol) and NaOH (11 mg, 0.281 mmol) in MeOH (4 mL). The mixture was refluxed for 3 h and then neutralized with aq. HCl (1 M). The crude mixture was then extracted with ether. After drying over anhydrous $MgSO_4$, a small aliquot was injected into a GC equipped with a Cyclodex-B column to determine the enantiomeric excess of the 1, 2-*trans* cyclohexanediol (t_R = 14.32 min for (*S, S*)-1, 2-*trans* cyclohexanediol, t_R = 14.75 min for (*R, R*)-1, 2-*trans* cyclohexanediol).

X-ray Crystallography. All data for compounds **2a**, **2d**, and **2k** were collected on a Bruker APEX-II CCD diffractometer. The intensity data were corrected for absorption and decay (SADABS).[41] The data were integrated with SAINT[42] and the structure was solved and

refined using SHELXTL.[43] The factors for the determination of the absolute structure were refined according established procedures.[44] Residue electrons were noted in the lattice of **2k**, which were found with the SQUEEZE routine from the PLATON package[45] to be the toluene solvate. X-ray crystal data, data collection parameters, and refinement parameters are summarized in Table 1 and further crystallographic details can be found in Supporting Information.

3.5. References

1. (a) Sakakura, T.; Kohno, K. *Chem. Commun.* **2009**, 1312-30. (b) Sakakura, T.; Choi, J. –C.; Yasuda, H. *Chem. Rev.* **2007**, *107*, 2365–87. (c) Aresta, M.; Dibenedetto, A. *Dalton Trans.* **2007**, 2975-92. (d) Tschan, M. J.-L.; Brule, E.; Haquette, P.; Thomas, C. M. *Polym. Chem.* **2012**, *3*, 836–851. (e) *Carbon Dioxide Recovery and Utilization;* Aresta, M., Ed. Kluwer Academic Publishers: Dordrecht, Netherlands, 2010.

2. (a) Kuran, W. *Prog. Polym. Sci.* **1998**, *23*, 919–992. (b) Ihata, O.; Kayaki, Y.; Ikariya, T. *Macromolecules* **2005**, *38*, 6429–6434.

3. For recent reviews: (a) Lu, X-B.; Darensbourg, D. J. *Chem. Soc. Rev.* **2012**, *41*, 1462–1484. (b) Kember, M. R.; Buchard, A.; Williams, C. K. *Chem. Commun.* **2011**, *47*, 141–163. (c) Klaus, S.; Lehenmeier, M. W.; Anderson, C. E.; Rieger, B. *Coord. Chem. Rev.* **2011**, *255*, 1460–1479. (d) Darensbourg, D. J. *Inorg. Chem.* **2010**, *49*, 10765–10780. (e) Darensbourg, D. J. *Chem. Rev.* **2007**, *107*, 2388–2410. (f) Coates, G. W.; Moore, D. R. *Angew. Chem. Int. Ed.* **2004**, *43*, 6618–6639. (g) Darensbourg, D. J.; Mackiewicz, R. M.; Phelps, A. L.; Billodeaux, D. R. *Acc. Chem. Res.* **2004**, *37*, 836−844. (h) Nakano, K.; Kosaka, N.; Hiyama, T.; Nozaki, K. *Dalton Trans.* **2003**, 4039–4050.

4. (a) Klaus, S.; Lehenmeier, M.; Herdtweck, E.; Degllmann, P.; Ott, A. K.; Rieger, B. *J. Am. Chem. Soc.* **2011**, *133*, 13151–13161. (b) Lehenmeier, M. L.; Bruckmeier, C.; Klaus, S.; Dengler, J. E.; Deglmann, P.; Ott, A. K.; Rieger, B. *Chem. Eur. J.* **2011**, *17*, 8858–8869. (c) Piesik, D. F-J.; Range, S.; Harder, S. *Organometallics* **2008**, *27*, 6178–6187. (d) Zhang, Z.; Cui, D.; Liu, X. *J. Polym. Sci., Part A: Polym. Chem.* **2008**, *46,* 6810–6817. (e) Xie, D.; Wang, X.; Zhao, X. J.; Wang, F. *Polym. Bull.* **2008**, *61*, 679–688. (f) Sugimoto, H.; Ohshima, H.; Inoue, S. *J. Polym. Sci., Part A: Polym. Chem.* **2003**, *41,* 3549–3553. (g) Thorat, S. D.; Phillips, P. J.; Semenov, V.; Gakh, A. *J. Appl. Polym. Sci.* **2003**, *89*, 1163–1176. (h) Pokharkar, V.; Sivaram, S. *Polymer* **1995**, *36*, 4851–4854.

5. (a) Inoue, S.; Koinuma, H.; Tsuruta, T. *J. Polym Sci., Part B,* **1969**, *7*, 287–292. (b) Inoue, S.; Koinuma, H.; Tsuruta, T. *Makromol. Chem.* **1969**, *130*, 210–220.

6. (a) Darensbourg, D. J.; Zimmer M. S.; Rainey, P.; Larkins, D. L. *Inorg. Chem.* **2000**, *39*, 1578–1585. (b) Sugimoto, H.; Inoue, S. *J. Polym. Sci., Part A: Polym. Chem.* **2004**, *42*, 5561–5573.

7. (a) Ren, W. –M.; Liu, Z.-W.; Wen, Y.-Q.; Zhang, R.; Lu, X.-B. *J. Am. Chem. Soc.* **2009**, *131*, 11509–11518. (b) Nakano, K.; Nakamura, M.; Nozaki, K. *Macromolecules* **2009**, *42*, 6972–6980. (c) Na, S. J.; S, S.; Cyriac, A.; Kim, B. E.; Yoo. J.; Kang, Y. K.; Han, S. J.; Lee, C.; Lee, B. Y. *Inorg. Chem.* **2009**, *48*, 10455–10465. (d) Darensbourg, D. J.; Maynard, E. L.; Holtcamp, M. W.; Klausmeyer, K. K.; Reibenspies, J. H. *Inorg. Chem.* **1996**, *35*, 2682–2684.

8. (a) Sugimoto, H.; Kuroda, K. *Macromolecules* **2008**, *41*, 312–317. (b) Sugimoto, H.; Ohtsuka, H.; Inoue, S. *J. Polym. Sci., Part A: Polym. Chem.* **2003**, *41,* 3549–3555.

9. (a) Kember, M. R.; Jutz, F.; Buchard, A.; White, A. J. P.; Williams, C. K. *Chem. Sci.* **2012**, *3*, 1245–1255. (b) Nakano, K.; Kobayashi, K.; Nozaki, K. *J. Am. Chem. Soc.* **2011**, 133, 10720–10723. (c) Buchard, A.; Kember, M. R. Sanderman, K.; Williams, C. K. *Chem. Commun.* **2011**, *47*, 212–214. (d) Darensbourg, D. J.; Fitch, S. B. *Inorg. Chem.* **2009**, *48*, 8668–8677. (e) Kember, M. R.; White, A. J. P.; Williams, C. K. *Inorg. Chem.* **2009**, *48*, 9535–9542.

10. (a) Cheng, M.; Lobkovsky, E. B.; Coates, G. W. *J. Am. Chem. Soc.* **1998**, *120*, 11018–11019. (b) Cheng, M.; Moore, D. R.; Reczek, J. J.; Chamberlain, B. M.; Lobkovsky, E. B.; Coates, G. W. *J. Am. Chem. Soc.* **2001**, *123*, 8738–8749. (c) Allen, S. D.; Moore, D. R.; Lobkovsky, E. B.; Coates, G. W. *J. Am. Chem. Soc.* **2002**, *124*, 14284–14285. (d) Moore, D. R.; Cheng, M.; Lobkovsky, E. B.; Coates, G. W. *Angew. Chem. Int. Ed.* **2002**, *41*, 2599–2602. (e) Moore, D. R.; Cheng, M.; Lobkovsky, E. B.; Coates, G. W. *J. Am. Chem. Soc.* **2003**, *125*, 11911–11924. (f) Byrne, C. M.; Allen, S. D.; Lobkovsky, E. B.; Coates, G. W. *J. Am. Chem. Soc.* **2004**, *126*, 11404–11405.

11. Brule, E.; Guo, J.; Coates, G. W.; Thomas, C. M. *Macromol. Rapid Commun.* **2011**, *32,* 169–185.

12. (a) Darensbourg, D. J.; Wilson, S. J. *J. Am. Chem. Soc.* **2011**, *133*, 18610–18613. (b) Wu, G-P.; Wei, S-H.; Ren, W-M.; Lu, X-B.; Darensbourg, D. J. *J. Am. Chem. Soc.* **2011**, *133*, 15191–15199.(c) Wu. G.-P.; Wei, S.-H.; Lu, X.-B.; Ren, W.-M.; Darensbourg, D. J. *Macromolecules* **2010**, *43*, 9202–9204.

13. (a) Kim, J. G.; Cowman, C. D.; LaPointe, A. M.; Wiesner, U.; Coates, G. W. *Macromolecules* **2011**, *44*, 1110–1113. (b) Ren, W.-M.; Zhang, X.; Liu, Y.; Li, J.-F.; Wang, H.; Lu, X.-B. *Macromolecules* **2010**, *43*, 1396–1402. (c) Seong, J. E.; Na, S. J.; Cyriac, A.; Kim, B.-W.; Lee, B. Y. *Macromolecules* **2010**, *43*, 903–908. (d) Jeske, R. C.; Rowley, J. M.; Coates, G. W. *Angew. Chem., Int. Ed.* **2008**, *47*, 6041–6044.

14. (a) Cyriac, A.; Lee, S. H.; Lee, B. Y. *Polym. Chem.* **2011**, *2*, 950–956. (b) Zhou, J.; Wang, W.; Villarroya, S.; Thurecht, K. J.; Howdle, S. M. *Chem. Commun.* **2008**, 5806–5808.

15. Nozaki, K.; Nakano, K.; Hiyama, T. *J. Am. Chem. Soc.* **1999,** *121,* 11008–11009.

16. Cheng, M.; Darling, N. A.; Lobkovsky, E. B.; Coates, G. W. *Chem. Commun.* **2000**, 2007–2008.

17. (a) Nakano, K.; Nozaki, K.; Hiyama, T. *J. Am. Chem. Soc.* **2003,** *125,* 5501–5510. (b) Nakano, K.; Hiyama, T.; Nozaki, K. *Chem. Commun.* **2005**, 1871–1873.

18. Xiao, Y.; Wang, Z.; Ding, K. *Chem. Eur. J.* **2005**, *11*, 3668– 3678.

19. (a) Nakano, K.; Hashimoto, S.; Nakamura, M.; Kamada, T.; Nozaki, K. *Angew. Chem., Int. Ed.* **2011,** *50*, 4868– 4871. (b) Li, B.; Wu, G.-P.; Ren, W.-M.; Wang, Y.-M.; Rao, D.-Y.; Lu, X.-B. *J. Polym. Sci. Part A* **2008**, *46*, 6102– 6113. (c) Shi, L.; Lu. X. –B.; Zhang, R.; Peng, X. –J.; Zhang, C. –Q.; Li, J. –F.; Peng, X.-M. *Macromolecules* **2006**, *39*, 5679– 5685. (d) Lu, X. –B.; Shi, L.; Wang, Y.-M.; Zhang, R.; Zhang, Y.-J.; Peng, X.-J.; Zhang, Z.-C.; Li, B.; *J. Am. Chem. Soc.* **2006**, *128*, 1664– 1674. (e) Cohen, C. T.; Chu, T.; Coates, G. W. *J. Am. Chem. Soc.* **2005**, *127*, 10869– 10878. (f) Qin, Z.; Thomas, C. M.; Lee, S.; Coates, G. W. *Angew. Chem. Int., Ed.* **2003,** *42*, 5484–5487. (g) Lu, X-B.; Wang, Y. *Angew. Chem. Int. Ed.* **2004**, *43*, 3574–3577.

20. Wu, G.-P.; Ren, W.-M.; Luo, Y.; Li, B.; Zhang, W.-Z.; Lu, X.-B. *J. Am. Chem. Soc.* **2012**, *134*, 5682–5688.

21. (a) Bourget-Merle, L.; Lappert, M. F. *Chem. Rev.* **2002**, *102*, 3031–3065. (b) Bourget-Merle, L.; Cheng, Y.; Doyle, D. J.; Hitchcock, P. B.; Khvostov, A. V.; Lappert, M. F.; Protchenko, V.; Wei, X. *ACS Symposium Series* **2006**, *917*, 192–207. (c) Chomitz, W. A.; Arnold, J. *Chem. Eur. J.* **2009**, *15*, 2020–2030.

22. (a) Gong, S.; Ma, H.; Haung, J. *Dalton Trans.* **2009**, 8237-8247. (b) Stanlake, L. J. E.; Stephan, D. W. *Dalton Trans.* **2011**, *40*, 5836–5841. (c) Dove, A. P.; Gibson, V. C.; Marshall, E. L.; White, A. J. P.; William, D. J. *Dalton Trans.* **2004**, 570–578. (d) Zhang, J.; Zhang, Z.; Chen, Z.; Zhou, X. *Dalton Trans.* **2012**, *41*, 357–361.

23. (a) Biyikal, M.; Lohnwitz, K.; Meyer, N.; Dochnahl, M.; Roesky, P. W.; Blechert, S. *Eur. J. Inorg. Chem.* **2010**, *7*, 1070–1081. (b) Wiese, S.; Badiei, Y. M.; Gephart, R. T.; Mossin, S.; Varonka, M. S.; Melzer, M. M.; Meyer, K.; Cundari, T. R.; Warren, T. H. *Angew. Chem., Int. Ed.* **2010**, *49*, 8850–8855. (c) Vela, J.; Smith, J. M.; Yu, Y.; Ketterer, N. A.; Flaschenriem, C. J.; Lachicotte, R. J.; Holland, P. L. *J. Am. Chem. Soc.* **2005**, *127*, 7857–7870. (d) Spielmann, J.; Harder, S. *Eur. J. Inorg. Chem.* **2008**, *9*, 1480–1486. (e) Zhao, G.; Basuli, F.; Kilgore, U. J.; Fan, H.; Aneetha, H.; Huffman, J. C.; Wu, G.; Mindiola, D. J. *J. Am. Chem. Soc.* **2006**, *128*, 13575–13585. (f) Fekl, U.; Kaminsky, W.; Goldberg, K. I. *J. Am. Chem. Soc.* **2003**, *125*, 15286–15287. (g) Bernskoetter, W. H.; Lobkovsky, E.; Chirik, P. J. *Chem. Commun.* **2004**, 764–765. (h) Bernskoetter, W. H.; Lobkovsky, E.; Chirik, P. J. *Organometallics* **2005**, *24*, 4367–4373.

24. (a) Peng, K.-F.; Chen, C.-T. *Eur. J. Inorg. Chem.* **2011**, 5182–5195. (b) Chen,M.-T.; Chang, P.-J.; Huang, C.-A.; Peng , K.-F.; Chen, C.-T. *Dalton Trans.* **2009**, 9068–9074. (c) Coeffard, V.; Muller-Bunz, H.; Guiry, P. J. *Org. Biomol. Chem.* **2009**, *7*, 1723–1734.

25. (a) Lee, B. Y.; Kwon, H. Y.; Lee, S. Y.; Na, S. J.; Han, S.-i.; Yun, H.; Lee, H.; Park, Y. –W. *J. Am. Chem. Soc.* **2005**, *127*, 3031–3043. (b) Bok, T.; Yun, H.; Lee, B. Y. *Inorg. Chem.* **2006**, *45*, 4228–4237.

26. (a) Drouin, F.; Oguadinma, P. O.; Whitehouse, T. J. J.; Prud'homme, R. E.; Schaper, F. *Organometallics* **2010**, *29*, 2139–2147. (b) El-Zoghbi, I.; Latreche, S.; Schaper, F. *Organometallics* **2010**, *29*, 1551–1559. (c) Oguadinma, P. O.; Schaper, F. *Organometallics* **2009**, *28*, 4089-4097. (d) Köhler, V.; Mazet, C.; Toussaint, A.; Kulicke, K.; Häussinger,

D.; Neuburger, M.; Schaffner, S.; Kaiser, S.; Pfaltz, A. *Chem. Eur. J.* **2008**, 14, 8530–8539. (e) Mazet, C.; Köhler, V.; Roseblade, S.; Toussaint, A.; Pfaltz, A. *Chimia*, **2006**, *60*, 195–198 (f) Dagorne, S.; Bellemin-Laponnaz, S.; Maisse-Francois, A. *Eur. J. Inorg. Chem.* **2007**, 913–925.

27. Binda, P. I.; Abbina, S.; Du, G. *Synthesis* **2011**, 2609–2618.

28. Abbreviations: DMP: dimethylphenyl; BTP: bis(trifluromethyl)phenyl; D*i*PP: diisopropylphenyl; Naph: 1-naphthyl.

29. See supporting information for further details.

30. Liang, L.-C.; Tsai, T.-L.; Li, C.-W.; Hsu, Y.-L.; Lee, T.-Y. *Eur. J. Inorg. Chem.* **2011**, 2948–2957.

31. (a) Chisholm, M. H.; Gallucci, J. C.; Phomphrai, K. *Inorg. Chem.* **2005**, *44*, 8004-10. (b) Dove, A. P.; Gibson, V. C.; Marshall, E. L.; White, A. J. P.; Williams, D. J. *Dalton Trans.* **2004**, 570–578.

32. Chisholm, M. H.; Gallucci, J. C.; Zhen, H.; Huffman, J. C. *Inorg. Chem.* **2001**, *40*, 5051-5054.

33. Roberts, C. C.; Barnett, B. R.; Green, D. B.; Fritsch, J. M. *Organometallics*, **2012**, *31*, 4133–4141.

34. Van Meerendonk, W. J.; Duchateau, R.; Koning, C. E.; Gruter, G.-J. M. *Macromol. Rapid Commun.* **2004**, *25*, 382–386.

35. Chen, C.-T.; Chan, C.-Y.; Huang, C.-A.; Chen, M.-T.; Peng, K.-F. *Dalton Trans.* **2007**, 4073– 4078.

36. Small, B. L.; Brookhart, M. *J. Am. Chem. Soc.* **1998**, *120*, 7143–7144.

37. (a) Eberhardt, R.; Allmendinger, M.; Luinstra, G. A.; Rieger, B. *Organometallics* **2003**, *22*, 211–214.(b) Kember, M. R.; Knight, P. D.; Reung,T. R. P.; Williams, C. K. *Angew. Chem. Int. Ed.* **2009**, *48*, 931–933. (c) Koning, C.; Wildeson, J.; Parton, R.; Plum, B.; Steeman, P.; Darensbourg, D. J. *Polymer* **2001**, *42*, 3995–4004.

38. Cohen, C. T.; Thomas, C. M.; Peretti, K. L.; Lobkvosky, E. B.; Coates, G. W. *Dalton Trans.* **2006**, 237–249.

39. Kotha, S. Statistical Analysis of the Stereo Defect Sequence Distribution of the Ziegler-Natta Isotactic Poly(propylene) in Light of the Crystallization Behavior of Its CITREF fractions. M.S. Dissertation, Florida state University, Tallahassee, FL, **2005**.

40. Cortright, S. B.; Johnston, J. N. *Angew. Chem., Int. Ed.* **2002**, *41*, 345–348.

41. Blessing, R. *Acta Crystallogr.* **1995**, *A51*, 33–38.

42. Bruker Analytical X-Ray Systems, SAINT: *Program for Reduction of Area Detector Data*; Bruker-AXS, Inc.: Madison, WI, **2003**.

43. Sheldrick, G. M. *Acta. Crystallogr. Sect. A*. **2008**, *64*, 112–122.

44. Flack, H. D. *Acta. Crystallogr*. **1983**, *A39*, 876–881.

45. Spek, A. L. PLATON, *A Multipurpose Crystallographic Tool*, Utrecht University, Utrecht, the Netherlands, **2003**.

CHAPTER-4

SYNTHESIS AND CHARACTERIZATION OF CHIRAL C_2-SYMMETRIC BIMETALLIC ZINC COMPLEXES OF AMIDO-OXAZOLINATES: ACTIVE INITIATORS FOR ASYMMETRIC COPOLYMERIZATION OF CO_2 AND CYCLOHEXENE OXIDE

4.1. Introduction

It is highly desirable to develop synthetic strategies for making biodegradable polymers using renewable resources instead of petroleum feedstocks, as depletion of petroleum resources is growing at a rapid rate.[1] Carbon dioxide (CO_2) is one of the most promising renewable resources because it is abundant, inexpensive, non-toxic, and non-flammable.[2] In particular, significant efforts have been directed towards the catalytic alternating copolymerization of aliphatic epoxides with carbon dioxide, due to a wide array of applications of the resulting polymeric materials.[3] Plenty of monomeric metal complexes including zinc,[4] aluminum,[5] calcium,[6] chromium,[7] cobalt,[3c,8] cadmium,[9] magnesium,[10] and yttrium[11] supported by various ligand frameworks have been well studied as viable initiators for the heterocoupling of cyclohexene oxide (CHO) with CO_2.

In recent years, the bimetallic metal complexes have also drawn considerable attention due to their promising applications in conventional catalysis in addition to their structural features.[12] Because of the cooperative effect between the two metal centers, these dinuclear systems can exhibit enhanced catalytic activity in several catalytic reactions such as olefin polymerization,[13] and alternating copolymerization of CHO and CO_2 [4g,6a,14,15] In

this context, a number of zinc based dinuclear complexes have been reported for copolymerization of CO_2 with CHO (Figure **38**).[15]

A well-defined, phenoxide-bridged dimeric zinc complex was reported by Darensbourg et. al. for the alternating copolymerization of CO_2 with CHO, producing corresponding copolymers with high molecular weight of up to 252,000 g/mol (Figure 38, **I**).[16] In 2003, a major breakthrough was reported by Coates and co-workers,[4g] in which a bimetallic β-diketiminate zinc complex was shown to promote copolymerization of CO_2 with cyclohexene oxide *via* a bimetallic enchainment process that operated by cooperative effect between the two metal centers bridged by alkoxides (Figure 38, **II**). Furthermore, Nozaki and co-workers reported a moderately selective chiral dimeric zinc catalyst for the asymmetric alternating copolymerization of CO_2 and CHO (Figure 38, **III**).[17,18]
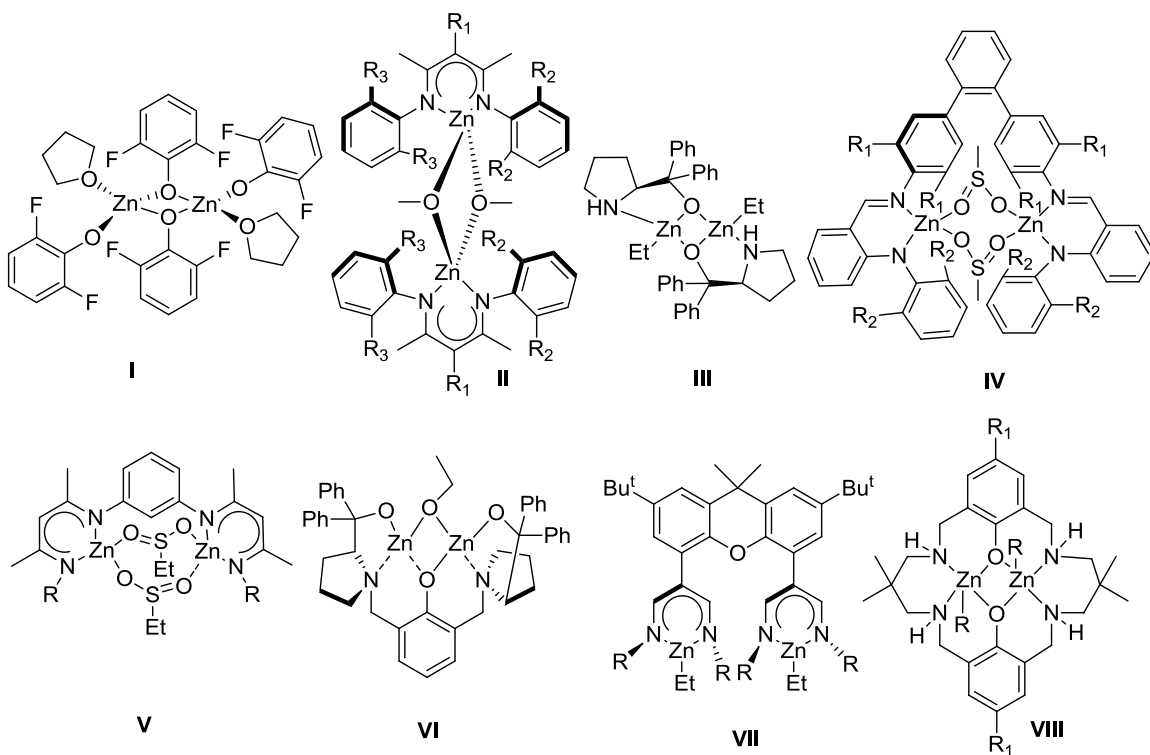
Figure 38. A set of dinuclear zinc complexes

Unlike the formation of the bimetallic complexes with bridging M-X bonds (X = OAc, OMe, OPh, etc), Piesik *et al* prepared a series of bimetallic zinc complexes of dinucleating bis(β-diketiminate) ligands that are connected by three different rigid frameworks such as *meta*-phenylene (Figure 38, **V**), *para*-phenylene, and 2, 6-pyridylene moieties.[6a] Copolymerization with *meta* phenylene bridged species was extremely fast while *para*-phenylene bridged complexes were less active. Surprisingly, 2, 6-pyridylene connected complexes were completely inactive even at very concentrated conditions. It emphasizes the choice of an appropriate linker/spacer is indispensable to achieve the maximum synergetic/cooperative effect between two metal centers. Lee and co-workers described a series of extremely active zinc anilido-aldimine complexes (Figure 38, **IV**) for the generation of poly(cyclohexene carbonate) even at very dilute conditions, giving unprecedented TONs of 670-2980.[14g]

Recently, we reported a series of novel mononuclear zinc complexes of amido-oxazolinate ligands for asymmetric alternating copolymerization of CO_2 and cyclohexene oxide, affording moderate isotactic PCHC with up to 90 % carbonate linkages.[4a] Since bimetallic complexes are expected to have superior activity when compared to their mononuclear counterparts, we set out to investigate the catalytic activity of bimetallic zinc complexes of amido-oxazolinate ligands, which are obtained by connecting two mononuclear zinc units with three different linkers. This also provides an opportunity to study the influence of rigidity of the linker on the efficiency of catalysts.

4.2. Results and Discussion

4.2.1. Ligand Design and Synthesis

The structure of linkers has shown profound effect on catalytic activity of the bimetallic complex in alternating copolymerization of CHO/CO_2.[14a] Depending on the nature of the linker, the two chelating systems in bimetallic complexes can be oriented either in face to face (such as **V** in Figure 38) or in parallel to each other (**VII**, Figure 38).[14g, 19] Furthermore, the linker in bimetallic complexes should keep the two metal centers in a proper distance (3.70 Å to 6.10 Å) to allow cooperative effects between the active sites.[3f] Because we are interested in investigating the effect of the linker in copolymerization process, the following three readily available amine sources were selected: m-phenylenediamine, 4-(4'-aminobenzyl) benzenamine, and 1,8-diaminoanthracene.[20] We hypothesized that the ligand structure constructed with a 1,8-diaminoanthracene linker provides the parallel arrangement while m-phenylenediamine incorporated ligand allows metal centers in a face-to-face orientation. The ligand with flexible linker, 4-(4'-aminobenzyl)benzenamine, may be amenable to both arrangements.

Synthetically we have constructed of a library of amido-oxazolinate lignads *via* modified Buchwald-Hartwig coupling reaction,[21] as palladium catalysis has been a powerful methodology for the C-X (X=N, O, C) bond formation.[22, 23] Initially, the same synthetic procedure with Pd(OAc)$_2$/BINAP was employed for the synthesis of binucleating ligands. However, it yielded multiple products with poor yields, and two peaks for NH protons around 9.65 and 9.74 ppm were observed in the ^{1}H NMR spectrum. We then performed the reaction using the second-generation Buchwald-Hartwig catalytic system, as it is an effective catalytic system for the coupling of highly electron rich aryl halides

with amines.[24] Thus ligands **1a-1c** were synthesized by a coupling reaction of bromophenyl-substituted oxazolines with *m*-phenylenediamine using a combination of 3 mol% $Pd_2(dba)_3$, 6 mol% *rac*-BINAP, and ^tBuONa in toluene at 120 °C (Scheme 5). The reaction pattern with flexible linker, 4-(4'-aminobenzyl)benzenamine, was also similar to that observed in the case of *m*-phenylenediamine. The desired pure products were obtained in high yields (85-90 %) after purification by column chromatography.
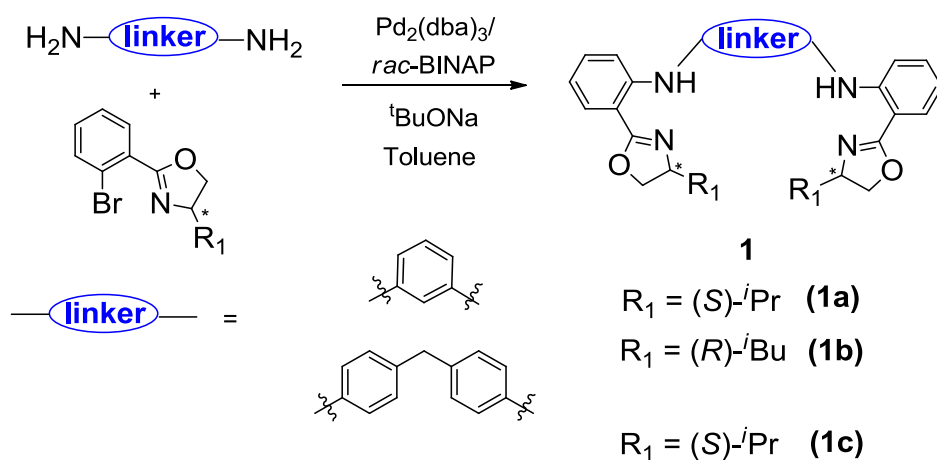
Scheme 5. Synthesis of binucleating ligands **1a-c**

The obtained ligands were characterized by NMR spectroscopy (^1H, ^{13}C, ^1H-^1H COSY, HETCOR). ^1H NMR spectra of **1a-1c** were consistent with the C_2 symmetry of the ligands. The analysis of ^{13}C NMR spectrum also further agrees with this interpretation having a single set of peaks. For instance, the ^1H NMR spectrum of **1a** has two up-field doublets (0.99 and 1.09 ppm), one septet (1.81 ppm), three resonances between 4-5 ppm, six peaks for aromatic protons (6.80-7.85 ppm), and a low intensity broad peak at 10.74 ppm for -NH proton consistent with the C_2-symmetric environment of the ligand. The resonance of the same -NH proton for the corresponding monomeric amido-oxazolinate ligands was typically around 9.00-10.0 ppm.[4a] This observation suggests stronger hydrogen bond in **1a** compared to its monomeric analogue. The two doublets in the up-field region

indicate the non-equivalent nature of methyl protons of *iso*-propyl group. ^{1}H NMR spectra of ligand **1b** and **1c** have similar features with **1a**. The distinction between two diastereotopic protons of –OCH$_2$ was identified by ^{1}H-^{1}H COSY and HETCOR NMR spectroscopy (Figure 39).
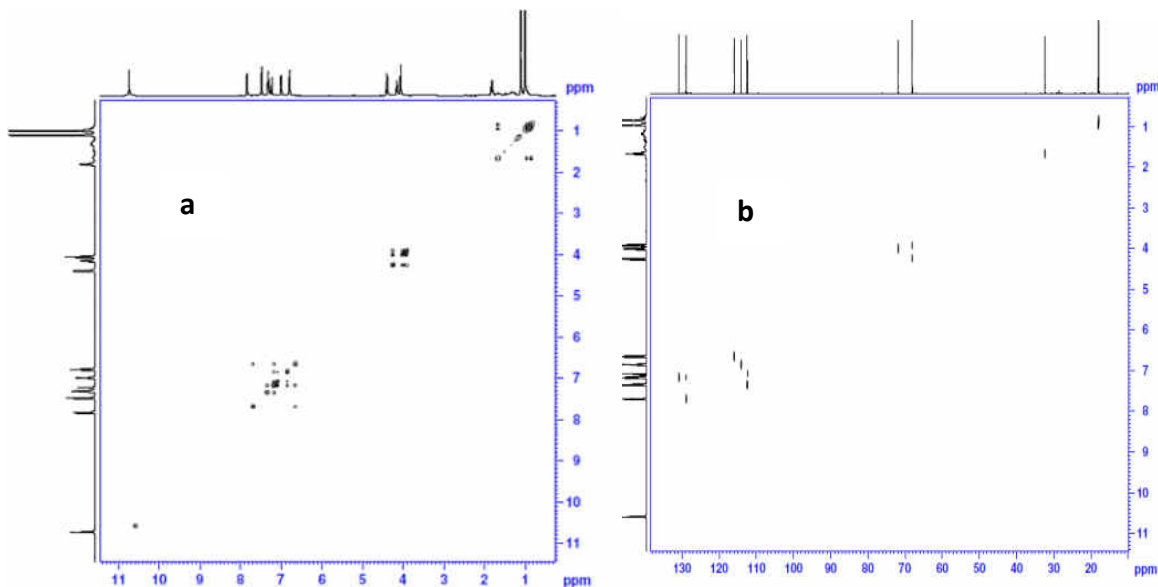
Figure 39. NMR spectra of ligand **1a:** (**a**) ^{1}H-^{1}HCOSY and (**b**) ^{1}H-DEPT-45 HETCOR

When the above synthetic route was employed for the synthesis of ligand **1d** using 1,8-diaminoanthracene as a linker, the conversion is very poor (~10%) irrespective of altering the reaction conditions such as heating the reaction mixture for prolonged times and adding excess amounts of catalyst and base, presumably due to the low solubility of 1,8-diaminoanthracene in refluxing toluene. Since Ullmann-type copper (I) mediated catalytic system is well known for the coupling of bromo substituted oxazolines with various chiral amines,[25] we attempted to use this catalytic system for the synthesis of ligand (**1d**). Nonetheless, no significant improvement in the yield of the desired product was observed, though in a few cases monoarylation products were observed. Recently,

Beletskaya et al. reported pd(dba)$_2$ based catalytic system for the diamination of 1,8-dichloroanthracenes and 1,8-dichloroanthraquinones with different amines including aliphatic and aromatic amines.[26] Inspired by this result, we followed an alternative synthetic route; starting from a new linker 1,8-dichloroanthraquinone instead of 1,8-diaminoanthracene. Diamination of 1,8-dichloroanthraquinone was performed with 2-(S)-4,5-dihydro-4-isopropyloxazol-2-yl)benzenamine,[27] giving the corresponding violet compound **4** in good yield (97 %) after purification by column chromatography. The characteristic –NH proton signal was observed in the low-field region of 11.58 ppm.
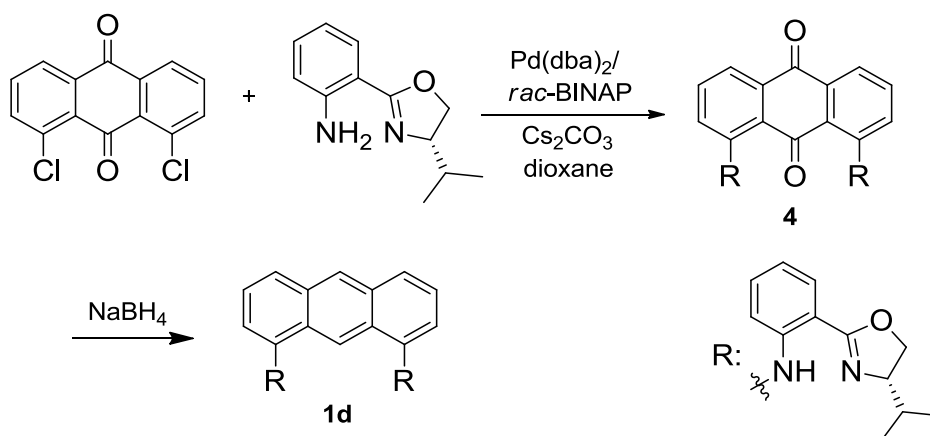
Scheme 6. Synthesis of ligand **1d**

Reduction of **4** with excess sodium borohydride in refluxing anhydrous *iso*-propanol[28] yielded yellow compound **1d** in moderate yield (61 %) (Scheme 6). In the ^{1}HNMR spectra, two new sharp singlets at 8.47 and 9.39 ppm, characteristic peaks of protons at 9 and 10 positions of the anthracene ring, were observed. It is also noticed that the -NH proton and methine proton peaks in **2d** shifted to low-field (12.58 ppm and 1.37 ppm respectively).

4.2.2. Synthesis of Zinc Complexes

The monomeric zinc complexes of bidentate amido-oxazolinate ligands have been prepared *via* metathesis with $Zn[N(SiMe_3)_2]_2$.[4a] Following a similar procedure, we metallated the bischelating ligands (**1a-1d**) with two equivalents of $Zn[N(SiMe_3)_2]_2$ in dry toluene at room temperature, affording the homoleptic bimetallic zinc complexes (**2a-2d**) as yellow precipitates in excellent yields (Scheme **7**). These complexes have shown pronounced sensitivity toward air and moisture as the monomeric zinc complexes.
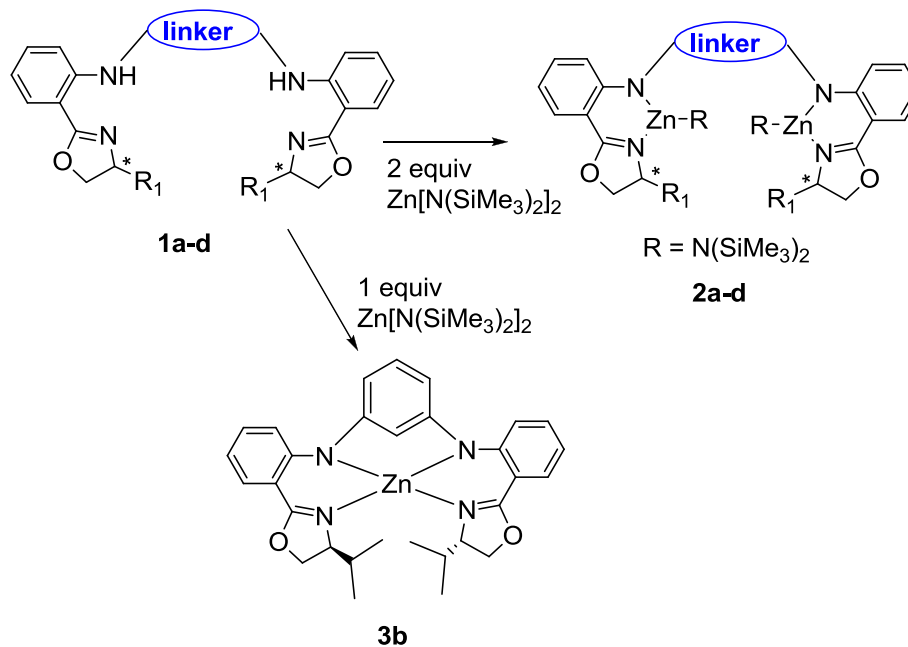
Scheme 7. Synthesis of zinc complexes **2a-2d** and **3b**

The obtained zinc complexes (**2a-2d**) haven been characterized by NMR spectroscopy. The disappearance of the N-H signal of the ligand and the appearance of the new broad peak for the 36 protons of silylamido group in the up-field region at -0.04 ppm (**2a**), -0.03 ppm (**2b**), -0.17 ppm (**2c**) demonstrate the formation of desired complexes (**2a-2c**). Interestingly, for complex **2d**, two peaks that integrate 18H appeared in the region of 0.25 and -0.30 ppm for the silyl protons of $-N(SiMe_3)_2$ group. In all complexes, the

resonances associated with the protons on the oxazoline ring and its substituents shifted downfield in the ^1H NMR spectrum. The same pattern is observed in the ^{13}C NMR spectroscopy as well. For instance, the signal for imine carbon in **2a** appeared at 169.45 ppm, in comparison to 163.00 ppm in **1a**. These observations confirmed the coordination between zinc metal center and nitrogen donors of the ligand, and revealed that the C_2 symmetry of the ligands was retained in solution upon the complex formation. The complete characterization is provided in the supporting information.

Along the dinuclear zinc complexes, a bis-ligated zinc complex **3b** was also synthesized to validate its activity in catalysis (see below). Treatment of ligand **1b** with exactly one equivalent of $Zn[N(SiMe_3)_2]_2$ in dry toluene at room temperature gave complex **3b**. Complex **3b** was isolated as a yellow color powder in a good yield (76 %). ^1H-NMR spectrum of **3b** features two different sets of peaks, indicating that two N,N-bidentate moieties in **3b** are in an asymmetric environment.

4.2.3. Copolymerization of CO_2 and CHO

In our previous chapter, we performed the alternating asymmetric copolymerization of CO_2 and CHO using monomeric zinc complexes of amido-oxazolinates at 500 psi of CO_2 and 75 °C to give an alternating poly(cyclohexene carbonate) with 72 % *m*-centered tetrads.[4a] Here, we are interested in comparing the activity and selectivity of bimetallic and monometallic zinc catalysts and understanding the possible co-operative effect in bimetallic complexes. The standard copolymerization reactions were carried out in neat CHO with a [Zn]/[cyclohexene oxide] ratio of 1:100 (Table 6). The effect of temperature and pressure of CO_2 on the present system was studied using catalyst **2a**. The selectivity and percentage of polycarbonate linkages were determined by measuring the relative

intensity of the methine proton signals of the carbonate linkage (δ = 4.6 ppm) of polymer.

At lower temperatures, catalyst **2a** was more selective toward poly(cyclohexene ether) (PCHE) formation without a detectable amount of poly(cyclohexene carbonate) (PCHC) (Table 6, entry **1** and **2**). In contrast, the monomeric zinc complexes showed no reactivity at all at RT. The structure of the pure homopolymer was verified by an assignable signal at 3.4 ppm (for the ether linkage) in the ^{1}H NMR spectrum. In the ^{13}C NMR spectrum, two broad peaks at 23.58 and 30.43 ppm for the methylene carbons of cyclohexene ring and a sharp peak at 68.30 ppm for the methine carbons were observed. A sharp peak at 1068 cm^{-1} and the absence of a peak around 1700-1740 cm^{-1} in the FTIR spectrum further confirmed the exclusive formation of poly(cyclohexene ether).

Table 6. Screening of the ceaction conditions for copolymerization of CO_2 and CHO[a]

entry	temp. (°C)	pressure (psi)	t/h	conv. (%)[b]	yield (%)[c]	M_n[d] (g/mol)	PDI	carbonate linkage(%)[e]	ether linkage(%)[e]
1	RT	500	48	97	76	139758	1.6	-	100
2	35	500	48	86	71	101182	1.6	-	100
3	50	100	48	72	41	8619	1.4	37	63
4	75	500	20	72	30	10566	1.4	78	22
5	100	500	20	84	17	304999	1.5	3	97
6[f]	75	500	20	54	25	4500	1.3	71	29
7[g]	75	500	24	60	28	148857	1.6	8	92

[a]All the reactions were performed using **2a** in neat CHO unless otherwise mentioned. [b]Determined by ^{1}H NMR spectroscopy. [c]Isolated yields of the major products. [d]Determined by GPC. [e]Carbonate linkages were determined by the integration of the methine protons of PCHC at 4.46 ppm and ether linkages were determined by the integration of the methine protons of PCHE at 3.4 ppm. [f]^{n}Bu$_4$NI was added as cocatalyst. [g]Toluene was used as solvent

It is evident that the catalyst **2a** turned its selectivity toward formation of polycarbonate linkage with increasing temperature (Table 6, entry **3** and **4**). At 500 psi of

CO$_2$, 75 °C, **2a** generated the polymer with 78 % carbonate linkages, comparable with similar monomeric zinc complexes (~85 % polycarbonate linkage). However, a further increase in reaction temperature (to 100°C) diminished the selectivity for polycarbonate linkages (Table 6, entry **5**). This behavior is quite similar to that observed in the case of monomeric zinc complexes of amido-oxazolinate ligands. The combination of **2a** and a co-catalyst (^{n}Bu$_4$NI) did not improve the content of carbonate linkages in the polymer back bone (entry **6**). At moderately dilute conditions, bimetallic complexes have given improved yields for CHO/CO$_2$ copolymers, because the viscosity of the reaction mixture is going down while the local concentration of active sites remains relatively high.[6a,19] Surprisingly, in the present system, dilution of the reaction mixture with toluene gave very high content of polyether linkages (Table 6, entry **7**). Overall these observations did not suggest the presence of a cooperative effect between the two zinc centers towards the copolymerization of CO$_2$ and CHO. Interestingly, we observed very broad molecular weights in the case of polymers that contained high ether linkages. This might be attributed to random polymerization process. The polymers with carbonate linkages have molecular weights closer to theoretical values.

Table 7. Asymmetric copolymerization of CO$_2$ and CHO with catalysts **2a-2d** and **3b**[a]

entry	catalyst	conversion (%)[b]	yield (%)[c]	M_n[d] (g/mol)	PDI	carbonate linkage(%)[e]	ether linkage(%)[e]
1	**2a**	72	30	10566	1.4	78	22
2	**2b**	76	36	232211	1.6	9	91
3	**2c**	70	41	120288	1.6	7	93
4	**2d**	60	5	7792	1.1	50	50
5	**3b**	43	17	193520	1.2	3	97

[a] All the reactions were performed with [CHO]:[catalyst] = 100:1 at 500 psi of CO$_2$, 75 °C in neat CHO for 24 h. [b] Determined by ^{1}H NMR spectroscopy. [c] Isolated yields of the major products. [d] Determined by GPC. [e] Carbonate linkages and ether linkages were determined by the relative intensity of methine protons of PCHC at 4.46 ppm and PCHE at 3.4 ppm

To investigate the influence of linker architecture in bimetallic catalysis, complexes **2a–2d** were employed for alternating copolymerization of CHO and CO_2 under optimized conditions (Table 7). While copolymerization with **2a** gave 78% polycarbonate incorporation in the polymer backbone, polymers obtained with complexes **2b-2c** have very low amount of carbonate linkages. Although catalysts **2a** and **2b** were incorporated with the same linker, the activity of **2a** is substantially higher than **2b** towards polycarbonates. It is believed that this negligible activity of **2b** is due to the high steric congestion around the metal center. Catalyst **2c** with a flexible linker is also shown to have high selectivity for the formation of poly(cyclohexene ether) (Table 7, entry **3**). It is reported that copolymerization activity is sensitive to the orientation of active sites; bimetallic catalysts in which two metal centers are arranged in face-face orientation are more active than their parallel counterparts.[14g] In agreement with the above observation, copolymerization reaction with **2d** gave alternating copolymer with moderate content (50%) of polycarbonate linkage (Table 7, entry **4**).
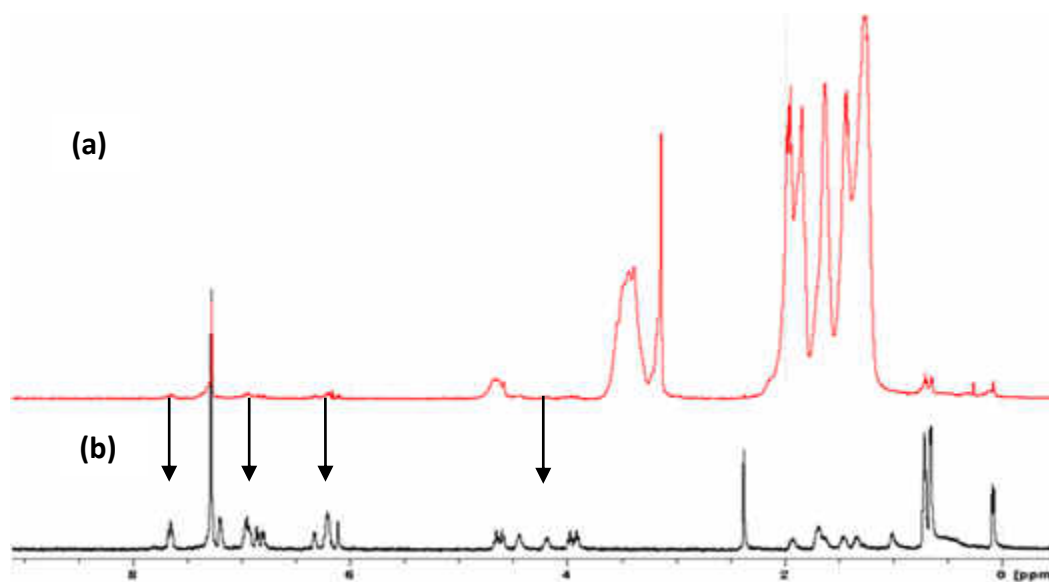
Figure 40. ^{1}H NMR spectra (a) Crude reaction mixture generated by catalyst **2b** (b) Bis(amido-oxazolinate) zinc complex **3b**

Notably, a new set of signals were observed during the copolymerization process, which were assigned to monomeric bis(amido-oxazolinate) zinc complex. This was confirmed by comparison with independently prepared mononuclear compound **3b**. The ^{1}H NMR spectrum of the crude reaction mixture produced by catalyst **2b** contained small peaks in the regions of 3.50-4.50 and 6.00-7.80 ppm, in agreement with the formation of monomeric bis(amido-oxazolinate) zinc complex (Figure 40).

The formation of low carbonate linkages can be attributed to conversion of bimetallic species into monomeric bis-ligated complexes. It is known that bischelating type complexes were inactive for copolymerization of CO_2 and CHO. We carried out a copolymerization reaction with **3b** at similar conditions, which indeed gave a polymer with 93% ether linkages (Table 7, entry **5**). Howerer, when a solution of complex **2b** in C_6D_6 (0.35 mL) was heated at 75 °C for 24 hr, ^{1}H NMR analysis showed no formation of bischelating zinc complex (**3b**). Only in the presence of CO_2, the nearly quantitative conversion of **2b** to **3b** could be observed, along with a small amount of pure ligand. Obviously the transformation is not simply a ligand exchange reaction. At this moment, we assume that this conversion has a significant role in providing high content of ether linkages in the polymer chain.

The microstructure (tacticity) of the resulting PCHC was characterized by ^{13}C NMR spectroscopy. According to the literature,[18g,29] four most prominent tetrad resonances ([*mmm*], [*mmr*], [*mrm*], and [*mrr*]) and two minor tetrad resonances ([*rrr*] and [*rmr*]) can be found in the carbonyl region of the ^{13}C NMR spectrum (154.0-153.30 ppm). In the case of isotactic PCHC, the most intensive peak at 154.02 ppm corresponds to *m*-centered tetrads ([*mmm*] and [*mmr*]) while the remaining two upfield resonances at δ = 153.50 and

153.35 ppm were assigned to r-centered tetrads ([*mrm*] and [*mrr*]). Along with the distinctive resonances in carbonyl region, two series of methylene triads resonances ([*mm*], [*mr*], and [*rr*]) corresponding to two non-equivalent methylene carbons of PCHC were observed in ^{13}C NMR spectrum. The two downfield resonances (δ = 29.91 and 23.28 ppm) correspond to [*mm*] triads, the two triads at δ = 29.59 and 23.06 correlates to [*mr*] triads, and the two highfield resonances (δ=29.05 and 22.54) can be attributed to the [*rr*] triads.
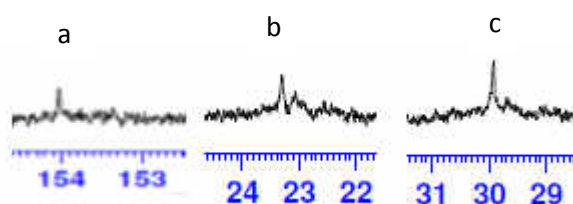
Figure 41. ^{13}C NMR spectrum of the poly(cyclohexene carbonate) generated by catalyst **2d:** (**a**) carbonyl region; (**b** and **c**) methylene region

On the basis of these assignments, poly(cyclohexene carbonate) obtained from **2a** is moderately isotactic with 75 % *m*-centered tetrads (see supporting information), higher than that obtained with the monomeric analogues. Remarkably, the ^{13}C NMR spectrum of PCHC generated by **2d** showed a large peak at 153.40 ppm correlating to the two combined [*mmm*] + [*mmr*] tetrads with very few additional resonances (Figure 41). This revealed that the obtained PCHC is highly isoenriched. To the best of our knowledge, this is the highest isoselectivity achieved for a bimetallic zinc catalyst in the copolymerization of CO_2 and CHO. In both cases, the other two characteristic tetrads in isotactic polymers [*rmr*] and [*rrr*] were not observed. For highly isotactic PCHC, it is noticeable that the intensity of [*rr*] triads is almost negligible. Such a highly selective PCHC was not generated in the case of monomeric zinc complexes of amido-oxazolinate ligands. The high selectivity might be due to the crowdedness around the reaction pocket created by the rigid linker in **2d.**

However, the stereoselectivity of catalyst **2a**, obtained by determination of enantiomeric excess 1,2-*trans*-cyclohexanediol produced from the hydrolysis of the PCHC, is low (*SS*/*RR*: 42/58). Future studies will be directed toward the mechanistic aspects of this copolymerization process.

4.3. Conclusion

In summary, a series of new chiral bimetallic zinc complexes (**2a-2d**) has been synthesized *via* metathesis of C_2-symmetric, dianionic, amido-oxazolinate ligands (**1a-1d**) with $Zn[N(SiMe_3)_2]_2$ in dry toluene. The formation of these complexes was identified by different NMR spectroscopic techniques (^1H NMR, ^{13}C NMR, COSY (^1H-^1H), and HETCOR) and elemental analysis. A monometallic bis(amido-oxazolinate) zinc complex, **3b**, was also synthesized to verify its catalytic activity for copolymerization of CO_2 and CHO. Although the transformation of bimetallic catalytic systems into bis-ligated complexes was observed, catalysts **2a** and **2d** are shown to be viable initiators for copolymerization of CO_2 and CHO. Catalyst **2d**, with the two metal centers oriented parallel to each other, is moderately active (yielding 50 % polycarbonate content) and generates highly isotactic PCHC.

4.4. Experimental Section

General Procedures: All reactions that involved air and/or moisture sensitive compounds were carried out using Schlenk line and glove box techniques. All chemicals were purchased from Aldrich except where noted. Toluene was distilled from Na/benzophenone. $CDCl_3$ and C_6D_6 were dried over CaH_2 and Na/benzophenone, respectively, and distilled and degassed prior to use. Carbon dioxide (Airgas, high purity, 99.995%) was used as received. Cyclohexene oxide was distilled from CaH_2 following three freeze−pump−thaw

cycles and stored in a glove box prior to use. Zinc bis(trimethylsilyl)amide was prepared according to the literature.[30] NMR spectra (^{1}H and ^{13}C) were recorded on a Bruker AVANCE-500 NMR spectrometer. Chiral GC analysis was carried out on an Agilent 7890 with FID detector using a chiral column (cyclodex-B, 30 m × 0.250 mm × 0.25 μm). The temperature program was as follows: injector temperature 250 °C, detector 300 °C, oven initial temperature 120 °C, hold for 30 min, ramp at 30 °C/min to 200 °C, hold for 10 min. Inlet flow: 85 mL/min (split mode, 68:1). Gel permeation chromatography (GPC) analysis was performed on a Varian Prostar, using a PLgel 5 μm Mixed-D column, a Prostar 355 RI detector, and THF as eluent at a flow rate of 1 mL/min (20 °C). Polystyrene standards were used for calibration.

Synthesis of Lignads

Synthesis of ligand 1a. An oven dried round bottom flask was loaded with (*S*)-2-(2-bromophenyl)-4,5-dihydro-4-isopropyloxazole (506 mg, 1.887 mmol), benzene-1,3-diamine (102 mg, 0.944 mmol), Pd$_2$(dba)$_3$ (52 mg, 6 mol%), *rac*-BINAP (71 mg, 12 mol%), sodium *tert*-butoxide (363 mg, 3.774 mmol), and dry toluene (25 mL) in a glove box. The resulting solution was refluxed for 20 hr and reaction mixture was filtered through a fritted funnel. The filtrate was concentrated and subjected to purification by silica gel chromatography (100:5 hexane/ethyl acetate) to afford the pure product as a yellow viscous liquid. Yellow-orange crystals were grown by slow evaporation of the diethylether solution of **1a** (401 mg, 88 %). ^{1}H NMR (500.1 MHz; CDCl$_3$; 298 K) 0.99 (3H, d, *J* = 6.77, CH(C*H*$_3$)$_2$),   1.09 (3H, d, *J* = 6.87 ,CH(C*H*$_3$)$_2$), 1.81 (1H, m, C*H*(CH$_3$)$_2$), 4.06 (1H, t, *J* = 8.18, NCH(R)C*H*$_2$O), 4.14 (1H, m, NC*H*(R)CH$_2$O), 4.40 (1H, t, *J* = 8.70 , NCH(R)C*H*$_2$O), 6.80 (1H, t, *J* = 7.78, *p*-Ph*H*(C$_6$H$_{10}$NO)NHPh), 6.99 (1H, d, *J* = 8.18, *o*-Ph*H*(C$_{12}$H$_{15}$N$_2$O)$_2$)

, 7.23 (1H, s, *o*-Ph*H*(C$_{12}$H$_{15}$N$_2$O)$_2$), 7.31 (2H, *m, m*-Ph*H*(C$_6$H$_{10}$NO)NHPh, *m*-Ph*H*(C$_{12}$H$_{15}$N$_2$O)$_2$), 7.48 (1H, d, *J* = 8.52, *o*-Ph*H*(C$_6$H$_{10}$NO)NHPh), 7.84 (1H, d, *J* = 8.69, *m*-Ph*H*(C$_{12}$H$_{15}$N$_2$O)$_2$), 10.74 (1H, br, N*H*). ^{13}C NMR (125.8 MHz; CDCl$_3$; 298 K): 19.11 ((CH)*Me*$_2$), 19.28 ((CH)*Me*$_2$), 33.67 ((*C*H)Me$_2$), 69.50 (NCH(R)*C*H$_2$O), 73.23(N*C*H(R)CH$_2$O), 110.80, 113.71, 113.86, 115.48, 117.33, 130.13, 130.22, (*C*Harom),132.18, 142.87, 145.59, 163.80 (*C*quart).

Synthesis of ligand 1b. An oven dried round bottom flask was loaded with (*R*)-2-(2-bromophenyl)-4,5-dihydro-4-isobutyloxazole (120 mg, 0.425 mmol), benzene-1,3-diamine (23 mg, 0.213 mmol), Pd$_2$(dba)$_3$ (12 mg, 6 mol%), *rac*-BINAP (16 mg, 12 mol%), sodium *tert*-butoxide (82 mg, 0.852 mmol), and dry toluene (10 mL) in a glove box. The resulting solution was refluxed for 20 hr and reaction mixture was filtered through a fritted funnel. The filtrate was concentrated and subjected to purification by silica gel chromatography (100:5 hexanes/ethyl acetate) to afford the pure product as yellow viscous liquid (93%, 101 mg). ^{1}H NMR (500.1 MHz; CDCl$_3$; 298 K) 1.0 (6H, d, *J* = 5.36, CH$_2$CH(C*H*$_3$)$_2$), 1.40 (1H, m, CH$_2$C*H*(CH$_3$)$_2$), 1.66 (1H, m, C*H*$_2$CH(CH$_3$)$_2$), 1.87 (1H, m, C*H*$_2$CH(CH$_3$)$_2$), 3.88 (1H, t, *J* = 6.80, NCH(R)C*H*$_2$O), 4.41 (2H, m, NC*H*(R)CH$_2$O, NCH(R)C*H*$_2$O), 6.74 (1H, t, *J* = 7.37, *p*-Ph*H*(C$_6$H$_{10}$NO)NHPh) 6.94 (1H, d, *J* = 7.90, *o*-Ph*H*(C$_{12}$H$_{15}$N$_2$O)$_2$)), 7.15 (1H, s, *o*-Ph*H*(C$_{13}$H$_{17}$N$_2$O)$_2$), 7.26 (2H, m, *m*-Ph*H*(C$_6$H$_{10}$NO)NHPh, *m*-Ph*H*(C$_{12}$H$_{15}$N$_2$O)$_2$), 7.39 (1H, d, *J* = 8.44, *o*-Ph*H*(C$_7$H$_{12}$NO)NHPh), 7.78 (1H, d, *J* = 7.89, *m*- Ph*H*(C$_7$H$_{12}$NO)NHPh), 10.55 (1H, br, N*H*). ^{13}C NMR (125.8 MHz; CDCl$_3$; 298 K): 22.90 (CH$_2$CH(*C*H$_3$)$_2$), 23.21 (CH$_2$CH(*C*H$_3$)$_2$), 26.07(CH$_2$*C*H(CH$_3$)$_2$), 45.86 (*C*H$_2$CH(CH$_3$)$_2$), 65.36 (N*C*H(R)CH$_2$O),

71.73 (NCH(R)CH$_2$O), 110.77, 113.76, 114.22, 115.91, 117.25, 130.12 (CHarom),132.09, 142.79, 145.65, 163.68 (Cquart).

Synthesis of ligand 1c. An oven dried round bottom flask was loaded with (R)-2-(2-bromophenyl)-4,5-dihydro-4-isobutyloxazole (514 mg, 1.917 mmol), 4-(4-aminobenzyl)benzenamine, (190 mg, 0.958 mmol) Pd$_2$(dba)$_3$(53 mg, 6 mol%), rac-BINAP(72 mg, 12 mol%), sodium *tert*-butoxide (368 mg, 3.834 mmol), and dry toluene (26 mL) in a glove box. The resulting solution was refluxed for 20 hr and reaction mixture was filtered through a fritted funnel. The filtrate was concentrated and subjected to purification by silica gel chromatography (100:5 hexane/ethyl acetate) to afford the pure product as a yellow viscous liquid (480 mg, 87.4%). ^{1}H NMR (500.1 MHz; CDCl$_3$; 298 K) 0.90 (3H, d, J = 6.71, CH(CH_3)$_2$), 0.96 (3H, d, J = 6.62, CH(CH_3)$_2$), 1.80 (1H, m, CH(CH$_3$)$_2$), 3.95 (1H, s, CH_2(Ph)$_2$), 4.03 (1H, t, J = 8.07, NCH(R)CH_2O), 4.13 (1H, m, NCH(R)CH$_2$O), 4.36 (1H, t, J = 8.79, NCH(R)CH_2O), 6.73 (1H, t, J = 7.44, p-PhH(C$_6$H$_{10}$NO)NHPh), 7.19 -7.25 (2H, m, ArH), 7.26 (1H, d, J = 6.97, o-PhHCH$_2$) 7.32 (1H, d, J = 8.44, m-PhHCH$_2$), 7.74 (1H, d, J = 8.17, m-PhH(C$_6$H$_{10}$NO)NHPh), 10.58 (1H, br, NH). ^{13}C NMR (125.8 MHz; CDCl$_3$; 298 K): 18.98 ((CH)Me_2), 19.21 ((CH)Me_2), 31.78 ((CH)Me$_2$), 41.04 (CH$_2$(Ph)$_2$), 69.21 (NCH(R)CH$_2$O), 73.08 (NCH(R)CH$_2$O), 110.32, 113.19, 116.81,122.13, 129.87, 130.11 (CHarom),132.07, 136.09, 139.70, 146.14, 163.82 (Cquat).

Synthesis of 1,-8-bis(2-(4,5-dihydro-4-isopropyloxazol-2-yl)phenylamino) anthracene -9,10-dione (4). An oven-dried Schlenk flask was loaded with 1,8-dichloroanthracene-9,10-dione (68 mg, 0.244 mmol), 2-(S)-4,5-dihydro-4-isopropyloxazol-2-yl)benzenamine (150 mg, 0.733 mmol), Pd(dba)$_2$ (11 mg, 8 mol%), rac-BINAP (18 mg, 12 mol%),

Cs$_2$CO$_3$(239 mg, 0.733 mmol), and dry 1,4-dioxane (10 mL) in a Glove box. After the reaction mixture was refluxed for 48 hr, the resulting solution was filtered and the filtrate was concentrated. The violet residue was purified by column chromatography (100:10 hexane/ethyl acetate) to give a violet pure product (97%, 145 mg). ^{1}H NMR (500.1 MHz; CDCl$_3$; 298 K) 0.67 (3H, d, J = 6.84, CH(CH_3)$_2$), 0.84 (3H, d, J = 6.66, CH(CH_3)$_2$), 1.61 (1H, m, CH(CH$_3$)$_2$), 4.00 (1H, m, NCH(R)CH_2O), 4.12 (1H, t, J = 4.12, NCH(R)CH$_2$O), 4.30 (1H, t, J = 8.37, NCH(R)CH_2O), 7.07 (1H, t, J = 7.51, p-PhH(C$_6$H$_{10}$NO)Ar), 7.39 (1H, t, J = 8.18, m-PhH(C$_6$H$_{10}$NO)Ar), 7.47 (1H, t, J = 7.75, ArH), 7.54 (1H, d, J = 8.32, ArH), 7.73 (1H, d, J = 8.58, o-PhH(C$_6$H$_{10}$NO)Ar), 7.83 (1H, d, J = 7.36, ArH), 7.89 (1H, d, J = 8.06, m-PhH(C$_6$H$_{10}$NO)Ar), 12.05 (1H, br, NH).

Synthesis of ligand 1d. To a solution of 1, 8-bis(2-(4,5-dihydro-4-isopropyloxazol-2-yl)phenylamino) anthracene-9,10-dione (132 mg, 0.215 mmol) in anhydrous isopropanol (10 mL), excess sodium borohydride (90 mg, 2.371 mmol) and sodium hydroxide (2 mg, 0.046 mmol) were added under nitrogen gas. The mixture was refluxed for 12 hr. The reaction progress was monitored with TLC (10:2 hexane/ethylacetate). The volatiles were removed by rotavapor and the residue was purified by column chromatography (100:8 hexane/ethyl acetate system) to afford the pure product (61 %, 76 mg). ^{1}H NMR (500.1 MHz; CDCl$_3$; 298 K) 0.52 (3H, d, J = 6.83, CH(CH_3)$_2$), 0.53(3H, d, J = 6.53, CH(CH_3)$_2$), 1.37 (1H, m, CH(CH$_3$)$_2$), 3.70 (1H, m, NCH(R)CH_2O), 3.88 (1H, t, J = 8.81, NCH(R)CH$_2$O), 4.32 (1H, t, J = 8.50, NCH(R)CH_2O), 6.80 (1H, t, J = 7.65, p-PhH(C$_6$H$_{10}$NO)Ar), 7.33 (1H, t, J = 8.21, m-PhH(C$_6$H$_{10}$NO)Ar), 7.48 (1H, t, J = 7.75, ArH), 7.64 (1H, d, J = 7.06, ArH), 7.67 (1H, d, J = 8.47, o-PhH(C$_6$H$_{10}$NO)Ar), 7.76 (1H, d, J = 8.73, ArH), 7.87 (1H, d, J = 7.86, m-PhH(C$_6$H$_{10}$NO)Ar), 8.47 (1H, s, ArH), 9.39

(1H, s, ArH), 11.58 (1H, br, NH). ^{13}C NMR (125.8 MHz; CDCl$_3$; 298 K): 18.79 ((CH)Me_2),

19.00 ((CH)Me_2), 33.43 ((CH)Me$_2$), 69.70 (NCH(R)CH$_2$O), 73.10(NCH(R)CH$_2$O),

110.98, 113.41, 115.13, 116.34, 117.13, 122.88, 125.69, 127.04, 127.80 (CHarom), 129.94,

132.16, 133.40, 138.08, 146.30, 163.72 (Cquart).

Synthesis of Zinc Complexes

Synthesis of zinc complex 2a. An oven dried Schlenk flask was loaded with ligand **1a**

(150 mg, 0.311 mmol) and Zn[N(SiMe$_3$)$_2$] (0.250 mL, 0.622 mmol) in toluene (6 mL) in a

glove box and the resulting yellow solution was stirred for 8 hr at room temperature. All

volatiles were removed *in vacuo* to afford the pure product as yellow powder; yield: 225

mg (78 %). ^{1}H NMR (500.1 MHz; CDCl$_3$; 298 K) -0.04 (18H, br, N(Si(Me)$_3$)$_2$), 0.85 (3H,

d, J = 6.73, CH(CH_3)$_2$), 1.0 (3H, d, J = 7.15, CH(CH_3)$_2$), 2.51 (1H, m, CH(CH$_3$)$_2$), 4.38

(1H, t, J = 7.16, NCH(R)CH_2O), 4.42 (1H, t, J = 8.86, NCH(R)CH$_2$O), 4.51 (1H, m,

NCH(R)CH_2O), 6.44 (1H, t, J = 7.61, p-PhH(C$_6$H$_{10}$NO)NPh), 6.88 (1H, br, o-

PhH(C$_6$H$_{10}$NO)NPh), 6.88 (1H, br, o-PhH(C$_{12}$H$_{15}$N$_2$O)$_2$), 7.09 (1H, t, J = 8.34, m-

PhH(C$_6$H$_{10}$NO)NPh), 7.26 (1H, s, o-PhH(C$_{12}$H$_{15}$N$_2$O)$_2$), 7.41 (1H, t, J = 7.92, m-

PhH(C$_{12}$H$_{15}$N$_2$O)$_2$), 7.77 (1H, d, J = 8.18, m-PhH(C$_{12}$H$_{15}$N$_2$O)$_2$). ^{13}C NMR (125.8 MHz;

CDCl$_3$; 298 K): 5.10 (N(SiMe_3)$_2$), 14.67 ((CH)Me_2), 19.35 ((CH)Me_2), 30.80 ((CH)Me$_2$),

66.35 (NCH(R)CH$_2$O), 69.31 (NCH(R)CH$_2$O), 104.26, 113.24, 117.86, 122.66, 128.47,

129.27 (CHarom),131.31, 134.00, 157.98, 169.45 (Cquat). Anal. Calcd. for

C$_{42}$H$_{68}$N$_6$O$_2$Si$_4$Zn$_2$.C$_7$H$_8$: C, 57.45; H, 7.48; N, 8.20. Found: C, 57.03; H, 6.93; N, 8.33.

Synthesis of zinc complex 2b. Complex **2b** was synthesized according to the same

procedure as described for **2a**. Ligand **2b** (217 mg, 0.425 mmol), Zn[N(SiMe$_3$)$_2$]$_2$ (0.34

mL, 0.850 mmol), and toluene (10 mL) were used. The pure product was obtained as

yellow powder (347 mg, 85 %). ^{1}H NMR (500.1 MHz; CDCl$_3$; 298 K) -0.03 (18H, br, N(Si(*Me*)$_3$)$_2$), 1.03 (6H, d, *J* = 7.03, CH$_2$CH(C*H*$_3$)$_2$), 1.51 (1H, m, CH$_2$C*H*(CH$_3$)$_2$), 1.68 (1H, m, C*H*$_2$CH(CH$_3$)$_2$), 2.31 (1H, m, *J* = , C*H*$_2$CH(CH$_3$)$_2$), 4.15 (1H, t, *J* = 8.38, NCH(R)C*H*$_2$O), 4.53 (1H, m, NC*H*(R)CH$_2$O), 4.64 (1H, t, *J* = 8.98, NCH(R)C*H*$_2$O), 6.43 (1H, t, *J* = 7.58, *p*-Ph*H*(C$_6$H$_{10}$NO)NPh), 6.88 (1H, br, *o*-Ph*H*(C$_6$H$_{10}$NO)NPh), 6.88 (1H, br, *o*-Ph*H*(C$_{12}$H$_{15}$N$_2$O)$_2$), 7.08 (1H, t, *J* = 7.61, *m*-Ph*H*(C$_6$H$_{10}$NO)NPh), 7.19 (1H, s, *o*-Ph*H*(C$_{12}$H$_{15}$N$_2$O)$_2$), 7.40 (1H, t, *J* = 7.92, *m*-Ph*H*(C$_{12}$H$_{15}$N$_2$O)$_2$), 7.77 (1H, d, *J* = 8.07, *m*-Ph*H*(C$_{12}$H$_{15}$N$_2$O)$_2$).^{13}C NMR (125.8 MHz; CDCl$_3$; 298 K): 5.18 (N(Si*Me*$_3$)$_2$), 21.93 (CH$_2$CH(C*H*$_3$)$_2$), 24.0 (CH$_2$CH(C*H*$_3$)$_2$), 25.94(CH$_2$C*H*(CH$_3$)$_2$), 45.32 (C*H*$_2$CH(CH$_3$)$_2$), 63.64 (NCH(R)C*H*$_2$O), 71.81 (NCH(R)CH$_2$O), 104.51, 113.28, 117. 90, 118.02, 122.54, 123.81 (*C*Harom), 131.39, 133.39, 157.86, 169.38 (*C*quart). Anal. Calcd. for C$_{44}$H$_{72}$N$_6$O$_2$Si$_4$Zn$_2$: C, 55.04; H, 7.56; N, 8.75. Found: C, 55.06; H, 6.26; N, 7.41.

Synthesis of zinc complex 2c. Complex **2c**: Complex **2c** was synthesized similarly as **2a**: Ligand **2c** (88 mg, 0.153 mmol), Zn[N(SiMe$_3$)$_2$]$_2$ (0.13 mL, 0.307 mmol), and toluene (4 mL) were used. Pure product was isolated as yellow powder in good yield (128 mg, 82 %). ^{1}H NMR (500.1 MHz; CDCl$_3$; 298 K) -0.23 (18H, br, N(Si(*Me*)$_3$)$_2$), 0.89 (3H, d, *J* = 6.75, CH(C*H*$_3$)$_2$), 1.03 (3H, d, *J* = 7.11, CH(C*H*$_3$)$_2$), 2.48 (1H, m, C*H*(CH$_3$)$_2$), 4.04 (1H, s, C*H*$_2$(Ph)$_2$), 4.37 (1H, t, *J* = 6.91, NCH(R)C*H*$_2$O), 4.43 (1H, t, *J* = 8.75, NC*H*(R)CH$_2$O), 4.51 (1H, m, NCH(R)C*H*$_2$O), 6.41 (1H, t, *J* = 7.34, *p*-Ph*H*(C$_6$H$_{10}$NO)NHPh), 6.75 (1H, d, *J* = 8.80, *o*-Ph*H*(C$_6$H$_{10}$NO)NHPh), 6.96 (2H, d, *J* = 8.07, *o*-Ph*H*CH$_2$), 7.07 (1H, t, *J* = 7.98, *m*-Ph*H*(C$_6$H$_{10}$NO)NHPh), 7.14 (2H, d, *J* = 8.42, *m*-Ph*H*CH$_2$), 7.80 (1H, d, *J* = 8.25, *m*-Ph*H*(C$_6$H$_{10}$NO)NHPh) ^{13}C NMR (125.8 MHz; CDCl$_3$; 298 K): 4.93 (N(Si*Me*$_3$)$_2$), 5.18 (N(Si*Me*$_3$)$_2$), 14.89 ((CH)*Me*$_2$), 19.45 ((CH)*Me*$_2$), 30.89 ((*C*H)Me$_2$), 41.08 (*C*H$_2$(Ph)$_2$),

67.87 (NCH(R)CH₂O), 69.76 (NCH(R)CH₂O), 104.24, 113.19, 117.28, 125.54, 126.77, 130.48 (CHarom), 131.52, 134.11,148.24, 157.35, 168.10 (Cquat).

Synthesis of zinc complex 2d. This complex was prepared according to the procedure described for complex **2a**. Ligand **2d** (19 mg, 0.033 mmol), Zn[N(SiMe₃)₂]₂ (27 µL, 0.066 mmol), and toluene (3 mL) were used and **2d** was obtained in a good yield as a yellow powder (30 mg, 87 %). ¹H NMR (500.1 MHz; C₆D₆; 298 K) -0.30 (9H, br, N(Si(*Me*)₃)₂), -0.29 (9H, s, N(Si(*Me*)₃)₂), 0.67 (6H, d, *J* = 6.83, CH(C*H*₃)₂), 2.45 (1H, m, C*H*(CH₃)₂), 3.90 (1H, t, *J* = 7.84, NCH(R)C*H*₂O), 4.04 (1H, t, *J* = 9.27, NC*H*(R)CH₂O), 4.19 (1H, m, NCH(R)C*H*₂O), 6.20 (1H, t, *J* = 7.17, Ar*H*), 6.67 (1H, d, *J* = 8.75, Ar*H*), 6.82 (1H, t, *J* = 7.10, Ar*H*), 7.32 (1H, s, Ar*H*), 7.40 (1H, d, *J* = 6.67, Ar*H*), 7.44 (1H, t, *J* = 8.53, Ar*H*), 7.73 (1H, d, *J* = 8.43, ArH), 7.83 (1H, d, *J* = 8.52, Ar*H*), 8.31 (1H, s, Ar*H*). ¹³C NMR (125.8 MHz; CDCl₃; 298 K): 3.73 (N(Si*Me*₃)₂), 16.35 ((CH)*Me*₂), 17.55 ((CH)*Me*₂), 28.97 ((*C*H)Me₂), 69.76 (NCH(R)*C*H₂O), 69.31 (N*C*H(R)CH₂O), 107.33, 110.62, 118.20, 119.50, 120.06, 124.83, 126.44, 126.63, 126.92 (*C*Harom), 129.23, 131.73, 133.26, 134.40, 145.16, 168.10 (*C*quart).

Synthesis of zinc complex 3b. A solution of ligand **1b** (180 mg, 0.352 mmol) and Zn[N(SiMe₃)₂]₂ (0.14 mL, 0.360 mmol) in dry toluene was stirred for 8 hr at RT. All volatiles were removed *in vacuo* to afford yellow solid (153 mg, 76 %). ¹H NMR (500.1 MHz; CDCl₃; 298 K) 0.58 (6H, d, *J* = 6.23, CH₂CH(C*H*₃)₂), 0.65 (6H, d, *J* = 6.23, CH₂CH(C*H*₃)₂), 0.94 (1H, br, CH₂C*H*(CH₃)₂), 1.29 (1H, br, CH₂C*H*(CH₃)₂), 1.39 (1H, br , C*H*₂CH(CH₃)₂), 1.63(2H, br , C*H*₂CH(CH₃)₂), 1.86 (1H, br, C*H*₂CH(CH₃)₂), 3.85 (1H, t, *J* = 9.11, NCH(R)C*H*₂O), 3.91 (1H, t, *J* = 8.81, NCH(R)C*H*₂O), 4.11 (1H, br, NC*H*(R)CH₂O), 4.38 (1H, br, NC*H*(R)CH₂O), 4.53 (1H, t, *J* = 8.64, NCH(R)C*H*₂O), 4.59

(1H, t, J = 8.39, NCH(R)CH_2O), 6.05 (1H, m, p-PhH(C$_6$H$_{10}$NO)NPh), 6.14 (3H, br, o-PhH(C$_6$H$_{10}$NO)NPh), 6.27 (1H, m, o-PhH(C$_{12}$H$_{15}$N$_2$O)$_2$), 6.73 (1H, d, J = 8.96, m-PhH(C$_6$H$_{10}$NO)NPh), 6.80 (1H, d, J = 8.97, m-PhH(C$_6$H$_{10}$NO)NPh), 6.89 (3H, m, m-PhH(C$_6$H$_{10}$NO)NPh), 7.14 (1H, d, J = 6.56, m-PhH(C$_6$H$_{10}$NO)NPh), 7.59 (1H, t, J = 8.90, m-PhH(C$_6$H$_{10}$NO)NPh). ^{13}C NMR (125.8 MHz; CDCl$_3$; 298 K): 21.70 (CH$_2$CH(CH_3)$_2$), 22.47, 22.49, 22.56, 22.66 25.52, 25.72, 45.45, 45.54, 63.47, 63.98, 71.78, 72.71, 104.39, 14.97, 117.71, 118.09, 119.08, 122.75, 125.53, 128.46, 129.29, 129.88, 131.18, 133.04, 138.10, 158.12, 158.32, 168.35, 168.42. Anal. Calcd. for C$_{32}$H$_{36}$N$_4$O$_2$Zn.CH$_2$Cl$_2$: C, 60.14; H, 5.81; N, 8.50. Found: C, 60.18; H, 5.81; N, 8.52.

Copolymerization of cyclohexene oxide/CO$_2$. In a Glovebox, a 60 mL Teflon-lined Parr high-pressure reactor vessel that was previously dried in an oven was charged with a zinc catalyst (1 mol %) and CHO (1 equiv). The vessel was sealed, taken out of the Glovebox, and brought to desired temperature and CO$_2$ pressure. After the mixture was stirred for the allotted time, it was cooled and a small aliquot of reaction mixture was taken for ^{1}H NMR spectroscopy to determine the conversion. When no further conversion was noted, the polymerization mixture was transferred into a round-bottom flask with CH$_2$Cl$_2$ (3−5 mL) and the polymer was precipitated from addition of methanol (18−30 mL). After separation, the polymer was dried in vacuo to constant weight to determine the yield.

Hydrolysis of polymers and chiral GC analysis. In a typical procedure, a small round-bottom flask was loaded with polycarbonate (20 mg, 0.141 mmol) and NaOH (11 mg, 0.281 mmol) in MeOH (4 mL). The mixture was refluxed for 4 h and then neutralized with HCl(aq) (1 M). The crude mixture was then extracted with ether. After drying over anhydrous MgSO$_4$, a small aliquot was injected into a GC equipped with a Cyclodex-B

column to determine the enantiomeric excess of the 1,2-trans-cyclohexanediol (t_R = 14.32 min for (*S*,*S*)-1,2-trans-cyclohexanediol, t_R = 14.75 min for (*R*,*R*)-1,2-transcyclohexanediol).

4.5. References

1. (a) Raquez, J-M.; Habibi, Y.; Murariu, M; Dubois, P. *Prog. Polym. Sci.* **2013**, *ASAP*. (b) Yao, K.; Tang, C. *Macromolecules* **2013**, *46*, 1689−1712. (c) Miller, S. A. *ACS Macro Lett*. **2013**, *2*, 550−554. (d) Tschan, M. J.-L.; Brule, E.; Haquette, P.; Thomas, C. M. *Polym. Chem.* **2012**, *3*, 836−851. (e) Yao, K.; Wang, J.; Zhang, W.; Lee, J. S.; Wang, C.; Chu, F.; He, X.; Tang, C. *Biomacromolecules* **2011**, *12*, 2171–2177. (f) Robert, C.; De Montignv, F.; Thomas, C. M. *Nature Commun*. **2011**, *2*, 586–591. (g) Klaus, S.; Vagin, S. I.; Lehenmeier, M. W.; Deglmann, P.; Brym, A. K.; Rieger, B. *Macromolecules* **2011**, *44*, 9508–9516. (h) Sakakura, T.; Kohno, K. *Chem. Commun.* **2009**, 1312−1330. (i) Sakakura, T.; Choi, J.-C.; Yasuda, H. *Chem. Rev.* **2007**, *107*, 2365−2387. (j) Aresta, M.; Dibenedetto, A. *Dalton Trans*. **2007**, 2975−2992. (k) Yu, L. Biodegradable Polymer Blends and Composites from Renewable Resources; A John Wiley & Sons: Hoboken, New Jersey, USA, **2009**.

2. (a) Tschan, M. J.-L.; Brule, E.; Haquette, P.; Thomas, C. M. *Polym .chem.* **2012**, *3*, 836−851 (b) Vechorkin, O.; Hirt, N.; Hu, X. *Org. Lett.* **2010**, *12*, 3567–3569. (c) Kember, R. M; Knight, P. D.; Reung, P. T. R.; Williams, C. K. *Angew. Chem., Int. Ed.* **2009**, *48*, 931–933. (d) Sakakura, T.; Kohno, K. *Chem. Commun. 2009*, 1312−1330. (e) Sakakura, T.; Choi, J.-C.; Yasuda, H. *Chem. Rev.* **2007**, *107*, 2365−2387. (f) Aresta, M.; Dibenedetto, A. *Dalton Trans*. **2007**, 2975−2992.

3. (a) Nakano, K.; Kobayashi, K.; Ohkawara, T.; Imoto, H.; Nozaki, K. *J. Am. Chem. Soc.* **2013**, *135*, 8456 −8459. (b) Geschwind, J.; Frey, H. *Macromolecules* **2013**, *46*, 3280–3287. (c) Luinstra, G. A.; Borchardt, E. *Adv. Polym. Sci*. **2012**, *245*, 29–48. (d) Lu, X-B.; Darensbourg, D. J. *Chem. Soc. Rev.,* **2012**, *41*, 1462–1484. (e) Kember, M. R.; Buchard, A.; Williams, C. K. *Chem. Commun*. **2011**, *47*, 141−163. (f) Klaus, S.; Lehenmeier, M. W.; Anderson, C. E.; Rieger, B. *Coord. Chem. Rev.* **2011**, *255*, 1460−1479. (g) Lehenmeier, M. W; Bruckmeier, C.; Klaus, S.; Dengler, J. E.; Deglmann, P.; Ott, A-K.; Rieger, B. *Chem. Eur. J.* **2011**, *17*, 8858–8869. (h) Darensbourg, D. J. *Inorg. Chem*. **2010**, *49*, 10765−10780. (i) Qin, Y.; Wang, X. *Biotechnol. J*. **2010**, *5*, 1164–1180. (j) Darensbourg, D. J. *Chem. Rev.* **2007**, *107*, 2388−2410 (k) Coates, W. G.; Moore, R. D. *Angew. Chem., Int. Ed.* **2004**, *43*, 6618–6639. (l) Darensbourg, D. J.; Mackiewicz, R. M.; Phelps, A. L.; Billodeaux, D. R. *Acc. Chem. Res*. **2004**, *37*, 836−844. (m) Nakano, K.; Kosaka, N.; Hiyama, T.; Nozaki, K. *Dalton Trans.* **2003**, 4039−4050.

4 (a) Abbina, S.; Du, G. *Organometallics* **2012**, *31*, 7394–7403. (b) Bok, T.; Yun, H.; Lee, B. Y. *Inorg. Chem.* **2006**, *45*, 4228–4237. (c) Cheng, M.; Lobkovsky, E. B.; Coates, G. W. *J. Am. Chem. Soc*. **1998**, *120*, 11018−11019. (d) Cheng, M.; Moore, D. R.; Reczek, J. J.; Chamberlain, B. M.; Lobkovsky, E. B.; Coates, G. W. *J. Am. Chem. Soc*. **2001**, *123*, 8738−8749. (e) Allen, S. D.; Moore, D. R.; Lobkovsky, E. B.; Coates, G. W. *J. Am. Chem. Soc*. **2002**, *124*, 14284−14285. (f) Moore, D. R.; Cheng, M.; Lobkovsky, E. B.; Coates, G. W. *Angew. Chem., Int. Ed*. **2002**, *41*, 2599−2602. (g) Moore, D. R.; Cheng, M.; Lobkovsky, E. B.; Coates, G. W. *J. Am. Chem. Soc*. **2003**, *125*, 11911−11924. (h) Byrne, C. M.; Allen, S. D.; Lobkovsky, E. B.; Coates, G. W. *J. Am. Chem. Soc*. **2004**, *126*, 11404−11405. (i)

Inoue, S.; Koinuma, H.; Tsuruta, T. *J. Polym. Sci., Part B* **1969**, *7*, 287−292. (j) Inoue, S.; Koinuma, H.; Tsuruta, T. *Makromol. Chem.* **1969**, *130*, 210−220.

5. (a) Nishioka, K.; Goto, H.; Sugimoto, H. *Macromolecules*, **2012**, *45*, 8172–8192. (b) Chisholm, M. H.; Zhou, Z. *J. Am. Chem. Soc*. **2004**, *126*, 11030–11039.

6. (a) Piesik, D. F.-J.; Range, S.; Harder, S. *Organometallics* **2008**, *27*, 6178–6187. (b) Darensbourg, D. J.; Choi, W.; Richers, C. P. *Macromolecules* **2007**, *40*, 3521–3523.

7. (a) Dean, R. K.; Dawe, L. N.; Kozak, C. M. *Inorg. Chem*. **2012**, *51*, 9095–9103. (b) Darensbourg, D. J.; Mackiewicz, R. M.; Rodgers, J. L.; Fang, C. C.; Billodeaux, D. R.; Reibenspies, J. H. *Inorg. Chem.* **2004**, *43*, 6024–6034. (c) Darensbourg, D. J.; Yarbrough, J. C.; Ortiz, C.; Fang, C. C. *J. Am. Chem. Soc.* **2003**, *125*, 7586–7591. (d) Darensbourg, D. J.; Yarbrough, J. C. *J. Am. Chem. Soc.* **2002**, *124*, 6335–6342. (e) Kruper, W. J.; Dellar, D. V. *J. Org. Chem.* **1995**, *60*, 725–727.

8. (a) Liu, J.; Ren, W-M.; Liu, Y.; Lu, X-B. *Macromolecules* **2013**, 46, 1343–1349. (b) Wu, G-P.; Ren, W-M.; Luo, Y.; Li, B.; Zhang, W-Z.; Lu, X-B. *J. Am. Chem. Soc.* **2012**, *134*, 5682–5688. (c) Ren , W-M.; Zhang, X.; Liu, Y.; Li, J-F.; Wang, H.; Lu, X-B. *Macromolecules*, **2010**, *43*, 1396–1402. (d) Qin, Z.; Thomas, C. M.; Lee, S.; Coates, G. W. *Angew. Chem., Int. Ed.* **2003**, *42*, 5484–5487. (e) Lu, X.-B.; Wang, Y. *Angew. Chem., Int. Ed*. **2004**, *43*, 3574–3577.

9. (a) Darensbourg, D. J.; Wildeson, J. R.; Lewis, S. J.; Yarbrough, J. C. *J. Am. Chem. Soc*. **2002**, *124*, 7075–7083. (b) Darensbourg, D. J.; Niezgoda, S. A.; Draper, J. D.; Reibenspies, J. H. *J. Am. Chem. Soc.* **1998**, *120*, 4690–4698.

10. (a) Kember, M. R.; Williams, C. K. *J. Am. Chem. Soc.* **2012**, *134*, 15676–15679. (b) Li, C-Y.; Wu, C-R.; Liu, Y-C.; Ko, B-T. *Chem. Commun.* **2012**, *48*, 9628–9630. (c) Xiao, Y.; Wang, Z.; Ding, K. *Macromolecules* **2006**, *39*, 128–137.

11. (a) Li, W.; Wu, W.; Wang, Y.; Yao, Y.; Zhanga, Y.; Shena, Q. *Dalton Trans*. **2011**, *40*, 11378–11381. (b) Vitanova, D. V.; Hampel, F.; Hultzsch, K. C. *J. Organomet. Chem.* **2005**, 690, 5182–5197. (c) Cui, D.; Nishiura, M.; Hou, Z. *Macromolecules*, **2005**, 38, 4089–4095.

12. (a) Chilleck, M. A.; Braun, T.; Herrmann, R.; Braun, B. *Organometallics* **2013**, *32*, 1067−1074. (b) Sun, S.; Sun, Q.; Zhao, B.; Zhang, Y.; Shen, Q.; Yao, Y. *Organometallics* **2013**, *32*, 1876−1881. (c) Lindsay, S.; Lo, S. K.; Maguire, O. R.; Bill, E.; Probert, M. R.; Sproules, S.; Hess, C. R. *Inorg. Chem.* **2013**, *52*, 898−909. (d) Sun, S.; Nie, K.; Tan, Y.; Zhao, B.; Zhang, Y.; Shena, Q.; Yao, Y. *Dalton Trans*. **2013**, *42*, 2870–2878. (e) Chuang, H-J.; Chen, H-L.; Huang, B-H.; Tsai, T-E.; Huang, P-L.; Liao, T-T.; Lin, C-C. *J. Poly. Sci. Pol. Chem.* **2013**, *51*, 1185–1196. (f) Li, L.; Wu, C.; Liu, D.; Li, S.; Cui, D. *Organometallics* **2013**, *32*, 3203–3209. (g) Dean, R. K.; Dawe, L. N.; Kozak, C. M. *Inorg. Chem.* **2012**, *51*, 9095−9103. (h) Wang, Y.; Zhao, W.; Liu, D.; Li, S.; Liu, X.; Cui, D.; Chen, X. *Organometallics* **2012**, *31*, 4182−4190. (i) Arbaoui, A.; Redshaw, C.; Sanchez-Ballester, N. M.; Elsegood, M. R. J.; Hughes, D. L. *Inorg. Chim. Acta* **2011**, *365*, 96–102.

(j) Devoille, A. M. J.; Richardson, P.; Bill, N. L.; Sessler, J. L.; Love. J. B. *Inorg. Chem.* **2011**, *50*, 3116–3126. (k) Devoille, A. M. J.; Richardson, P.; Bill, N. L.; Sessler, J. L.; Love, J. B. *Inorg. Chem.* **2011**, *50*, 3116–3126. (l) Kember, M. R.; White, A. J. P.; Williams, C. K. *Macromolecules* **2010,** *43*, 2291–2298. (m) Kember, M. R.; Knight, P. D.; Reung, P. T. R.; Williams, C. K. *Angew. Chem., Int. Ed.* **2009**, *48*, 931–933. (n) Yao, W.; Mu, Y.; Gao, A.; Gao, W.; Ye, L. *Dalton Trans.* **2008**, 3199–3206. (o) Doyle, D. J.; Gibson, V. C.; White, A. J. P. *Dalton Trans.* **2007**, 358–363.(p) Xiao, Y.; Wang, Z.; Ding, K. *Macromolecules* **2006**, *39*, 128–137. (q) Xiao, Y.; Wang, Z.; Ding, K. *Chem. Eur. J.* **2005**, *11*, 3668–3678.

13. (a) Kong, S.; Song, K.; Liang, T.; Guo, C-Y.; Sun, W-H.; Redshaw, C. *Dalton Trans.* **2013**, *42*, 9176–9187. (b) Li, H.; Marks, T. J. *PNAS*, **2006**, *103*, 15295–15302.

14. (a) Nakano, K.; Hashimotoa, S.; Nozaki, K. *Chem. Sci.* **2010**, *1*, 369–373. (b) Range, S.; Piesik, D. F.-J.; Harder, S. *Eur. J. Inorg. Chem.* **2008**, 3442–3451. (c) Pilz, M. F.; Limberg, C.; Lazarov, B. B.; Kai C.; Hultzsch, K. C.; Ziemer, B. *Organometallics* **2007**, *26*, 3668–3676. (d) Noh, E. K.; Na, S. J.; Sujith, S.; Kim, S-W.; Lee, B.Y. *J. Am. Chem. Soc.* **2007**, *129*, 8082–8083. (e) Lu, X-B.; Shi, L.; Wang, Y-M.; Zhang, R.; Zhang, Y-J.; Peng, X-J.; Zhang, Z-C.; Li, B.; *J. Am. Chem. Soc.* **2006**, *128*, 1664–1674. (f) Xiao, Y.; Wang, Z.; Ding, K. *Chem. Eur. J.* **2005**, *11*, 3668–3678. (g) Lee, B. Y.; Kwon, H. Y.; Lee, S. Y.; Na, S. J.; Han, S-I.; Yun, H.; Lee, H.; Park, Y-W. *J. Am. Chem. Soc.* **2005**, *127*, 3031–3037.

15. (a) Kember, M. R.; White, A. J. P.; Williams, C. K. *Inorg. Chem.* **2009**, *48*, 9535–9542. (b) Knight, P. D.; White, A. J. P.; Williams, C. K. *Inorg. Chem.* **2008**, *47*, 11711–11719. (c) Kroger, M.; Folli, C.; Walter, O.; Doring, M. *Adv. Synth. Catal.* **2006**, *348*, 1908–1918. (d) Bok, T.; Yun, H.; Lee, B. Y. *Inorg. Chem.* **2006**, *45*, 4228–4237. (e) Allen, S. D.; Moore, D. R.; Lobkovsky, E. B.; Coates, G. W. *J. Organomet. Chem.* **2003**, *68,* 137–148. (f) Nakano, K.; Nozaki, K.; Hiyama, T. *J. Am. Chem. Soc.* **2003**, *125*, 5501–5510. (g) Moore, D. R.; Cheng, M.; Lobkovsky, E. B.; Coates, G. W. *Angew. Chem., Int. Ed.* **2002**, *41,* 2599–2603.

16. Darensbourg, D. J.; Wildeson, J. R.; Yarbrough, J. C.; Reibenspies. J. H. *J. Am. Chem. Soc.* **2000**, *122,* 12487–12496.

17. (a) Nozaki, K.; Nakano, K.; Hiyama, T. *J. Am. Chem. Soc.* **1999**, *121*, 11008−11009. (b) Nakano, K.; Nozaki, K.; Hiyama, T. *J. Am. Chem. Soc.* **2003**, *125*, 5501−5510. (c) Nakano, K.; Hiyama, T.; Nozaki, K. *Chem. Commun.* **2005**, 1871−1873.
18. Nakano, K.; Hashimoto, S.; Nakamura, M.; Kamada, T.; Nozaki, K. *Angew, Chem., Int. Ed.* **2011**, *50*, 4868−4871.

19. Pilz, M. F.; Limberg, L.; Lazarov, B. B.; Hultzsch, K. C.; Ziemer, B. *Organometallics* **2007**, *26*, 3668–3676.

20. Dahan, A.; Ashkenazi, T.; Kuznetsov, V.; Makievski, S.; Drug, E.; Fadeev, L.; Bramson, M.; Schokoroy, S.; Rozenshine-Kemelmakher, E.; Gozin, M. *J. Org. Chem.* **2007**, *72*, 2289–2296.

21. Binda, P. I.; Abbina, S.; Du, G. *Synthesis* **2011**, 2609−2618.

22. (a) Cheng, X-F.; Li, Y.; Su, Y-M.; Yin, F.; Wang, J-Y.; Sheng, J.; Vora, H. U.; Wang, X-S.; Yu, J-Q. *J. Am. Chem. Soc.* **2013**, *135*, 1236–1239. (b) Nicolai, S.; Sedigh-Zadeh. R.; Waser, J. *J. Org. Chem.* **2013**, 78, 3783–3801. (c) Cannon, J. S.; Olson, A. C.; Overman, L. E.; Solomon, N. S. *J. Org. Chem.* **2012**, *77*, 1961–1973. (d) Tardiff, B. J.; McDonald, R.; Ferguson, M. J.; Stradiotto, M. *J. Org. Chem.* **2012**, *77*, 1056–1071. (e) Giri, R.; Maugel, N; Li, J. J; Wang, D.-H.; Breazzano, S. P.; Saunders, L. B.; Yu, J.-O. *J. Am. Chem. Soc.* **2007**, *129,* 3510–3511. (f) Molander, G.A.; Canturk, B. *Angew. Chem., Int. Ed.* **2009**, *48*, 9240–9246. (g) Shen, Q.; Hartwig, J. *J. Am. Chem. Soc.* **2006**, *128*, 10028–10029.

23. (a) Cheung, C. W.; Surry, D. S.; Buchwald, S. L. *Org. Lett.* **2013**, *ASAP*. (b) Raders, S. M.; Moore, J. N.; Parks, J. K.; Miller, A. D.; Leibing, T. M.; Kelley, S. P.; Rogers, R. D.; Shaughnessy, K. H. *J. Org. Chem.* **2013**, *78*, 4649–4664. (c) Bruno, N, C.; Tudge, M. T.; Buchwald, S. L. *Chem. Sci.* **2013**, *4*, 916–920. (d) Shrestha, R.; Mukherjee, P.; Tan, Y.; Litman, C. Z.; Hartwig, J. F. *J. Am. Chem. Soc.* **2013**, *135*, 8480–8483.

24. (a) Doherty, S.; Knight, J. G.; Smyth, C. H.; Sore, N. T.; Rath, R. K.; McFarlane, W.; Harrington, R. W.; Clegg, W. *Organometallics* **2006,** *25,* 4341–4350. (b) Wolfe, J. P.; Wagaw, S.; Buchwald, S. L. *J. Am. Chem. Soc.* **1996**, *118*, 7215–7219. (c) Driver, M. S.; Hartwig, J. F. *J. Am. Chem. Soc.* **1996**, *118*, 7217-7223.

25. Shafir, A.; Buchwald, S. *J. Am. Chem. Soc.* **2006**, *128*, 8742–8743.

26. Beletskaya, I. P.; Bessmertnykh, A. G.; Averin, A. D.; Denat, F.; Guilard, R. *Eur. J. Org. Chem.* **2005**, 281–305.
27. Doherty, S.; Knight, J. G.; Mcrae, A.; Harrington, R. W.; Clegg, W. *Eur. J. Org. Chem.* **2008**, 1759–1766.

28. Dahan, A.; Ashkenazi, T.; Kuznetsov, V.; Makievski, S.; Drug, E.; Fadeev, L.; Bramson, M.; Schokoroy, S.; Rozenshine-Kemelmakher, E.; Gozin, M. *J. Org. Chem.* **2007**, *72*, 2289–2296.

29. (a) Li, B.; Wu, G.-P.; Ren, W.-M.; Wang, Y.-M.; Rao, D.-Y.; Lu, X.-B. *J. Polym. Sci., Part A: Polym. Chem.* **2008**, *46*, 6102−6113. (b) Cohen, C. T.; Thomas, C. M.; Peretti, K. L.; Lobkvosky, E. B.; Coates, G. W. *Dalton Trans.* **2006**, 237−249. (c) Shi, L.; Lu, X.-B.; Zhang, R.; Peng, X.-J.; Zhang, C.-Q.; Li, J.-F.; Peng, X.-M. *Macromolecules* **2006,** *39*, 5679−5685. (d) Xiao, Y.; Wang, Z.; Ding, K. *Chem. Eur. J.* **2005**, *11*, 3668−3678. (e) Cohen, C. T.; Chu, T.; Coates, G. W. *J. Am. Chem. Soc.* **2005,** *127*, 10869−10878. (f) Cheng, M.; Darling, N. A.; Lobkovsky, E. B.; Coates, G. W. *Chem. Commun.* **2000**, 2007−2008.

30. Darensbourg, D. J.; Holtcamp, M. W.; Struck, G. E.; Zimmer, M. S.; Niezgoda, S. A.; Rainey, P.; Robertson, J. B.; Draper, J. D.; Reibenspies, J. H. *J. Am. Chem. Soc*. **1999**, *121*, 107−116.

CHAPTER 5

RING OPENING POLYMERIZATION OF LACTIDES WITH ZINC COMPLEXES OF
AMIDO-OXAZOLINATES: GENERATION OF HIGHLY ISOTACTIC
POLY(LACTIDE)

5.1. Introduction

Poly(lactide) (PLA) is a linear aliphatic polyester, derived from ring opening

polymerization (ROP) of a cyclic dimer of lactic acid, i.e., lactide, which is produced by

fermentation of biomass followed by chemical depolymerization.[1,2,3,4] The most commonly

used biomass-feedstock for the production of PLA are corn, tapioca roots, sugarcane, sugar

beets, wheat, and other starch-enriched products.[3,5,6] Nowadays, PLA is becoming a

promising bio-derived polymer that can be used in variety of applications ranging from

bulk commodity materials to bio-medicinal products such as fibers, staples, sutures, drug

delivery agents, and artificial tissue matrices.[7,8,9,10,11] The plausible micro structures of PLA

via ROP process will depend on catalyst, monomer, and reaction conditions. ROP of

racemic or meso lactides can provide different microstructures as they are associated with

two different chiral centers (Scheme 7). The control of tacticity or microstructures of the

poly(lactide) *via* stereoselective ROP of *rac*-lactides has received significant attention, as

microstructures of the PLA have profound influence on their physical, thermal, mechanical

as well as their degradation properties.[12,13,14,15,16] For instance, pure isotactic PLA has a

melting point (T_m) of 180 °C and glass transition temperature (T_g) of 50°C, whereas

heterotactic PLA, a semicrystalline polymer, possesses a T_m of 130 °C and insignificant

glass transition temperature. Interestingly, a stereoblock PLA that is a 50:50 mixture of PLLA and PDLA is a highly crystalline material than heterotactic and isotactic PLLA or PDLA and displays T_m and T_g of up to 230°C and 58°C respectively.[11,17] Stereoblock PLAs accommodating poly(ethylene glycol) are found with faster degradation as well as shorter erosion times than corresponding isoenriched PLAs.[1813] Several metal alkoxides, such as Sn(R-COO)$_2$,[19,20,21] Al(OR)$_3$ [22,23] are well-known for ROP of racemic or meso-lactides, however, they yielded amorphous atactic PLAs with random arrangements of stereosequences (-*RSSRSRSRSR*- for meso lactide and *RRSSSSRR*- for *rac*-lactides) (Scheme 7). To achieve the desired control in stereoselective ROP, a single site catalyst with well-defined chiral pocket is required.

Over the past three decades, a wide variety of single-site catalysts, using different metal centers including Zn,[24] Al,[25] In,[26] Mg,[27] and rare earth metals[28] have been developed for stereoselective ROP of *rac*-lactides. Many studies confirmed that ROP of *rac*-lactides followed coordination-insertion chain growth mechanism; polymerization proceeds with retention of configuration of the lactide monomer by cleavage of its acyl-oxygen bond.[14,29]
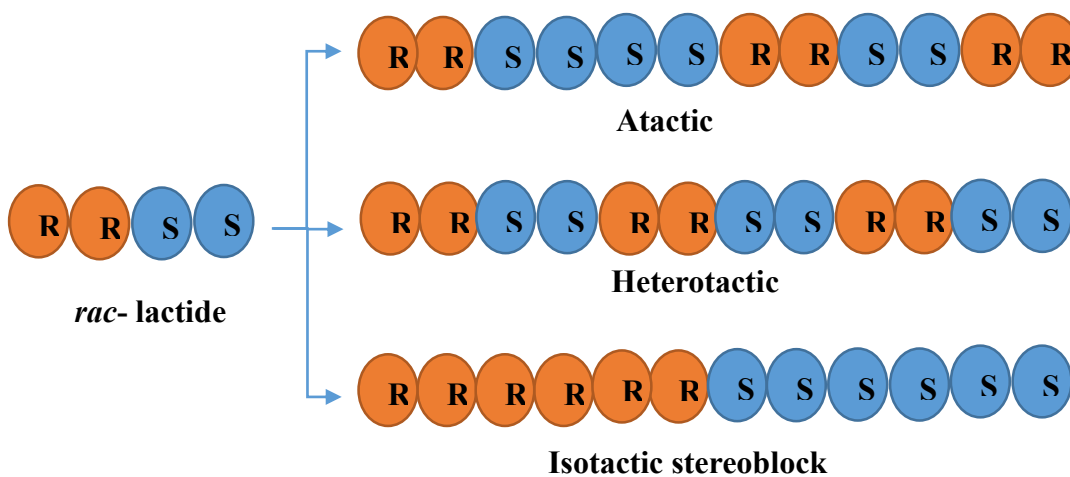
Scheme 7. Microstructures derived from ROP of *rac*-lactides

Spassky and co-workers first reported a chiral salen complex [(R)-(SalBinap)-AlOCH₃] for ROP of *rac*-lactide that exhibited a kinetic preference for (R,R)-enantiomer than (S,S)-enantiomer (20:1), yielding a stereoblock PLA with T_m of 187 °C (Scheme 17).[30] In another study, Duda *et al* employed chiral Schiff's base/aluminum alkoxide catalytic system for ROP of *rac*-lactides to produce stereo block PLA that has very high melting point (T_m) of 210 °C.[31]

Later on, Coates and co-workers have shown that zinc complexes of β-diketiminate ligands are active initiators for ROP of *rac*-lactides, producing highly stereoregular heteotactic PLA (P_r = 0.94) *via* chain-end control mechanism [32]. Subsequently, Chisholm and co-workers showed that zinc complexes of β-diketiminate ligands with monosubstituted aryl N-substituents can polymerize *rac*-lactides and generate the highly selective heterotactic PLA (P_r = 0.90).[33] Schaper and co-workers have reported that zinc complexes of chiral diketiminate ligands with aliphatic substituents are effective initiators for ROP of *rac*-lactides, yielding heterotactic PLA (P_r = 0.84-0.87).[34] More recently, Rodriguez and co-workers reported the synthesis of isotactic PLA (P_m = 0.77) from ROP of *rac*-lactide using an alkylzinc complex of enantiopure hybrid scorpionate/cyclopentadiene ligand, controls the stereochemistry by enantiomorphic site control mechanism.[35] Although zinc-based catalysts are among the most active initiators for ROP of *rac*-lactides, generation of highly selective stereoblock PLA using zinc based initiators is still a significant scientific goal.

Recently, we reported the synthesis of a family of mononuclear zinc complexes of amido-oxazolinate ligands for asymmetric alternating copolymerization of CO_2 and

cyclohexene oxide, yielding a moderate isotactic PCHC.[36] We hypothesized that our present system controls the stereochemistry of the polymeric chain by an enantiomorphic site control mechanism; however, this mechanism may be competitive with a chain-end control mechanism, since the obtained poly(cyclohexene carbonates)s are moderately isotactic. These results intrigued us to investigate the efficiency and stereo selectivity of our catalytic systems for ROP of *rac*-lactides. Herein, we expand our initial discoveries in ROP of *rac*-lactides using zinc complexes of amido-oxazolinate ligands.

5.2. Results and Discussion

5.2.1. Synthesis of Zinc Amide Complexes

Our previous results showed that the monomeric zinc complexes of amido-oxazolinate ligands were viable catalysts for the asymmetric alternating copolymerization of CO_2 and CHO, affording moderate isotactic PCHC with 90 % carbonate linkages.[36] The monomeric zinc complexes of amido-oxazolinate ligands have been synthesized *via* deprotonation of ligands with $Zn[N(SiMe_3)_2]_2$ in dry toluene. A series of seven zinc complexes of amido-oxazolinate ligands, with different geometrical parameters, were assessed for their ROP efficiency of *rac*-lactides (Scheme 9).

	R_1	R_2
a	2,6-DMP	(S)-^{i}Pr
b	2,6-DMP	(R)-Ph
c	2,6-DMP	(S)-^{s}Bu
d	2,6-D^{i}PP	(S)-^{i}Pr
e	(R)-CHMeNaph	(S)-^{i}Pr
f	(S)-SO^{t}Bu	(R)-^{i}Bu
g	3,5- BTP	(R)-Ph
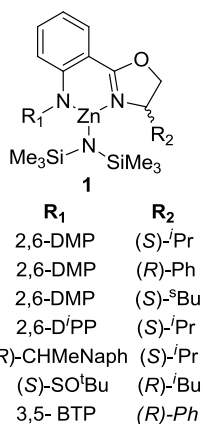
Scheme 9. A series of zinc amide complexes

5.2.2. Synthesis of Zinc Alkyl Complexes

Due to the promising catalytic activity of zinc alkyl complexes in polymerization reactions,[37] we explored the complexation chemistry of C_1-symmetric amido-oxazolinate ligands with diethyl zinc and examine the ability of resulting diethyl zinc complexes as potential catalysts for ROP of *rac*-lactides. The synthesis of zinc ethyl complexes was carried out as reported in the literature.[38] The corresponding amido-oxazolinate ligands were treated with excess of diethyl zinc in dry toluene and stirred for 1.5 hr at RT. The volatile impurities were removed in vacuum, complexes **2a** and **2b** were isolated as yellow solids in 76 % and 69 % yields respectively (Scheme 10). The formation of diethyl zinc complexes was confirmed by ^{1}H NMR spectroscopy. Both complexes exhibit similar type of ^{1}H NMR spectra; a quartet around 0.17-0.21 ppm (**2a**), -0.35 ppm (**2b**) for ZnCH_2CH$_3$ and a triplet around 1.25-1.40 ppm (**2a**), 0.53 ppm (**2b**) for ZnCH$_2$CH_3 were observed. Due to the restricted N-aryl bond rotation, there are two different singlets (δ=2.09 and 2.13 ppm) were found for methyl protons of the side arm (-ArCH_3) in both complexes **2a** and **2b**.

	R_1	R_2
a	2,6-DMP	(S)-^{i}Pr
b	2,6-DMP	(R)-Ph
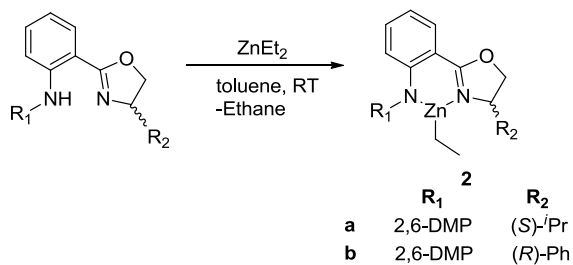
Scheme 10. Synthesis of zinc alkyl complexes

5.2.3. Polymerization Studies

The polymerization activity of the zinc complexes of amido-oxazolinate ligands (**1a-1g**, **2a**, and **2b**) for ROP was examined with *rac*-lactide. All ROP of *rac*-lactides

reactions were carried out in toluene unless otherwise mentioned. Preliminary studies were conducted using **1a** in the presence of benzyl alcohol as it is known that benzyl alcohol is a good chain transfer agent.

Table 8. Screening of the conditions for ring opening polymerization of *rac*-lactide
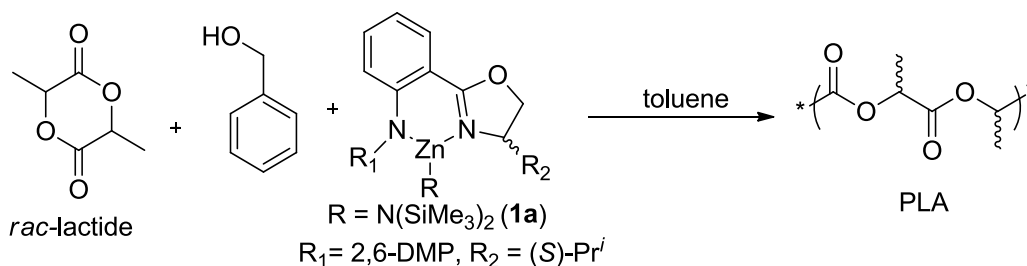
entry	temp.(°C)	time(min)	con.(%)^a	$M_{n,calcd}$(g/mol)^b
1	RT	1200	71	10234
2	50	600	93	13405
3	75	120	82	11819
4	100	20	82	11819
5^c	50	30	98	14125

All polymerization reactions were carried out using 1 mol % of catalyst and benzyl alcohol combination. ^{a}Determined by ^{1}H NMR spectroscopy. ^{b}Calculated by 144.14×(LA/I) × conversion of monomer. ^{c}Reaction was performed without BnOH

Complex **1a** gave decent conversion at room temperature (Table 8, entry **1**). Not surprisingly, a rise in reaction temperature is accompanied by increase in catalytic activity of **1a** (Table 8). Interestingly, pure zinc amide complex **1a**, without benzyl alcohol, was also proven as active catalyst at 50°C with moderate TOFs 196 h^{-1}.

Further, to observe the influence of ligand architecture on catalytic behavior, the remaining complexes (**1b-1g**) were examined for polymerization of *rac*-lactide without adding benzyl alcohol (Table 9). Except catalyst **1e** (Table 9, entry **6**), the remaining catalysts have similar activity, gave 95-98% conversion at 50 °C within 30 min. It implied that influence of substituents of ligand framework is less profound on polymerization activity of catalyst. The low activity of catalyst **1e** might be attributed to its geometrical

features; the less bulky chiral substituent on amido nitrogen might have free rotation, which might block the monomer entrance to the active site.[38,39] It could be also possible that the aliphatic N-substituents decrease the Lewis acidity of the metal center than the N-aromatic substituents, lead to lessening the polymerization activity of the catalyst. A similar phenomenon was also observed when zinc complexes of β-diketiminate ligands were employed for ROP of *rac*-lactides at identical reaction conditions.[34,40]

Table 9. Ring opening polymerization of *rac*-lactide using zinc complexes (**1a-1g**)

entry	cat.	time (min)	con. (%)[a]	M_n (g/mol)[b]	$M_{n,calcd}$ (g/mol)[c]	PDI	T_m[d]	P_r/ P_m[e]
1	**1a**	30	98	30006	14125	1.30	176.0	0.23/0.77
2	**1b**	30	96	17950	13837	1.07	184.3	0.24/0.76
3	**1c**	30	96	30152	13837	1.10	195.0	0.20/0.80
4	**1d**	30	97	26145	13981	1.12	202.0	0.31/0.69
5	**1e**	30	80	29371	11531	1.05	194.1	0.28/0.72
6	**1f**	30	95	21160	13693	1.37	195.8	0.22/0.78
7	**1g**	30	93	37423	13405	1.12	204.0	0.14/0.86
8[f]	**1a**	30	95	40060	13693	1.13	208.3	0.20/0.80
9[g]	**1a**	125	91	34455	13116	1.12	167.5	isotactic
10[h]	**1a**	8	91	45463	13116	1.15		0.23/0.77

All polymerization reactions were carried out using 1 mol % of catalyst at 50°C. [a]Determined by ^{1}H NMR spectroscopy. [b]Measured by GPC using polystyrene standards and molecular weights were corrected by equation: $0.58 \times M_n$(GPC). [c]Calculated by $144.14 \times$(LA/I)×conversion of monomer. [d]Determined by DSC. [e]P_m (Probability of forming a new *m*-dyad) is determined by the integration of methine region of the homonuclear decoupled ^{1}H NMR spectrum of the polymer. [f]1:200 eq. of catalyst and monomer were used. [g](cis)-Lactide was used. [h]Performed using bulk conditions without solvent

The catalyst **1a** displayed high TOFs (392 h^{-1}) at the same temperature (Table 9, entry **8**). At bulk conditions, catalyst **1a** exhibited very high TOFs 700 h^{-1} (Table 9, entry **9**). The resultant polymers were analyzed by gel permeation chromatography (GPC) and it is revealed that, in most cases, experimentally found number-average molecular weight of polymers has large difference from theoretically derived values. This large disparity most likely due to participation of different initiating groups derived from a reaction between impurities in the system (such as adventitious water and lactic acid) and –N(SiMe₃)₂ group.

Subsequently, it leads to propagation of polymeric chain much faster than the initiation of the chain. Overall, these zinc amide initiators are highly active and produced better molecular weight distributions than their isoelectronic analogues such as zinc amide complexes of β-diketiminate ligands.[40] We did not observe any catalyst decomposition to *bis*-ligated complexes and it is evidenced by short polymerization reaction times.[24f] The ROP polymerization reaction with L-lactide gave isotactic PLA without any additional products, which are usually derived from either epimerization or transesterifications (Table 9, entry **9**). High isotacticity of the PLLA is confirmed by the homonuclear decoupled ^{1}H NMR spectrum as it is showed a single peak at δ 5.17 ppm for methinee proton of the PLA. The obtained PLLA is crystalline, highly isotactic in nature, and possess a melting point of 167.5 °C, which is consistent with observed temperature (167-178 °C) in the literature.[41,42]

To further screen the effect of initiating group, ROP of *rac*-lactides was performed using zinc ethyl complexes **2a** and **2b** (Table 10). Zinc ethyl complex **2a** was shown with low activity than **1a** (Table 10, entry **2**). Catalyst **2a** showed significant higher activity (TOF = 38 h^{-1}) than the corresponding traditional zinc complexes of β-diketiminate complexes (TOF = 10 h^{-1}).[40] From the analysis of the GPC data, it is confirmed that polymers, generated by catalysts **1a** and **2a**, have similar distribution of molecular weights. It suggested that irrespective of initiating group, the propagation step of polymerization would be same. In contrast to this, long polymerization times were observed if catalyst **1a** was used with the combination of benzyl alcohol (Table 10, entry **3**). This resulted from either slow initiation process or catalyst decomposition to bis(ligated) complexes in the presence of BnOH.

Table 10. Influence of initiating group in ROP of *rac*-lactide

R = N(SiMe$_3$)$_2$ (**1a**), Et (**2a**),
N(SiMe$_3$)$_2$ (**1a**) + HOBn,
R$_1$= 2,6-DMP, R$_2$ = (*S*)-Pr^i
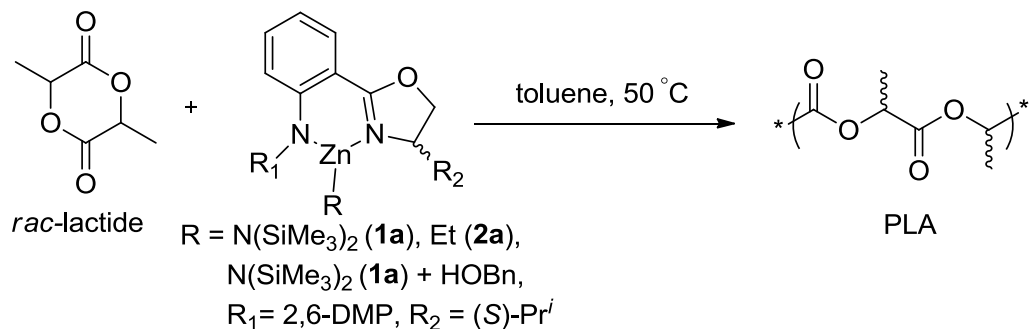
entry	catlyst	time (hr)	con.(%)^a	$M_{n,calcd}$(g/mol)^b	P_r/ P_m^{c}
1	**1a**	0.5	98	14125	0.23/0.77
2	**2a**	2.5	96	13837	0.15/0.85
3^e	**1a**	10	93	13405	0.39/0.61

All polymerization reactions were carried out using 1 mol % of catalyst. ^{a}Determined by ^{1}H NMR spectroscopy. ^{b}Calculated by 144.14×(LA/I)×conversion of monomer. ^{c}P_m (probability of forming a new *m*-dyad) is determined by the integration of methine region of the homonuclear decoupled ^{1}H NMR spectrum of the polymer

The performance of **1a** for ROP of *rac*-lacides was also compared in three differentsolvents, such as toluene, DCM, and THF at 50 °C (Table 11). The activity of catalyst **1a** in different solvents is found in the following order; toluene > DCM > THF. The lower activity of **1a** in THF might be attributed to strong competition between THF and lactide units for coordination to the metal center.[43] The rather moderate activity of the

Table 11. Influence of solvent on ROP of *rac*-lactide

entry	solvent	time (min)	con.(%)^a	$M_{n(calcd)}$^{b}	T_m^{c}	P_r/P_m^{d}
1	toluene	30	98	14125	176.0	0.23/0.77
2	THF	30	84	12108	171.5	0.29/0.71
3	DCM	30	89	12828	174.6	0.22/0.78

All polymerization reactions were carried out using 1 mol % of catalyst at 50 °C. ^{a}Determined by ^{1}H NMR spectroscopy. ^{b}Calculated by 144.14×(LA/I)×conversion of monomer. ^{c}Determined by DSC. ^{d}P_m (probability of forming a new *m*-dyad) is determined by the integration of methine region of the homonuclear decoupled ^{1}H NMR spectrum of the polymer

catalyst **1a** in DCM is probably due to its slightly higher polarity of DCM than that of toluene.

Reaction temperature also has a dramatic influence on the polymerization behavior of the catalysts. The effect of temperature on catalytic activity is significant; prolonged reaction times were observed as the reaction temperature was decreased (Table 12). Interestingly, catalyst **1a** showed decent activity even at 0 °C (Table 12, entry **4**).

Table 12. Influence of temperature on ROP of *rac*-lactide

entry	temp.(°C)	time(hr)	con.(%)[a]	$M_{n(calcd)}$[b]	T_m[c]	P_r/P_m[d]
1	75	0.25	93	13405	179.0	0.24/0.76
2	50	0.50	98	14125	176.0	0.23/0.77
3	RT	24	66	9513	188.9	0.20/0.80
4	0	72		13549	214.0	0.10/0.90

All polymerization reactions were carried out using 1 mol % of catalyst **1a** at 50 °C. [a]Determined by ^{1}H NMR spectroscopy.[b]Calculated by 144.14×(LA/I) ×conversion of monomer. [c]Determined by DSC. [d]P_m (probability of forming a new *m*-dyad) is determined by the integration of methine region of the homonuclear decoupled ^{1}H NMR spectrum of the polymer

5.2.4. Analysis of Microstructures

Physical, mechanical, and degradation properties of the polymers are intensively dependent on tacticity of the polymer backbone. Determination of tacticity of PLA was carried out by measuring the integrals of methine region of polymers in the homonuclear decoupled ^{1}H NMR spectra. Five different stereo errors for PLA, *rmr*, *mmr/rmm*, *mmr/rmm*, *mmm*, and *mrm*, are observed in between 5.15-5.25 ppm on homonuclear decoupled ^{1}H NMR spectrum after decoupling the methane protons of the PLA. P_m values of the PLAs are determined by $P_m = 1 - P_r$, where $P_r = 2$ [(*rmr*, *mmr/rmm*)]/(*rmr*, *mmr/rmm* + *mmr/rmm*, *mmm*, *mrm*). It is known that zinc-based initiators are highly selective toward hetrotactic PLA.[32,33,34] In contrast to this, all zinc initiators (**1a-1g**, **2a**) showed very high selectivity toward isotactic dyad (Table 8). The analysis of microstructures revealed that

PLAs are obtained by ROP of *rac*-lactides using catalysts (**1a-1g**) displayed significant high P_m values of 0.72-0.86. To date, this is the highest P_m value ($Pm = 0.86$) obtained using chiral zinc complex, **1g** (Table 9, entry **7** and Figure 42, **a**). The electron withdrawing group (3, 5-BTP) and phenyl group combination provide the suitable geometry that might induce the high isoselectivity of **1g**. The high selectivity (P_m) of **1g** is further confirmed by its high melting point (T_m) of 204 °C (Table 9, entry **7**). This is far different from melting point of pure isotactic PLA that displayed 167.5 °C in our case. It is known that stereoblock isotactic polymer, which is a stereo complex of pure enantiomeric isotactic polylactic acids, has higher melting points than pure isotactic PLAs.[44,45,46,47] The high melting point, presumably, is due to high crystallinity of the PLAs that is aroused by highly ordered arrangement of stereogenic centers.
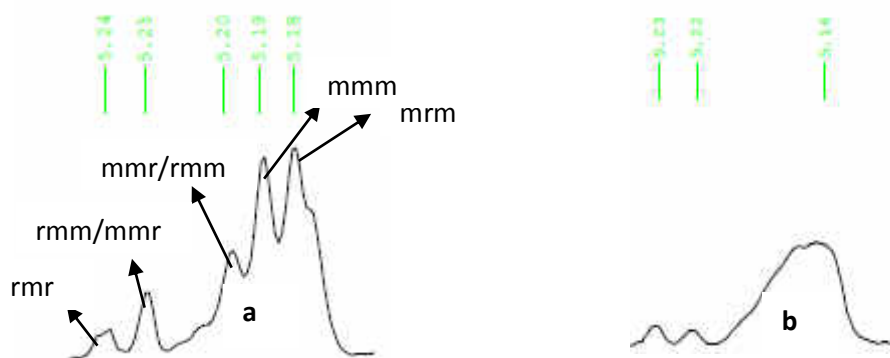
Figure 42. Homonuclear decoupled ^{1}H NMR spectra: (**a**) derived by catalyst **1g**, (**b**) derived by catalyst **1a** at 0 °C

From the obtained data, substitution on oxazoline ring (R_2 position) has notable influence on steteroselectivity. It is observed that in our earlier results, the ^{i}Bu group attached at R_2 position of the zinc complex of amido-oxazolinate ligand is oriented approximately perpendicular to the plane of the six membered chelate ring and pointing toward metal center.[36a] We presume, similar geometrical features in catalyst **1c** may lead to better

selectivity and allowing monomer units more selectively to the metal center (Table 9, entry **3**). In catalyst **1e**, the less bulky group on amido nitrogen might cause for its low isoselectivity (Table 9, entry **5**). In contrast to this, additional interactions between sulfinamido side arm and metal center in **1f** might provide better shielding and this helped in obtaining high isoselectivity (Table 9, entry **6**). Surprisingly, even at bulk conditions, catalyst **1a** displayed remarkably high isoselectivity, $P_m = 0.77$ (Table 9, entry **10**).

A point worthwhile noting is that, at identical reaction conditions, isoselectivity (P_m) of the zinc complex with ethyl initiating group, **2a**, was improved to 0.85 (Table 10, entry **2**). It is also noteworthy that reaction temperature has prominent influence on the level of stereoselectivity. Diminution of the reaction temperature to 0 °C led to remarkable increase in P_m value to 0.90 (Table 12, entry **4** and Figure 42b). This might be due to more kinetic preference of either (R,R) or (S,S)-lactide units.[40] The other confirmation for high isoselectivity of PLA is its high melting point; it was determined by differential scanning calorimetry (DSC), illustrated in Figure 43.
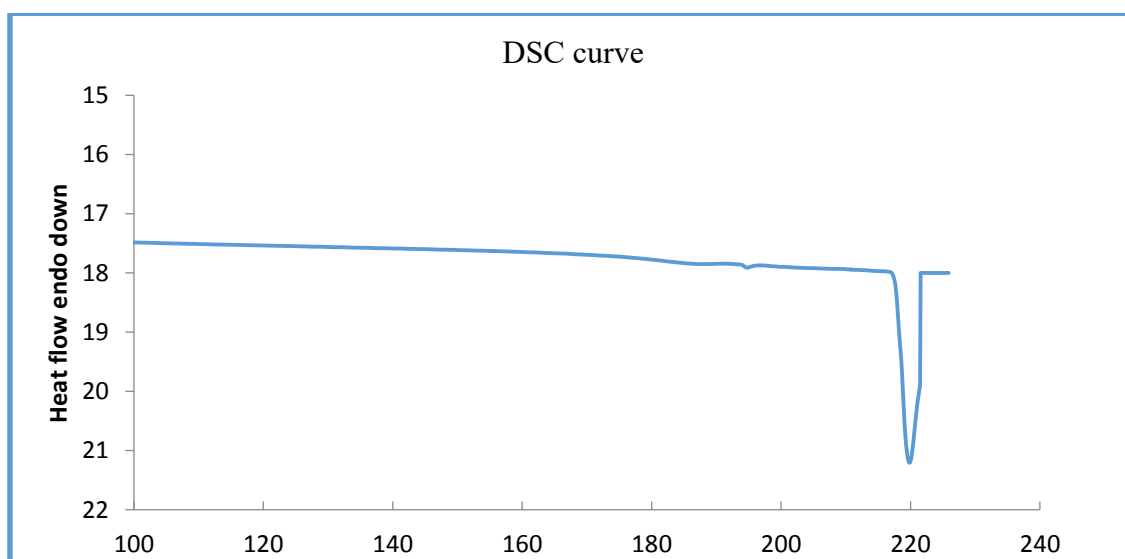
Figure 43. DSC curve of PLA generated by **1a** at 0 °C

Even at high temperature 75 °C, the catalyst **1a** displayed high P_m value 0.76 (Table 12, entry **1**). The role of solvent is also influential on ROP polymerization activity of catalysts. The polymerization behavior of **1a** in THF is different from non-coordinating solvents, such as toluene or DCM. Electronic factors may have a role here as Lewis acidity of the metal center is decreased in the case of coordinating solvents.

5.2.5. Kinetics of Polymerization

In order to understand the mechanistic details of ROP of *rac*-lactides, kinetic studies of ROP have been systematically examined. The kinetics of ROP of *rac*-lactide reaction were investigated at different temperatures (23 °C, 35 °C, 45 °C, and 55 °C) and monomer/initiator ratios using catalyst **1a** in toluene. In all cases, the semi logarithmic conversion-time plots demonstrate the polymerization reactions followed approximately first-order kinetics in lactide concentration (up to 80% monomer conversion) (Figure 44).
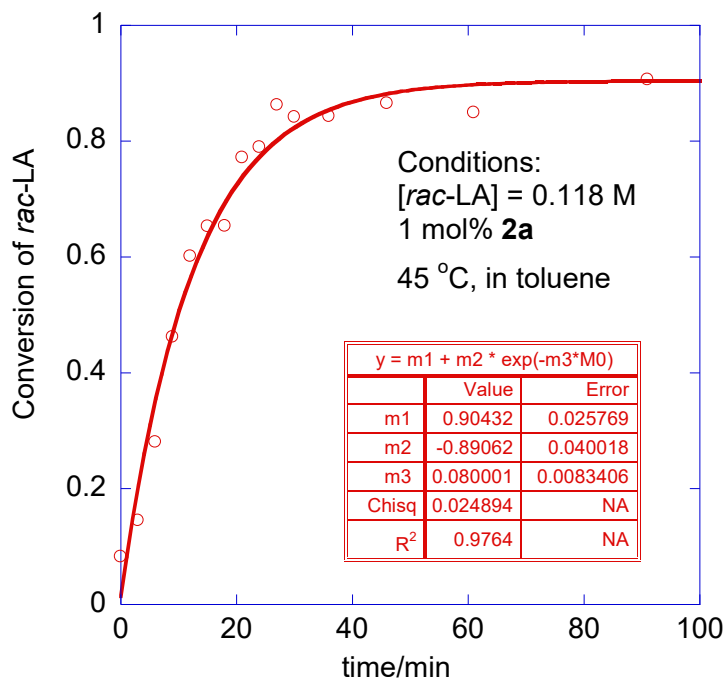
Figure 44. Plot of *rac*-LA conversion vs time (Exponential fitting gives a first order rate constant of $k_{obs} = 0.080 \pm 0.008$ min^{-1})

The observed rate constant (k_{obs}) was found to be 0.080 ± 0.008 min^{-1} for ROP of *rac*-lactides, in which [monomer]/[cat.] was 100 in toluene at 45 °C. Since, the rate of polymerization reaction of *rac*-lactide can be expressed as -d/dt[monomer] = k_{obs}[monomer]^x, in which $k_{obs} = k_p$[initiator]^y, where k_p is the propagation rate constant. To determine the dependence of order of the reaction in terms of initiator concentration, we explored the relationship between k_{obs} and concentration of zinc complex **1a** in toluene at 35 °C (Figure 45). The linear relationship between $\ln(k_{obs})$ **vs** [**1a**] indicates the order of the reaction in terms of **1a** initiator is 0.93 ± 0.14.
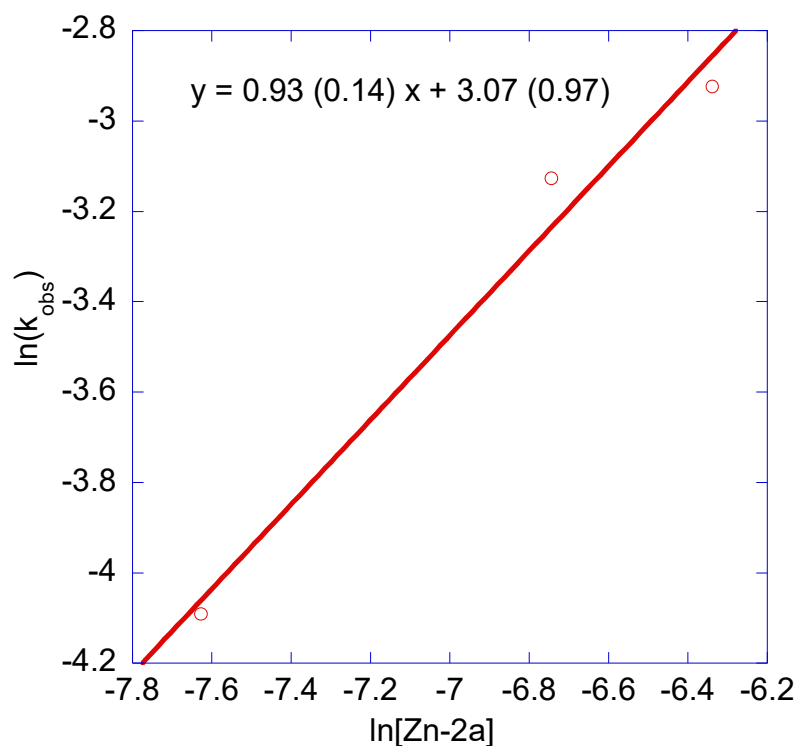
Figure 45. Dependence of PLA formation on catalyst (**1a**) concentration

Thus the overall rate law can be written as rate = k[cat.][monomer]. Activation parameters of the polymerization were obtained from the Eyring plot at 23-55 ˚C: $\Delta H^{\neq} = 54$ (± 7) kJ mol^{-1} and $\Delta S^{\neq} = -112$ (± 21) J mol^{-1} K^{-1}. These values are comparable with the literature

reports and in agreement with coordination-insertion mechanism with an ordered transition state.[26e,48]

Hence, our catalytic systems showed high isotactic selectivity, we examined the kinetics of ROP of both *rac*-and (*S, S*)-lactides. It revealed that polymerization rate of *rac*-lactide will be almost 1.6 times higher than that of *cis*-lactide (Figure 46). We assume that our catalytic systems might prefer the (*R, R*) entiomeric face rather than the (*S, S*) chiral face. However, further experimentation is required to confirm this selectivity and they are under progress.
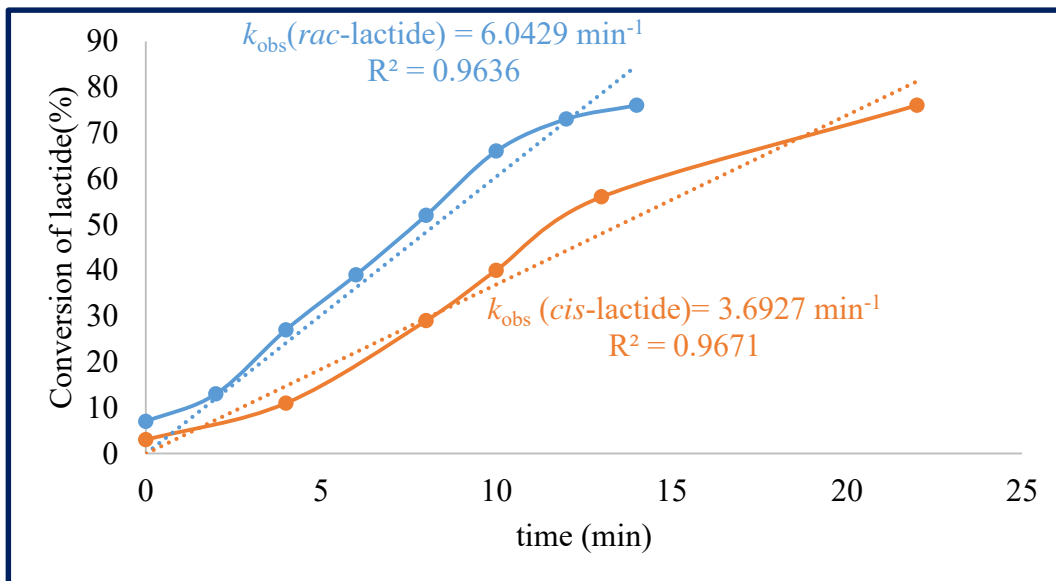
Figure 46. Plots of *rac*, *cis*-lactide conversion vs time

5.2.6. MALDI-TOF Analysis

The PLA samples were inspected by matrix-assisted laser desorption/ionization time-of-flight mass spectrometry (MALDI-TOF MS) in order to determine the structural composition and end groups of the oligomers. MALDI-TOF spectrum was run using α-cyano-4-hydroxycinnamic acid as a matrix and 5 mM sodium acetate as an ionization

agent. MALDI-TOF analysis of oligomeric fractions of the PLA generated by **1a** with the combination of benzyl alcohol (Table 8, entry **1**) revealed that MALDI spectrum has both odd-numbered and even-numbered oligomers (Figure 47). The even-numbered oligomers are formed due to the ring-opening polymerization of *rac*-lactide, whereas the formation odd-numbered oligomers can be explained on the basis of ester-exchange reactions (transesterification) that do occur along the polymerization process.[49] It is also known that either high catalyst loadings or prolonged polymer separation procedures might account for transesterification reactions that can be occurred parallel to polymerization reactions.[50,49e] In our case, the high catalyst loadings might be a plausible source for transesterification reactions as catalyst (40-50 mg) was used for ROP of *rac*-lactides and most of the oligomer samples were prepared immediately right after the completion of the reaction.

DP$_n$	$M_{n,obs}$ (g/mol)	$M_{n,theo}$ (g/mol)
16	1175.2	1176.0
17	1247.2	1248.1
18	1319.2	1320.2
19	1391.2	1392.2
20	1463.3	1464.3
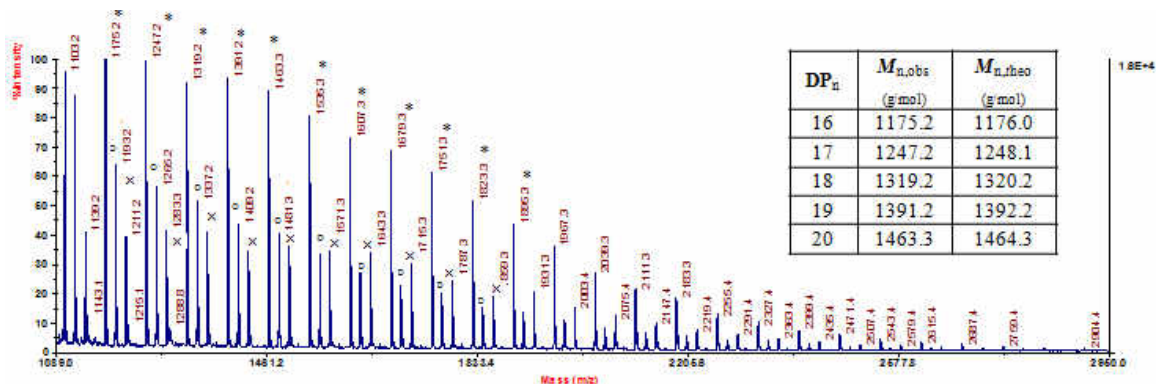
Figure 47. MALDI-TOF spectrum of PLA sample, obtained with **1a+BnOH**, with three different distributions (* indicates the distribution **A**, ° indicates the distribution **B**, × indicates the distribution C). Theoretical molecular weights were calculated by following equation: $M_{n,\ theo} = (DP_n \times M_{Wt\ of\ half\text{-}lactide\ unit}) \times M_{wt\ of\ Na}$, where, DP$_n$ is the degree of polymerization, $M_{wt\ of\ Na} = 23.09$ g/mol, $M_{wt\ of\ half\text{-}lactide\ unit} = 72.06$ g/mol

Three distinct mass distributions were observed in the spectrum with three different end groups and the consecutive peaks in all three series were separated by increments of 72 Da. mass units corresponding to exactly half-lactide unit (-CH(CH$_3$)C(O)O-).

The series **A** has a set of peaks (n = 9-40) with the mass ratio (m/z) of n.72+ 23

(M.Wt of Na) (Figure 48). This series corresponds to cycli oligomers of the PLA. The

second series has **B** a set of peaks (n = 10-38) with the mass ratio of (m/z) of n.72+23(M.Wt

of Na) +90, indicates that this oligomer was capped both H and alcohol (–

OCH(CH$_3$)C(O)OH) (Figure 48). The formation of the carboxylic acid end group can be

explained by the hydrolysis of ester group in the presence of small traces of water in the

polymerization process. The third series **C** has a set of peaks (n = 11-38) with the mass

ratio of (m/z) of n.72+23(M.Wt. of Na) +108, indicates that this oligomer was capped both

H and –OC$_7$H$_8$O end groups (Figure 48). The formation of this end group provides the

strong evidence for ring opening polymerization of lactides that proceeds *via* coordination-

insertion mechanism; coordination of carbonyl group to the metal center followed by

insertion of benzoxy group to the nucleophilic carbon center.[51]

Distribution A (*):

Distribution B (°):
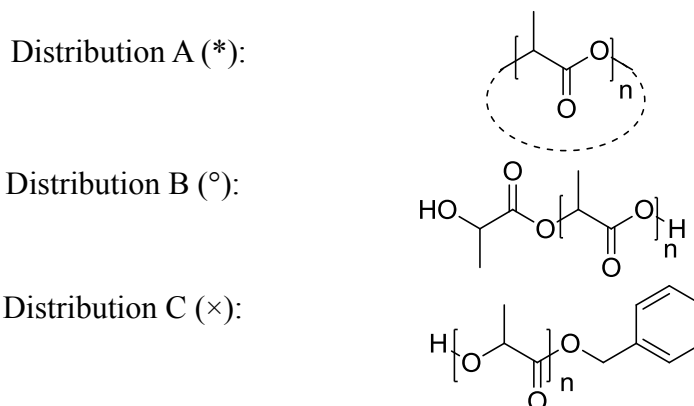
Distribution C (×):

Figure 48. Three plausible distributions with different end groups

The first two distributions (**A**, **B**) are repeated for the PLA that is generated by **2a**

(Supporting Information S26,). Interestingly, only one type distribution (**B**) was observed

for PLA that is obtained by **1a** (n = 10-30), oligomer was capped both H and–

OC(O)CH(CH$_3$)COH end groups (Figure 49).
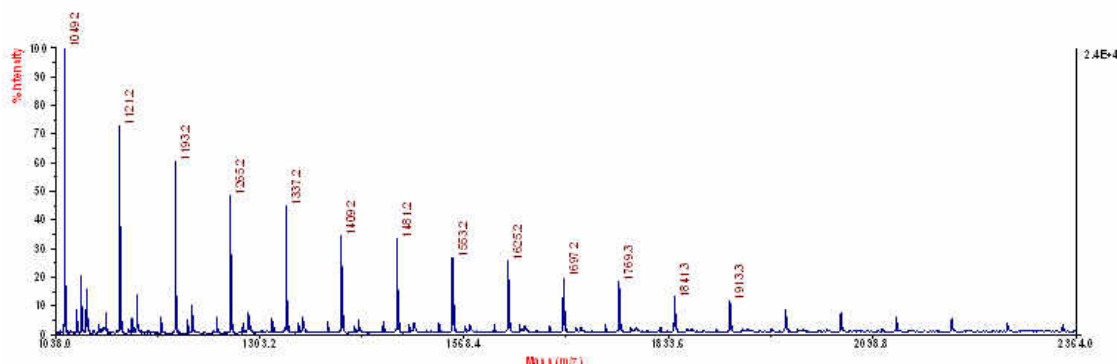
Figure 49. MALDI-TOF spectrum of PLA sample obtained with **1a** (RT) with single distribution

5.3. Conclusions

Herein, we have explored a series of zinc complexes of amido-oxazolinate ligands for the ring opening polymerization of *rac*-lactides at mild reaction conditions. These catalysts deliver a viable synthetic route to produce highly selective steroblock PLA ($P_m = 0.90$), an unprecedented selectivity in the case of zinc-based catalysts. The ligand geometrical parameters strongly influence the polymerization behavior of the catalytic systems. Our future directions will be focused toward understanding mechanistic complexity of this polymerization process and physical and mechanical properties of these polymeric architectures.

5.4. Experimental Conditions

General Conditions: All reactions with air- and/or moisture sensitive compounds were carried out under dry nitrogen using a glove box or standard Schlenk line techniques. All chemicals were purchased from Aldrich unless otherwise noted. (*L, L*)-lactide was recrystallized using ethyl acetate and sublimed four times. *Rac*-lactide was also purified by sublimation. $CDCl_3$ was distilled over CaH_2 and degassed prior to use. Toluene, THF, and DCM were distilled under nitrogen from Na/benzophenone. Carbon dioxide (high purity, 99.995%) was purchased from Airgas and used as received. Zinc bis(trimethylsilyl)amide

was prepared according to the literature.[52] NMR spectra were recorded on a Bruker AVANCE-500 NMR spectrometer (^{1}H, ^{13}C, and homonuclear decoupled ^{1}H NMR). The base line corrections in homonuclear decoupled NMR spectrum were performed using cubic spline fitting. Matrix-assisted laser desorption/ionization time-of-flight mass spectrometry (MALDI-TOF MS) spectra were run using α-cyano-4-hydroxycinnamic acid as a matrix and 5 mM sodium acetate as a ionization agent. Gel permeation chromatography (GPC) analysis was performed on a Varian Prostar, using a PLgel 5 μm Mixed-D column, a Prostar 355 RI detector, and THF as eluent at a flow rate of 1 mL/min (20 °C). Polystyrene standards were used for calibration.

Synthesis of Zinc alkyl complexes

General Procedure: To a solution of ligand in toluene (6-10 mL), excess of diethyl zinc (3.5 eq) was added in a glove box. The resulting solution was stirred until complete conversion of ligand

into complex was observed ^{1}H NMR.

Complex **2a**. Yield: 76 %. ^{1}H NMR (500.1 MHz; CDCl$_3$; 298 K): 0.17 (2H, q, J = 8.1,-CH_2CH$_3$), 0.95 (3H, d, J = 6.34, -CH(CH_3)$_2$), 1.05 (3H, d, J = 6.70, -CH(CH_3)$_2$), 1.30 (3H, t, J = 7.65, - CH$_2$CH_3), 2.18 (3H, s, ArMe), 2.20 (3H, s, ArMe), 2.42 (1H, m, -CH(CH$_3$)$_2$), 4.38 (1H, m, NCH(R)CH$_2$O), 4.47 (2H, m, NCH(R)CH_2O), 6.25 (1H, d, J = 8.82, ArH), 6.45 (1H, t, J = 7.31, ArH), 7.05-7.11 (2H, m, ArH), 7.24 (1H, m, ArH), 7.32 (1H, t, J = 7.96, ArH), 7.90 (1H, d, J = 8.10, ArH). ^{13}C NMR(125.8 MHz; CDCl$_3$; 298 K): -1.36 (ZnCH$_2$CH$_3$), 11.84 (CH(CH$_3$)$_2$), 15.90 (CH(CH$_3$)$_2$), 18.61 (CH(CH$_3$)$_2$), 21.65 (ZnCH$_2$$CH_3$), 32.10 (CH(CH$_3$)$_2$), 67.34 (N$C$H(R)CH$_2$O), 69.71 (NCH(R)$CH_2$O), 103.81,

112.13, 114.95, 123.84, 125.48, 126.13, 128.41 (*C*Harom), 133.26, 134.18, 138.03, 148.40, 156.38, 168.90 (*C*quat).

Complex **2b**.Yield: 69 %. ^{1}H NMR (500.1 MHz; CDCl$_3$; 298 K): -0.32 (2H, m, -C*H*$_2$CH$_3$), 0.53 (3H, t, *J* = 8.57, -CH$_2$C*H*$_3$), 2.07 (3H, s, Ar*Me*), 2.09 (3H, s, Ar*Me*), 4.40 (1H, t, *J* = 8.10, NC*H*(R)CH$_2$O), 4.88 (1H, t, *J* = 8.68, NCH(R)C*H*$_2$O), 5.53 (1H, t, J = 8.24, NCH(R)C*H*$_2$O), 6.20 (1H, d, *J* = 9.01, Ar*H*), 6.44 (1H, t, *J* = 8.10, Ar*H*), 6.97 (2H, t, *J* = 8.20, Ar*H*), 7.09-7.20 (4H, m, Ar*H*), 7.36 (1H, m, Ar*H*) 7.39 (2H, m, Ar*H*), 7.90 (1H, d, *J* = 8.16, Ar*H*). ^{13}C NMR(125.8 MHz; CDCl$_3$; 298 K): -2.41 (Zn*C*H$_2$CH$_3$), 11.50 (Ar*Me*), 18.65 (Ar*Me*), 21.65 (ZnCH$_2$*C*H$_3$), 68.72 (N*C*H(R)CH$_2$O), 73.82 (NCH(R)*C*H$_2$O), 103.44, 112.33, 115.23, 123.86, 125.50, 126.88, 128.44, 128.58, 128.80, 129.24, 129.37, 131.07 (*C*Harom), 133.91, 134.48, 141.47, 148.31, 156.57, 169.57 (*C*quat).

General procedure for ROP of *rac*-lactides. A flame-dried Schlenk flask was charged with a mixture of catalyst (1 mol%) and *rac*-lactide in toluene (30-45 mL) in a glove box. The flask was heated to desired temperature and stirring was continued until complete conversion was observed by ^{1}H NMR spectroscopy. The same procedure was used for ROP of *cis*-lactide.

General Procedure for Kinetic Experiments. A flame dried Schlenk flask was equipped with catalyst (1 mol%) and *rac*-lactide in toluene (30-45 mL) in a glove box. The flask was heated to the desired temperature and small aliquots were collected at regular intervals.

5.5. References

1. Lunt, J. *Polym. Degrad. Stab.* **1998**, *59*, 145–152.

2. Jung, Y. K.; Kim, T. Y.; Park, S. J.; Lee, S. Y. *Biotechnol. Bioeng.* **2010**, *105*, 161–171.

3. Auras, R.; Lim, L-T.; Selke, S. E. M.; Tsuj, H. *Poly(Lactic Acid): Synthesis, Structures, Properties, Processing, and Applications;* John Wiley & Sons: Hoboken, NJ, USA, 2010.

4. Drumright, R. E.; Gruber, P. R.; Henton, D. E. *Adv. Mater.* **2000**, *12*, 1841–1846.

5. Darensbourg, D. J.; Karroonnirun, O. *Organometallics* **2010**, *29*, 5627–5634.

6. Harvey, L. D. D. *Energy and the New Reality 2: Carbon-free Energy Supply;* Taylor & Francis: NY, USA, 2010.

7. Jeong, B.; Bae, Y. H.; Lee, D. S.; Kim, S. W. Nature **1997**, *388*, 860–862.

8. Mathers, R. T.; Meier, M. A. R. *Green Polymerization Methods:Renewable Starting Materials, Catalysis and Waste Reduction;* Wiley-VCH: Weinheim, Germany, 2011.

9. Gross, R. A.; Kalra, B. *Science* **2002**, *297*, 803–807.

10. Auras, R.; Harte, B.; Selke, S. *Macromol. Biosci.* **2004**, *4*, 835–864.

11. Wang, G-J.; Ho, K-H.; Hsueh, C-C. *Microsyst. Technol.* **2008**, *14*, 989–993.

12. Paakinaho, K.; Ellaa, V.; Syrjala, S.; Kellomaki, M. *Polym. Deg. Stab.* **2009**, *94*, 438–442.

13. Agatemor, C.; Shave, M. P. *Biomacromolecules* **2013**, *14*, 699–708.

14. Stanford, M. J.; Dove, A. P. *Chem. Soc. Rev.* **2010**, *39*, 486–494.

15. Becker, J. M.; Pounder, R. J.; Dove, A. P. *Macromol. Rapid Commun.* **2010**, *31*, 1923–1927.

16. Fukushima, K.; Kimura, Y. *Polym. Int.* **2006**, **55**, 626–642.

17. Tsuji, H.; Horii, F.; Hyon, S. H.; Ikada, Y. *Macromolecules* **1991**, *24*, 5651–5656.

18. Tsuji, H. *Macromol. Biosci.* **2005**, *5*, 569–597.

19 . Nijenhuis, A. J.; Grijpma, D. W.; Pennings, A. J. *Macromolecules* **1992**, *25*, 6419–6424.

20. Stridsberg, K.; Ryner, M.; Albertsson, A.-C. *Macromolecules* **2000**, *33*, 2862–2869.

21. Kricheldorf, H. R.; Lee, S.-R.; Bush, S. *Macromolecules* **1996**, *29*, 1375–1381.

22. Brochu, S.; Prudhomme, R. E.; Barakat, I.; Jerome, R. *Macromolecules* **1995**, *28*, 5230–5239.

23. Ma, H.; Okuda, J. *Macromolecules* **2005**, *38*, 2665–2673.

24. (a) Rezayee, N. M.; Gerling, K. A.; Rheingold, A. L.; Fritsch, J. M. *Dalton Trans.* **2013**, *42*, 5573–5586. (b) Petrus, R.; Sobota, P. *Dalton Trans.* **2013**, 42, 13838–13844. (c) Otero, A.; Fernaandez-Baeza, J.; Sanchez-Barba, L. F.; Tejeda, J.; Honrado, M.; Garces, A.; Lara-Sanchez, A.; Rodriguez, A. M. *Organometallics* **2012**, *31*, 4191−4202. (d) Petrus, R.; Sobota, P. *Organometallics* **2012**, *31*, 4755−4762. (e) Chen, H-Y.; Peng, Y-L.; Huang, T-H.; Sutar, A. K.; Miller, S. A.; Lin, C-C. *J. Mol. Catal. A: Chem.* **2011**, *339*, 61–71. (f) Roberts, C. C.; Barnett, B. R.; Green, D. B.; Fritsch, J. M. *Organometallics* **2012**, *31*, 4133−4141. (g) Song, S.; Zhang, X.; Ma, H.; Yang, Y. *Dalton Trans.* **2012**, *41*, 3266–3278. (h) Chen, H-Y.; Tang, H-Y.; Lin, C-C. *Macromolecules* **2006,** *39,* 3745–3752. (i) Darensbourg, D. J.; Karroonnirun, O. *Inorg. Chem.* **2010**, *49*, 2360–2371.

25 (a) Bouyahyi, M.; Roisnel, T.; Carpentier, J.-F. *Organometallics* **2012**, *31*, 1458−1466. (b) Chen, H.-L.; Dutta, S.; Huang, P.-Y.; Lin, C.-C. *Organometallics* **2012**, *31*, 2016−2025. (c) Koller, J.; Bergman, R. G. *Organometallics* **2011**, *30*, 3217−3224. (d) Darensbourg, D. J.; Karroonnirun, O.; Wilson, S. J. *Inorg. Chem.* **2011**, *50,* 6775−6787. (e) Liu, Z.; Gao, W.; Zhang, J.; Cui, D.; Wu, Q.; Mu, Y. *Organometallics* **2010**, *29*, 5783−5790. (f) Chisholm, M. H.; Gallucci, J. C.; Quisenberry, K. T.; Zhou, Z. *Inorg. Chem.* **2008**, *47*, 2613−2624. (g) Wu, J.; Pan, X.; Tang, N.; Lin, C.-C. *Eur. Polym. J.* **2007**, *43*, 5040−5046.

26. (a) Aluthge, D. C.; Patrick, B. O.; Mehrkhodavandi, P. *Chem. Commun.* **2013**, *49*, 4295–4297. (b) Yu, I.; Acosta-Ramirez, A.; Mehrkhodavandi, P. *J. Am. Chem. Soc.* **2012**, *134*, 2758–12773. (c) Normand, M.; Kirillov, E.; Roisnel, T.; Carpentier, J.-F. *Organometallics* **2012**, *31*, 1448−1457. (d) Peckermann, I.; Kapelski, A.; Spaniol, T. P.; Okuda, J. *Inorg. Chem.* **2009**, *48*, 5526–5534. (e) Douglas, A. F.; Patrick, B. O.; Mehrkhodavandi, P. *Angew. Chem., Int. Ed.* **2008**, *47*, 2290–2294.

27 (a) Sanchez-Barba, L. F.; Garces, A.; Fernandez-Baeza, J.; Otero, A.; Alonso-Moreno, C.; Lara-Sanchez, A.; Rodriguez, A. M. *Organometallics* **2011**, *30*, 2775−2789. (b) Wang, L.; Ma, H. *Macromolecules* **2010**, *43*, 6535–6537. (c) Tsai, Y.-H.; Lin, C.-H.; Lin, C.-C.; Ko,B.-T. *J. Polym. Sci., Part A: Polym. Chem.* **2009**, *47*, 4927−4936. (d) Poirier, V.; Roisnel, T.; Carpentier, J.-F.; Sarazin, Y. *Dalton Trans.* **2009**, *44*, 9820−9827. (e) Huang, Y.; Hung, W.-C.; Liao, M.-Y.; Tsai, T.-E.; Peng, Y.-L.; Lin, C.-C. *J. Polym. Sci., Part A: Polym. Chem.* **2009**, *47*, 2318−2329. (f) Ayala, C. N.; Chisholm, M. H.; Gallucci, J. C.; Krempner, C. *Dalton Trans.* **2009**, *42*, 9237−9245. (g) Tang, H.-Y.; Chen, H.-Y.;Huang, J.-H.; Lin, C.-C. *Macromolecules* **2007,** *40,* 8855–8860.

28 (a) Sinenkov, M.; Kirillov, E.; Roisnel, T.; Fukin, G.; Trifonov, A.; Carpentier, J.-F. *Organometallics* **2012**, *31*, 4133−4141. (b) Li, G.; Lamberti, M.; Mazzeo, M.; Pappalardo,

D.; Roviello, G. Pellecchia, C. *Organometallics* **2012**, *31*, 1180−1188. (c) Mahrova, T. V.; Fukin, G. K.; Anton V. Cherkasov, A. V.; Trifonov, A. A.; Ajellal, N.; Carpentier, J.-F. *Inorg. Chem.* **2009**, *48*, 4258–4266. (d) Ma, H.; Spaniol, T. P.; Okuda, J. *Inorg. Chem.* **2008**, *47*, 3328–3339. (e) Bonnet, F.; Cowley, A. R.; Mountford, P. *Inorg. Chem.* **2005**, *44*, 9046–9055. (f) Ovitt, T. M.; Coates, G. W. *J. Am. Chem. Soc.* **2002**, *124*, 1316–1327.

29. Dijkstra, J. P.; Du, H.; Feijen, J. *Polym. Chem.* **2011**, *2*, 520–527.

30. Spassky, N.; Wisniewski, M.; Pluta, C.; Le Borgne, A. *Macromol. Chem.Phys.* **1996**, *197*, 2627–2637.

31. Majerska, K.; Duda, A. *J. Am. Chem. Soc.* **2004**, *126*, 1026–1027.

32. Cheng, M.; Attygalle, A. B.; Lobkovsky, E. B.; Coates, G. W. *J. Am. Chem. Soc.* **1999**, *121,* 11583–11584.

33. Chisholm, M. H.; Phomphrai, K. *Inorg. Chim. Acta* **2003**, *350*, 121–125.
34. Drouin, F.; Oguadinma, P. O.; Whitehorne, T. J. J.; Prudhomme, R. E.; Schaper, F. *Organometallics* **2010**, *29*, 2139–2147.

35. Honrado, M.; Otero, A.; Fernandez-Baeza, J.; Sanchez-Barba, L. F.; Lara-Sanchez, A.; Tejeda, J.; Carrion, M. P.; Martinez-Ferrer, J.; Garces, A.; Rodrıguez, A. M. *Organometallics* **2013**, *32*, 3437−3440.

36. (a) Abbina, S.; Du, G. *Organometallics* **2012**, 31, 7394–7403. (b) Binda, P. I.; Abbina, S.; Du, G. *Synthesis* **2011**, 2609−2618.

37. (a) Otero, A.; Fernandez-Baeza, J.; Sanchez-Barba, L. F.; Tejeda, J.; Honarado, M.; Garces, A.; Lara-Sanchez, A.; Rodriguez, A. M. *Organometallics* **2012**, *31*, 4191–4202. (b) Li, J-Y.; Li, C-Y.; Tai, W-J.; Lin, C-H.; Ko, B-T. *Inorg. Chem. Commun.* **2011**, *14*, 1140–1144. (c) Alonso-Moreno, C.; Garces, A.; Sanchez-Barba, L. F.; Fajardo, M.; Fernandez-Baeza, J.; Otero, A.; Lara-Sanchez, A.; Antinolo, A.; Broomfield, L.; Lopez-Solera, M. I.; Rodríguez, A. M. *Organometallics* **2008**, *27*, 1310–1321. (d) Wheaton, C. A.; Hayes, P. G.; Ireland, B. J. *Dalton Trans.* **2009**, 4832–4846.

38. Cheng, M.; Moore, D. R.; Reczek, J. J.; Chamberlain, B. M.; Lobkovsky, E. B.; Coates, G. W. *J. Am. Chem. Soc.* **2001**, *123,* 8738–8749.

39. Chen, C.-T.; Chan, C.-Y.; Huang, C.-A.; Chen, M.-T.; Peng, K.-F. *Dalton Trans.* **2007**, 4073−4078.

40. Chamberlain, B. M.; Cheng, M.; Moore, D. R.; Ovitt, T. M.; Lobkovsky, E. B.; Coates, G. W. *J. Am. Chem. Soc.* **2001**, *123*, 3229–3238.

41. Becker, J. M.; Pounder, R. J.; Dove, A. P. *Macromol. Rapid Commun.* **2010**, *31*, 1923−1937.

42. Zhong, Z.; Dijkstra, J. P.; Feijen, J. *J. Am. Chem. Soc.* **2003**, *125*, 11291−11298.

43. Chisholm, M, H.; Gallucci, J. C.; Phomphrai, K. *Inorg. Chem.* **2005**, *44*, 8004–8010.

44. Tsuji, H.; Ikada, Y. *Polymer* **1999**, *40*, 6699–6708.

45. Ovitt, T. M.; Coates, G. W. *J. Polym. Sci.: Part A: Polym. Chem.* **2000**, *38*, 4686–4692.

46. Tang, Z.; Chen, X.; Yang, Y.; Pang, X.; Sun, J.; Zhang, X.; Jing, X. *J. Polym. Sci.: Part A: Polym. Chem.* **2004**, *42*, 5974–5982.

47. Tang, Z.; Chen, X.; Pang, X.; Yang, Y.; Zhang, X.; Jing, X. *Biomacromolecules* **2004**, *5*, 965–970.

48. Chisholm, M. H.; Eilerts, N. W. *Chem. Commun.* **1996**, 853–854.

49. (a) El-Zoghbi, I.; Whitehorne, T. J. J.; Schaper, F. *Dalton Trans.* **2013**, *84,* 132-147. (b) Dyer, H. E.; Huijser, S.; Susperregui, N.; Bonnet, F.; Schwarz, A. D.; Duchateau, R.; Maron, L.; Mountford, P. *Organometallics* **2010**, *29*, 3602–3621. (c) Jalabert, M.; Fraschini, C.; Prudhomme, R. E. *J. Polym. Sci.: Part A: Polym. Chem.* **2006**, *45*, 194–1955. (d) Klok, H-A.; Hwang, J. J.; Iyer, S. N.; Stupp, S. I. *Macromolecules* **2002**, *35*, 746–759. (e) Zhong, Z.; Dijkstra, P. J.; Feijen, J. *J. Am. Chem. Soc.* **2003**, *125*, 11291–11298.

50. Montaudo, G.; Montaudo, M. S.; Puglisi, C.; Samperi, F.; Spassky, N.; LeBorgne, A.; Wisniewski, M. *Macromolecules* **1996**, *29*, 6461–6465.

51. Petrus, R.; Sobota, P. *Organometallics* **2012**, *31*, 4755–4762.

52. Darensbourg, D. J.; Holtcamp, M. W.; Struck, G. E.; Zimmer, M. S.; Niezgoda, S. A.; Rainey, P.; Robertson, J. B.; Draper, J. D.; Reibenspies, J. H. *J. Am. Chem. Soc.* **1999**, *121*, 107−116.

CHAPTER–6

RING OPENING COPOLYMERIZATION OF CYCLIC ANHYDRIDES AND
STYRENE OXIDE

6.1. Introduction

Until today, the most commonly consumed polymers are derived from oil-based feedstocks and this production causes many severe problems i.e. dwindling of fossil fuel resources as well as other environmental issues.[1,2] To overcome the issues with the conventional polymers, spectacular improvements during the last three decades have been made in synthesis of biodegradable and environmentally adaptable polymers using renewable resources.[3,4,5] Among the explored polymers, polyesters are an important class of polymers as they are widely used ina variety of applications, including drug delivery systems, artificial tissues, and commodity materials. Moreover, most of the polyesters are biodegradable and biocompatible.[6,7,8,9] In general, most of the polyesters can be synthesized from either polycondensation of diols and diacids or by ring-opening polymerization (ROP) of cyclic esters. Although these methods have been used for quite some time, they have suffered from several problems, such as drastic reaction conditions, side reactions, and limited choices of monomer units.[10,11,12,13]

To establish a more efficient synthetic route for the generation of polyesters (ABABABAB type), more attention turned into ring opening copolymerization of epoxides with cyclic anhydrides[14,15,16,17,18] since the ring opening copolymerization is became a popular route for the synthesis of polycarbonates *via* copolymerization of CO_2 and

epoxides.[19] The initial discovery by Inoue and coworkers showed that (porphyrin)Al(III) catalysts can copolymerize cyclic anhydrides with epoxides and CO_2; however, activity of these catalysts is very low (TOFs ~2 h^{-1}).[20,15a] Subsequent reports by Inoue *et al*[15b] and Maeda *et al*[14] also described the copolymerization of anhydrides with epoxides, but these systems suffered with obtaining low molecular weight copolymers and homopolymerization of epoxides. The major breakthrough was reported by Coates and co-workers who illustrate that zinc complexes of β-diketiminate ligands are active for copolymerization of aliphatic anhydrides and variety of epoxides, yielding copolymers with high molecular weight (up to 55 000 gm/mol) and narrow molecular weight distributions.[21,22] Later on, Duchateau and co-workers more vigorously studied ring opening copolymerization of variety epoxides and anhydrides using salen based metal (Co, Cr, Al, and Mn) complexes.[12,23]

We have previously reported zinc complexes of amido-oxazilinate ligands as viable initiators for asymmetric alternating copolymerization of epoxides and CO_2.[24] In addition to this, we have also confirmed that the same zinc complexes can also act as catalysts for ring opening polymerization of *rac*-lactides.[25] On the basis of these initial results, we anticipated that our catalytic systems might serve as active catalytic systems for the ring-opening copolymerization of oxianes and cyclic anhydrides. Herein, we report the highly active catalytic systems, zinc complexes of amido-oxazolinate ligands, for the synthesis of polyesters *via* alternating copolymerization of styrene oxide (SO) and cyclic anhydrides (succinic anhydride (SA), maleic anhydride (MA), and phthalic anhydride (PA)) and its mechanistic aspects.

6.2. Results and Discussions

6.2.1 Screening of the Polymerization Reaction Conditions

Initially, to screen the ring copolymerization reaction conditions, polymerization of styrene oxide (SO) with maleic anhydride (MA) was carried out at 100°C using zinc complex **1** (Scheme 11) in toluene. These zinc-based catalysts previously were shown to be active for cyclohexene oxide /CO_2 copolymerization and ROP of *rac*-lactides. This copolymerization reaction did not produce any copolymer even at prolonged reaction times without catalyst (Scheme 11, entry **1**). This emphasizes the need of catalyst for this copolymerization reaction. Catalyst **1a** produced moderate TOFs at 303 h^{-1} at 100 °C in toluene, generating alternating copolymers (Scheme 11, entry **2**). The formation of polymer was confirmed by NMR spectroscopy (^{1}H and ^{13}C). The olefinic protons in the polymer are observed at 6.27 ppm and the protons from the styrene oxide are found at 6.25 and 4.40-4.60 ppm. The formation of side product, phenyl acetaldehyde, was confirmed by proton resonances at 3.80 and 9.80-9.85 ppm on ^{1}H NMR spectrum.

Later on, at similar conditions, polymerization reactions were performed involving SO to [Zn] ratios of 250:1, 500:1, 1000:1, 2500:1, and 4000:1. Catalyst **1a** showed very high TOFs 8000 h^{-1} at 100 °C (Scheme 11, entry **6**). As far as we know, catalyst **1a** showed the highest TOFs for ring opening copolymerization of maleic anhydride and styrene oxide. In all cases, phenyl ethanol was observed in significant amounts. This formation of phenyl ethanol, an isomerized product of styrene oxide, is reported in the literature. Chisholm and co-workers studied the formation of PE and its influence on copolymerization process.[26] We also believed that adventitious water that is trapped in anhydrides might help the formation of PE. Even after careful sublimation of anhydrides, the moisture was not

eliminated completely. The trace amounts water produce corresponding acids that can help the transformation of styrene oxide into phenyl ethanol.

Scheme 11. Screening of the reaction conditions of ring opening co-polymerization of styrene oxide and maleic anhydride[a]
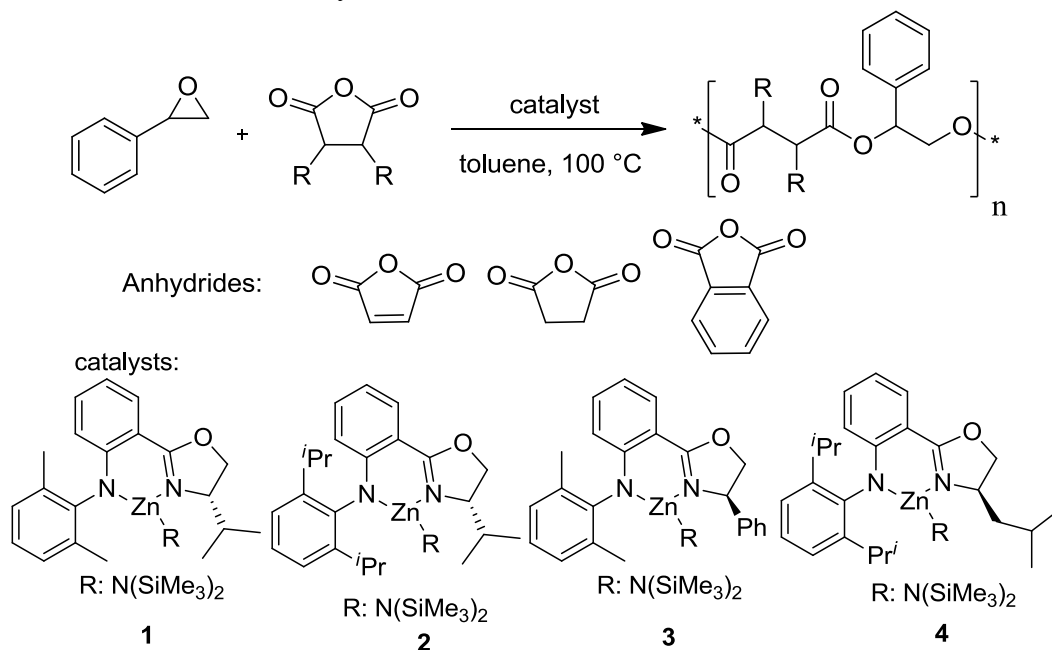
entry	epoxide	anhydride	[cat]/[monomer]	time (min)	ratio of polyester/PE[c]
1[b]	SO	MA	-	1440	-
2	SO	MA	1:100	20	76/24
3	SO	MA	1:200	20	76/24
4	SO	MA	1:500	20	76/24
5	SO	MA	1:1000	20	76/24
6	SO	MA	1:2500	30	75/25
7	SO	MA	1:4000	30	76/24

PE: Phenyl ethanol, MA: Maleic anhydride, SO: styrene oxide. [a]All reaction were performed using catalyst **1** in toluene (1-4 mL) at 100 °C. [b]Performed without catalyst. [c]Determined by measuring the intensities of peaks on ^{1}H NMR spectroscopy. In all cases, 100 % conversion was achieved with respective of SO

6.2.2. Effect of Catalyst Structure on Catalytic Behavior

To study the influence of the steric and electronic features of the catalyst on their polymerization behavior, we decided to use the catalysts (**1-4**) for ring opening polymerization of SO with different anhydrides (MA, PA, SA) with an

oxirane:anhydride:catalyst ratio of 200:200:1 in toluene at 100 °C (Table **13**). Evidently, catalyst **1,** with ^{i}Pr group and 2,6-DMP on amido-oxazolinate ligand framework, afforded perfectly alternating polymer chains with a significantly higher degree of polymerization than the remaining catalysts (**2-4**). Catalyst **3,** with (*R*)-Ph group and 2,6-DMP on amido-oxazolinate ligand framework, showed low TOFs for all conversions except the conversion of SO and SA (Table 13). From the data, it can be believed that the substitution on amido nitrogen can alter the activity of the catalyst. In case of catalysts **2** and **4,** the conversion of MA and SO is faster than SO and PA while catalysts **1** and **3** gave faster degree of polymerization for SO and PA. Except the coupling of SO and SA, catalysts (**1-4**) exhibit the following order **1**>**2**>**4**>**3** for all remaining polymerization reactions.

Table 13. Results of copolymerization of SO with different anhydrides[a]

entry	catalyst	anhydride	time	ratio of polyester/PE[b]
1	1	PA	30	76/24
2	1	MA	35	78/22
3	1	SA	240	85/15
4	2	PA	90	79/12
5	2	MA	60	80/20
6	2	SA	720	87/13
7	3	PA	150	76/24
8	3	MA	195	76/24
9	3	SA	570	82/18
10	4	PA	120	80/20
11	4	MA	105	77/23
12	4	SA	660	79/21

PE: Phenyl ethanol, MA: Maleic anhydride, SA: Succinic anhydride. PA: Phthalic anhydride. [a]All reaction were performed using 0.5 mol% of catalyst in toluene (2 mL) at 100 °C. [b]Determined by measuring the intensities of peaks in the ^{1}H NMR spectroscopy. In all cases, 100 % conversion was achieved with respective SO, determined by ^{1}H NMR spectroscopy

Polystyrene succinate (PSS), obtained from ring opening of copolymerization of SO and SA ((SO-SA)$_n$), possesses three different types of microstructures (Figure 50). The microstructures of the PSS (HT, HH, and TT junctions) can be easily identified by ^{13}C

NMR spectroscopy. As per previous assignments, the peaks at 171.82 and 171.28 ppm correspond to HT junctions.[26] The two chemical shifts at 171.60 and 171.20, respectively, relate to TT and HH junctions. The split in HH junction relates *iso*, *syn* diads of the HH junctions of the PSS. ^{13}C NMR spectrum of the carbonyl region of PSS, obtained by catalyst **3**, is shown in Figure **51** and it clearly indicates the presence of four resonances that correlate to four microstructures of PSS. The peaks at 171.20 ppm and 171.16 ppm correspond to *i* and *s* HH-junctions.
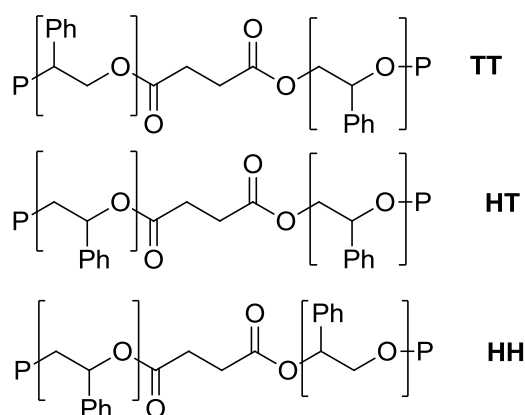

Figure 50. Regiostructures of poly(styrene succinate): Tail-Tail (TT), Head-Tail (HT), and Head-Head (HH) junctions
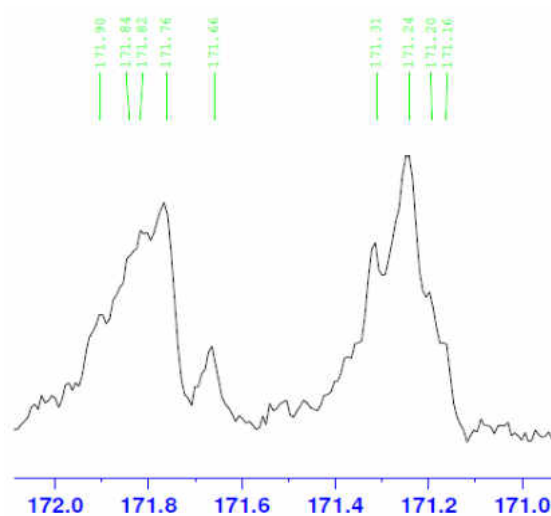

Figure 51. Carbonate region of the ^{13}C NMR spectrum of PSS generated from SO and SA by catalyst **3**

6.2.3. Effect of Anhydride

To investigate the influence of anhydride on copolymerization process, three anhydrides (PA, MA, and SA) were chosen. All polymerization reactions catalyzed by complexes (**1-4**) yielded 100% conversions in terms styrene oxide concentration and gave perfectly alternating copolymers without any ether bonds. The ring strain can dramatically influence the polymerization behavior. In general, for a given epoxide, styrene oxide, the relative rate of hetero coupling with anhydride was found in the following order, PA>MA>SA (Figure 51). The conversion of SA and SO with all catalysts (**1-4**) was rather low. This can be explained by low ring strain of anhydride.
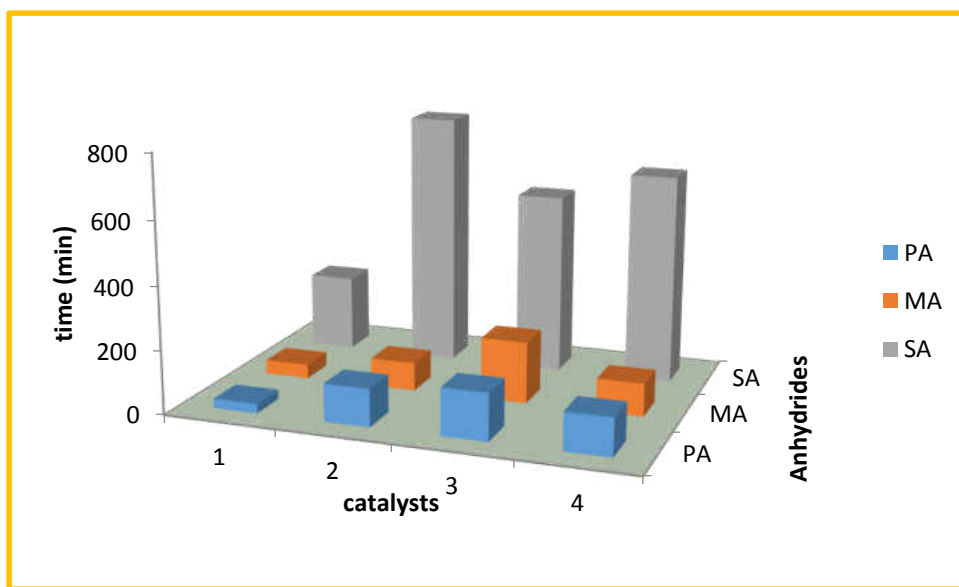

Figure 52. Ring opening copolymerization of SO and anhydrides catalyzed by **1-4**

6.3. Conclusions

In conclusion, we have demonstrated the catalytic activity of zinc complexes of amido-oxazolinate ligands for ring-opening copolymerization of anhydrides and styrene oxide. Among the four catalysts, catalyst **1** proved to be the most active catalyst. A study on the copolymerization of styrene oxide and anhydrides, different anhydrides exhibited a

trend following in the order of PA>MA>SA. The catalytic system appeared to be well suited for stereoselective ring opening copolymerization of anhydrides and styrene oxide. Further studies are in progress.

6.4. Experimental Section

General Conditions. All reactions with air- and/or moisture sensitive compounds were carried out under dry nitrogen using a glove box or standard Schlenk line techniques. All chemicals were purchased from Aldrich unless otherwise noted. Styrene oxide was distilled over CaH_2 and degassed prior to use. All anhydrides were sublimed before use for polymerization reactions. $CDCl_3$ was distilled over CaH_2 and degassed prior to use. Toluene was distilled under nitrogen from Na/benzophenone. Synthesis of catalysts (**1-4**)[24] and zinc bis(trimethylsilyl)amide[24] were prepared according to the reported literature methods. All NMR spectra (^{1}H and ^{13}C) were recorded on a Bruker AVANCE-500 NMR spectrometer). Matrix-assisted laser desorption/ionization time-of-flight mass spectrometry (MALDI-TOF MS) spectra were run using *trans*-2-[3-(4-tertbutylphenyl)-2-methyl-2-propenylidene]malononitrile (DCTB) as a matrix agent and 5 mM sodium acetate as a ionization agent. Gel permeation chromatography (GPC) analysis was performed on a Varian Prostar, using a PLgel 5 μm Mixed-D column, a Prostar 355 RI detector, and THF as eluent at a flow rate 1 ml/min (20 °C). Polystyrene standards were used for calibration.

General procedure for copolymerization reactions. An oven dried 50 mL round bottom side neck flask was charged with a mixture of anhydride (1 eq), SO (1 eq) and catalyst (0.5 mol%) in toluene (1-2 mL) in Glove box. The flask was heated at 100 °C until complete conversion was observed by ^{1}H NMR spectroscopy. The unreacted monomers and catalyst

were separated from polymers by dissolving the crude reaction mixture in methanol (4-5 mL) and 1M HCl (0.25 mL) and followed by filtration.

Characterization of compounds in Table 13.

Copolymer of styrene oxide and phthalic anhydride (entry 5). ^{1}H NMR (500MHz, CDCl$_3$): 4.10-4.60 (br, -PhCHC*H$_2$*COO-, 2H), 5.90-6.50 (br, -PhC*H*CH$_2$COO, 1H), 5.90-6.50 (br, -COO*H*C=C*H*COO, 2H).

Copolymer of styrene oxide and phthalic anhydride (entry 10). ^{1}H NMR (500MHz, CDCl$_3$): 4.30-4.65 (br, -PhCHC*H$_2$*COO-, 2H), 6.10-6.40 (br, -PhC*H*CH$_2$COO, 1H), 6.10-6.40 (br, -COOPh*H*COO-, 4H).

Copolymer of styrene oxide and phthalic anhydride (entry 12). ^{1}H NMR (500MHz, CDCl$_3$): 2.50-2.80 (br, -COOCH$_2$CH$_2$COO-, 4H), 4.29 (br, -PhCHC*H$_2$*COO, 2H), 6.08 (br, -PhC*H*CH$_2$COO, 1H).

6.5. References

1. Dechy-Cabaret, O.; Martin-Vaca, B.; Bourissou, D. *Chem. Rev.* **2004**, *104*, 6174–6176.

2. Gandini, A. *Macromolecules* **2008**, *41,* 9492–9504.

3. Okada, M. *Prog. Polym. Sci.* **2002**, *27*, 87–133.

4. Dechy-Cabaret, O.; Martin-Vaca, B.; Bourissou, D. *Chem. Rev.* **2004**, *104*, 6147–6176.

5. Pilla, S. *Handbook of Bioplastics and Biocomposites Engineering Applications;* John Wiley & Sons, Inc: Hoboken, New Jersey, **2011**.

6. Coulembier, O.; Degee, P.; Hedrick, J. L.; Dubois, P. *Prog. Polym. Sci.* **2006**, *31*, 723–747.

7. Ikada, Y.; Tsuj, H. *Macromol. Rapid Commun.* **2000**, *21,* 117–132.

8. Vink, E. T. H.; Rabago, K. R.; Glassner, D. A.; Springs, B.; O'Connor, R. P.; Kolstad, J.; Gruber, P. R. *Macromol. Biosci.* **2004**, *4*, 551–564.

9. Chasin, M.; Langer, R. *Biodegradable Polymers as Drug Delivery Systems*; Marcel Dekker Inc: New York, **1990**.

10. (a) Thomas, C. M. *Chem. Soc. Rev.* **2010**, *39*, 165–173. (b) Robert, C.; de Montigny, F.; Thomas, C. T. *Nature Commun.* **2011**, *2*, 586−592.

11. Kricheldorf, H. R. *Chem. Rev.* **2009**, *109*, 5579−5594.

12. Huijser, S.; Nejad, E. H.; Sablong, R.; Jong, C. D.; Koning, C. E.; Duchateau, R. *Macromolecules* **2011**, *44*, 1132–1139.

13 . Yoneyama, M.; Kakimoto, M.; Imai, Y. *Macromolecules* **1989**, *22*, 2593–2596.

14. Maeda, Y.; Nakayama, A.; Kawasaki, N.; Hayashi, K.; Aiba, S.; Yamamoto, N. *Polymer* **1997**, *38*, 4719–4725.

15. Aida, T.; Inoue, S. *J. Am. Chem. Soc.* **1985**, *107*, 1358–1364. (b) Aida, T.; Sanuki, K.; Inoue, S. *Macromolecules* **1985**, *18*, 1049–1055.

16. Eberhardt, R.; Allmendinger, M.; Rieger, B. *Macromol. Rapid Commun.* **2003**, *24*, 194–196.

17. Darensbourg, D. J.; Poland, R. P.; Escobedo, C. *Macromolecules* **2012**, *45*, 2242−2248.

18. Maeda, Y. *Polymer* **1997**, *38*, 4719–4725.

19. Nakano, K.; Kobayashi, K.; Ohkawara, T.; Imoto, H.; Nozaki, K. *J. Am. Chem. Soc*. **2013**, *135*, 8456–8459. (b) Geschwind, J.; Frey, H. *Macromolecules* **2013**, *46*, 3280–3287. (c) Lu, X.-B.; Darensbourg, D. J. *Chem. Soc. Rev*. **2012**, *41*, 1462–1484.

20. Inoue, S.; Koinuma, H.; Tsuruta, T. *J. Polym. Sci. Polym. Lett.* 1**969**, *7*, 287–292.

21. Jeske, R. C.; DiCiccio, A. M.; Coates, G. W. *J. Am. Chem. Soc.* **2007**, *129*, 11330–11330−11331.

22. Jeske, R.; Rowley, J.; Coates, G. *Angew. Chem., Int. Ed.* **2008**, *47*, 6041–6044.

23. (a) Nejad, E. H.; Melis, C. G. W.; Vermeer, T. J.; Koning, C. E.; Duchateau, R. *Macromolecules* **2012**, *45*, 1770−1776. (b) Nejad, E. H.; Paoniasari, A.; Melis, C. G. W.; Koning, C. E.; Duchateau, R. *Macromolecules* **2013***, 46,* 631−637.

24. Abbina, S.; Du. G. *Organometallics* **2012**, *31*, 7394–7403.

25. Abbina, S.; Du. G. Manuscript in Preparation.

26. Harrold, N. D.; Li, Y.; Chisholm, M. H. *Macromolecules* **2013**, *46*, 692−698.

UNEXPECTED FORMATION OF CHIRAL PINCER CNN NICKEL COMPLEXES
WITH β-DIKETIMINATO TYPE LIGANDS VIA C-H ACTIVATION: SYNTHESIS,
PROPERTIES, STRUCTURE AND COMPUTATIONAL STUDIES

7.1. Introduction

Ligands play an essential role in catalysis, especially when regio, stereo, and enantioselectivities are concerned, as they can provide appropriate stereochemical and electronic environments around the active metal centers. Among the various chelating ligands available in the literature, tridentate pincer ligands are one of the most widely applied systems.[1] The prototypical DXD-type pincer ligands feature two donor atoms (D) such as tertiary phosphine or amine linked through an aromatic or aliphatic skeleton encompassing a carbon- or nitrogen-bound anionic anchor (X) (Figure 53). In particular, NCN and PCP pincer complexes with overall C_2 symmetry are widespread, and this design, with the carbon-metal bond located between two lateral arms, leads to stabilization of the C-M bond and could improve the robustness of catalytic systems.[2] It is also important that such framework can be fine-tuned to allow rational design of catalysts. Variations of donor and anchor atoms have greatly expanded the range of pincer ligands, in which D can be N, P, S, O, C, etc., and X can be C, Si, N, P, B, etc.[1,3]

D, D' = N, P, S, O, C, etc

X = C, N, P, Si, B, etc

Figure 53. General representation of pincer ligands

Among these variations, the unsymmetric pincer ligands of the DXD' type have received increasing attention.[4,5] The two donor groups (D and D') can be markedly different, which may result in unique and novel properties in the pincer complexes. Transition metal complexes based on the CNN pincer have been synthesized and employed in the catalytic cross coupling,[6] hydrogenation of esters,[5a] and transfer hydrogenation of ketones.[7] The carbon donors in these systems are typically based on aryl (**1a-b**) or N-heterocyclic carbene (**1c-f**) carbons (Figure 54). The introduction of chiral substituents in the pincer framework constitutes of a common strategy for enantioselective catalysis.[8,9] However, pincer complexes with both unsymmetric and chiral ligands have been relatively less developed,[10] presumably because of lack of a general synthetic strategy, and only a few complexes incorporating chiral CNN pincer ligands, derived from **1a** and **1e**, have been reported.[11]

Nickel is one of the first metals incorporated in the pincer complexes[12] and numerous pincer nickel complexes have appeared in the literature.[13] Their applications in bond activation and

catalysis such as C-C coupling, dehydrogenation, and hydroamination have been extensively studied.[6a-b,14,15] The potential exhibited by these complexes has encouraged further development of ligand precursors bearing analogous chelating systems and isoelectronic features.[16] In this report we describe the synthesis and characterization of a series of rare chiral CNN pincer nickel complexes with C_1-symmetry β-diketiminato type ligands, in which the carbon donor arm is formed via an intramolecular C-H activation. Besides the unexpected C-H activation for both sp^3- and sp^2-hybridized carbon atoms, these complexes are of interest in catalysis given that the chiral ligand precursors are readily available and tunable. The C_1-symmetric systems have received increasing
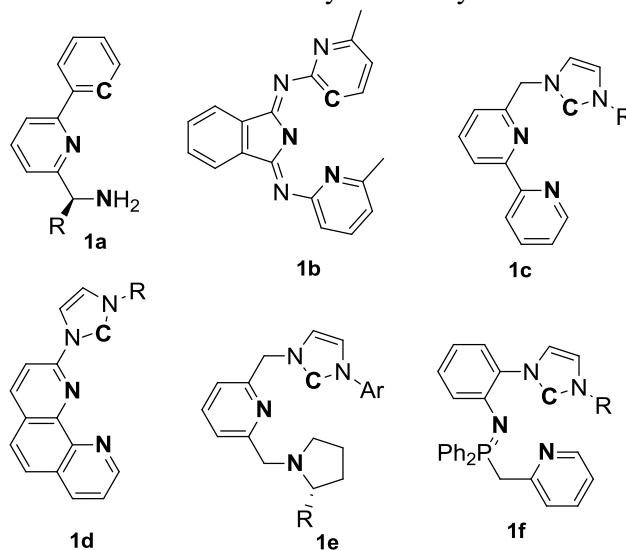

Figure 54. Some examples of CNN pincer ligands. (Donor atoms are in bold)

attention in recent years[17] and the unsymmetric donor sets could be advantageous when two donor groups influence the reactivity and selectivity in different manners.[18] The presence of sp^3-C in the pincer framework may also lead to structural and electronic versatilities that can open up new opportunities in catalysis.[19]

7.2. Results and Discussion
7.2.1. Synthesis of Ligands

The chiral, unsymmetric anilido-imine ligands, **2a-e**, have been obtained as analogues of conventional β-diketiminato framework, via a palladium catalyzed Buchwald-Hartwig amination reaction (Scheme 12).[20] In the case of **2e**, because of the low and inconsistent yields, an alternative, Cu-catalyzed amination reaction protocol[21] was employed. This protocol seems to be more

2a, R = (*S*)-^{i}Pr
2b, R = (*S*)-^{sec}Bu
2c, R = (*R*)-^{i}Bu
2d, R = (*R*)-Ph

2e, R = (*R*)-^{i}Bu
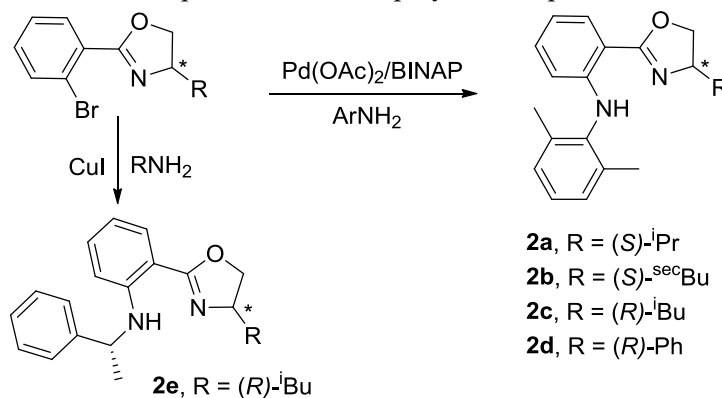
Scheme 12. Synthesis of ligands **2a–2e** via amination reaction

consistent and reliable for alkyl amines, although yields are still generally moderate (~40%).

These ligands can be deprotonated with a strong base such as ^{n}BuLi at low temperature. Thus, the lithium salt of ligand **2d** was prepared by lithiation with stoichiometric amount of ^{n}BuLi and isolated as a yellow crystalline solid in good yields. The ^{1}H NMR indicates that the coordination environment of the lithium center is completed with two THF solvent molecules. It was further noted that isolation of lithium salts was not necessary and the subsequent metallation reactions were carried out using *in-situ* generated lithium compounds without further purification.

7.2.2. Preparation of Pincer Nickel Complexes 3a-3d

Treatment of lithium salts of ligand **2a-d** with *trans*-NiCl(Ph)(PPh$_3$)$_2$ at room temperature resulted in an immediate color change and dark-red crystals **3a-d** were consistently formed after allowing solutions standing for 2-5 days. The isolated compounds appeared rather sensitive to air, as the color blackened within minutes upon exposure to the air, but could be stored under an inert atmosphere for months. They are quite soluble in THF and toluene and have been characterized by various spectroscopic and analytic techniques including ^{1}H, ^{13}C, and ^{31}P NMR spectroscopy. In the ^{1}H NMR of **3a** in benzene-d_6 (Figure 55), the most striking features include the six-proton dimethyl group of the free ligands becoming a three-proton singlet, and the appearance of two new 1-proton multiplets at 2.76 and 1.38 ppm. The two multiplets are coupled with each other and connected to the same carbon atom, as indicated by 2D NMR analysis.[22] These observations suggest the metallation of one methyl group of the aniline moiety, leading to a coordinated methylene group (NiCH_2) with two diastereotopic protons riding on the same carbon (Scheme 13). Because of coupling with the phosphorus nuclei, the methylene protons are both multiplets, and this is further supported by a doublet of NiCH_2 at 26.43 ppm ($^2J_{C-P}$ = 25.3 Hz) in the ^{13}C NMR.[23] The ^{1}H NMR spectra for **3b-d** reveal the similar features that coordinated methylene protons exhibit two signals at 2.66 and 1.45 ppm for **3b**, 2.47 and 1.64 ppm for **3c**, and 2.48 and 1.56 ppm for **3d**, respectively; the NiCH_2 signals appear as doublets at 26.38 ppm for **3b**, 26.61 for **3c**, and 26.52 for **3d**, respectively, in ^{13}C NMR ($^2J_{C-P}$ = 25.2 -26.5 Hz) due to coupling with the phosphorus nuclei.
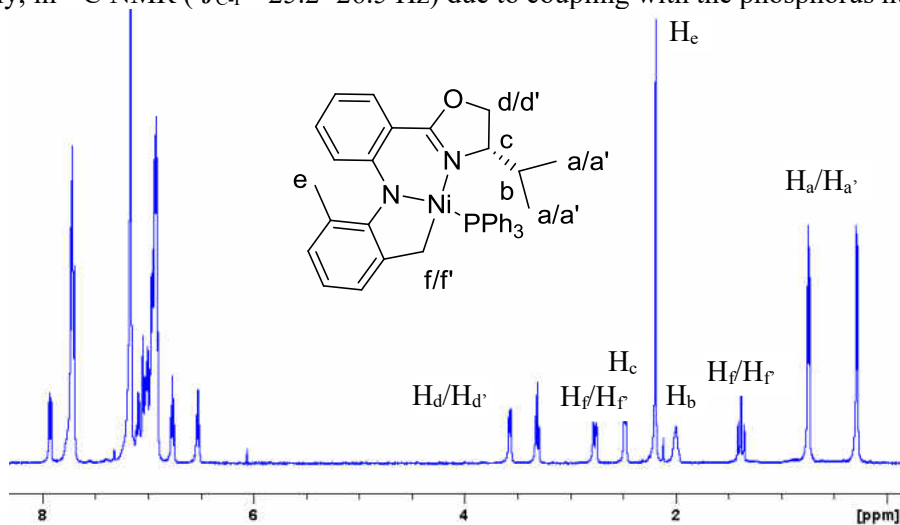

Figure 55. ^{1}H NMR of complex **3a** in C$_6$D$_6$ with partial assignment

The proposed structures of the Ni complexes were further verified by single-crystal X-ray diffraction experiments. The X-ray crystal data, data collection, and refinement parameters are summarized in Table 14. A single crystal X-ray structure of **3a** is presented in Figure 56. In agreement with the NMR data, one of the aniline methyl substituents is metallated with nickel, forming a five-membered metallacycle. This, along with the imine nitrogen atom, resulted in an unsymmetric, CNN pincer type coordination mode of the supposedly bidentate ligand.
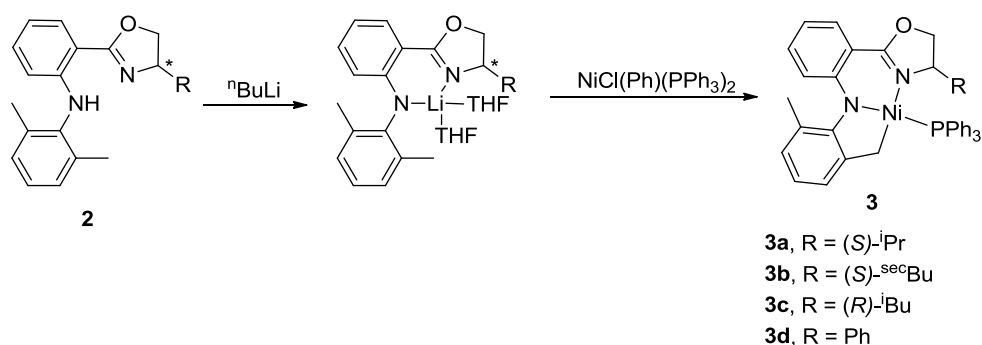
Scheme 13. Synthesis of pincer complexes **3a-d**

3a, R = (S)-ⁱPr
3b, R = (S)-secBu
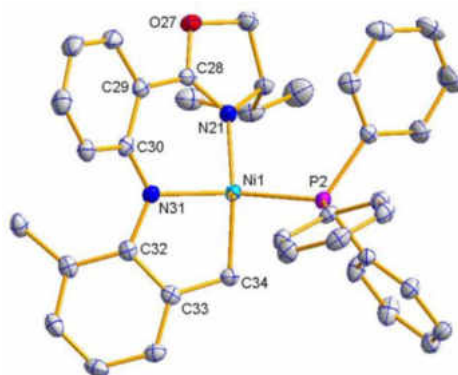3c, R = (R)-ⁱBu
3d, R = Ph

Figure 56. Molecular structure of compound **3a** with thermal ellipsoids drawn at the 50% probability level

The triphenylphosphine ligand completed the distorted square-planar environment around the nickel center. The Ni-P bond length of 2.1336(6) Å is in the typical range for similar compounds,[24] while the Ni-C bond distance of 1.930(2) Å is considerably shorter than the Ni-C(sp³) bond (1.97 Å) in a PCP pincer complex,[25] but longer than the Ni-C(sp²) bonds (1.88 Å) seen in the other pincer complexes.[26]

Complexes **3a-3c** are isomorphic with similar structural parameters; selected bond lengths and bond angles are listed in Table 15. The bond distances of Ni-N$_{imino}$ (1.920-1.935 Å) are slightly longer than that of Ni-N$_{amido}$ (1.908-1.920 Å), presumably because of the stronger interaction with anionic amido nitrogens. Both of them are in the normal range compared with other reported nickel compounds.[27] The coordination plane around nickel, however, appears to be severely distorted. While the N$_{imino}$-Ni-C bond angles of ~163˚ are not unusual for the trans angles involving the lateral donors in pincer systems, the N$_{amido}$-Ni-P bond angles of ~153˚ are much smaller than the typical linear arrangement for the trans angles involving the central atom of the pincer ligand.[28] Presumably, this reflects a rather strong steric strain of the nickel coordination environment. Consistent with this, the two adjacent chelating rings deviate significantly from coplanarity, with dihedral angles of 22.7(1)° (**3a**), 23.9(2)° (**3b**), and 23.6(1)° (**3c**), respectively. The six-membered ring adopts an envelope-like conformation with the Ni atom in the flap position. The Ni atoms are displaced by 0.6571(2) (**3a**), 0.6650(6) (**3b**), and 0.6984(3) (**3c**) Å from the plane through other five atoms of the six-membered rings. The dihedral angles between the aniline phenyl ring and the central phenyl skeleton ring are in the range 46.9(1)° (**3a**), 48.6(2)° (**3b**), and 50.0(1)° (**3c**). Comparison of structural features of complexes **3b** and **3c** suggests that the absolute configuration at the 4-oxazoline position has a profound influence on the overall configuration of the complexes. A side-by-side comparison of structures of **3b** and **3c**, roughly along the C-Ni-N$_{imino}$, is shown in

179

Figure 57. The 2,6-disubstituted aniline phenyl moiety bends towards the same direction of the substituent at the oxazoline chiral center, while the backbone aromatic ring, as well as the PPh$_3$ group, points towards the opposite direction, in order to minimize the steric interactions.

7.2.3. Racemization and Structure of 3d

When ligand **2d**, with a phenyl substituent at the 4-oxazoline position, was employed, similar benzylic C-H activation occurred and CNN pincer complex was readily obtained. However, the chiral center at the 4-oxazoline position somehow racemized. The compound crystallized in a different crystal system (triclinic for **3d** *vs* orthorhombic for **3a-c** and **3e**) that contains a pair of enantiomers in the unit cell related by an inversion center.[22] The geometrical parameters are similar to those in **3a-c**, but the distortion appears to be less severe. The racemization of **3d** is further supported by the CD measurement, which showed no observable signals. In comparison, the CD spectrum of ligand **2d** showed distinctive features. Moreover, the single crystal X-ray structure of **2d** was determined, which is in accordance with the ligand chirality with the same absolute configuration (*R*) at the 4-oxazoline position as the starting (*R*)-2-phenylglycinol. Additionally, the free ligand itself takes on a planar configuration with the N-H proton located between amido and imino nitrogens, forming an inner N-H···N hydrogen bond. The dimethyl phenyl unit resides nearly perpendicular to the above-mentioned plane. Comparison with the ligand parameters in the nickel complex further confirmed the distortion upon coordination (Figure 58). Particularly, the nearly coplanar oxazoline ring and the central phenyl ring in the free ligand are now twisted at 25.20(5)°, and the dihedral angle between the aniline phenyl ring and the central phenyl skeleton ring is 59.01(5)° in the complex.

7.2.4. Synthesis and Structure of 3e

Inspired by the formation of complexes **3a-d**, we were interested to see if C-H bonds other than the benzylic one can be activated and form pincer complexes within this type of ligands. Thus, ligand **2e**, in which a chiral alkyl moiety was introduced adjacent to the amine nitrogen, was examined. Following a similar procedure, a dark red crystal was obtained from reaction of *trans*-NiCl(Ph)(PPh$_3$)$_2$ and *in-situ* generated lithium salt of ligand **2e**. The ^{1}H NMR spectrum in benzene-d_6 showed the absence of the N-H signal of the free ligand. The benzylic proton, however, is still observed at 4.99 ppm as a quartet, shifted downfield compared with free ligand (4.55 ppm). These observations are consistent with a proposed structure with C$_1$ symmetry (Scheme 14).
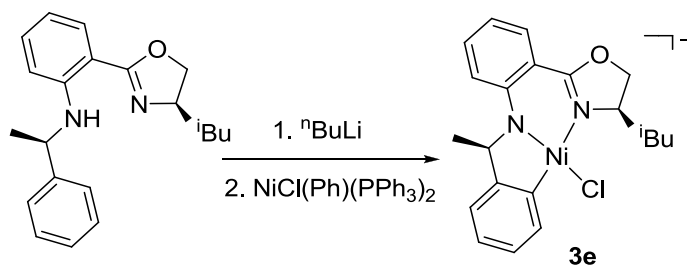
Scheme 14. Synthesis of pincer complex **3e**

Table 14. X-ray Crystal Data, Data Collection Parameters, and Refinement Parameters

	3a	3b	3c	3d	3e	2d	4
formula	$C_{38}H_{37}N_2NiOP$	$C_{39}H_{39}N_2NiOP$	$C_{39}H_{39}N_2NiOP$	$C_{41}H_{35}N_2NiOP$	$C_{93}H_{84}ClLiN_2NiO_5P_4$	$C_{23}H_{22}N_2O$	$C_{75}H_{73}Ni_2P_5$
FW	627.41	641.43	641.43	661.39	1534.70	342.43	1366.74
crystal system	Orthorhombic	Orthorhombic	Orthorhombic	Triclinic	Orthorhombic	Orthorhommbic	Triclinic
space group	$P2_12_12_1$	$P2_12_12_1$	$P2_12_12_1$	P-1	$P2_12_12_1$	$P2_12_12_1$	P-1
a, Å	9.7830(2)	9.7903(2)	9.84280(10)	9.2807(2)	11.4071(3)	10.7615(11)	12.7404(4)
b, Å	15.0674(2)	15.3617(4)	15.0952(3)	11.2227(3)	20.7893(7)	10.8922(11)	12.8703(4)
c, Å	21.6014(15)	21.5085(15)	21.8779(15)	17.2906(4)	33.113(2)	15.7770(16)	24.2765(7)
α, deg				108.2600(10)			77.185(2)
β, deg				92.2040(10)			88.302(2)
γ, deg				103.0970(10)			61.962(2)
V, Å^3	3184.1(2)	3234.8(2)	3250.6(2)	1654.02(7)	7852.6(6)	1849.3(3)	3413.08(18)
Z	4	4	4	2	4	4	2
d_{calc}, g cm^{-3}	1.309	1.317	1.311	1.328	1.298	1.230	1.330
T/K	123	123	123	173	123	173	173
μ, mm^{-1}	0.692	0.683	0.680	0.670	0.418	0.076	0.716
2θ range, deg	3.118-27.484	3.111-27.482	3.094-27.484	1.25-33.09	3.003-24.710	2.29-28.22	0.86-28.30
data collected	22147	11925	23395	25654	32597	15880	86941
unique data	7309	7097	7369	10575	13331	4274	16805
R_{int}	0.025	0.036	0.021	0.0215	0.101	0.0249	0.1086
Data in Refinement	7294	7083	7355	10575	13292	4274	16805
data with I>2.0σ(I)	6875	5413	6970	8835	8596	4021	9748
variables	389	398	398	415	965	237	813
$R(F_o)^a$	0.0246	0.0456	0.0276	0.0351	0.0596	0.0381	0.0561
$R_w(F_o^2)^b$	0.0438	0.0748	0.0553	0.0951	0.0818	0.1014	0.1373
GOF	0.9425	0.9724	0.9765	1.047	0.9568	1.038	0.933
Flack	-0.002(7)	-0.01(2)	0.004(9)		-0.036(16)		

^{a} $R = \Sigma \, ||F_o| - |F_c||/ \Sigma |F_o|$ for $F_o^2 > 2 \, \Sigma(F_o^2)$; ^{b} $R_w = [\Sigma \, w \, (|F_o^2| - |F_c^2|)^2/ \Sigma \, w \, |F_o^2|^2]^{1/2}$

Table 15. Selected Bond Distances (Å) and Bond Angles (deg) in Complexes 3a−e Determined by X-ray crystallography.

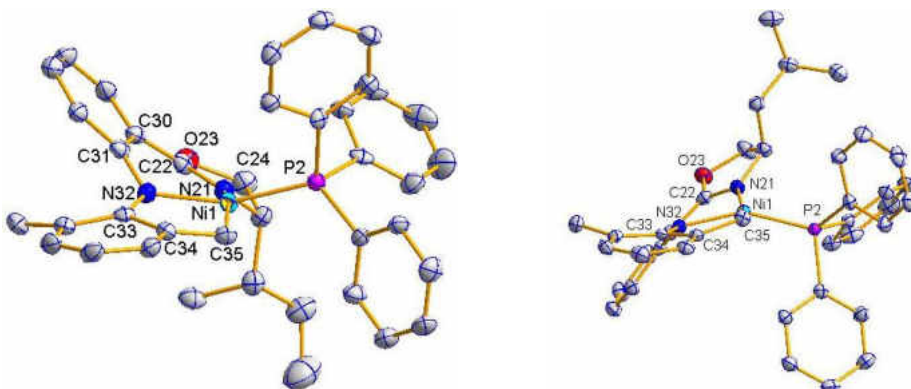|	3a	3b	3c	3d	3e
Ni−C	1.9320 (15)	1.934(4)	1.9303(18)	1.9308(15)	1.887(5)
Ni−Namido	1.9197 (14)	1.914(4)	1.9177(16)	1.9081(11)	1.887(4)
Ni−Nimino	1.9199 (14)	1.926 (4)	1.9343(17)	1.9358(12)	1.942(4)
Ni−P/Cl	2.1335(4)	2.1327(12)	2.1333(5)	2.1631(4)	2.2100(15)
Nimino−Ni−C	162.77(7)	164.05(19)	162.74(8)	171.60(6)	176.1(2)
Namido−Ni−P/C	152.69(4)	153.91(12)	152.84(5)	167.39(4)	174.92(12)

181

Figure 57. Side view of the structures **3b** (left) and **3c** (right)
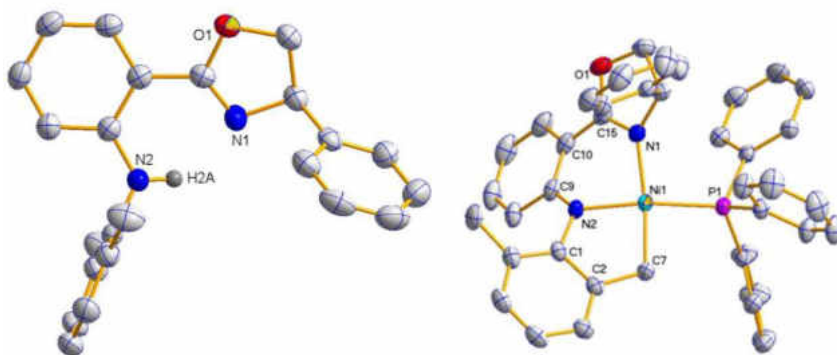

Figure 58. Molecular structure of ligand **2d** (left) and its nickel complex **3d** (right)

X-ray crystal structure analysis confirmed the pincer coordination mode of the ligand, in which the cyclometallation takes place on the *ortho*-phenyl position of the amine arm to form a five-membered chelation ring (Figure 59). Selected bond lengths and bond angels are listed in Table 15. Unlike complexes **3a-d**, one Cl atom is coordinated to nickel atom instead of PPh$_3$. The nickel atom resides in a distorted square planar geometry constructed by N3, N14, C17, and Cl2 with the bond distances of N3-Ni1 = 1.942(4), N14-Ni1 = 1.887(4), C17-Ni = 1.887(5), and Ni-Cl2 = 2.210(2). Clearly the Ni-C17 bond distance is much shorter than those in complexes **3a-d**. Presumably, this is because the PPh$_3$ group was replaced by a smaller Cl atom, which reduces steric crowdedness around the metal center. In addition, PPh$_3$ has a much stronger trans influence than chloride, further reducing the Ni-C distance in **3a-d**. Absence of PPh$_3$ ligand makes the nickel coordination environment more planar, and the deviation of Ni from the coordination plane is only 0.0354(6) Å. Li(OPPh$_3$)$_4{}^+$ is found as the counter cation in the crystal structure; presumably oxygen comes from adventitious air during the reaction process.

7.2.5. UV-vis and CD Spectroscopy of Ni Complexes 3a–3d

UV-vis and CD spectra of Ni complexes **3a–3d** are presented in Figure 60 and are summarized in the Experimental Section. In general, all complexes exhibit four features in their UV-vis spectra. The first low intensity band ($\varepsilon \sim 200$ M^{-1} cm^{-1}) is located at ~650 nm, which is followed by two intense bands at ~440 ($\varepsilon \sim 2500$ M^{-1} cm^{-1}) and ~320 ($\varepsilon \sim 9000$ M^{-1} cm^{-1}) nm, with one low-intensity broad shoulder observed at ~500 nm. The CD spectra of the Ni complexes **3a–**

3d are shown in Figure 60 and agree well with the UV-vis spectra. All *(R)*-isomers have a strong *negative* signal, which corresponds to the low-energy transition observed in the UV-vis spectra at ~650 nm. This band follows the low-intensity negative signal at ~510 nm, which correlates with the position of shoulder observed in UV-vis spectra of corresponding complexes. Absorption band at ~440 nm has a positive amplitude for all *(R)*-isomers and fits well with a position of intense band observed in UV-vis spectra of the target nickel complexes. Finally, one low intensity (~380 nm) and one high-intensity negative CD signal dominate in the UV region of CD spectra of complexes **3a–3d**. In agreement with the expectations, the CD spectrum of *(S)*-isomer of complex **3c** is a mirror image of the CD spectrum of *(R)*-isomer. As it has already been mentioned above, complex **3d** has no signals in CD spectrum, which confirms its racemization during a metal-insertion reaction.
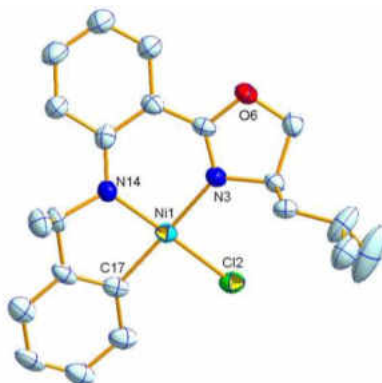

Figure 59. X-ray crystal structure of compound **3e**. Cationic counter ion is omitted for clarity

7.2.6. DFT-PCM and TDDFT-PCM Calculations

A tentative interpretation of the UV-vis and CD spectra of nickel (II) complexes **3a–3d** is quite challenging. In particular, the following questions should be addressed: (i) Taking into consideration the "soft base" character of new CNN pincer ligand, is the highest occupied molecular orbital (HOMO) predominantly nickel- or CNN π-centered MO? (ii) Is the lowest occupied molecular orbital (LUMO) π* MO centered on pincer CNN ligand or soft PPh$_3$ fragment? (iii) Are low-intensity band at~665 nm and a shoulder at ~510 nm classic nickel (II) d-d transitions? (iv) Is the intense band observed at ~440 nm charge-transfer or π-π* in nature? Thus, the further insight into the electronic structure and UV-vis as well as CD spectroscopy of the target nickel complexes **3a–3d** was gained on the basis of DFT-PCM and TDDFT-PCM calculations which have been shown to provide accurate energetic and spectroscopic parameters for a large variety of transition-metal complexes[29] including nickel-containing compounds.[30] Since UV-vis and CD spectra of all investigated nickel complexes are very close to each other, we have only calculated electronic structure, UV-vis, and CD spectra of *(R)*- and *(S)*-isomers of complex **3c**. As shown in Supporting Information, Table S1, the predicted geometries from DFT-PCM calculations are in good agreement with the X-ray experimental parameters. The DFT-PCM predicted MO energy diagram for **3c** is presented in Figure 61, while an analysis of the orbital compositions is provided in Figure 62. and Supporting Information, Table S2. In addition, the frontier orbitals of the complex **3c** are also pictured in Figure 61.

The X3LYP/6-31G(d) DFT-PCM calculations predict that the HOMO in the complex **3c** is a predominantly π-orbital with an electron density delocalized over diphenylamide fragment of the ligand with the metal contribution of ~10%. This orbital is energetically well-separated (~0.8 eV) from the closely spaced predominantly nickel-centered HOMO-1 to HOMO-3 MOs. HOMO-1 is dominated by nickel d$_{z2}$ AO contribution, while HOMO-2 and HOMO-3 have prominent nickel d$_{xz}$ and d$_{yz}$ characters, respectively. The other set of MOs, which is important for understanding of the

UV-vis and CD spectra of **3c** (HOMO-4 to HOMO-9), is predominantly localized over PPh$_3$ and chiral pincer ligands (Figures 61 and 62 and Supporting Information, Table S2). For instance, HOMO-4 has distinct Π-character and is localized over C$_6$H$_3$CH$_2$ fragment. Similarly, HOMO-5 and HOMO-6 are Π -orbitals delocalized over the pincer ligand, while HOMO-7 and HOMO-8 have distinct PPh$_3$ localization. Except LUMO+2, which has ~10% of nickel d$_{x2-y2}$ character,
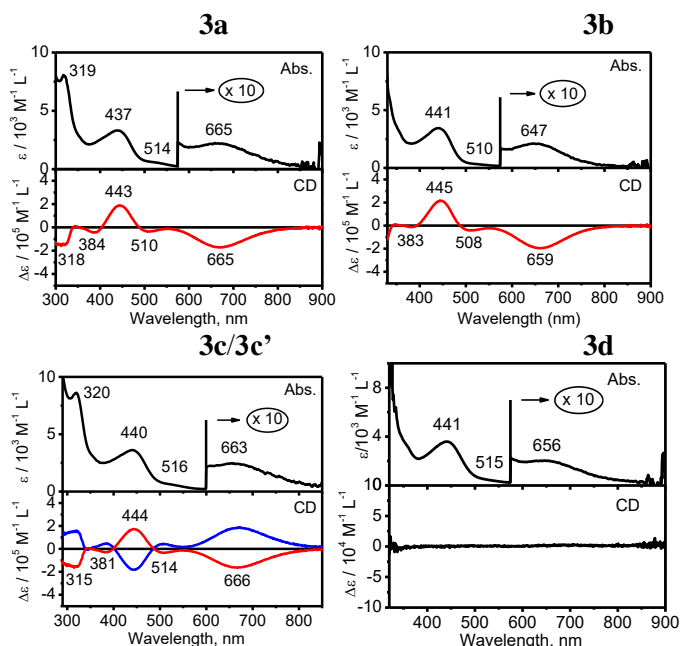

Figure 60. UV-vis and CD spectra of **3a–3d** in CH$_2$Cl$_2$
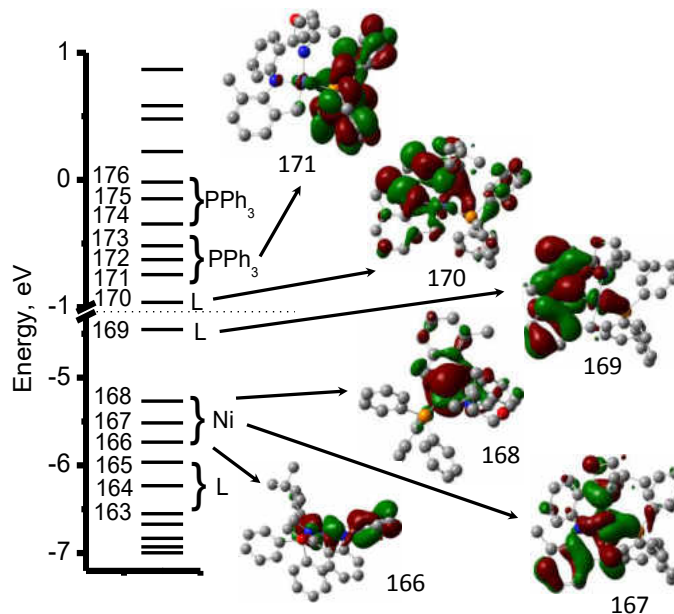
Figure 61. Molecular energy diagram and frontier orbitals of complex **3c** calculated using DFT-PCM approach and X3LYP exchange-correlation functional. HOMO–LUMO energy gap is indicated by the dotted line
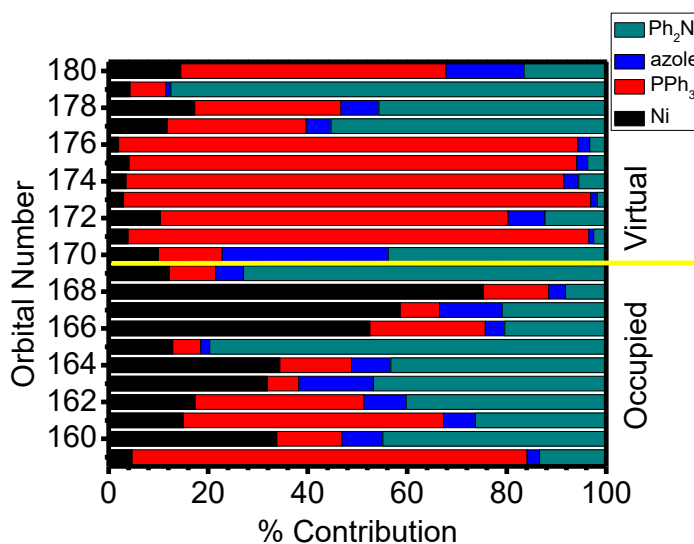
184

Figure 62. Molecular orbitals contribution analysis of complex **3c** calculated at DFT-PCM level using X3LYP exchange-correlation functional. Black bars are contribution of Ni ion, red bars are contribution of PPh$_3$ ligand, blue bars are contribution of oxazoline part of the pincer ligand, blue-gray bars are contribution of PhNPh part of the pincer ligand

LUMO to LUMO+10 MOs are dominated either by PPh$_3$ (LUMO+1 to LUMO+6) or pincer ligand (LUMO, LUMO+7 to LUMO+9) contributions and could be characterized as π* MOs.

The further interpretation of the UV-vis and CD spectra of complex **3c** was solidified on the basis of TDDFT-PCM calculations (Figure 63 and Supporting Information). TDDFT-PCM predicted vertical excitation energies, oscillator strengths, and rotary strengths of **3c** calculated with and without solvent equilibration are virtually identical. UV-vis and CD spectra in the 400 - 900 nm range could be described using first six low-energy excitations. The first low-intensity band experimentally observed as a weak band at ~665 nm in UV-vis spectrum and as a strong positive signal in CD spectrum of **3c** is associated with the first transition predicted by TDDFT-PCM method. This excited state consists of ten significant single-electron contributions, has ~74% of intra- and inter-ligand π-π* character and ~26% of MLCT character, and dominated by HOMO → LUMO (~47%) and HOMO → LUMO+2 (~14%) transitions. The first transition has intra (pincer)-ligand character, while the second one can be described as the charge-transfer transition from the pincer ligand to PPh$_3$ fragment. In agreement with experimental data, the oscillator strength of this transition is small, while rotary strength is positive and large. The second and third excited states are responsible for the broad, low intensity shoulder observed in UV-Vis spectrum of **3c** between 500 and 600 nm and weak positive CD signal observed in the same region. These transitions have pure MLCT character and dominated by HOMO-1 (Ni d$_{z2}$) → LUMO (~40%, pincer π* MO), LUMO+2 (~25%, PPh$_3$ π* MO) for excited state 2 or HOMO-2 (Ni d$_{xz}$) → LUMO, LUMO+2 (~25%, pincer π* MO), LUMO+2 (~20%, PPh$_3$ π* MO) for excited state 3 transitions. In addition, ~22% of excited state 3 could be described as HOMO-3 (Ni d$_{yz}$) →LUMO, LUMO+1, LUMO+7, and LUMO+8 single-electron excitations. Again, in agreement with experimental data, TDDFT-PCM predicted rotary strengths of the excited states 2 and 3 are positive and significantly smaller compared to that in the first excited state. According to TDDFT-PCM calculations, excited state 4 is the main contributor to the 440 nm band observed in UV-vis spectrum of **3c**. This excited state consists of five major single-electron contributions, has ~90% of π-π* character, and dominated by HOMO →LUMO (~64%) and HOMO → LUMO+2 (~26%) transitions. In agreement with experimental CD spectrum, TDDFT-PCM calculations predict strong negative signal associated

with this excited state. Excited state 5 could be associated with the higher-energy shoulder of the 440 nm band, a positive signal in CD spectrum observed at ~375 nm. This excited state has 17 single-electron contributions, has ~83% of π-π* and ~17% of MLCT character, and has no dominant contribution (the largest single-electron contribution is ~11% for HOMO →LUMO+2 transition). Again, TDDFT-PCM calculations predict positive amplitude for CD signal associated with this excited state. Finally, the shoulder at ~350 nm observed in UV-vis and CD spectra of **3c** and a weak negative signal observed in its CD spectrum in this region can be assigned to the excited state 6. This excited state has pure π-π* character and could be described as almost pure HOMO → LUMO+1 (PPh$_3$, π* MO) single electron transition (~96%). TDDFT-PCM calculations predict that the higher energy regions of UV-vis and CD spectra of **3c** consist of numerous overlapping excited states and thus it is impossible to provide a clear assignment for intense 320 nm and higher energy bands.

Overall, TDDFT-PCM calculations are in good agreement with the experimental UV-vis and CD data and allow us to assign the observed spectra in 400-900 nm region to four excited states with predominantly π-π* character and two excited states with predominantly MLCT character.
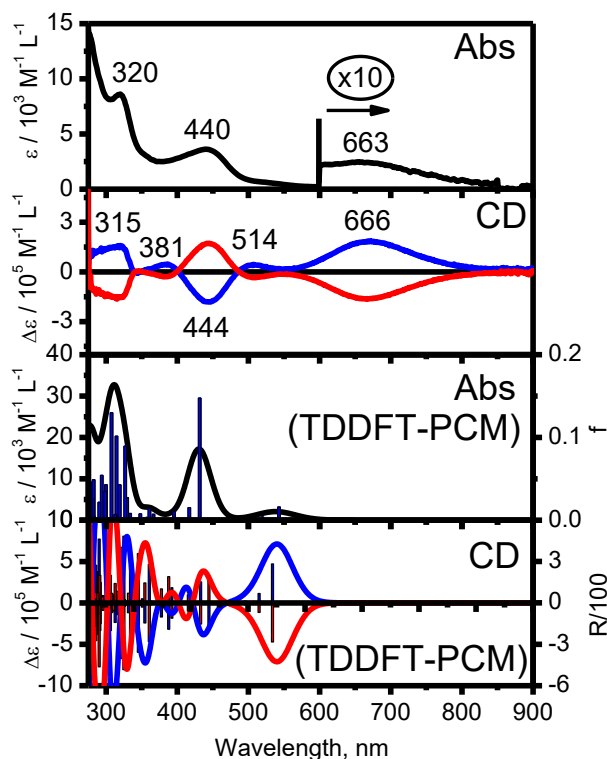

Figure 63. Experimental UV-vis and CD data (top) and TDDFT-PCM predicted UV-vis and CD spectra (bottom) of complex **3c**. Blue lines represent (*S*)-isomer and red lined represent (*R*)-isomer of chiral complex.

7.2.7. Discussions

A few anilido imine complexes of nickel have been reported as analogues of conventional β-diketimine or α-diimine based complexes, mostly for applications in catalytic olefin polymerization.[31] Usually they are obtained as mono- or dinuclear Ni(II) species by reaction of free or deprotonated ligands with a nickel precursor such as Ni(OAc)$_2$, NiCl$_2$, NiBr$_2$, NiCl$_2$(THF)$_{1.5,}$

NiCl$_2$(py)$_4$, and Ni(acac)$_2$, with or without the presence of a base. When *trans*-NiCl(Ph)(PPh$_3$)$_2$ was employed as the precursor, formation of a three coordinate Ni(I) complex (**NN**)Ni^I(PPh$_3$) was observed.[27a, 32] Analogous results were obtained for the conventional β-diketiminato ligand, leading to reduction of Ni(II) and formation of three coordinate Ni(I) complexes.[33] However, when less bulky ketiminato and salicylaldiminato ligands were allowed to react with *trans*-NiCl(Ph)(PPh$_3$)$_2$, square planar Ni(II) complexes from simple metathesis were obtained as the main products.[33,34] It should be emphasized that in none of these reactions C-H activation of ligands has been observed. Therefore, it is surprising to note that in the present system, one of the benzylic or aryl C-H bonds on the aniline side arm was cyclometallated, and the ligand functioned as a tridentate, dianionic chelate and led to the formation of unsymmetric CNN pincer type complexes.

A large number of pincer complexes with a C backbone or arm have been prepared; vast majority of them is introduced through direct metallation, transmetallation, or cyclometallation of C(sp^2)-H bonds.8 In comparison, examples with C(sp^3)-H bonds, either benzylic or aliphatic, are relatively less common,[12,35] although the coordination-assisted C(sp^3)-H bond activation by palladium is well-documented.[36] It also appears that the metallation occurs only when the metal center is easily accessible to the CH bond so that substitution at the sp^3 carbon is feasible.[37] Thus, results here are even more striking, considering the typical orientation the *ortho*-dimethyphenyl group adopts and the strong distortion the ligand would have to go through to form the observed complexes. We have described the distorted coordination environment around the Ni center. The sensitivity of these complexes towards air may also be a reflection of the strain in the system.

Another puzzling yet important aspect is the observation of racemization of chiral oxazolines in compound **3d**, apparently during the complex formation. Oxazoline and its derivatives have been employed extensively in transition metal asymmetric catalysis,[38] but racemization of chiral oxazolines upon metal coordination or during catalysis is rarely reported. Gabbai and coworkers noted that a chiral oxazoline palladium complex, (*S,S*)-di-*μ*-(acetate)-bis[2-[2-(4-carbomethoxy) oxazolinyl]phenyl-C,N]-dipalladium(II), underwent racemization reaction when serving as a catalyst for the hydrolysis of organophosphorus.[39] However, the mechanism of racemization is not well-understood. One possibility is that deprotonation of hydrogen at 4-oxazoline may occur due to the enhanced acidity when a phenyl (as in **3d**) or carbomethoxy (as in the dipalladium complex) group is attached. Isomerization to 3-oxazoline or non-selective recombination of proton and carbanion resulted in racemization (Scheme 15). It is unclear what could serve as a base to deprotonate the 4-H. Fortunately, no racemization is observed when aliphatic substituents are present at the 4-oxazoline position, as seen in **3a-c** in our study.
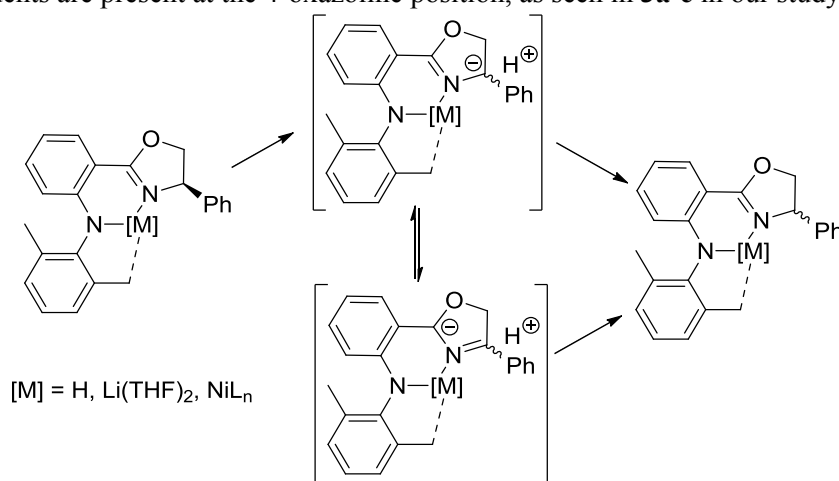
Scheme 15. Possible pathways for racemization of **3d**

It has been suggested that the steric bulk of the chelating NN ligands in combination of the

bulky PPh₃ played a key role in the reduction of Ni(II) and the formation of three-coordinated Ni(I).[27a] We suspect that unexpected formation of CNN pincer complexes via C-H activation may have a similar steric origin. Presumably, the ligand is first coordinated to nickel(II) in an N, N-bidentate fashion, with PPh₃ in the less congested side and phenyl group adjacent to aniline moiety. Because of the proper steric interaction with the environment, particularly the chiral oxazoline quadrant, the dimethylphenyl group was forced out of its normal perpendicular position, with one methyl leaning close towards the Ni center. This may lead to an agostic interaction or a σ-complex that eventually resulted in the elimination of benzene and the formation of the carbon nickel bond, possibly through a conventional concerted σ-bond metathesis or a σ-complex assisted metathesis pathway (Scheme 16). Such mechanisms are common for electrophilic early transition metal systems,[40] but it can occur with late transition metals as well.[41] The observation of the nickel product in the same oxidation state and the absence of biphenyl from phenyl coupling in the products are in agreement with this mechanism. An oxidative addition pathway involving a high valent nickel, formally Ni^{IV}, seems less likely, but could not be ruled out.[42] Further studies are required to elucidate the reaction mechanism and to utilize this C-H activation chemistry.
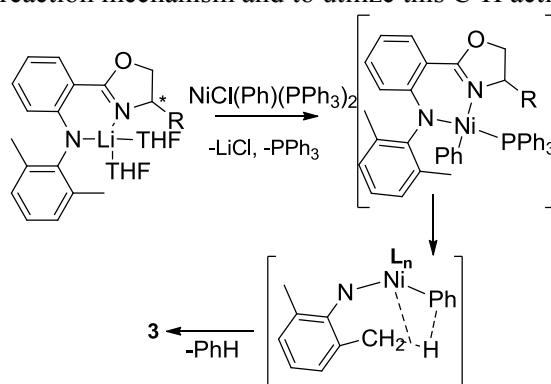
Scheme 16. A possible pathway for complexes **3a-d**

One of our initial goals is to prepare nickel (II) complexes incorporating chiral, monoanionic β-diketimine type ligands. Therefore, we explored a number of commonly used nickel precursors listed above in the synthesis. Though signs of reactions were noted in several occasions, only the procedure with *trans*-NiCl(Ph)(PPh₃)₂ afforded the isolable and identifiable nickel complexes, leading to the formation of pincer complexes via unexpected C-H activation. However, the yields are generally low; and the highest so far obtained is ~35% with **3a**, despite numerous attempts to improve the reactions.

Efforts were also made to isolate and characterize other Ni-containing products formed in the reaction. The paramagnetic species were often observed in the crude reaction mixture, as indicated by the appearance of ¹H NMR signals in the +50 and -50 ppm range. Another type of byproducts features two nickel centers without incorporation of the anilido imine ligands. One of them was isolated as a dark-green crystals and characterized by X-ray diffraction crystallography, which revealed a dinuclear structure of (PPh₃)₂Ni(μ-PPh₂)₂Ni(PPh₃), **4**.[22] These observations may explain, at least in part, the low yields generally obtained, and they also indicate the complexity of the process.

7.3. Conclusions

In summary, we have synthesized and characterized a series of chiral and unsymmetrical CNN pincer nickel complexes with C_1 symmetry ligands via a coordination assisted cyclometallation process. Both C(sp³)-H and C(sp²)-H bonds may be activated, showing the diversity it may bring. The absolute configuration of chiral groups exerts considerable influence on the overall structural arrangement. The fact that both benzylic and aryl C-H bonds are activated

with similar ease suggests that the geometries of the intermediates favor activation, regardless of the energetics of the process. These findings open new possibility for a pincer ligand design based on the anilido imine framework and appear promising for further investigations. Current efforts aim to establish the general applicability of the synthetic approach, further probe the origin of the observed activity by varying substituent groups on both arms, and explore if the activity can be harnessed for practical C-H activations. In addition, these nickel complexes are chiral with easily tunable substituents and their potential applications in asymmetric catalysis will be investigated.

7.4. Experimental Section

General. All air- or moisture-sensitive reactions were carried out under a dry nitrogen atmosphere, employing standard Schlenk line and drybox techniques. Tetrahydrofuran, toluene, and diethyl ether were dried over potassium hydroxide and distilled over Na/benzophenone prior to use. DMF was distilled over CaH_2. Deuterated solvents were purchased from Cambridge Isotope Laboratory, dried over sodium or calcium hydride, degassed, and distilled by vacuum transfer. *trans*-$NiCl(Ph)(PPh_3)_2$ was prepared according to a literature procedure.[43]

All ^1H and ^{13}C NMR spectra were recorded on a Bruker AVANCE-500 NMR spectrometer and referenced to TMS or the residue peaks in $CDCl_3$ or C_6D_6. ^{31}P NMR was referenced to $P(OEt)_3$ at 137 ppm. The elemental analyses were performed by Midwest Microlab, Indianapolis, IN. UV-Vis data were obtained on Jasco-720 or Cary 17 spectrophotometers. Circular Dichroism (CD) data were recorded using OLIS DCM 17 CD spectropolarimeter. GC-MS analyses were performed on an HP 5890 GC/HP 5971/B MSD system with electron impact ionization (70 eV).

Ligand 2e by Cu-Catalyzed Amination.[21] An oven-dried Schlenk flask was charged with a magnetic stir bar, CuI (10 mg, 0.05 mmol, 5 mol%) and K_3PO_4 (2 mmol, 425 mg), then evacuated and backfilled with nitrogen three times. Under a counter-flow of nitrogen, *R*-(+)-α-methylbenzylamine (181 mg, 1.5 mol), oxazoline derivative (302 mg, 1 mmol), and DMF (0.5 mL) were added by syringe. Finally, 2-isobutyrylcyclohexanone (34 mg, 0.2 mmol, 20 mol%) was added via syringe, the flask was sealed and the mixture was heated at the 110 °C for 24 hours. Upon completion of the reaction, the mixture was allowed to cool to room temperature, diluted with ethyl acetate, and passed through a fritted glass filter to remove the inorganic salts. The solvent was removed with the aid of rotary evaporator. The residue was purified by column chromatography on silica gel and the product was dried under vacuum for at least 1 h. Colorless crystals of the product could be obtained in ethyl acetate by slow evaporation. The typical yield was ~40%. The identity of **2e** was compared with literature[20a] and confirmed by ^1H NMR and GC-MS.

Lithium Salt L^{2d}Li(THF)$_2$: Ligand **2d** (1 mmol) was dissolved in 10 mL of THF and cooled to -78°C. To it was added an n-butyl lithium solution in hexane (0.625 mL, 1.6 M) at low temperature. The solution changed from colorless to dark-green and then orange. It was allowed to stir for 2 hours at -78°C and then warm to room temperature with stirring. THF was then removed under vacuum and the yellow residue was washed with hexane. Light yellow needle-like crystals could be obtained by diffusion of hexane into a THF solution of the lithium salt. The yield is 0.39 g (80%). ^1H NMR (500 MHz, C_6D_6): δ 8.40 (d, 1 H, J = 8.41 Hz), 7.21 (m, 3 H), 7.13 (m, 1 H), 6.99 (m, 5 H), 6.58 (d, 1 H, J = 6.55 Hz), 6.48 (t, 1 H, J = 6.47 Hz), 4.78 (t, 1 H, J = 4.78 Hz), 4.16 (t, 1 H, J = 4.15 Hz), 3.72 (t, 1 H, J = 3.70 Hz), 3.11 (m, 8 H, THF), 2.36 (s, 3 H), 2.31 (s, 3 H), 1.13 (m, 8 H, THF) ppm. ^{13}C NMR (126 MHz, C_6D_6): δ 170.32, 158.76, 153.66, 144.70, 133.88, 133.28, 133.21, 133.17, 129.23, 128.87, 127.27, 121.59, 115.68, 109.10, 105.69, 73.27, 70.09, 68.13 (THF), 25.68 (THF), 19.31, 19.23.

Synthesis of 3a. The following procedure is typical: **2a** (30.8 mg, 0.1 mmol) was dissolved in 5 mL of THF which was cooled to -78°C. At this temperature 50 μL of BuLi (0.1 mmol) was added and the resulting yellow solution was stirred at low temperature for 1 hour and then was allowed to warm to room temperature. All volatiles were removed under vacuum. The yellow residue was dissolved in 5 mL of toluene, and then mixed with the orange solution of $NiCl(Ph)(PPh_3)_2$ (0.1

mmol) in 5 mL of toluene. The red to dark-red solution was stirred overnight at ambient temperature. After filtration and removal of solvent, the residue was dissolved in small amount of toluene and layered up with hexanes. After a few days, the red crystals formed and were collected. The yield is 22 mg (35%).^{1}H NMR (500 MHz, C_6D_6): δ 7.92 (d, J = 7.9 Hz, 1H), 7.79 – 7.65 (m, 6H, o-PPh$_3$), 7.12 – 7.06 (m, 1H), 7.06-6.99 (m, 3H), 6.99-6.89 (m, 9H, m,p-PPh$_3$), 6.76 (t, J = 7.3 Hz, 1H), 6.52 (t, J = 7.2 Hz, 1H), 3.57 (dd, J = 8.6, 2.2 Hz, 1H, NCH(R)CH_2O), 3.31 (t, J = 8.6 Hz, 1H, NCH(R)CH_2O), 2.76 (dd, J = 13.5, 5.0 Hz, 1H, NiCH_2), 2.54 – 2.42 (m, 1H, NCH(R)CH$_2$O), 2.19 (s, 3H, ArCH_3), 2.04-1.96 (m, 1H, CHMe$_2$), 1.38 (dd, J= 14.3, 14.3 Hz, 1H, NiCH_2), 0.74 (d, J = 6.7 Hz, 3H, CHMe_2), 0.28 (d, J = 6.9 Hz, 3H, CHMe_2). ^{13}C NMR (126 MHz, C_6D_6): δ 163.57, 156.54, 155.37, 145.66, 134.66, 133.79, 133.48, 133.15, 130.34, 129.53 – 128.08, 126.92, 124.68, 120.53, 119.87, 112.90, 111.24, 69.81 (NCH(R)CH$_2$O), 67.73 (NCH(R)CH$_2$O), 33.44 (CHMe$_2$), 26.43 (d, [2]J_{C-P}= 25.3 Hz, NiCH$_2$), 21.05 (ArCH$_3$), 18.56 (CHMe_2), 15.40 (CHMe_2). ^{31}P NMR (202 MHz, C_6D_6): δ 32.04. UV-vis (DCM, ε M^{-1} cm^{-1}): 319 (8010), 437 (3310), 514sh (622), 665 (220).

Synthesis of 3b. The procedure is the same as **3a** while ligand **2b** (32.2 mg, 0.1 mmol) was used. The yield is 15.2 mg (24%). Elemental analysis: Calc. $C_{39}H_{39}N_2$NiOP, C, 73.03; H, 6.13; N, 4.37. Found: C, 72.74; H, 5.99; N, 4.26. ^{1}H NMR (500 MHz, C_6D_6): δ 7.93 (dd, J = 7.9, 1.6 Hz, 1H), 7.75 – 7.66 (m, 6H, o-PPh$_3$), 7.16 (s, 2H), 7.12 – 7.01 (m, 3H), 6.94 (m, 9H, m,p-PPh$_3$), 6.77 (t, J = 7.3 Hz, 1H), 6.53 (ddd, J = 7.9, 6.7, 1.2 Hz, 1H), 3.58 (dd, J = 8.7, 2.9 Hz, 1H, NCH(R)CH_2O), 3.27 (t, J = 8.7 Hz, 1H, NCH(R)CH_2O), 2.66 (dd, J = 13.8, 5.5 Hz, 1H, NiCH_2), 2.60 (dt, J = 8.6, 2.9 Hz, 1H, NCH(R)CH$_2$O), 2.20 (s, 3H, ArCH_3), 1.96 – 1.90 (m, 1H, CHCH$_3$(Et)), 1.45 (dd, J = 14.2, 14.2 Hz, 1H, NiCH_2), 0.70 (d, J = 6.8 Hz, 1H, CHCH_3(Et)), 0.49 (t, J = 6.0 Hz, 3H, CHCH$_3$(CH$_2$CH_3)), 0.47 – 0.40 (m, 2H, CHCH$_3$(CH_2CH$_3$)). ^{13}C NMR (126 MHz, C_6D_6): δ 163.62, 156.48, 155.31, 145.55, 145.50, 134.69, 134.61, 133.58, 133.26, 133.11, 130.37, 130.23, 126.91, 124.83, 120.47, 119.86, 112.88, 111.10, 69.23 (NCH(R)CH$_2$O), 67.63 (NCH(R)CH$_2$O), 40.47 (CHCH$_3$(Et)), 26.38 (d, [2]J_{C-P}= 25.3 Hz, NiCH$_2$), 26.29 (CHCH$_3$(CH$_2$CH$_3$)), 21.08 (ArCH$_3$), 12.41 (CHCH$_3$(CH$_2$$CH_3$)), 11.85 (CH$CH_3$(CH$_2CH_3$)). ^{31}P NMR (202 MHz, C_6D_6): δ 33.02. UV-vis (DCM, ε M^{-1} cm^{-1}): 441 (3490), 510sh (390), 647 (210).

Synthesis of 3c. The procedure is the same as **3a**. **2c** (32.2 mg, 0.1 mmol) was used. Yield: ~15%. ^{1}H NMR (500 MHz, C_6D_6): δ 7.99 (d, J = 8.5 Hz, 1H), 7.74 (dd, J = 9.4, 7.7 Hz, 6H, o-PPh$_3$), 7.12 – 7.07 (m, 3H), 6.99 – 6.89 (m, 10H, m,p-PPh$_3$+ArH), 6.79 (t, J = 7.3 Hz, 1H), 6.56 (ddd, J = 7.9, 5.5, 2.3 Hz, 1H), 3.50 (dd, J = 8.2, 2.7 Hz, 1H, NCH(R)CH_2O), 3.23 (t, J = 8.1 Hz, 1H, NCH(R)CH_2O), 2.52 – 2.44 (m, 2H, NCH(R)CH$_2$O + NiCH_2), 2.21 (s, 3H, ArCH_3), 1.89 – 1.80 (m, 1H, CH_2CHMe$_2$), 1.64 (dd, J = 13.8, 13.8 Hz, 1H, NiCH_2), 1.18 (ddd, J = 13.8, 11.1, 4.9 Hz, 1H, CH_2CHMe$_2$), 1.03 – 0.94 (m, 1H, CH$_2$CHMe$_2$), 0.61 (d, J = 6.6 Hz, 3H, CH$_2$CHMe_2), 0.28 (d, J = 6.6 Hz, 3H, CH$_2$CHMe_2). ^{13}C NMR (126 MHz, C_6D_6): δ 163.96, 156.19, 155.27, 145.13, 134.92, 134.83, 133.37, 133.09, 132.99, 130.40, 130.06, 128.89, 128.79, 127.01, 124.94, 120.35, 120.01, 112.91, 110.95, 71.35 (NCH(R)CH$_2$O), 63.89 (NCH(R)CH$_2$O), 45.83 (CH$_2$CHMe$_2$), 26.61 (d, [2]J_{C-P} = 26.5 Hz, NiCH$_2$), 25.69 (CH$_2$$CHMe_2$), 24.08 (Ar$CH_3$), 22.02 (CH$_2CHMe_2$), 21.38 (CH$_2CHMe_2$). ^{31}P NMR (202 MHz, C_6D_6): δ 34.20. UV-vis (DCM, ε M^{-1} cm^{-1}): 320 (8620), 440 (3620), 516sh (673), 663 (240). The complex **3c'** was prepared analogously, starting from ligand **2c'** with a (S)-[i]Bu substituent at the 4-oxazoline position. The ^{1}H NMR data are virtually identical with **3c**.

Synthesis of 3d. The procedure is the same as **3a**. **2d** (34.2 mg, 0.1 mmol) was used. Yield: ~20%. ^{1}H NMR (500 MHz, C_6D_6): δ 7.94 (d, J = 8.5 Hz, 1H), 7.53 (m, 6H, o-PPh$_3$), 7.20 – 7.12 (m, 4H), 7.01-6.96 (m, 5H), 6.95 (m, 3H), 6.86 (td, J = 7.9, 5.0 Hz, 6H), 6.76 (t, J = 7.5 Hz, 1H), 6.55 (m, 1H), 3.58 (m, 1H, NCH(R)CH$_2$O), 3.50 (m, 2H, NCH(R)CH_2O), 2.48 (dd, J = 13.8, 5.5 Hz, 1H, NiCH_2), 2.29 (s, 3H, ArCH_3), 1.56 (m, 1H, NiCH_2). ^{13}C NMR (126 MHz, C_6D_6): δ 165.71, 156.11, 155.66, 145.13, 145.07, 143.01, 134.88, 134.79, 133.33, 133.28, 133.02, 130.29, 129.32, 126.97, 126.80, 124.90, 124.88, 120.47, 120.22, 120.21, 113.05, 110.55, 74.99 (NCH(R)CH$_2$O), 68.50 (NCH(R)CH$_2$O), 26.52 (d, [2]J_{C-P} = 25.2 Hz, NiCH$_2$), 21.43 (ArCH$_3$).^{31}P NMR (202 MHz, C_6D_6): δ 34.27. UV-vis (DCM, ε M^{-1} cm^{-1}): 441 (3590), 515sh (550), 656 (200).

Synthesis of 3e. The procedure is the same as **3a**. **2e** (0.1 mmol) was used. Yield: ~10%. ^{1}H NMR (500 MHz, C$_6$D$_6$) δ 8.16 (t, J = 8.4 Hz, 2H), 7.82 – 7.56 (m, 24H), 7.20-6.96 (m, 40H), 6.48 (t, J = 7.2 Hz, 1H), 6.44 (t, J = 6.7 Hz, 1H), 4.99 (q, J = 5.8 Hz, 1H, NC*H*(Ar)CH$_3$), 4.85 (t, 1H, NC*H*(R)CH$_2$O), 3.73 (dd, J = 7.5, 2.5 Hz, 1H, NCH(R)C*H*$_2$O), 3.60 (t, J = 8.0 Hz, 1H, NCH(R)C*H*$_2$O), 2.38 (t, J = 10.6 Hz, 1H, C*H*$_2$CHMe$_2$), 1.63 (d, J = 6.1 Hz, 3H, NCH(Ar)C*H*$_3$), 1.45 – 1.39 (m, 1H, CH$_2$C*H*Me$_2$), 1.00 (m, 1H, C*H*$_2$CHMe$_2$), 0.97 (d, J = 6.4 Hz, 3H, CH$_2$CH*Me*$_2$), 0.65 (d, J = 6.5 Hz, 3H, CH$_2$CH*Me*$_2$). ^{31}P NMR (202 MHz, C$_6$D$_6$): δ 25.35. ^{13}C NMR was not obtained due to its low solubility.

X-ray Crystallography. Single crystal X-ray diffraction of compounds **2d**, **3d**, and **4** were collected on a Bruker Apex diffractometer equipped with an Oxford Cryosystems 700 Series Cryostream cooler, and that of compounds **3a-c** and **3e** were collected on a Rigaku RAPID II diffractometer equipped with XStream Cryosystem. Mo K$_\alpha$ radiation (λ = 0.71073 Å) was used on both instruments. X-ray crystal data, data collection parameters, and refinement parameters are summarized in Table 14 and more crystallographic details can be found in Supporting Information.

DFT-PCM and TDDFT-PCM Calculations. The initial geometry of complex **3c** was taken from the X-ray data and optimized at the DFT level, using a hybrid X3LYP exchange-correlation functional. We choose this exchange-correlation functional after 12 exchange-correlation functional were compared for CD intensities calculations on chiral model nickel (II) complexes (full comparison on all tested exchange-correlation functional will be published elsewhere). Equilibrium geometries were confirmed by frequency calculations and specifically by the absence of the imaginary frequencies. Solvation effects were modeled using the polarized continuum model (PCM) approach.[44] DCM was used as the solvent in all calculations to match with experimental data. All single-point DFT-PCM and TDDFT-PCM calculations were conducted using a X3LYP functional.[45] The first 70 states were considered in all PCM-TDDFT calculations in order to cover UV and visible range of the spectrum. In all cases, 6-31G(d) basis set was used for all atoms.[46] All calculations were performed using Gaussian03 or 09 software. Molecular orbital analysis was conducted using the QMForge program.[47]

7.5. References

1. (a) van Koten, *Top. Organomet. Chem*. **2013**, *40*, 1–20 and references therein. (b) Schneider, S.; Meiners, J.; Askevold, B. *Eur. J. Inorg. Chem*. **2012**, 412–429. (c) Nishiyama, H.; Ito, J.-I. *Chem. Commun*. **2010**, *46*, 203–212. (d) Pugh, D.; Danopoulos, A. A. *Coord. Chem. Rev*. **2007**, *251*, 610–641. (e) Dupont, J.; Consorti, C. S.; Spencer, J. *Chem. Rev*. **2005**, *105*, 2527–2572. (f) Peris, E.; Crabtree, R. H. *Coord. Chem. Rev*. **2004**, *248*, 2239–2246. (g) Albrecht, M.; van Koten, G. *Angew. Chem., Int. Ed.* **2001,** *40*, 3750–3781.

2. (a) Bonnet, S.; Li, J.; Siegler, M. A.; von Chrzanowski, L. S.; Spek, A. L.; van Koten, G.; Klein Gebbink, R. J. M. K. *Chem. Eur. J.* **2009,** *15*, 3340–3343. (b) Benito-Garagorri, D.; Kirchner, K. *Acc. Chem. Res.* **2008,** *41*, 201–213.

3. Niu, J.-L.; Hao, X.-Q.; Gong, J. –F.; Song, M.-P. *Dalton Trans*. **2011**, *40*, 5135–5150.

4. Moreno, I.; SanMartin, R.; Ines, B.; Herrero, M. T.; Dominguez, E. *Curr. Org. Chem*. **2009**, *13*, 878–895.

5. (a) Balaraman, E.; Fogler, E.; Milstein, D. *Chem. Commun*. **2012**, *48*, 1111–1113. (b) Bossi, G.; Putignano, E.; Rigo, P.; Baratta, W. *Dalton Trans*. **2011**, 8986–8995. (c) Sun, Y.; Koehler, C.; Tan, R.; Annibale, V. T.; Song, D. *Chem. Commun*. **2011**, *47*, 8349–8351. (d) Fogler, E.; Balaraman, E.; Ben-David, Y.; Leitus, G.; Shimon, L. J. W.; Milstein, D. *Organometallics*, **2011**, *30*, 3826–3833. (e) Kozlov, V. A.; Aleksanyan, D. V.; Nelyubina, Y. V.; Lyssenko, K. A.; Vasil'ev, A. A.; Petrovskii, P. V.; Odinets, I. L. *Organometallics* **2010**, *29*, 2054–2062. (f) Hao, X.-Q.; Wang, Y.-N.; Liu, J.-R.; Wang, K.-L.; Gong, J.-F.; Song, M.-P. *J. Organomet. Chem*. **2010**, *695*, 82–89. (g) Jones, G. D.; Martin, J. L.; McFarland, C.; Allen, O. R.; Hall, R. E.; Haley, A. D.; Brandon, J. R.; Konovalova, T.; Desrochers, P. J.; Pulay, P.; Vicic, D. A. *J. Am. Chem. Soc*. **2006,** *12*, 13175–13183. (h) Poverenov, E.; Gandelman, M.; Shimon, L. J. W.; Rozenberg, H.; Ben-David, Y.; Milstein, D. *Chem. Eur. J.* **2004**, *10*, 4673–4684.

6. (a) Gu, S.; Chen, W. *Organometallics*, **2009**, *28*, 909–914. (b) Zhang, C.; Wang, Z.-X. *Organometallics* **2009,** *28*, 6507–6514. (c) Broring, M.; Kleeberg, C.; Kohler, S. *Inorg. Chem*. **2008**, *47*, 6404–6412.

7. (a) Baratta, W.; Bosco, M.; Chelucci, G.; Del Zotto, A.; Siega, K.; Toniutti, M.; Zangrando, E.; Rigo, P. *Organometallics*, **2006**, *25*, 4611–4620. (b) Baratta, W.; Ballico, M.; Del Zotto, A.; Herdtweck, E.; Magnolia, S.; Peloso, R.; Siega, K.; Toniutti, M.; Zangrando, E.; Rigo, P. *Organometallics* **2009**, *28*, 4421–4430.

8. Selander, N.; Szabo, K. J. *Chem. Rev*. **2011**, *111*, 2048–2076.

9. (a) Feng, J.-J.; Chen, X.-F.; Shi, M.; Duan, W.-L. *J. Am. Chem. Soc*. **2010,** *132*, 5562–5563. (b) Li,J.; Lutz, M.; Spek, A. L.; van Klink, G. P. M.; van Koten, G.; Gebbink, R. J. M. K. *Organometallics* **2010**, *29*, 1379–1387. (c) Iglesias-Sigueenza, J.; Ros, A.; Diez, E.; Magriz, A.; Vazquez, A.; Alvarez, E.; Fernandez, R.; Lassaletta, J. M. *Dalton Trans*. **2009**, 8485–8488. (d) Gosiewska, S.; Herreras, S. M.; Lutz, M.; Spek, A. L.; Havenith, R. W. A.; van Klink, G. P. M.; van Koten, G.; Gebbink, R. J. M. K. *Organometallics* **2008**, *27*, 2549−2559. (e) Fossey, J. S.; Russell, M. L.; Abdul Malik, K. M.; Richards, C. J. *J. Organomet. Chem*. **2007**, *692*, 4843–4848. (f) Gosiewska, S.; Martinez, S. H.; Lutz, M.; Spek, A. L.; van Koten, G.; Gebbink, R. J. M. K. *Eur. J. Inorg. Chem*. **2006**, 4600–4607. (g) Wallner, O. A.; Olsson, V. J.; Eriksson, L.; Szabo, K. J. *Inorg. Chim. Acta* **2006**, *359*, 1767–1772.

10. (a) Zhang, B.-S.; Wang, W.; Shao, D.-D.; Hao, X.-Q.; Gong, J.-F.; Song, M. P. *Organometallics* **2010**, *29*, 2579–2587. (b) Felluga, F.; Baratta, W.; Fanfoni, L.; Pitacco, G.; Rigo, P.; Benedetti, F. *J. Org. Chem*. **2009**, *74*, 3547–3550.

11. (a) Boronat, M.; Corma, A.; Gonzalez-Arellano, C.; Iglesias, M.; Sanchez, F. *Organometallics* **2010**, *29*, 134–141. (b) Baratta, W.; Chelucci, G.; Magnolia, S.; Siega, K.; Rigo, P. *Chem. Eur. J.* **2009**, *15*, 726–732. (c) Baratta, W.; Benedetti, F.; Del Zotto, A.; Fanfoni, L.; Felluga, F.; Magnolia,

S.; Putignano, E.; Rigo, P. *Organometallics* **2010**, *29*, 3563–3570. (d) Baratta, W.; Ballico, M.; Chelucci, G.; Siega, K.; Rigo, P. *Angew. Chem., Int. Ed.* **2008**, *47*, 4362 –4365.

12. Moulton, C. J.; Shaw, B. L. *Dalton Trans*. **1976**, 1020–1024.

13. Zargarian, D.; Castonguay, A.; Spasyuk, D. M. *Top. Organomet. Chem*. **2013**, *40*, 131–174.

14. Wang, Z.-X.; Liu, N. *Eur. J. Inorg. Chem.* **2012**, 901–911.

15. (a) Scok, Z.; Vechorkin, O.; Harkins, S. B.; Scopelliti, R.; Hu, X. L. *J. Am. Chem. Soc.* **2008,** *130*, 8156–8157. (b) Liang, L.-C.; Chien, P.-S.; Huang, Y.-L. *J. Am. Chem. Soc.* **2006,** *128*, 15562–15563; (c) Zhang, C.; Wang, Z.-X. *Organometallics* **2009,** *28*, 6507–6514; (d) Phapale, V. B.; Buñuel, E.; García-Iglesias, M.; Cárdenas, D. J. *Angew. Chem. Int. Ed.* **2007,** *46*, 8790–8795.

16. Nishiyama, H. *Chem. Soc. Rev.* **2007,** *36*, 1133–1141.

17. Monfette, S.; Turner, Z. R.; Semproni, S. P.; Chirik, P. J. *J. Am. Chem. Soc.* **2012,** *134*, 4561–4564.

18. Pfaltz, A.; Drury, W. J., III *Proc. Natl. Acad. Sci. USA* **2004**, *101*, 5723–5726.

19. Gelman, D.; Musa, S. *ACS Catal*. **2012**, *2*, 2456−2466.

20. (a) Binda, P. I.; Abbina, S.; Du, G. *Synthesis* **2011**, 2609–2618. (b) Abbina, S.; Du, G. *Organometallics* **2012**, *31*, 7394–7403.

21. (a) Shafir, A.; Buchwald, S. L. *J. Am. Chem. Soc.* **2006,** *128*, 8742-8743. (b) Kwong, F. Y.; Buchwald, S. L. *Org. Lett.* **2003,** *5*, 793–796.

22. See Supporting Information for more details.

23. (a) Langer, J.; Görls, H.; Fischer, R.; Walter, D. *Organometallics* **2005,** *24*, 272–279; (b) Liang, L.-C.; Chien, P.-S.; Lee, P.-Y. *Organometallics* **2008,** *27*, 3082–3093.

24. Carmona, E.; Gonzalez, F.; Poveda, M. L.; Atwood, J. L.; Rogers, R. D., *J. Chem. Soc., Dalton Trans*. **1980**, 2108–2116.

25. Gwynne, E. A.; Stephan, D. W. *Organometallics* **2011**, *30*, 4128–4135.

26. (a) Ito, J.-I.; Ujiie, S.; Nishiyama, H. *Chem. Commun*. **2008**, 1923–1925. (b) Spasyuk, D. M.; Zargarian, D.; van der Est, A. *Organometallics* **2009**, *28*, 6531–6540. (c) Zhang, B.-S.; Wang, W.; Shao, D.-D.; Hao, X.-Q.; Gong, J.-F.; Song, M. P. *Organometallics* **2010**, *29*, 2579–2587.

27. (a) Wang, H.-Y.; Meng, X.; Jin, G. –X. *Dalton Trans*. **2006**, 2579–2585. (b) Eckert, N. A.; Bones, E. M.; Lachicotte, R. J.; Holland, P. L. *Inorg. Chem*. **2003**, *42*, 1720–1725.

28. Pandarus, V.; Zargarian, D. *Chem. Commun*. **2007**, 978–980.

29. (a) Firme, C. L.; Pontes, D. de L.; Antunes, O. A. C. *Chem. Phys. Lett.* **2010**, *499*, 193–198. (b) Kalamse, V.; Wadnerkar, N.; Chaudhari, A. *J. Phys. Chem. C* **2010**, *114*, 4704–4709. (c) Meylemans, H. A.; Damrauer, N. H. *Inorg. Chem.* **2009**, *48*, 11161–11175. (d) Alparone, A.; Reis, H.; Papadopoulos, M. G. *J. Phys. Chem. A* **2006**, *110*, 5909–5918. (e) Solntsev, P. V.; Dudkin, S. V.; Sabin, J. R.; Nemykin, V. N. *Organometallics*, **2011**, *30*, 3037–3046. (f) Solntsev P. V.; Spurgin, K. L.; Sabin, J. R.; Heikal, A. A.; Nemykin, V. N. *Inorg. Chem.* **2012**, *51*, 6537–6547. (g) Solntsev, P. V.; Sabin, J. R.; Dammer, S. J.; Gerasimchuk, N. N.; Nemykin, V. N. *Chem. Commun.* **2010**, 6581–6583. (h) Nemykin, V. N.; Rohde, G. T.; Barrett, C. D.; Hadt, R. G.; Sabin, J. R.; Reina, G.; Galloni, P.; Floris, B. *Inorg. Chem.* **2010**, *49*, 7497–7509. (i) Nemykin, V. N.; Hadt, R. G. *J. Phys. Chem. A* **2010**, *114*, 12062–12066. (j) Nemykin, V. N.; Kobayashi, N.; Chernii, V. Y.; Belsky, V. K. *Eur. J. Inorg. Chem.* **2001**, 733–743. (k) Nemykin, V. N.; Makarova, E. A.; Grosland, J. O.; Hadt, R. G.; Koposov, A. Y. *Inorg. Chem.* **2007**, *46*, 9591–9601. (l) Nemykin, V. N.; Maximov, A. Y.; Koposov, A. Y. *Organometallics* **2007**, *26*, 3138–3148. (m) Sabin, J. R.; Varzatskii, O. A.; Voloshin, Y. Z.; Starikova, Z. A.; Novikov, V. V.; Nemykin, V. N. *Inorg. Chem.* **2012**, *51*, 8362–8372. (n) Nitta, H.; Kawata, I. *Chem. Phys.* **2012**, *405*, 93–99. (o) Jacquemin, D.; Mennucci, B.; Adamo, C. *Phys. Chem. Chem. Phys.* **2011**, *13*, 16987–16998. (p) Solomon, E. I.; Hadt, R. G. *Coord. Chem. Rev.* **2011**, *255*, 774–789. (q) Mitsopoulou, C. A. *Coord. Chem. Rev.* **2010**, *254*, 1448–1456. (r) Moore, E. G.; Samuel, A. P. S.; Raymond, K. N. *Acc. Chem. Res.* **2009**, *42*, 542–552. (s) Vlcek, A.; Zalis, S. *Coord. Chem. Rev.* **2007**, *251*, 258–287. (t) Decker, A.; Clay, M. D.; Solomon, E. I. *J. Inorg. Biochem.* **2006**, *100*, 697–706. (u) Petrenko, T.; Kossmann, S.; Neese, F. *J. Chem. Phys.* **2011**, *134*, 054116/1–054116/14. (v) Ray, K.; DeBeer G. S.; Solomon,

E. I.; Wieghardt, K.; Neese, F. *Chem. Eur. J.* **2007**, *13*, 2783–2797. (w) Gennari, M.; Retegan, M.; DeBeer, S.; Pecaut, J.; Neese, F.; Collomb, M.-N.; Duboc, C. *Inorg. Chem.* **2011**, *50*, 10047–10055. (x) Gennari, M.; Orio, M.; Pecaut, J.; Bothe, E.; Neese, F.; Collomb, M.-N.; Duboc, C. *Inorg. Chem.* **2011**, *50*, 3707–3716. (y) Lehnert, N.; Cornelissen, U.; Neese, F.; Ono, T.; Noguchi, Y.; Okamoto, K.-I.; Fujisawa, K. *Inorg. Chem.* **2007**, *46*, 3916–3933.

30. (a) Chmielewski, P. J.; Szterenberg, L.; Siczek, M. *Chem. Eur. J.* **2011**, *17*, 1009–1020. (b) Bridgeman, A. J.; Courcot, B.; Nguyen, T. *Dalton Trans.* **2012**, *41*, 5362–5367. (c) Nemykin, V. N.; Polshyna, A. E.; Makarova, E. A.; Kobayashi, N.; Lukyanets, E. A. *Chem. Commun.* **2012**, *48*, 3650–3652. (d) Yamazaki, A.; Akitsu, T. *RSC Advances* **2012**, *2*, 2975–2980. (e) Dumas, A.; Luedtke, N. W. *Chem. Eur. J.* **2012**, *18*, 245–254. (f) Sripothongnak, S.; Ziegler, C. J.; Dahlby, M. R.; Nemykin, V. N. *Inorg. Chem.* **2011**, *50*, 6902–6909. (g) Yoshinari, N.; Igashira-Kamiyama, A.; Konno, T. *Chem.Eur. J.* **2010**, *16*, 14247–14251. (h) Soloshonok, V. A.; Ono, T.; Ueki, H.; Vanthuyne, N.; Balaban, T. S.; Burck, J.; Fliegl, H.; Klopper, W.; Naubron, J.-V.; Bui, T. T. T. *J. Am. Chem. Soc.* **2010**, *132*, 10477–10483. (i) Van Heuvelen, K. M.; Cho, J.; Dingee, T.; Riordan, C. G.; Brunold, T. C. *Inorg. Chem.* **2010**, 49, 6535−6544. (j) Wu, T.; Li, C.-H.; Li, Y.-Z.; Zhang, Z.-G.; You, X.-Z. *Dalton Trans. 2010*, *39*, 3227−3232. (k) Van Heuvelen, K. M.; Kieber-Emmons, M. T.; Riordan, C. G.; Brunold, T.C. *Inorg. Chem.* **2010**, *49*, 3104−3112. (l) Kieber-Emmons, M. T.; VanHeuvelen, K. M.; Brunold, T. C.; Riordan, C. G. *J. Am. Chem. Soc*. **2009**, *131*, 440−441. (m) Peralta, G. A.; Seth, M.; Ziegler, T. *Inorg.Chem.* **2007**, *46*, 9111−9125. (n) Armstrong, D. W.; Cotton, F. A.; Petrovic, A. G.; Polavarapu, P. L.; Warnke, M. M. *Inorg. Chem.* **2007**, *46, 1535−1537.* (o) Basu, P.; Nigam, A.; Mogesa, B.; Denti, S.; Nemykin, V. N. *Inorg. Chim. Acta* **2010**, *363*, 2857−2864.

31. Hu, H. ; Gao, H.; Zhu, F.; Wu, Q. *Zhongguo Kexue: Huaxue* **2012**, *42*, 628–635.

32. Li, J.; Tian, D.; Song, H.; Wang, C.; Zhu, X.; Cui, C.; Cheng, J.-P. *Organometallics* **2008**, *27*, 1605–1611.

33. Zhang, D.; Jin, G. –X.; Weng, L.-H.; Wang, F. *Organometallics* **2004**, *23*, 3270–3275.

34. (a) Wang, C.; Friedrich, S.; Younkin, T. R.; Li, R. T.; Grubbs, R. H.; Bansleben, D. A.; Day, M.W. *Organometallics* **1998**, *17*, 3149–3151. (b) Connor, E. F.; Younkin, T. R.; Henderson, J. I.; Waltman, A. W.; Grubbs, R. H. *Chem. Commun*. **2003**, 2272–2273.

35. (a) Julia-Hernandez, F.; Arcas, A.; Bautista, D.; Vicente, J. *Organometallics* **2012**, *31*, 3736–3744. (b) Vicente, J.; Arcas, A.; Julia-Hernandez, F.; Bautista, D.; Jones, P. G. *Organometallics* **2010**, *29*, 3066–3076. (c) Pandarus, V.; Zargarian, D. *Organometallics* **2007**, *26*, 4321–4334.

36. (a) Giri, R.; Maugel, N.; Foxman, B. M.; Yu, J.-Q. *Organometallics* **2008**, *27*, 1667–1670. (b) Mawo, R. Y.; Mustakim, S.; Young, V. G., Jr.; Hoffmann, M. R.; Smoliakova, I. P. *Organometallics* **2007**, *267*, 1801-10. (c) Song, G.; Li, X.; Song, Z.; Zhao, J.; Zhang, H. *Chem. Eur. J.* **2009**, *15*, 5535–5544. (d) Herrmann, W. A.; Brossmer, C.; Ofele, K. *Angew. Chem., Int. Ed.* **1995,** *34*, 1844.

37. Deeming, A. J.; Rothwell, I. P. *J. Orgnomat. Chem.* **1981**, *205*, 117.

38. (a) Desimoni, G.; Faita, G.; Jørgensen, K. A. *Chem. Rev*. **2011**, *111*, PR284–PR437. (b) Desimoni, G.; Faita, G.; Jørgensen, K. A. *Chem. Rev*. **2006**, *106*, 3561–3651. (c) Hargaden, G. C.; Patrick J. Guiry, P. J. *Chem. Rev*. **2009**, *109*, 2505–2550.

39. Kim, M.; Liu, Q.; Gabbaï, F. P. *Organometallics* **2004**, *23*, 5560–5564.

40. Rothwell, I. P. *Acc. Chem. Res*. **1988**, *21*, 153–159.

41. Perutz, R. N.; Sabo-Etienne, S. *Angew. Chem. Int. Ed*., **2007**, *46*, 2578–2592.

42. Higgs, A. T.; Zinn, P. J.; Simmons, S. J.; Sanford, M. S. *Organometallics* **2009**, *28*, 6142–6144.

43. Zeller, A.; Herdtweck, E.; Strassner, T. *Eur. J. Inorg. Chem*. **2003**, 1802–1806.

44. Tomasi, J.; Mennucci, B.; Cammi, R. *Chem. Rev*. **2005**, *105*, 2999–3093.

45. (a) Xu, X.; Goddard, W. A., III. *Proc. Natl. Acad. Sci. USA* **2004**, *101*, 2673–2677. (b) Lee, C.; Yang, W.; Parr, R. G. *Phys. Rev. B* **1988**, *37*, 785–789.

46. McLean, A. D.; Chandler, G. S. *J. Chem. Phys.* **1980**, *72*, 5639–5648.

47. Tenderholt, A. L. QMForge, Version 2.1. Stanford University, Stanford, CA, USA.

APPENDIX II

SCOPE AND MECHANISTIC STUDIES OF CATALYTIC HYDROSILYLATION WITH A
HIGH VALENT NITRIDORUTHENIUM(VI)

8.1. Introduction

Reduction of unsaturated organic compounds is an important transformation in academic and industrial research. Particularly, catalytic hydrosilylation of carbonyl compounds, the addition of a Si-H bond across a C=O double bond, has been extensively studied.[1] Because of the mild nature and ease of handling of hydrosilanes, they are often used as a convenient alternative to hydrogenation,[2] especially in asymmetric synthesis.[3] The field has been traditionally dominated by catalysts based on low-valent precious metals platinum, rhodium, and iridiumm.[2,3] Oxidative addition of Si-H to low-oxidation-state, late transition metals is believed to be a key step in the reaction.[4]

Therefore, it is noteworthy that a high-valent *cis*-dioxo rhenium(V) compound, $Re(O)_2I(PPh_3)_2$, was found to effectively catalyze the hydrosilylation of aldehydes and ketones.[5] This represents a new reactivity mode for high-valent transition metals in reduction catalysis[6] because such complexes are typically involved in catalytic oxidation and oxygen atom transfer reactions.[7,8,9] Significant progress has been made in the use of high-valent complexes in catalytic reductions and the understanding of their reaction mechanisms.[10,11] A number of catalysts have been identified, mostly high valent rhenium (V, VII)[12,13] and molybdenum (IV, VI)[14,15,16] complexes bearing terminal oxo or imido groups. They have proved effective in a variety of reduction reactions, such as hydrosilylation of ketones and aldehydes,[17,18] reduction of imines,[19] esters,[20] amides,[21] azides,[22] nitriles,[23] nitro compounds,[24] and sulfoxides.[25] Asymmetric reduction of ketones and imines has been achieved with good to excellent enantioselectivity.[26,27] Furthermore, other sigma bonds such as H-H and B-H can be activated by high valent transition metals, as hydrogenation of alkynes,[28,29] and reduction with boranes[30,31,32,33] have been demonstrated. Because of their high oxidation state, these complexes are usually moisture- and air-stable, allowing the reaction to be carried out conveniently on the bench top under air. In addition to the synthetic utility of these reactions, the high valent transition metal catalysts also provide a new paradigm in which important mechanistic questions can be addressed as related to σ-bond activation.[34,35]

Several mechanisms have been proposed for the high-valent, transition metal catalyzed hydrosilylation. For the *cis*-dioxo $ReO_2I(PPh_3)_2$ catalyst, the Si-H bond adds across one of the two Re=O bonds to afford a siloxy rhenium hydride, followed by carbonyl insertion and silylether elimination (Scheme 17, path A).[36,37] Depending on the substrates, the resting state of the catalyst may vary. Related MoO_2Cl_2 catalyst likely follows a similar mechanism.[38,39] However, this unconventional pathway seem to be unique to catalysts bearing *cis*-dioxo groups, as Si-H addition to Re=O is not observed for the monooxorhenium catalysts such as $ReOCl_3(PPh_3)_2$.[40] In these systems, silane activation is believed to proceed via η^2-silane σ-adduct, followed by heterolytic

cleavage at the electrophilic rhenium center (Scheme 17, path B). The rhenium hydride formation step may not be needed if the reaction proceeds in a more concerted manner,[41,42] resembling the situation in catalytic silane alcoholysis reactions.[43] As in the ionic hydrogenation mechanism, a carbonyl coordination step is not required.[44] Indeed, a non-hydride ionic hydrogenation mechanism is supported by a computational study.[45] On the ground of a stoichiometric labeling experiment, an alternative mechanism, in which the metal center simply activates the carbonyls as a Lewis acid, is suggested for imido-molybdenum catalysts, as well as the rhenium catalysts mentioned above.[46,47] In another study, expected Si-O elimination (the last step of path A in Scheme 17) from intermediate is not observed.[48] The disparity in mechanistic understanding is perhaps not too surprising because hydrosilylation is often complicated and a universal mechanism is not expected for different catalysts and substrates. In any event, the roles of the multiply bonded terminal ligands and hydrides in silane activation remain unclear in catalysis.
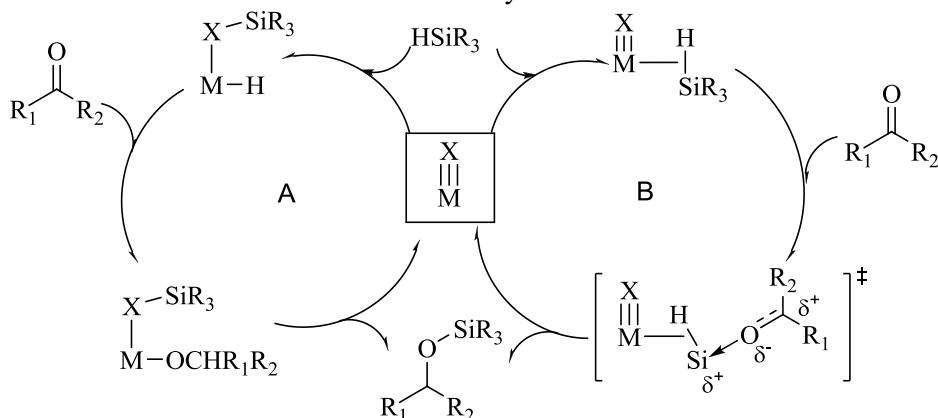
Scheme 17. Proposed mechanism of oxo and imido Re and Mo catalyzed hydrosilylation

Given the utility of this novel type of catalysts in reductions, we became interested in related transition metal compounds. We have recently communicated the application of a cationic nitride Ru(VI) complex, [Ru(VI)N(saldach)(MeOH)$^+$][ClO$_4^-$] (**1**, where saldach is the dianion of *racemic* N,N'-cyclohexan-di-yl-bis(salicylideneimine), Figure 64),[49] which is isoelectronic with rhenium (V) and Mo (IV) with a d^2 electron configuration, in catalytic hydrosilylation of aldehydes and ketones.[50] Herein, we describe a detailed study of **1**/PhSiH$_3$ system in catalytic reduction of various carbonyl compounds and imines. Furthermore, we present evidence that more than one pathway, including a radical pathway, is at play for the current hydrosilylation.
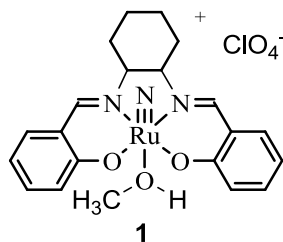
Figure 64. RuN catalyst

8.2. Results and Discussion

As mentioned previously, high valent transition metal catalysts can effectively reduce a variety of unsaturated organic substrates. We have shown that RuN(saldach)$^+$ is an effective catalyst for the reduction of a few ketones and aldehydes by primary silane.[50] To extend the scope of the reaction, we have examined a number of different substrates, with particular attention on the hydrosilylation of carbonyl and imine compounds.

197

8.2.1. Reduction of Carbonyl Compounds

Using the standard conditions (~0.5 mmol substrate, 1.5 equivalents of $PhSiH_3$, 1 mol% catalyst **1**, ~120 °C in benzene), we carried out the hydrosilylation of a diverse set of representative aliphatic and aryl carbonyl compounds, including acyclic, cyclic, aryl, acyclic conjugated enone, and cyclic conjugated enone, etc. [51] The selected results are summarized in Table 16. As noted before, reduction of aldehydes was efficient, typically complete within two hours, except for *p*-nitro benzaldehyde, which is surprisingly sluggish (Table 16, entry **3**). Substituents such as halo, hydroxyl, and nitro groups are tolerated, although there is evidence that the nitro group may be reduced further after the carbonyl reduction. The α,β-unsaturated cinnamaldehyde underwent 1,2-addition reaction of silane, leading to corresponding alcohol in 74% yield (entry 6), and 1,4 addition product is not observed.

In comparison with aldehydes, the reduction of ketones was relatively slow, taking ~20 h to completion. In most of the cases, the corresponding alcohols are successfully isolated by column chromatography in good yields. Sometimes, deoxygenation of carbonyl to corresponding alkyl compounds can be observed. For example, 4-ethyl-anisole is isolated in 27% yield along with the desired alcohol in the reduction of 4-methoxy acetophenone (entry 8). On the other hand, α,β-unsaturated enones seem to be challenging substrates in the reaction. The acyclic *trans*-chalcone gave rise to a complex mixture, from which only ~16% expected 1,2-reduction product is isolated (entry 12). Other isolated products include 16% 1,4 reduction product and the deoxygenation product (18%). In the case of a cyclic enone, 3-methyl, 2-cyclohexenone, no 1,4-addition product was observed and the desired unsaturated alcohol was identified by both GC-MS data and ^{1}H NMR spectroscopy, although the conversion is low (entry 13).

8.2.2. Reduction of Imines
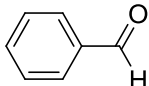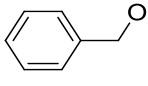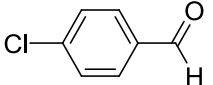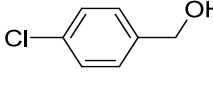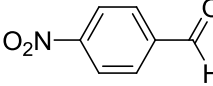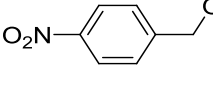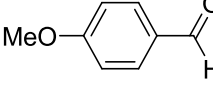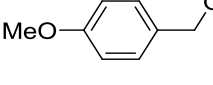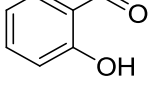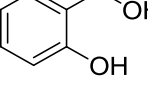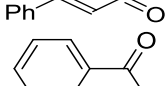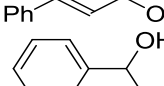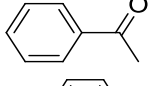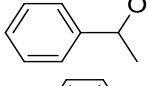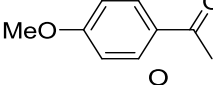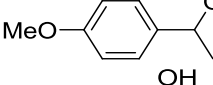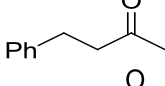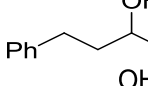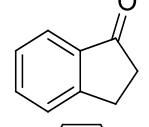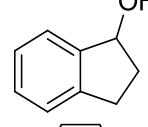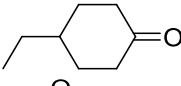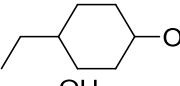
Synthesis of amines from imines is an important transformation in pharmaceutical and agricultural chemistry that can be achieved with a stoichiometric reducing agent or catalytic hydrogenation.[52] Alternatively, this can be done via catalytic hydrosilylation and a number of high-valent Re- and Mo-based systems have been shown to effect the reduction of imines. To expand the substrate scope of the $Ru^{VI}N$-$PhSiH_3$ system, we examined a number of imines under the standard reaction conditions employed for carbonyl compounds. The results are summarized in Table 17.

It is evident that the C=N double bonds in imine react readily under these conditions, leading to the formation of corresponding amines upon workup. The reactivity is comparable with that of ketones and slower than aldehydes. The imines derived from anilines are generally slower than imines derived from alkyl amines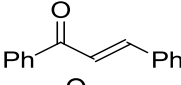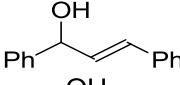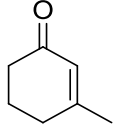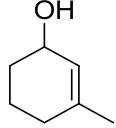 (Table 17, entries 1-4 vs 5-6). As expected, similar level of functional group tolerance is observed. The reduction of imine derived from isopropyl amine, $PhCH=N^iPr$, seems to stop after ~33% conversion, and prolonged reaction time failed to improve the conversion (entry 3). Similar reactivity was seen with an imine derived from 2,6-dimethyl aniline (entry 6). Apparently, the steric bulk near the imino nitrogen plays a significant role in the reduction reaction.

8.2.3. Product Profile

Although the desired reduction products, alcohols and amines, can generally be isolated in good yields, it has been noted that the initial reaction products are rather complex. For example, in the crude reaction mixture of an imine and $PhSiH_3$, various products can be detected by GC-MS (Scheme 18). In the case of aldehydes and ketones, mono-, di-, and trialkoxy silanes are observed among the products, with the dialkoxysilane being dominant. The preference for dialkoxy silane formation has been observed in other catalytic hydrosilylations.[15,53,54] This suggests that $PhSiH_2(OR)$ is more active than $PhSiH_3$ in the reaction. Further reduction to deoxygenation products are typically noted for ketones when longer reaction time is needed for complete

Table 16. Hydrosilylation of Carbonyl Compounds Catalyzed by RuN[a]

entry	substrate	product	time	conversion[b]	% yield[c]
1			40 min	100	73
2			2 h	100	76
3			26 h	100	78
4			1.5 h	100	73
5			2 h	100	84
6			1.5 h	100	74
7			18 h	100	67
8			13 h	100	36[d]
9			20 h	100	86
10			8 h	83	65
11			20 h	100	89
12			20 h	100	16[e]
13			20 h	54	-

[a]Reaction conditions: 0.3-0.8 mmol substrate, 1.5 equivalent of PhSiH$_3$ and catalyst **1** (1 mol%) in heated toluene or benzene (~120 °C). [b]Based on NMR integration. [c]Isolated yields. [d]p-Ethylanisole was isolated in 27% yield. [e]Other products isolated include 1, 3-diphenylpropan-1-ol (15%) and 1, 3-diphenylpropan-1-one (16%).

conversion. After acidic workup, however, the majority of the species isolated are the orresponding alcohols or amines. In comparison, the Re^{V}O-catalyzed hydrosilylation of acetophenone was accompanied mostly with the formation of ethylbenzene and *dl*, *meso*-di(1-phenyl-ethyl)ethers.[13] The different product profiles suggest that these catalysts may have different features in the reaction.

8.2.4. Redistribution at Silicon

Very notable is the presence of silane redistribution products, mostly Ph_2SiH_2, with a small amount of Ph_3SiH (Scheme 19). SiH_4, the other possible redistribution product, has not been

Table 17. Hydrosilylation of Imines Catalyzed by RuN[a]

entry	substrate	product	time	conversion	% yield[b]
1			12 h	100	85
2			24 h	100	58
3			24 h	33	-
			48 h	33	-
4			18 h	65	60
5			18 h	50	-
			46 h	97	85
6			24 h	40	-
			72 h	63	60

[a]Reaction conditions: 0.4-0.8 mmol imine, 1.5 equivalent of $PhSiH_3$ and catalyst (1 mol%) in heated toluene or benzene. [b]Isolated yields.
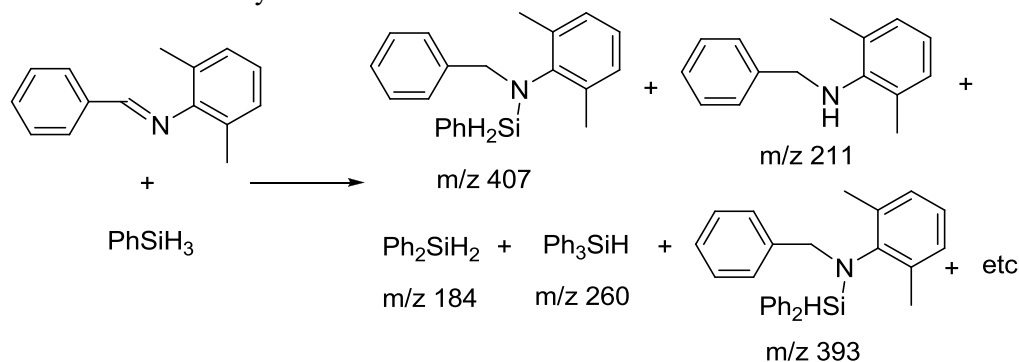
Scheme 18. Products in hydrosilylation of an imine (The top two species are the major products).

detected, supposedly due to its high volatility and reactivity. Sometimes, hydrosilylation products derived from Ph_2SiH_2 can be detected (see Scheme 18). In the literature, silane redistribution reactions have been observed in the presence of low valent, late transition metal complexes, such as Ru, Rh,[55] Ir,[56] or others.[57] However, in high-valent transition-metal-catalyzed hydrosilylations with $PhSiH_3$, silane redistribution has been rarely reported.[14,15,21] To further probe this reactivitywith the present ruthenium catalyst, reaction in the absence of carbonyl substrate was

carried out under similar conditions with catalytic amount of **1**. The conversion of PhSiH$_3$ reached a plateau of ~25% after 24 h. Among the products, Ph$_2$SiH$_2$ can be easily identified by both ^{1}H NMR (5.1 ppm) and GC-MS (m/z 184; t_R = 13.55 min). A small amount of Ph$_3$SiH can be detected by GC/MS (m/z 260) in the crude mixture, along with silane dehydrocoupling product PhH$_2$SiSiH$_2$Ph (m/z 214). It is unclear how the redistribution occurs. One obvious choice is catalysis by low valent Ru resulting from reduction by PhSiH$_3$; However, the observation that the redistribution stops before completion seems to suggest that high-valent Ru is important in the present redistribution.

$$2\ PhSiH_3 \rightleftharpoons Ph_2SiH_2 + SiH_4$$

$$2\ Ph_2SiH_2 \rightleftharpoons Ph_3SiH + PhSiH_3$$

Scheme 19. Redistribution of PhSiH$_3$

8.2.5. Mechanistic Consideration

To probe the mode of activation with the RuN catalyst, stoichiometric reactions of **1** and substrates were studied. Treatment of **1** with a carbonyl substrate, PhCHO, showed no observable change in the NMR or UV-vis spectra. On the other hand, reaction between **1** and PhSiH$_3$ in CH$_3$CN is indicated by the facile color change from reddish brown to green. Although the reaction product was not isolated, ESI-MS analysis revealed predominantly a peak at m/z 422, in agreement with a Ru^{III}(saldach)$^+$ species.[58] These observations do not support a Lewis acid catalyzed carbonyl activation pathway;[46] rather, a silane activation pathway is more likely, though it should be noted that the observation of Ru(VI) reduction by silane is not necessarily related to a silane activation pathway, and the possibility of Lewis acid catalysis can not be completely ruled out.

The question is then how silane is activated in the reaction, as diverse pathways have been proposed for high-valent catalysts.[10,11] Compared with isoelectronic Re(V) and Mo(IV), Ru(VI) is certainly more oxidizing, because complex **1** can abstract hydrogen from relatively weak C-H bonds via a hydrogen atom transfer mechanism.[59] It is thus conceivable that RuN abstracts hydrogen from silane in the initial step, generating a silyl radical, PhH$_2$Si$^•$. This could explain the formation of disilane via combination of two silyl radicals. Radical pathway in catalytic hydrosilylation has been indicated for a titanium(IV)/silane system via single electron transfer process.[60] In a high-valent Mo catalyzed hydrosilylation, radical mechanism could provide a feasible pathway based on the computational studies.[61]

To investigate the possibility of radical involvement, the catalytic reduction of PhCHO (1 equivalent) by PhSiH$_3$ (1.5 equivlents) was carried out in the presence of one equivalent of a silyl radical scavenger, 2,2,6,6-tetramethyl-1-piperidinyloxyl (TEMPO).[62] The hydrosilylation reaction slowed down, as shown in Figure 65, but still was able to finish. At the end of the reaction, 2,2,6,6-tetramethyl-1-piperidine, the reduction product derived from TEMPO, was detected in ~ 0.5 equivalent (relative to PhCHO). Control experiment shows that TEMPO reacts with PhSiH$_3$ under similar conditions, but takes much longer (>48h). These observations are suggestive of the involvement of a silyl radical in the catalytic reaction.[63]

In addition, cyclopropyl phenyl ketone was employed in catalytic hydrosilylation as a mechanistic probe; formation of cyclopropyl ring-opening products indicates a radical mechanism.[64] Analysis of the crude reaction products showed again a complex mixture, but both direct hydrosilylation and ring-opening products were detected (Scheme 20). After hydrolysis, mono and dialkoxy silanes (**E** and **F**) disappeared, and the major components are identified in a ratio of **A**:**B**:**C**:**D** = 2.4:1.0:1.7:5.2. The reappearance of the starting ketone (such as **A**) upon workup has been noted previously,[50] presumably through a silyl enol ether intermediate. The presence of cyclopropyl ring-opening products **B** (and **C**) clearly suggests the involvement of a radical pathway, but perhaps not as a principal contributor. As to the major pathway or pathways,

a heterolytic cleavage of the SiH bond activated by coordination to the highly electrophilic RuN unit[49] can be surmised, similar to that of monooxo Re^V based systems in Scheme 17B. However, a more detailed conclusion can not be reached at this point.

The effect of electronic factors was further studied with a series of substituted benzaldehydes in competition reactions with PhCHO. Both electronic-donating (4-OMe) and electron-withdrawing groups (4-Cl, 4-NO$_2$) seem to accelerate the reaction, lending further support for a radical contribution.[65] However, a linear free energy relationship between relative rates and $\sigma^{\cdot}$ or other Hammet constants (σ and σ^+) could not be established, which may be a reflection of the presence of multiple pathways. Curiously, at competition conditions, reduction of *p*-nitro benzaldehyde is much faster, even faster than benzaldehyde.
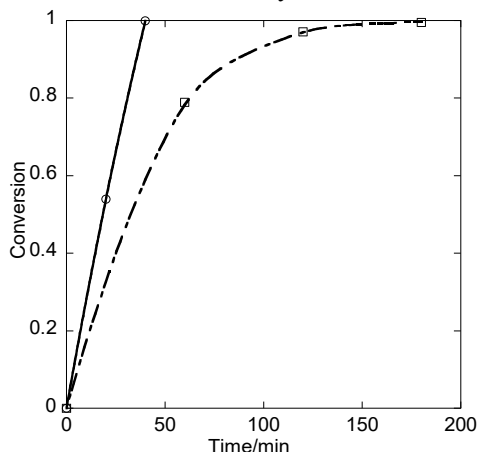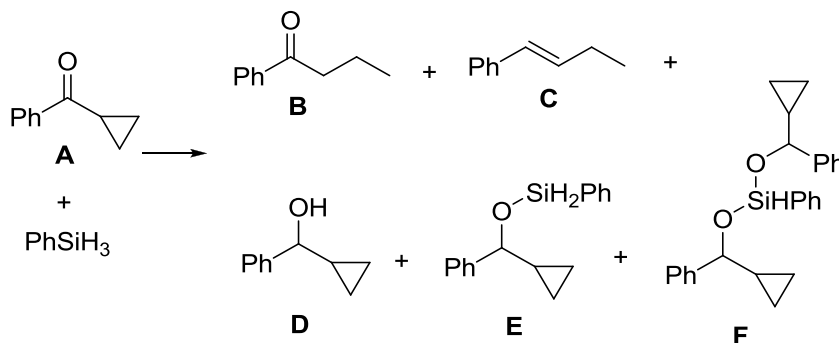

Figure 65. Time profile for the catalytic hydrosilylation of PhCHO in the absence (circle) and presence (square) of 1 equiv of TEMPO

**Scheme 20**. Hydrosilylation products derived from cyclopropyl phenyl ketone

8.2.6. Involvement of Ru^{III}

Low valent Ru species have been studied extensively as hydrosilylation/hydrogenation catalysts.[66] In the present system, Ru^{VI}N can be easily reduced in the presence of PhSiH$_3$. Ru^{VI}N complexes could also undergo N-N coupling reactions to afford Ru^{III}.[49] A recent work has called attention to low-valent rhenium, which may be responsible for hydrosilylation with oxorhenium(V) catalysts.[67] It is also worth mentioning that the Brookhart's [(POCOP)Ir^{III}H]$^+$ system has been proposed to catalyze hydrosilylation of carbonyl compounds through an ionic mechanism featuring an η^1-silane intermediate.[68] Thus, we investigated the possibility of Ru(III) as the actual catalyst. An independently prepared Ru(III)-saldach complex, [Ru(saldach)(H$_2$O)$_2^+$][PF$_6^-$][69], did not exhibit much reactivity at similar conditions, but in situ generation for Ru(III) from Ru(VI)N and PhSiH$_3$ in C$_6$D$_6$ seem to lead to decomposition. In additiona, under catalytic conditions, the reaction mixture maintained an orange-brown color throughout, not the green color, characteristic of Ru^{III},

observed in the absence of carbonyl substrates. Furthermore, ESI-MS analysis of the reaction mixture under catalytic conditions reveals the absence of mononuclear $[Ru^{VI}N]^+$ or $[Ru^{III}]^+$; instead, the majority of the Ru-containing species is observed at m/z 858 and 892, with correct isotopic patterns for a dinuclear form, possibly $[(saldach)Ru]_2N$, though its nature remains uncertain. These observations do not support Ru^{III} as the primary active catalyst, but it may still be involved in a minor pathway.

8.2.7. Reduction of Other Unsaturated Substrates

A wide variety of unsaturated substrates has been subjected to high-valent rhenium- and molybdenum-catalyzed reductions. To further examine the scope of the present $Ru^{VI}N$ system, we tested a few less active, unsaturated groups, including ester, amide, nitro, and alkyne. In these reactions, the desired reduction products can be observed (Scheme 21), but the conversions are low (10-35%). It is also noted the consumption of $PhSiH_3$ is considerably larger than the unsaturated substrates, though the products were not always tractable. In addition to Ph_2SiH_2, which is easily detected by both NMR and GC-MS, we suspect that phenylsilane oligomers/polymers were formed in these reactions, as indicated by the presence of broad but feartureless signals between 4-6 ppm in ^1H NMR.
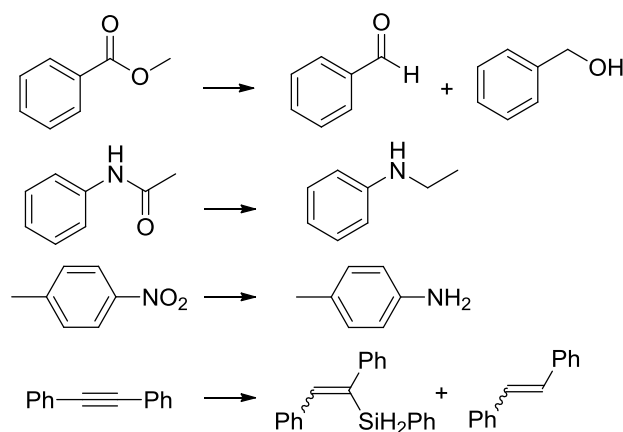
Scheme 21. Catalytic reduction of some unsaturated substrates

8.3. Conclusion

In summary, we have demonstrated that a high-valent nitridoruthenium(VI) compound, $[RuN(saldach)(CH_3OH)]^+[ClO_4]^-$ (**1**), is an effective catalyst for hydrosilylation of unsaturated organic substrates, particularly aldehydes, ketones, and imines. The reaction mixture contains various species, including the redistribution products of $PhSiH_3$. This and other mechanistic studies indicate that the catalysis likely proceeds by silane activation via several pathways; in particular, evidence for a radical pathway is presented. Efforts are underway to improve the performance of this type of RuN-based catalysts and gain more insights of the mechanist aspects.

8.4. Experimental Section

General. The ruthenium catalyst was prepared according to the literature.[49] Imine substrates were obtained by condensation of corresponding carbonyl compounds and amines. All other reagents and reactants were obtained commercially and used as received. All ^1H and ^{13}C NMR spectra were recorded on a Bruker AVANCE-500 NMR spectrometer and referenced to the residue peaks in $CDCl_3$ (7.26) or C_6D_6 (7.16). UV-vis measurement was performed on a PerkinElmer Lamda 35 spectrophotometer. GC-MS analyses were performed on an HP 5890 GC/HP 5971/B MSD system

with electron impact ionization (70 eV) and a DB5 column (30m x 0.53 mm ID, 0.25 μm thick; initial temperature 50 °C, initial time 1 min; ramp rate 10 °C/min; final temperature 310 °C, final time 5 min). High resolution mass spectrometry (HRMS) was performed using high-resolution time of flight G1969A instrumentation (Agilent, Santa Clara, CA, USA).

Catalytic hydrosilylation. In a typical procedure, RuN catalyst **1** (3-5 mg, 1 mol%), substrate (0.5 – 0.8 mmol, 1.0 equivalent), C_6D_6 (0.30-0.35 mL), and $PhSiH_3$ (1.5 equiv) were charged into a J Young NMR tube, usually in that order. Trimethylphenyl silane or hexamethyl benzene was used as internal standard (5-20 %). This was then mixed and heated in an oil bath at ~120 ˚C. The reaction progress was monitored by periodically taking ¹H NMR. The reduction for ketones is typically complete within 1 day, and aldehyde substrates take only 2 h or less. After the reaction was complete or nearly complete, the reaction mixture was transferred to a round bottom flask with diethylether, and hydrolyzed with aqueous HCl or tetrabutylammonium fluoride (TBAF). Before and after the hydrolysis, a small sample was taken for GC-MS analysis. After hydrolysis, the organic layer was extracted with ether and then subject to column chromatography on silica with appropriate mixture of hexane-EtOAc as eluent. The reduction products were identified by ¹H NMR and GC-MS analysis in comparison with literature data or authentic samples.

8.5. References

1. Ojima, I.; Li, Z.; Zhu, J. in *The Chemistry of Organic Silicon Compounds, Vol. 2*. Rappoport, Z.; Apeloig, Y. Ed. Wiley: New York, **1998**, pp 1687–1792.

2. de Vries, J. G., Elsevier, C. J., Eds. *The Handbook of Homogeneous Hydrogenation*; Wiley-VCH: Weinheim, Germany, 2007, Vol. 1–3.

3. Noyori, R. *Asymmetric Catalysis in Organic Synthesis,* Wiley: New York, **1994**.

4. Chalk, A. J.; Harrod, J. F. *J. Am. Chem. Soc.* **1965**, *87*, 16–21.

5. Kennedy-Smith, J. J.; Nolin, K. A.; Gunterman, H. P.; Toste, F. D. *J. Am. Chem. Soc.* **2003**, *125*, 4056–4057.

6. Thiel, W. R. *Angew. Chem, Int. Ed.* **2003**, *42*, 5390–5392.

7. Owens, G. S.; Arias, J.; Abu-Omar, M. M. *Catal. Today* **2000,** *55*, 317–363.

8. Romao, C. C.; Kuhn, F. E.; Herrmann, W. A. *Chem. Rev.* **1997**, *97*, 3197–3246.

9. Espenson, J. H. *Adv. Inorg.. Chem.* **2003**, *54*, 157–202.

10. Sousa, S. C. A.; Cabrita, I.; Fernandes, A. C. *Chem. Soc. Rev.* **2012**, *41*, 5641–5653.

11. Du. G.; Abu-Omar, M. M. *Curr. Org. Chem.* **2008**, *12*, 1185–1198.

12. Royo, B.; Romao, C. C. *J. Mol. Catal. A: Chem.* **2005**, *236*, 107–120.

13. Du, G.; Abu-Omar, M. M. *Organometallics* **2006**, *25*, 4920–4923.

14. Ziegler, J. E.; Du, G.; Fanwick, P. E.; Abu-Omar, M. M. *Inorg. Chem.* **2009**, *48*, 11290–11296.

15. Peterson, E.; Khalimon, A. Y.; Simionescu, R.; Kuzmina, L. G.; Howard, J. A. K.; Nikonov, G. I. *J. Am. Chem. Soc.* **2009**, *131*, 908–909.

16. Pontes da Costa, A.; Reis, P. M.; Gamelas, C.; Romao, C. C.; Royo, B. *Inorg. Chim. Acta* **2008,** *361,* 1915–1921.

17. Ison, E. A.; Trivedi, E. R.; Corbin, R. A.; Abu-Omar, M. M. *J. Am. Chem. Soc.* **2005**, *127*, 15374–15375.

18. Du, G.; Fanwick, P. E.; Abu-Omar, M. M. *Inorg. Chim. Acta* **2008**, *361*, 3184–92.

19. Fernandes, A. C.; Romao, C. C. *Tetrahedron Lett.* **2005**, *46*, 8881–8883.

20. Pehlivan, L.; Metay, E.; Laval, S.; Dayoub, W.; Delbrayelle, D.; Mignani, G.; Lemaire, M. *Eur. J. Org. Chem.* **2011**, *36*, 7400–7406.

21. Fernandes, A. C.; Romao, C. C. *J.Mol. Cat. A: Chem.* **2007**, *272*, 60–63.

22. Maddani, M. R.; Moorthy, S. K.; Prabhu, K. R. *Tetrahedron* **2010**, *66*, 329–333.

23. Cabrita, I.; Fernandes, A. C. *Tetrahedron* **2011**, *67*, 8183–8186.

24. de Noronha, R. G.; Romao, C. C.; Fernandes, A. C. *J. Org. Chem.* **2009**, *74*, 6960–6964.

25. Cabrita, I.; Sousa, S. C. A.; Fernandes, A. C. *Tetrahedron Lett.* **2010**, *51*, 6132–6135.

26. Nolin, K. A.; Ahn, R. W.; Kobayashi, Y.; Kennedy-Smith, J. J.; Toste, F. D. *Chem. Eur. J.* **2010**, *16*, 9555–9562.

27. Nolin, K. A.; Ahn. R. W.; Toste, F. D. *J. Am. Chem. Soc.* **2005**, *127*, 12462–12463.

28. Reis, P. M.; Costa, P. J.; Romao, C.C.; Fernandes, J.A.; Calhorda, M. J.; Royo, B. *Dalton Trans.* **2008**, 1727–1733.

29. Ortiz, C. G.; Abboud, K. A.; Cameron, T. M.; Boncella, J. M. *Chem. Commun.* **2001**, 247–248.

30. Khalimon, A. Y.; Farha, P.; Kuzmina, L. G.; Nikonov, G. I. *Chem. Commun.* **2012**, 455–457.

31. Fernandes, A. C.; Fernandes, J. A.; Romao, C. C.; Veiros, L. F.; Calhorda, M. J. *Organometallics* **2010** *29*, 5517–5525.

32. Fernandes, A.C.; Fernandes, J.A.; Paz, F.A. A.; Romao, C.C. *Dalton Trans.* **2008**, 6686–6688.

33. Fernandes, A. C.; Romao, C. C. *Tetrahedron Lett.* **2007**, *48*, 9176–9179.

34. Calhorda, M. J.; Costa, P. J. *Dalton Trans.* **2009**, 8155–8161.

35. Shirobokov, O. G.; Gorelsky, S. I.; Simionescu, R.; Kuzmina, L. G.; Nikonov, G. I. *Chem.*

Commun. **2010**, *46*, 7831–7833.

36. Nolin, K. A.; Krumper, J. R.; Pluth, M. D.; Bergman, R. G.; Toste, F. D. *J. Am. Chem. Soc*. **2007**, *129*, 14684–14696.
37. Chung, L. W.; Lee, H. G.; Lin, Z.; Wu, Y.-D. *J. Org. Chem.* **2006**, *71*, 6000–6009.
38. Reis, P. M.; Romao, C. C.; Royo, B. *Dalton Trans.* **2006**, 1842–1846.
39. Drees, M.; Strassner, T. *Inorg. Chem.* **2007**, *46*, 10850–10859.
40. Du, G.; Fanwick, P. E.; Abu-Omar, M. M. *J. Am. Chem. Soc*. **2007**, *129*, 5180–5187.
41. Buhl, M.; Mauschick, F. T. *Organometallics* **2003**, *22*, 1422–1431.
42. Chang, S.; Scharrer, E.; Brookhart, M. *J. Mol. Cat. A: Chem*. **1998**, *130*, 107–119.
43. Luo, X. L.; Crabtree, R. H. *J. Am. Chem. Soc*. **1989**, *111*, 2527–2535.
44. Bullock, R. M. *Chem. –Eur. J.* **2004**, *10*, 2366–2374.
45. Gu, P.; Wang, W.; Wang, Y.; Wei, H. *Organometallics* **2013**, *32*, 47–51.
46. Shirobokov, O. G.; Kuzmina, L. G.; Nikonov, G. I. *J. Am. Chem. Soc*. **2011**, *133,* 6487–6489.
47. Khalimon, A. Y.; Shirobokov, O. G.; Peterson, E.; Simionescu, R.; Kuzmina, L. G.; Howard, J. A.; Nikonov, G. I. *Inorg. Chem.* **2012**, *51*, 4300–4313.
48. Khalimon, A. Y.; Ignatov, S. K.; Simionescu, R.; Kuzmina, L. G.; Howard, J. A.; Nikonov, G. I. *Inorg. Chem.* **2012**, *51*, 754–756.
49. Man, W.-L.; Tang, T.-M.; Wong, T.-W.; Lau, T.-C.; Peng, S.-M.; Wong, W.-T. *J. Am. Chem. Soc*. **2004**, *126*, 478–479.
50. Truong, T. V.; Kastl, E. A.; Du, G. *Tetrahedron Lett*. **2011**, 52, 1670–1672.
51. Brown, H. C.; Park, W. S.; Cho, B. T.; Ramachandran, P. V. *J. Org. Chem.* **1987**, *52*, 5406–5412.
52. Ohkuma, T.; Noyori, R. In *Comprehensive Asymmetric Catalysis, Suppl. 1*, Jacobsen, E. N.; Pfaltz, A.; Yamamota, H. Eds.; Springer: New York, **2004**.
53. Yang, J.; Tilley, T. D. *Angew. Chem. Int. Ed*. **2010**, *49*, 10186–10188.
54. Spielmann, J.; Harder, S. *Eur. J. Org. Chem.* **2008**, 1480–1486.
55. Rosenberg, L.; Davis, C. W.; Yao, J. *J. Am. Chem. Soc*. **2001**, *123*, 5120–5121.
56. Park, S.; Kim, B. G.; Gottker-Schnetmann, I.; Brookhart, M. *ACS Catal*. **2012**, *2*, 307–316.
57. Radu, N. S.; Hollander, F. J.; Tilley, T. D.; Rheingold, A. L. *Chem. Commun*. **1996**, *21*, 2459–2460.
58. See Supporting Information for more details.
59. Man, W.-L.; Lam, W. W. Y.; Kwong, H.-K.; Yiu, S.-M.; Lau, T.-C. *Angew. Chem. Int. Ed.* **2012**, *51*, 9101–9104.
60. Petit, C.; Favre-Reguillon, A.; Albela, B.; Bonneviot, L.; Mignani, G.; Lemaire, M. *Organometallics* **2009**, *28*, 6379–6382.
61. Costa, P. J.; Romao, C. C.; Fernandes, A. C.; Royo, B.; Reis, P. M.; Calhorda, M. J. *Chem. Eur. J.* **2007**, *13*, 3934–3941.
62. Chatgilialoglu, C.; Guerrini, A.; Lucarini, M.; Pedulli, G. F.; Carrozza, P.; Da Roit, G.; Borzatta, V.; Lucchini, V. *Organometallics* **1998**, *17*, 2169–2176.
63. Albeniz, A. C.; Espinet, P.; Lopez-Fernandez, R.; Sen, A. *J. Am. Chem. Soc*. **2002**, *124*, 11278–11279.
64. Yang, D.; Tanner, D. D. *J. Org. Chem.* **1986**, *51*, 2267–2270.
65. Dust, J. M.; Arnold, D. R. *J. Am. Chem. Soc*. **1983**, *105*, 1221–1227.
66. Kitamura, M.; Noyori, R. In *Ruthenium in Organic Synthesis*; Murahashi, S. I., Ed.; Wiley-VCH: Weinheim, Germany, **2004**; *pp* 3–52.
67. Smeltz, J. L.; Boyle, P. D.; Ison, E. A. *Organometallics* **2012**, *31*, 5994–5997.
68. Park, S.; Brookhart, M. *Organometallics* **2010**, *29*, 6057–6064.
69. Man, W.; Kwong, H.; Lam, W.W.Y.; Xiang, J.; Wong, T.; Lam, W.; Wong, W.; Peng, S.; Lau, T. *Inorg. Chem.* **2008,** *47,* 5936–5944.

APENDIX III: LIST OF ABBREVIATIONS AND ACRONYMS

BDI	β-diketiminate
BINAP	bis(diphenylphosphino)-1,1'-binaphthyl
BPA	bisphenol-A
BPA-PC	poly(bisphenol-A carbonate)
CDC	centers for disease control and prevention
CHO	cyclohexene oxide
$Co(OAc)_2$	cobalt acetate
CO_2	carbon dioxide
Cs_2CO_3	cesium carbonate
DCM	dichloromethane
DMAP	4-dimethylaminopyridine
DMP	dimethylphenyl
EO	ethylene oxide
MA	maleic anhydride
M_n	number average molecular weight
M_w	weight average molecular weight
PA	phthalic anhydride
PC	poly(carbonate)

PCC	poly(cyclohexene carbonate)
PCHC	poly(cyclohexene carbonate)
Pd(OAc)$_2$	palladium acetate
PDI	polydispersity index
PDLA	D-poly(lactic acid)
PE	phenyl ethanol
PLA	poly(lactic acid)
PLLA	L-poly(lactic acid)
PO	propylene oxide
PPC	poly(propylene carbonate)
ROP	ring opening polymerization
SA	succinic anhydride
Salcy	salicylidene
Salen	*N,N*-bis(salicylidene)-1,2-diaminoalkane
Sc	supercritical
SO	styrene oxide
T_g	glass transition temperature
THF	tetrahydrofuran
T_m	melting point
TOF	turnover frequency
TPP	5,10,15,20-tetraphenylporphinato
Zn(OAc)$_2$	zinc acetate
ZnEt$_2$	diethylzinc

α   enantioselective parameter